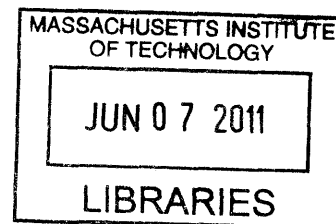


Nature's Approach Toward Ring Formation and Structural Diversity in Ergot Alkaloid Biosynthesis

by

Johnathan Zandrew Cheng

B.S. Chemistry
University of Hawaii, 2007



SUBMITTED TO THE DEPARTMENT OF CHEMISTRY
IN PARTIAL FULFILLMENT OF THE REQUIREMENTS FOR THE
DEGREE OF DOCTOR OF PHILOSOPHY
AT THE
MASSACHUSETTS INSTITUTE OF TECHNOLOGY

ARCHIVES

JUNE 2011

© 2011 Massachusetts Institute of Technology. All rights reserved

Signature of Author

Department of Chemistry
March 31, 2011

Certified by ____

Sarah E. O'Connor
Associate Professor of Chemistry
Thesis Supervisor

Accepted by ____

Robert W. Field
Professor of Chemistry
Chairman, Departmental Committee on Graduate Students

This doctoral thesis has been examined by a committee of the Department of Chemistry as follows:

Professor Barbara Imperiali

Chair _____

Professor Sarah E. O'Connor

Thesis Supervisor _____

Professor Catherine L. Drennan

Committee Member _

Nature's Approach Toward Ring Formation and Structural Diversity in Ergot Alkaloid Biosynthesis

by

Johnathan Zandrew Cheng

Submitted to the Department of Chemistry
on March 31, 2011 in Partial Fulfillment of the
Requirements for the Degree of Doctor of Philosophy in
Chemistry

ABSTRACT

Ergot alkaloids are fungal-derived secondary metabolites well known for a diverse array of pharmacological effects both beneficial and detrimental to human health. Historically, the ergot alkaloids have been known to cause ergotism in populations that consume grain contaminated by ergot alkaloid producing fungus. However, naturally isolated and semi-synthetic derivatives of certain ergot alkaloids have also been used to treat migraines, Parkinsonism, and tumor growth.

Different fungal species such as *Aspergillus fumigatus*, *Claviceps purpurea*, and *Neotyphodium lolii* produce ergot alkaloids that have distinct structural features yet share a common tetracyclic ergoline ring scaffold. Mechanistic details regarding the formation of the common ergoline ring are not well understood, though the genes encoding the enzymes that carry out these cyclizations are believed to be well conserved across divergent fungal species. Here we describe *in vivo* gene disruption experiments in *Aspergillus fumigatus* that allowed us to identify candidate enzymes that were directly involved with the intramolecular cyclization of the ergoline ring. Additionally, we discuss the cloning and heterologous expression of these genes to further characterize their catalytic function.

Old Yellow Enzyme homologues from the ergot gene clusters of *Aspergillus fumigatus* and *Neotyphodium lolii* were shown to catalyze the formation of the D ring of the ergoline skeleton. These enzymes catalyzed either reductase or isomerase type reactions to yield distinct pathway intermediates. Mutational analysis was used to engineer an Old Yellow Enzyme that displayed both reductase and isomerase activities, thereby elucidating the mechanistic basis behind this switch in enzymatic activity. These findings present a mechanistic rationale behind nature's biosynthetic strategy toward ring cyclization and the introduction of structural diversity into the ergot alkaloid class of natural products.

Thesis Supervisor: Sarah E. O'Connor
Title: Associate Professor of Chemistry

ACKNOWLEDGMENTS

I am deeply grateful for numerous individuals in my life who I would like to give thanks:

First and foremost my advisor Professor Sarah O'Connor for giving me the opportunity and honor to join her lab and study such a fascinating topic in natural products biosynthesis. Your leadership, insight, knowledge, and dedication to students have always been an inspiration to me. I am forever grateful for your kind support and encouragement that have guided me through these years.

Professor Dan Panaccione and his students Christine Coyle and Kerry Goetz, for their contributions and insightful discussions that have allowed us to share such a productive research collaboration.

My thesis committee Professor Barbara Imperiali and Professor Catherine Drennan for their advice and guidance in my studies.

All the O'Connor lab members who I've had the pleasure of working and getting to know over the years as fellow scientists and good friends. A special thanks to postdoctoral researchers Xudong Qu and Hyang-Yeol Lee for being my mentors in lab, their expertise in molecular biology and organic chemistry were invaluable. My colleague Weslee Glenn for our discussions and management of lab duties. I am truly fortunate to learn from such a great group.

MIT Chemistry Department and the MIT-Dupont Presidential Fellowship for their financial support. Other sponsors of my education, you are my inspiration to give back to the community.

Additionally, my MIT professors, staff, and friends who have contributed to my growth and learning during my graduate studies. Professors at the University of Hawaii, undergraduate advisor Professor Qing Li and Professor Michael Cooney. I thank all the teachers and friends in my lifetime for your involvements that have inspired my passion for science.

Most importantly, none of this would have been possible without the support of my family, my mother Jean and father Joe who have always given my brother and I the utmost priority in their lives. My brother Julian who I can always share a good laugh with. My Uncles Gabe, Francis, and Perry who have always been supportive and positive influences in my life. Grandma Iva who encouraged me to go to the east coast for graduate school. My Grandpa, Grandma, and other family for your daily blessings and watching over us from above.

TABLE OF CONTENTS

ABSTRACT	3
ACKNOWLEDGMENTS	4
TABLE OF CONTENTS.....	5
LIST OF TABLES	8
LIST OF ABBREVIATIONS.....	9
CHAPTER 1 . BACKGROUND AND SIGNIFICANCE	10
HISTORICAL SIGNIFICANCE OF ERGOT ALKALOIDS.....	11
ERGOT ALKALOID CLASSES.....	12
ERGOT ALKALOID PRODUCERS	15
ERGOT ALKALOID BIOSYNTHESIS	18
FUNCTIONAL CHARACTERIZATION OF LATE ERGOT ALKALOID BIOSYNTHETIC ENZYMES.....	27
RESEARCH GOAL AND THESIS OVERVIEW.....	30
CHAPTER 2 . ASSIGNING FUNCTION TO GENES INVOLVED IN EARLY STEP ERGOT ALKALOID BIOSYNTHESIS	36
INTRODUCTION	37
EXPERIMENTAL METHODS.....	40
RESULTS AND DISCUSSION	43
CONCLUSION.....	64
REFERENCES.....	66
CHAPTER 3 . ROLE OF REDOX ENZYMES INVOLVED WITH THE FORMATION OF ERGOLINE RING D.....	69
INTRODUCTION	70
EXPERIMENTAL METHODS.....	80
RESULTS AND DISCUSSION	107
CONCLUSION.....	126
REFERENCES.....	128
CHAPTER 4 . CONTROLLING PATHWAY DIVERGENCE IN ERGOT ALKALOID BIOSYNTHESIS	131
INTRODUCTION	132
EXPERIMENTAL METHODS.....	139
RESULTS AND DISCUSSION	145
CONCLUSION.....	165
REFERENCES.....	167
CHAPTER 5 . ROLE OF REDOX ENZYMES INVOLVED WITH THE FORMATION OF ERGOLINE RING C.....	169
INTRODUCTION	170
EXPERIMENTAL METHODS.....	173
RESULTS AND DISCUSSION	178
CONCLUSIONS.....	205
REFERENCES.....	206
CHAPTER 6 . CONCLUSIONS AND FUTURE DIRECTIONS.....	210
CONCLUSIONS.....	211
FUTURE DIRECTIONS.....	215
REFERENCES.....	228
CURRICULUM VITAE - JOHNATHAN ZANDREW CHENG	232

TABLE OF FIGURES

FIGURE 1.1. ERGOT ALKALOID NATURAL PRODUCTS AND SEMI-SYNTHETIC DERIVATIVES.....	13
FIGURE 1.2. 6,8-DIMETHYLERGOLINE TETRACYCLIC RING STRUCTURE.....	14
FIGURE 1.3. EARLY AND LATE PATHWAY STEPS OF ERGOT ALKALOID BIOSYNTHESIS	17
FIGURE 1.4. PROPOSED INTERMEDIATES OF ERGOT ALKALOID BIOSYNTHESIS.....	19
FIGURE 1.5. PROPOSED ERGOT ALKALOID BIOSYNTHETIC GENE CLUSTERS	24
FIGURE 1.6. LATE STEP ERGOT BIOSYNTHETIC PATHWAY	29
FIGURE 2.1. EARLY ERGOT PATHWAY ENZYMES AND THE CYCLIZATION OF ERGOLINE RING C AND D.....	39
FIGURE 2.2. LC-MS TRACE OF <i>A. FUMIGATUS</i> WILD TYPE CULTURE EXTRACT	44
FIGURE 2.3. LC-MS TRACE OF <i>A. FUMIGATUS</i> Δ <i>DMAW</i> CULTURE EXTRACT.....	45
FIGURE 2.4. LC-MS TRACE OF <i>A. FUMIGATUS</i> Δ <i>EASF</i> CULTURE EXTRACT.....	47
FIGURE 2.5. FLUORESCENCE HPLC ERGOT ALKALOID PROFILES Δ <i>EASE</i> AND Δ <i>EASC</i>	50
FIGURE 2.6. LC-MS TRACE OF <i>A. FUMIGATUS</i> Δ <i>EASE</i> CULTURE EXTRACT	51
FIGURE 2.7. LC-MS TRACE OF <i>A. FUMIGATUS</i> Δ <i>EASC</i> CULTURE EXTRACT.....	52
FIGURE 2.8. FLUORESCENCE HPLC ERGOT ALKALOID PROFILES Δ <i>EASA</i>	58
FIGURE 2.9. LC-MS TRACE OF <i>A. FUMIGATUS</i> Δ <i>EASA</i> CULTURE EXTRACT	59
FIGURE 2.10. LC-MS TRACE OF <i>A. FUMIGATUS</i> Δ <i>EASA</i> + <i>C. PURPUREA</i> <i>EASA</i>	62
FIGURE 3.1. PROTEIN SEQUENCE ALIGNMENTS OF <i>EASA_AF</i> AND <i>OYE</i> HOMOLOGUES.	71
FIGURE 3.2. REPRESENTATIVE SUBSTRATES OF VARIOUS <i>OYE</i> HOMOLOGUES.....	73
FIGURE 3.3. CATALYTIC CYCLE FOR <i>OYE</i> WITH NADPH AND 2-CYCLOHEXENONE SUBSTRATE	74
FIGURE 3.4. CATALYTIC ACTIVE SITE RESIDUES OF <i>OYE1</i>	76
FIGURE 3.5. PROPOSED ACTIVE SITE MECHANISM OF <i>EASA_AF</i>	77
FIGURE 3.6. HOMOLOGY MODEL OF <i>EASA_AF</i> WITH CHANOCLOAVINE-I-ALDEHYDE	78
FIGURE 3.7. SDS-PAGE OF <i>EASA</i> (<i>A. FUMIGATUS</i>).....	83
FIGURE 3.8. CHARACTERISTIC <i>EASA_AF</i> FLAVIN ABSORBANCE SPECTRUM	85
FIGURE 3.9. RELEASED FLAVIN FROM <i>EASA_AF</i> IDENTIFIED AS FMN BY HPLC.....	86
FIGURE 3.10. ISOLATION AND PURIFICATION OF CHANOCLOAVINE-I-ALDEHYDE	88
FIGURE 3.11. LC-MS TRACE OF <i>A. FUMIGATUS</i> EXTRACT AND PURIFIED CHANOCLOAVINE-I-ALDEHYDE.	89
FIGURE 3.12. LC-MS TRACE OF PURIFIED CHANOCLOAVINE-I-ALDEHYDE.	90
FIGURE 3.13. ¹ H-NMR CHANOCLOAVINE-I-ALDEHYDE.....	92
FIGURE 3.14. LC-MS TRACE OF AGROCLAVINE STANDARD.....	94
FIGURE 3.15. LC-MS TRACE OF FESTUCLAVINE STANDARD.....	95
FIGURE 3.16. ¹ H-NMR AGROCLAVINE	97
FIGURE 3.17. ¹ H-NMR FESTUCLAVINE.....	98
FIGURE 3.18. CHANOCLOAVINE-I-ALDEHYDE STANDARD CURVE BY LC-MS	101
FIGURE 3.19. STABILITY OF CHANOCLOAVINE-I-ALDEHYDE UNDER ASSAY BY LC-MS	102
FIGURE 3.20. SDS-PAGE OF <i>EASG</i> (<i>A. FUMIGATUS</i>).....	105
FIGURE 3.21. LC-MS TRACES OF <i>EASA_AF</i> ASSAY.....	110
FIGURE 3.22. LC-MS TRACES OF <i>EASA_AF</i> ASSAY WITH CONTROLS	112
FIGURE 3.23. LC-MS TRACES OF <i>EASA_AF</i> CYCLIC IMINIUM PRODUCT.....	115
FIGURE 3.24. RACEMIZATION OF THE DIHYDROCHANOCLOAVINE ALDEHYDE.....	116
FIGURE 3.25. LC-MS TRACES OF NACNBH ₃ REDUCED CYCLIC IMINIUM INTERMEDIATE.....	118
FIGURE 3.26. ¹ H-NMR <i>EASA_AF</i> ENZYME PRODUCT REDUCED WITH NACNBH ₃	119
FIGURE 3.27. COMPARISON OF ¹ H-NMR SPECTRA OF COMPOUNDS USED IN THIS STUDY	120
FIGURE 3.28. COMPARISON OF ¹ H-NMR AROMATIC REGION	121
FIGURE 3.29. PROPOSED FUNCTIONAL ROLES OF <i>EASA_AF</i> AND <i>EASG</i>	125
FIGURE 4.1. ERGOT ALKALOID BIOSYNTHESIS IN DIVERGENT FUNGAL SPECIES.....	134
FIGURE 4.2. EARLY ISOTOPE FEEDING STUDIES	135
FIGURE 4.3. ALIGNMENTS OF <i>EASA</i> SEQUENCES FROM SEVERAL ERGOT ALKALOID PRODUCING FUNGI.....	136
FIGURE 4.4. SDS-PAGE OF <i>EASA</i> (<i>N. LOLII</i>)	142
FIGURE 4.5. CHARACTERISTIC <i>EASA_NL</i> FLAVIN ABSORBANCE SPECTRUM.....	143
FIGURE 4.6. LC-MS TRACES OF <i>EASA_AF</i> + <i>EASG</i> WITH CONTROLS.....	148
FIGURE 4.7. LC-MS TRACES OF ACTIVE <i>EASA_NL</i> + <i>EASG</i> WITH CONTROLS	149
FIGURE 4.8. LC-MS TRACES OF <i>EASA_AF</i> , <i>EASA_NL</i> , OR <i>EASA_NL_F176Y</i> WITH INACTIVE <i>EASG</i>	150

FIGURE 4.9. LC-MS TRACES OF EASA_AF, EASA_NL, AND EASA_NL_F176Y WITH INACTIVE EASG SYNTHETICALLY REDUCED WITH NACNBH ₃ OR NACNBD ₃ .	151
FIGURE 4.10. ALIGNMENT OF EASG SEQUENCES.	152
FIGURE 4.11. LC-MS TRACES OF OF EASA_AF, EASA_NL, AND EASA_NL_F167Y WITH EASG.	153
FIGURE 4.12. LC-MS TRACES OF EASA_AF, EASA_NL, AND EASA_NL_F176Y WITH EASG SYNTHETICALLY REDUCED WITH NACNBH ₃ OR NACNBD ₃	155
FIGURE 4.13. CHANOCCLAVINE-I-ALDEHYDE AND THE ISOMERIZATION OF THE C8-C9 ALKENE.	159
FIGURE 4.14. LC-MS TRACES OF EASA_NL_F176Y + EASG WITH CONTROLS	163
FIGURE 4.15. LC-MS TRACES OF EASA_AF_Y178F + EASG	164
FIGURE 5.1. PROPOSED EASE AND EASC MECHANISM FOR THE CYCLIZATION OF ERGOLINE RING C	172
FIGURE 5.2. SDS-PAGE GEL OF DMAW (<i>C. PURPUREA</i>).	180
FIGURE 5.3. HPLC TRACES OF DMAW ASSAYS.	181
FIGURE 5.4. LC-MS TRACES OF DMAW ASSAYS.	182
FIGURE 5.5. SDS-PAGE GEL OF EASC (<i>A. FUMIGATUS</i>).	184
FIGURE 5.6. EASC CATALASE ACTIVITY FOR H ₂ O ₂ .	185
FIGURE 5.7. UV-VIS SPECTRUM EASC.	186
FIGURE 5.8. SDS-PAGE OF EASE (<i>A. FUMIGATUS</i>)	189
FIGURE 5.9. UV-VIS SPECTRA OF EASE_AF	190
FIGURE 5.10. PROPOSED MECHANISMS FOR FAD DEPENDENT OXIDATIONS	195
FIGURE 5.11. ALIGNMENT OF EASE (<i>A. FUMIGATUS</i>) AND BBE (<i>E. CALIFORNICA</i>).	196
FIGURE 5.12. ALIGNMENT OF EASE (<i>A. FUMIGATUS</i>) AND MREA (<i>A. ORYZAE</i>)	197
FIGURE 5.13. ALIGNMENT OF EASC (<i>A. FUMIGATUS</i>) AND CATALASEA (<i>S. CEREVISIAE</i>)	198
FIGURE 5.14. PROPOSED MECHANISM FOR EASC	199
FIGURE 5.15. PROPOSED MECHANISM FOR EASE.	202
FIGURE 6.1. PROPOSED INCORPORATION OF DEUTERIUM LABEL VIA NADPD INTO EROLINE RING D TO EXPLORE STEREOSELECTIVITY OF THE PROPOSED EASA_AF REDUCTASE AND EASG.	219
FIGURE 6.2. PROPOSED INCORPORATION OF DEUTERIUM LABEL VIA NADPD INTO EROLINE RING D TO EXPLORE THE STEREOSELECTIVITY OF THE PROPOSED EASA_NL ISOMERASE AND EASG.	220

LIST OF TABLES

TABLE 2.1. <i>A. FUMIGATUS</i> GENE DISRUPTED MUTANTS AND THE ACCUMULATION OF PATHWAY INTERMEDIATES DETECTED BY LC-MS.	43
TABLE 2.2. CONVERSION OF EXOGENOUS CHANOC LAVINE-I INTO DOWNSTREAM ERGOT ALKALOIDS BY CULTURES OF <i>A. FUMIGATUS</i>	55
TABLE 3.1. EXACT MASS OF COMPOUNDS DETERMINED BY HIGH RESOLUTION MS.....	111
TABLE 4.1. EXACT MASS OF COMPOUNDS DETERMINED BY HIGH RESOLUTION MS.....	154

LIST OF ABBREVIATIONS

This thesis uses standard abbreviations for nucleic acids (one-letter code) and amino acids (one and three-letter codes).

°C	degrees centigrade
DMAPP	dimethylallyl pyrophosphate
DMAT	4-dimethylallyl-L-tryptophan
DmaW	4-dimethylallyl tryptophan synthase
cDNA	complementary deoxyribonucleic acid
DNA	deoxyribonucleic acid
DTT	dithiothreitol
EasA	Old Yellow Enzyme homologue
EasA_Af	<i>Aspergillus fumigatus</i> Old Yellow Enzyme homologue
EasA_Nl	<i>Neotyphodium lolii</i> Old Yellow Enzyme homologue
EasC	<i>Aspergillus fumigatus</i> catalase
EasD	<i>Aspergillus fumigatus</i> NAD ⁺ dependent dehydrogenase
EasE	<i>Aspergillus fumigatus</i> FAD monooxygenase/dehydrogenase
EasF	S-Adenosylmethionine dependent methyltransferase
EasG	NADPH dependent reductase
ESR	electron spin resonance
FAD	flavin adenine dinucleotide
FMN	flavin mononucleotide
HPLC	high performance liquid chromatography
IPTG	isopropyl-β-thiogalactopyranoside
k _{cat}	turnover number
kDa	kilodalton
K _m	Michaelis constant
LC-MS	liquid chromatography mass spectrometry
NADP ⁺	nicotinamide adenine dinucleotide phosphate (oxidized)
NADPH	nicotinamide adenine dinucleotide phosphate (reduced)
Ni-NTA	nickel nitrilotriacetic acid
N-Me-DMAT	4-dimethylallyl-L-abrine
N-Me-L-Trp	N _α -methyl-L-tryptophan, L-abrine
NMR	nuclear magnetic resonance
OYE	Old Yellow Enzyme
RNA	ribonucleic acid
PCR	polymerase chain reaction
SDS	sodium dodecyl sulfate
SDS-PAGE	sodium dodecyl sulfate polyacrylamide gel electrophoresis
UV-Vis	Ultraviolet-Visible

Chapter 1 . Background and Significance

Historical Significance of Ergot Alkaloids

Ergot alkaloids are formed in sclerotia, a dark dense mass of fungal mycelium, produced upon the infection of grass and grains by parasitic fungi of the genus *Claviceps*. These compounds are also produced in a variety of other fungi, including the genera *Aspergillus* and *Neotyphodium*.¹ Ergot alkaloids have long been a part of human history. Ergot has been documented for use in obstetrics as early as 1100 BC in China. Both ergot grain disease and their bioactive properties have also been noted throughout Egyptian, Assyrian, and Greek history.² Ergot alkaloids rose to notoriety during the Middle Ages in Central Europe being the cause of mass poisonings in both humans and animals which fed on grass or grains that were contaminated by ergot producing fungi.³ Symptoms included gangrene, convulsions, and hallucination, that were collectively known as “St. Anthony’s Fire” or “Ergotism”. Ergot alkaloids were also associated with historical events of mass hysteria during the Great Fear of the French Revolution as well as the Salem Witch Trials.^{1,2}

It was not until the latter part of the 17th century, when ergotism was finally correlated to the consumption of infected rye containing ergot alkaloids, increased human awareness and knowledge reduced these mass poisonings. The use of ergot compounds in modern western medicine for post partum hemorrhage occurred in the early 19th century. Further research and screening of ergot derivatives for oxytocic activity in 1938 resulted in the synthesis of lysergic acid diethylamide (LSD) hallucinogen that has since become infamous for its use as an illicit recreational drug.²

The notorious history and abuse of ergot compounds have often overshadowed its beneficial medicinal properties. In present times, ergot alkaloids are the inspiration for

numerous semi-synthetic derivatives that have been applied for a wide range of medicinal purposes including the treatment of migraines, parkinsonism, and tumor growth. The diverse bioactivity exhibited by ergot alkaloids is related to its ability to act as an agonist or antagonist toward neuroreceptors for dopamine, serotonin, and adrenaline.^{4, 5} Semi-synthetic derivatives of ergot alkaloids aim to tailor their activity toward specific receptors while reducing their adverse side effects (Figure 1.1). A number of previous studies have yielded insight into the structure activity relationships of the ergot alkaloids.⁵⁻¹¹ Ergot alkaloids remain a valuable resource to be fully explored for novel pharmaceutical analogs.

Ergot Alkaloid Classes

All naturally produced ergot alkaloid structures are composed of the tetracyclic ergoline ring (Figure 1.2A). Ergot alkaloids may be divided into classes based on the substituents that are attached on the ergoline scaffold; these include the clavines, simple lysergic acid derivatives, and ergopeptides.^{1, 7} The clavines include such structures which are all hydroxy and dehydro versions of the 6,8-dimethylergoline structure (Figure 1.2B). Simple lysergic acid derivatives consist of an attached alkyl amide or small peptide (Figure 1.2C). Ergopeptides consists of a D-lysergic acid and a cyclic tripeptide moiety (Figure 1.2D).

Figure 1.1. Ergot alkaloid natural products and semi-synthetic derivatives displaying diverse bioactivity by interactions with different neurotransmitter receptors. The tetracyclic ergoline ring common to all ergot alkaloids is shown in red.

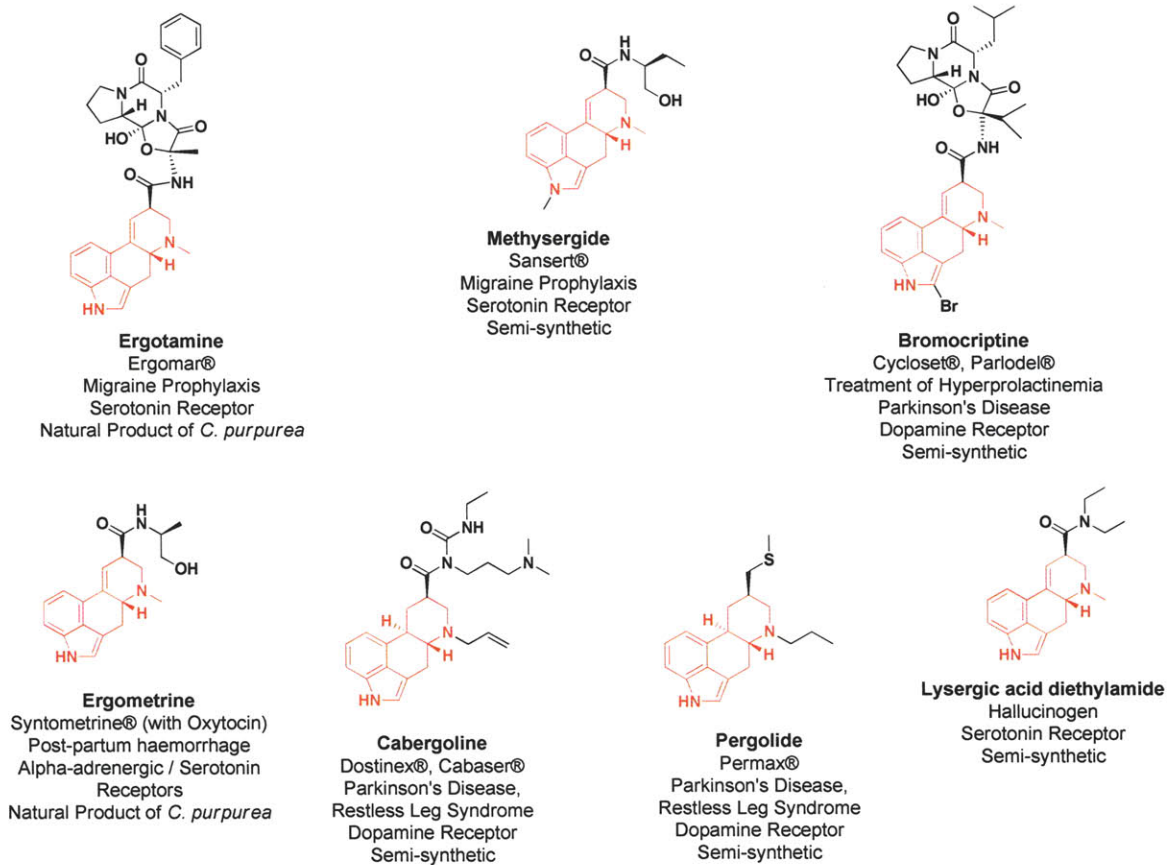
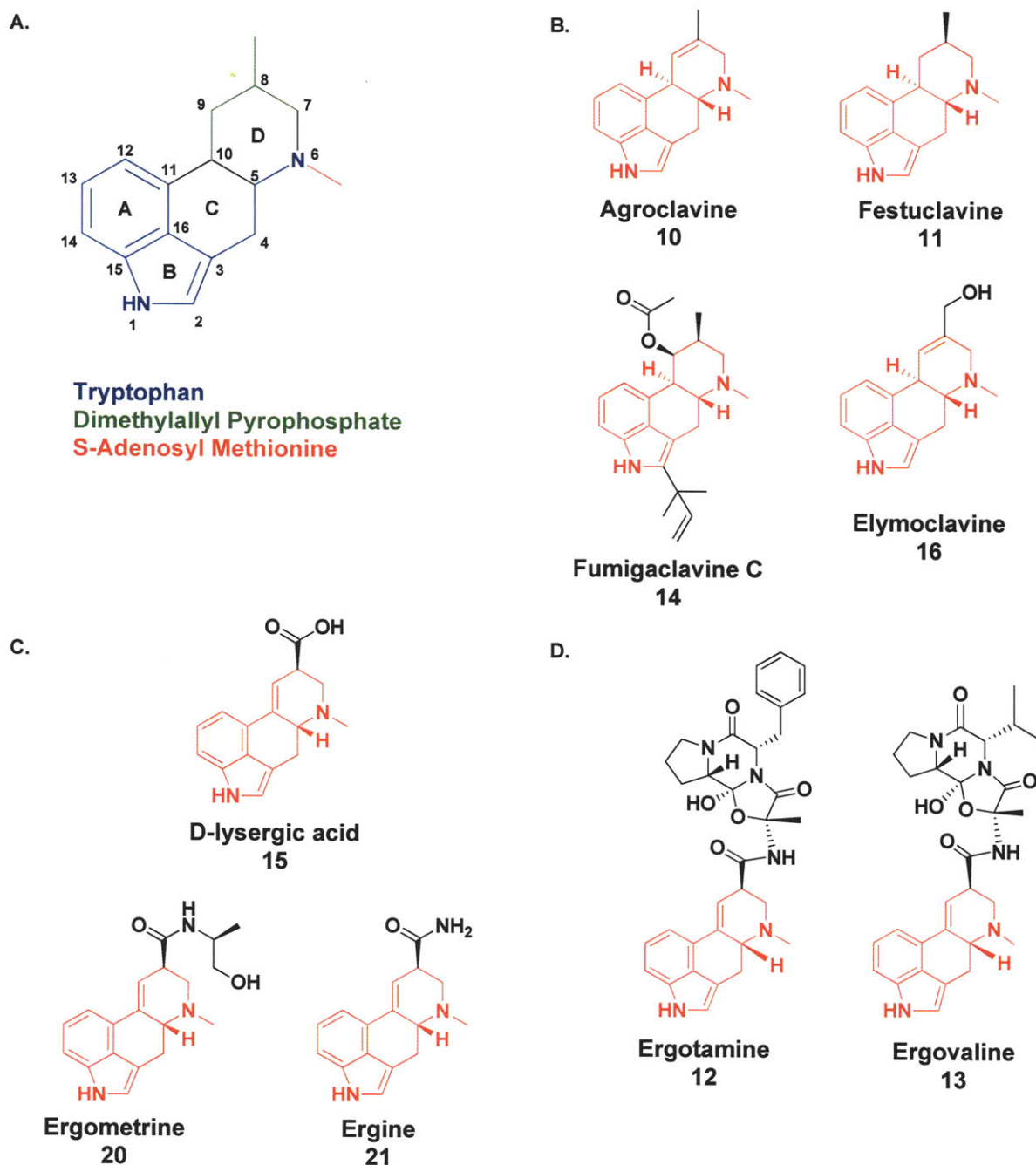


Figure 1.2. A. 6,8-dimethylergoline tetracyclic ring structure. Conventional ergoline ring numbering and lettering are designated for each ring. B. Clavines include hydroxy and dehydro versions of the 6,8-dimethylergoline structure. C. Simple lysergic acid derivatives consist of the basic D-lysergic acid structure with attachment of an amide in the form of an alkyl amide or small peptide. D. Ergopeptides consists of a D-lysergic acid with a cyclic tripeptide moiety.



Ergot Alkaloid Producers

Ergot alkaloid producing fungi occupy distinct ecological niches, Clavicipitaceous species such as *Claviceps purpurea* and *Neotyphodium lolii* from the order Eurotiales are plant parasites, while *Aspergillus fumigatus* from the order Hypocreales is an opportunistic pathogen of mammals.^{1, 12-14} These distantly related fungal lineages produce unique ergot alkaloid profiles.

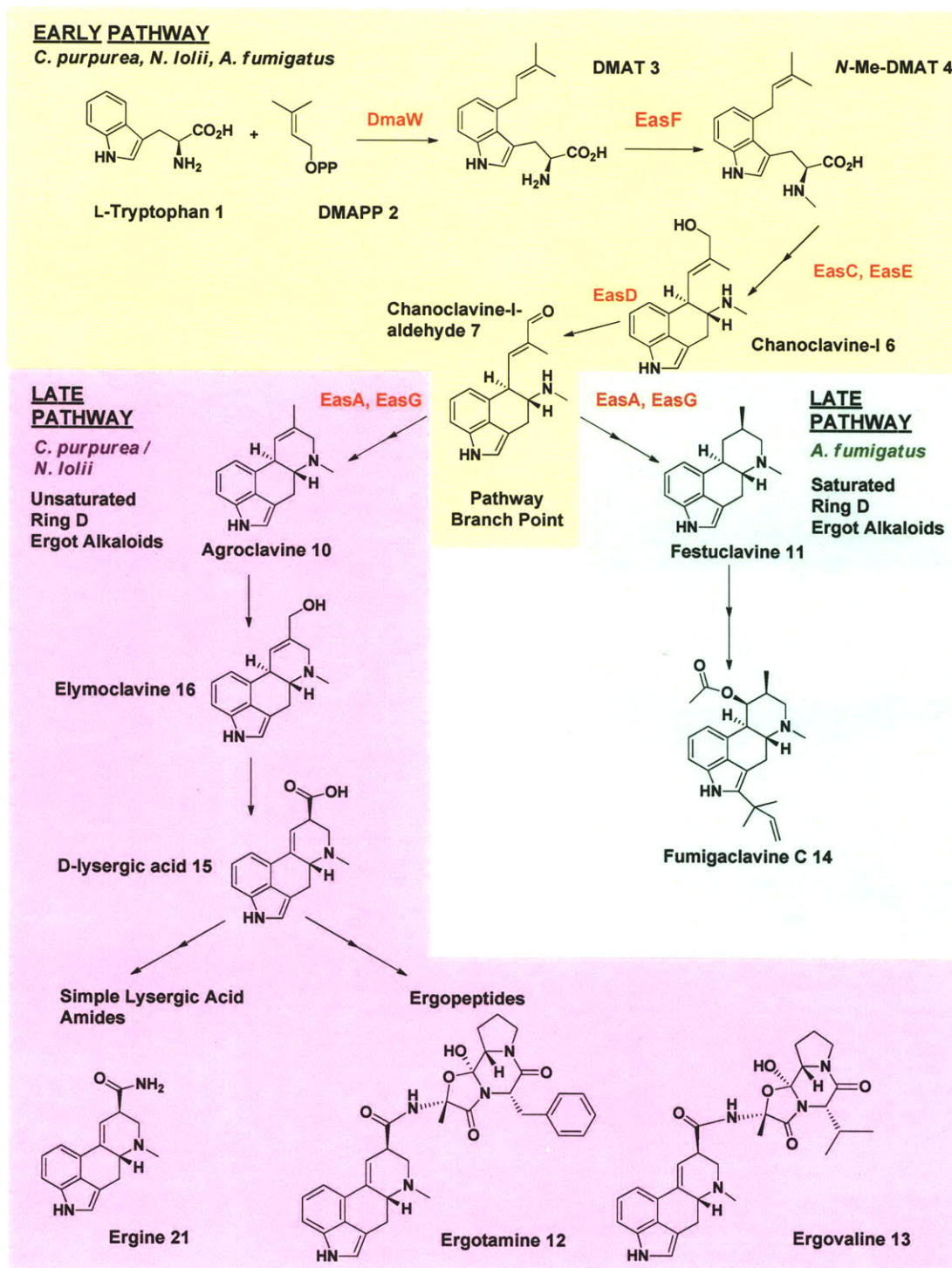
Ergot alkaloids that are derivatives of lysergic acid and ergopeptides (Figure 1.2 C, D) are associated with Clavicipitaceous fungi *Claviceps purpurea* and *Neotyphodium lolii*, and are believed to aid in protecting the fungi from predation by mammals. By contrast, fumigaclavine ergot alkaloids are only produced by *A. fumigatus* during conidiation, though their biological role to aid in survival of conidia during invasive aspergillosis is not completely understood.^{1, 15}

A unique quality to fungal genes coding for the biosynthesis of secondary metabolites is their clustering on a single genetic locus. In contrast, genes for primary metabolism are not localized in clusters.¹² For fungi the clustering of genes for secondary metabolite production are believed to improve efficiency of gene regulation and thereby confer selective advantage. Other hypotheses postulate that this clustering may be a result of horizontal gene transfer from prokaryotes.^{12, 16}

The ergot alkaloid biosynthetic genes are clustered in *A. fumigatus*^{14, 17} as well as Clavicipitaceous fungi *C. purpurea*^{18, 19} and *N. lolii*.^{20, 21} Shared gene homologues between *A. fumigatus*, *C. purpurea*, and *N. lolii* are believed to participate in early steps of ergot biosynthesis, while species-unique genes are responsible for downstream modifications to yield either fumigaclavines in *A. fumigatus* or ergopeptides / lysergic

acid derivatives in Clavicipitaceous fungi (Figure 1.3).^{1, 14, 22-24} Therefore, it is believed that the distantly related *A. fumigatus* and Clavicipitaceous fungi share a common origin for their ability to produce ergot alkaloids (Figure 1.3). A notable difference between these ergot alkaloid classes is the fully saturated D ring of the ergoline (Figure 1.2A) structure found in the clavine type alkaloids from *A. fumigatus*. In contrast, ergot alkaloids of Clavicipitaceous fungi *C. purpurea* and *N. lolii*, have an unsaturated ergoline D ring.²⁵ More information regarding the early and late step genes of ergot alkaloid biosynthetic clusters are presented in the following sections.

Figure 1.3. Early biosynthetic pathway steps are proposed to be conserved across divergent fungi. Later biosynthetic pathway steps create diverse ergot alkaloid profiles in different fungal species. Clavicipitaceous fungi *C. purpurea* and *N. lolii* are associated with production of ergot alkaloids with an unsaturated ergoline D ring. *A. fumigatus* is associated with the production of ergot alkaloids with a saturated ergoline D ring.

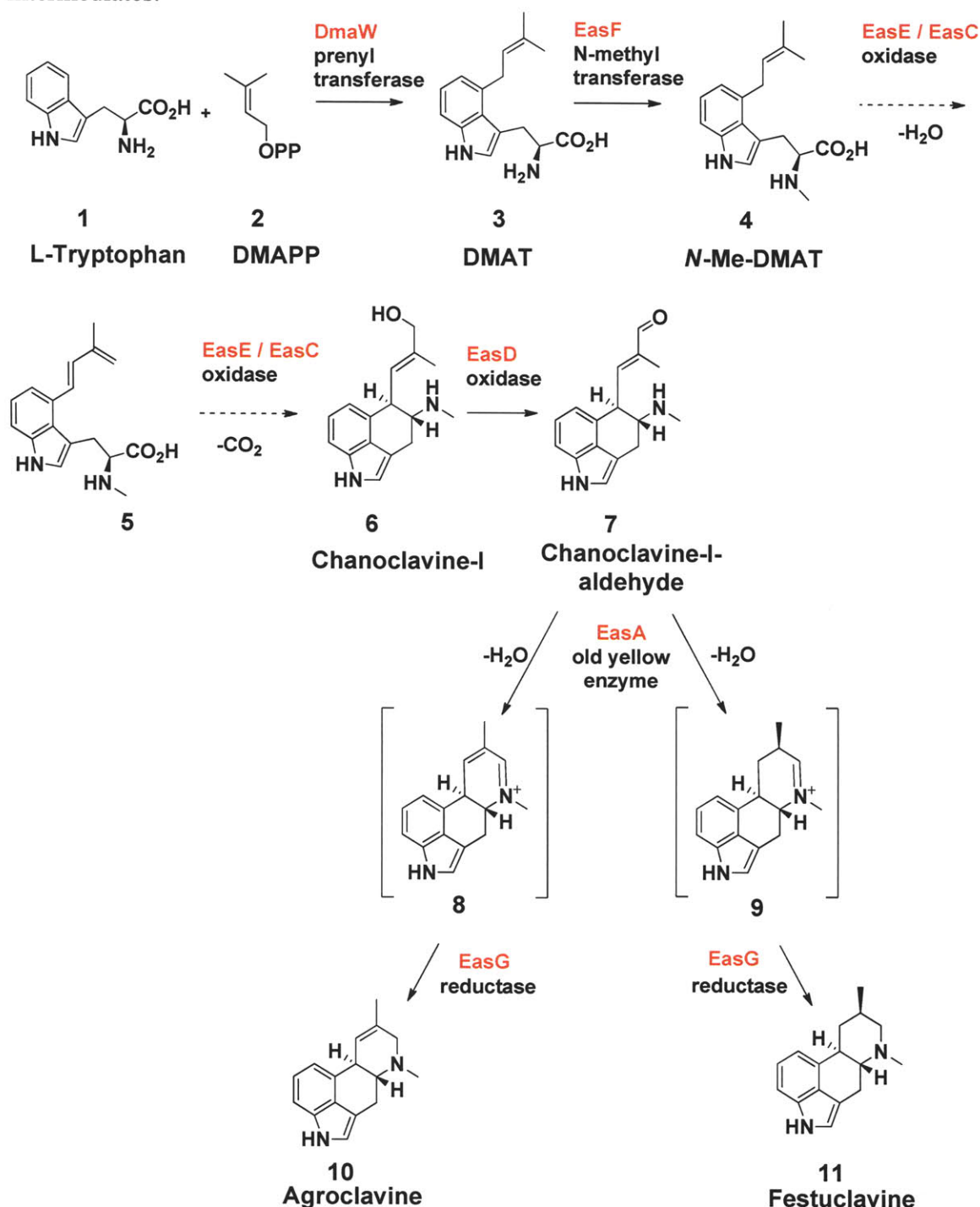


Ergot Alkaloid Biosynthesis

Proposed Ergot Alkaloid Biosynthetic Pathway

Much of the early pathway of ergot alkaloid biosynthesis had been investigated through extensive isotope feeding studies with cultures of *C. purpurea*.²⁶⁻³⁸ These studies were instrumental in proposing a biosynthetic pathway for ergot compounds (Figure 1.4). The first committed step in ergot alkaloid biosynthesis is the prenylation of L-tryptophan **1** with dimethylallyl pyrophosphate (DMAPP) **2**, to yield 4-dimethylallyl-L-tryptophan (DMAT) **3**. The next step involves the N-methylation of DMAT **3** to yield 4-dimethyl-L-abrine (*N*-Me-DMAT) **4**.³⁸ Subsequently, a proposed series of successive oxidation steps catalyze the intramolecular cyclization of the prenyl and indole moieties to form ring C in tricyclic chanoclavine-I **6**. Chanoclavine-I **6** in turn is oxidized to form chanoclavine-I-aldehyde **7**, which is the last common precursor of ergot alkaloid producing fungi prior to pathway divergence. At this branch point of ergot alkaloid pathways, chanoclavine-I-aldehyde **7** undergoes another intramolecular cyclization resulting in the formation of ring D of tetracyclic agroclavine **10** (*C. purpurea*, *N.lolii*) or festuclavine **11** (*A. fumigatus*).^{1, 5, 25} Thereafter, the pathway diverges where agroclavine **10** and festuclavine **11** are further derived into respective lysergic acid amides/peptides and fumigaclavines (Figure 1.3).³⁹⁻⁴³ Many of the enzymes associated with each of these pathway steps were found to be encoded by ergot alkaloid biosynthetic gene clusters in divergent fungal species.

Figure 1.4. Proposed early steps of ergot alkaloid biosynthesis up to chanoclavine-I-aldehyde **7**. Later pathway steps diverge to give either agroclavine **10** or festuclavine **11** derived ergot alkaloids in different fungal species. Solid arrows represent biosynthetic steps that have been studied *in vitro* and are associated with the corresponding enzyme homologs (red) encoded by the ergot gene clusters. Dashed arrows represent proposed steps that are not well understood but associated with the remaining ergot cluster genes encoding oxidases EasC and EasE. Brackets represent hypothetical cyclized iminium **8**, **9** intermediates.



Ergot Alkaloid Biosynthetic Gene Clusters

The ergot biosynthetic gene clusters of *A. fumigatus*, *C. purpurea*, and *N. lolii* share a set of homologues that are associated to early pathway ergot alkaloid biosynthesis (Figure 1.5). These conserved set of homologous genes across divergent fungal species are attributed to the early steps of ergoline biosynthesis from the prenylation of L-tryptophan **1** up to the cyclization of ring D (Figure 1.4).¹⁴

The first determinant step for entry into the ergot biosynthetic pathway is catalyzed by the 4-dimethylallyl prenyltransferase (DmaW) enzyme purified to homogeneity from cultures of ergot alkaloid producing *C. fusiformis* (formerly annotated as *Claviceps purpurea*).³¹ It was shown to prenylate L-tryptophan **1** via an electrophilic aromatic substitution mechanism.³² Using a reverse genetics approach, the group of Tsai et al. successfully identified and cloned the gene coding for L-tryptophan dimethylallyl prenyl transferase (DmaW) from *C. fusiformis*. Eventually this allowed the identification of other ergot alkaloid biosynthetic genes from *C. purpurea* via chromosome walking.^{18,}

19

The *C. purpurea* gene cluster for ergotamine **12** biosynthesis (68.5kb) was identified by the Tudzynski group (Figure 1.5B).^{18, 19} Gene open reading frames were assigned putative functions based on sequence similarity to previously characterized enzymes.¹⁸ Importantly, this gene cluster included a homologue of *dmaW* prenyltransferase and open reading frames encoding the non-ribosomal peptide synthetase (NRPS) module and lysergylpeptidyl synthetase 1 and 2 (*Lps1* and *Lps2*) genes that are involved with the later biosynthetic pathway formation of ergopeptides (Figure 1.6).^{39, 42, 44} Additionally it was observed that comparison of cluster sequences

within *C. purpurea* strain P1 (ergotamine producer) with strain *C. purpurea* ECC93 (ergocristine producer) displayed conservation of most genes associated with the early pathway formation of the ergoline ring, yet displayed high variation in genes associated with the NRPS production of the peptide ergot moiety.¹⁸ These observations supported the hypothesis that clustered early pathway genes are responsible for similar steps of biosynthesis of the ergoline ring, while variations in genes encoding the later step NRPS modules confer intraspecies diversification of peptide ergot alkaloids.

Clustered genes for ergot biosynthesis in a different fungal species *Neotyphodium* sp. Lp1 (a natural hybrid *Neotyphodium lolii* x *Epichloe typhina*) were initially studied by Panaccione et al., where disruption of the *Lps1* homologue (*LpsA*) involved in ergopeptide biosynthesis resulted in the loss of downstream alkaloid ergovaline **13**.^{41, 45} In another gene knockout experiment with *Neotyphodium* sp. Lp1, Wang et al. demonstrated that disruption of a *dmaW* homologue led to loss of ergovaline **13** production.²⁰ Complementation of the gene with the *dmaW* homologue from *C. fusiformis* restored ergot alkaloid production.^{20, 45} Later, the Fleetwood group of identified part of the ergot alkaloid cluster for ergovaline **13** biosynthesis (~19kb) in *N. lolii* using both chromosome walking and southern blot (Figure 1.5D).²¹ Again it was noted that genes associated with the early steps of ergoline biosynthesis were conserved across other ergot producing fungal species, while later pathway genes were divergent. Notably, it was demonstrated that the *LpsB* gene in *N. lolii*, a homologue of the *C. purpurea* *Lps2* in ergotamine **12** synthesis, was associated with ergovaline **13** production.²¹ This observation again reinforced the hypothesis that the biosynthesis of the ergoline ring is encoded by a set of conserved genes, while later pathway genes are

divergent across different fungal species, creating the resulting diversity in ergot alkaloid profiles.

The *A. fumigatus* ergot biosynthetic gene cluster is associated to the production of fumigaclavines and festuclavine **11**¹⁴. The gene cluster that is responsible for the production of these ergot alkaloids had been previously identified via gene disruption of *dmaW* in *A. fumigatus* and heterologous expression and characterization of the dimethylallyltryptophan synthase *dmaW* gene (annotated as *fgaPT2*) in *Saccharomyces cerevisiae*.^{14, 17} The extension of this *dmaW* sequence information allowed identification of the biosynthetic cluster for fumigaclavine C **14** (22kb) of *A. fumigatus* (Figure 1.5A). Further analysis of gene function in this cluster led to the characterization of *easF* and *easD* gene products that are attributed to the early step ergot pathway.^{46, 47} This cluster again contained a set of genes, homologous with the other known Clavicipitaceous fungal species *C. purpurea* and *N. lolii*, that were likely to be associated with the early ergot alkaloid synthetic pathway. Notably, no homologues for the later pathway lysergyl peptide synthase genes were observed^{18, 21}, correlating with the fact that *A. fumigatus* does not produce lysergic acid derived ergopeptides. Instead the *A. fumigatus* gene cluster displayed unique genes that were later shown to be associated with the decoration of the fumigaclavine structure. Some of these downstream ergot pathway genes from *A. fumigatus* have been cloned, expressed, and functionally characterized in the transformation of festuclavine **11** into fumigaclavine C **14** (Figure 1.6).^{40, 43}

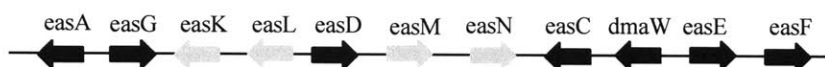
In summary, when comparing the ergot biosynthetic gene clusters of *A. fumigatus* to the Clavicipitaceous fungi *C. purpurea* and *N. lolii*, the shared set of homologous genes that are associated with early pathway ergot biosynthesis are conserved (Figure

1.5). This set of genes was attributed to the early steps of ergoline biosynthesis up to the cyclization of the D ring (Figure 1.3).¹⁴ In contrast, the genes that are unique to *A. fumigatus* are proposed to be responsible for further decoration of festuclavine **11** to give fumigaclavine C **14**, while genes that are unique to Clavicipitaceous fungi such as *C. purpurea* and *N. lolii* are involved with the transformation of agroclavine **10** to the respective ergopeptides ergotamine **12** and ergovaline **13** (Figure 1.3). Notably, the availability of this gene sequence information expedited the successful cloning and functional characterization of ergot biosynthetic enzymes from *A. fumigatus*, *C. purpurea* and *N. lolii*.^{17, 20, 48}

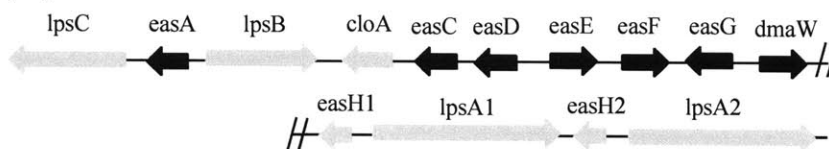
Figure 1.5. Proposed ergot alkaloid biosynthetic gene clusters.

A. *Aspergillus fumigatus*^{14, 17} B. *Claviceps purpurea*¹⁸ C. *Claviceps fusiformis*⁴⁹ D. *Neotyphodium lolii*²¹ location and orientation of proposed clustered genes *dmaW*, *cloA*, *easC*, *easD*, and *lpsA* with respect to the reported contig are unknown (dashed box). *DmaW* and *lpsA* have been identified and functionally assigned in closely related *Neotyphodium* sp. *Lp1*^{20, 41}.

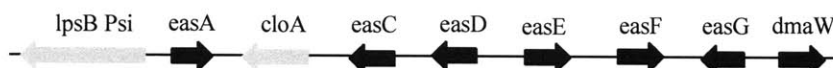
A. *Aspergillus fumigatus*



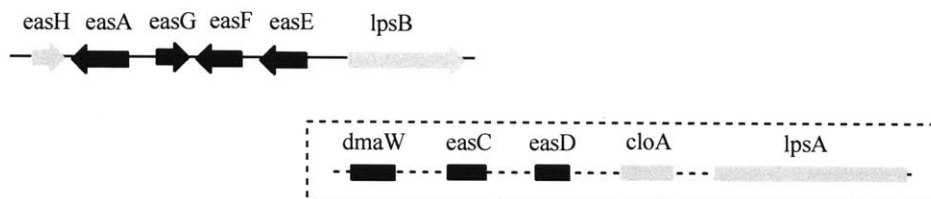
B. *Claviceps purpurea*



C. *Claviceps fusiformis*



D. *Neotyphodium lolii*



Common Genes to All Ergot Alkaloid Producers (Early Biosynthetic Pathway)

Species Unique Genes (Late Biosynthetic Pathway)

Functional Characterization of Early Ergot Alkaloid Biosynthetic Enzymes

A number of genes in the ergot alkaloid biosynthetic clusters have been previously studied yielding insight into the function of their associated gene products. The first determinant step for entry into the ergot biosynthetic pathway is catalyzed by the dimethylallyl prenyltransferase (DmaW), which has been purified to homogeneity from cultures of ergot alkaloid producing *C. fusiformis*.³¹ DmaW was shown to prenylate L-tryptophan **1** via electrophilic aromatic substitution.³² DmaW homologues from *A. fumigatus* and other Clavicipitaceous fungi such as *C. purpurea* and *N. lolii* have also been characterized.^{17, 20, 48}

The next early pathway enzyme EasF is responsible for the *N*-methylation of DMAT **3** and was first purified by Otsuka et al. from cell free cultures of *C. purpurea*.³⁸ EasF displayed activity for methylating the amine nitrogen of dimethylallyl tryptophan with the *S*-adenosyl methionine (SAM) co-factor. Later, with the identification of the ergot biosynthetic gene cluster in *A. fumigatus*, the *easF* gene was successfully cloned and heterologously expressed. EasF displayed the predicted *N*-methyltransferase activity, yielding *N*-Me-DMAT **4** (dimethylallyl L-abrine) from DMAT **3**.⁴⁷

Following the *N*-methyltransferase EasF, two successive oxidations are proposed to transform *N*-Me-DMAT **4** to chanoclavine-I **6** thus forming ergoline ring C. These two oxidation steps of the pathway are predicted based on feeding studies conducted by Floss et al.^{30, 33} Two notable observations from these studies were (1) observation that a proposed diene intermediate **5** was incorporated into downstream ergot alkaloids of *C. purpurea*³⁴ and (2) molecular oxygen was incorporated into chanoclavine-I **6**.³³ Enzyme candidates of the ergot clusters that were capable of carrying out oxidation reactions were

proposed to be EasC and EasE, which display protein sequence similarity to other catalases and FAD oxygenases, respectively. The involvement of the *easE* gene product in the oxidations of *N*-Me-DMAT **4** to chanoclavine-I **6** in *C. purpurea* has also been demonstrated by gene disruption experiments.⁵⁰ Details regarding the function of EasC and EasE and their putative role in carrying out the formation of ring C are not well understood and were one of the focuses of our research efforts (Chapter 5).

The next enzyme of the ergot pathway, EasD, is an NAD⁺ binding oxidase capable of oxidizing the hydroxyl group of chanoclavine-I **6** to yield chanoclavine-I-aldehyde **7**. EasD was successfully cloned and characterized from *A. fumigatus* by Wallwey et al.⁴⁶

The next enzymes of the pathway, EasA and EasG, are required for the cyclization of chanoclavine-I-aldehyde **7** to form ergoline ring D, representing the branching point of ergot alkaloid biosynthesis into either festuclavine **11** (*A. fumigatus*) or agroclavine **10** derived alkaloids (*C. purpurea* / *N. lolii*). Homologues of EasA in the ergot cluster show protein sequence similarity to enzymes of the Old Yellow Enzyme (OYE) family. OYE enzymes display activity toward the reduction of α , β -unsaturated ketones and aldehydes.^{51, 52} Therefore, EasA served as a likely candidate capable of reducing the α , β -unsaturated carbon-carbon double bond of chanoclavine-I-aldehyde **7** to yield the hypothetical cyclized iminium intermediates **8** and **9** toward ring D formation (Figure 1.4). The EasG protein encoded by the gene cluster displays similarity to Rossmann fold NADPH reductases^{53, 54}, and its likely function is to reduce the proposed cyclized iminium products **8** and **9** of EasA to form agroclavine **10** (*C. purpurea* / *N. lolii*) or festuclavine **11** (*A. fumigatus*) respectively. The details of EasA and EasG

function, mechanism, and role in cyclization of the D ring in diverse fungal species were not fully understood and served as the focus of our study (Chapters 3 and 4).

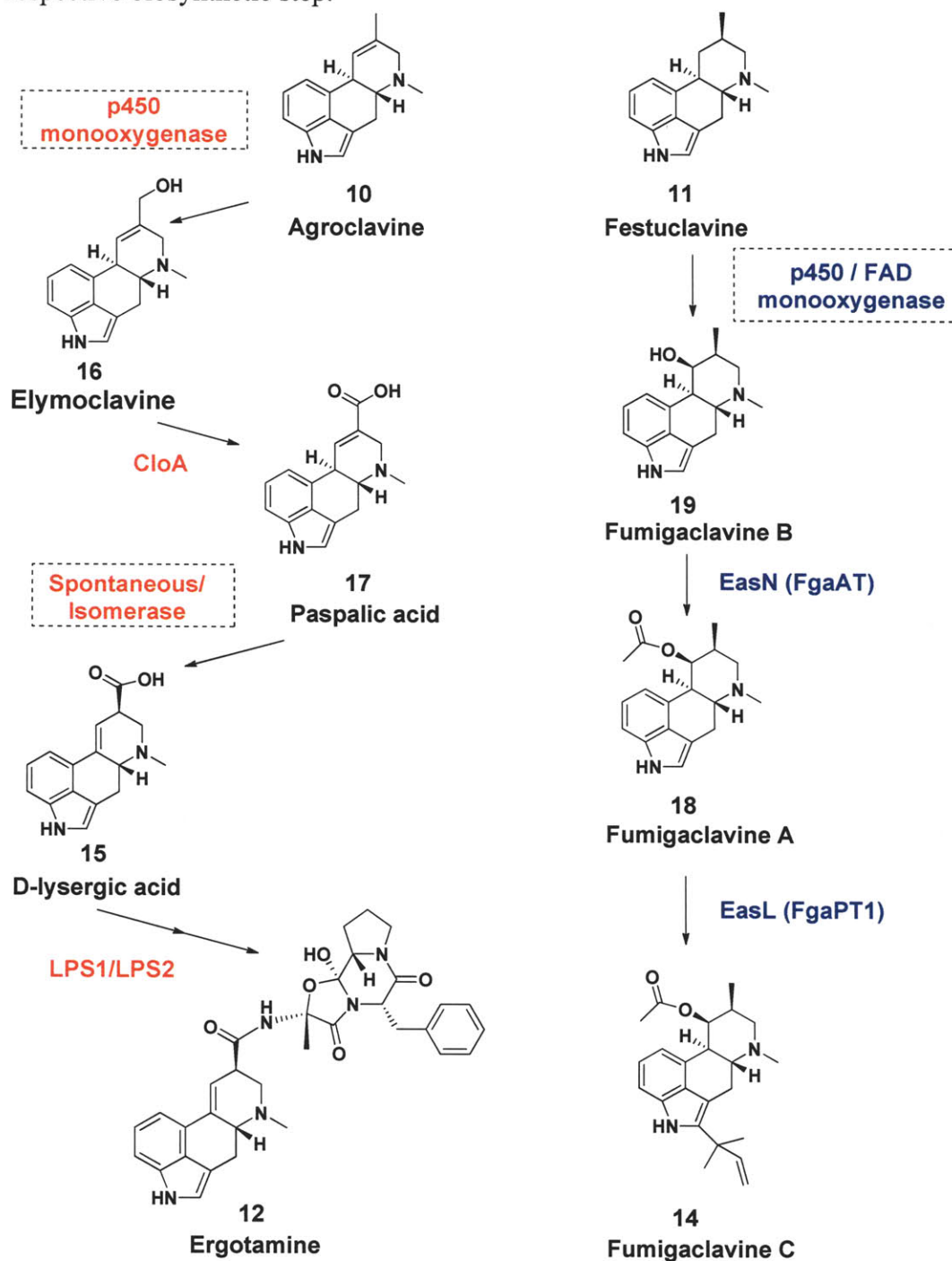
Functional Characterization of Late Ergot Alkaloid Biosynthetic Enzymes

Early pathway steps establish the ergoline ring up to either the festuclavine **11** or agroclavine **10** intermediate compound. The enzymes involved with the transformations in later step ergot alkaloid pathway biosynthesis are attributed to the pathway divergence of ergot alkaloid profiles observed in different fungal species. The Clavicipitaceous fungi *C. purpurea* and *N. lolii* carry late step pathway genes encoding non-ribosomal peptide synthetases (NRPS) domains for the conversion of agroclavine **10** into ergopeptides. Several of these genes have been studied by gene disruption or *in vitro* characterization (Figure 1.6).^{21, 42, 44, 49, 55} These studies have shown evidence that ergopeptide formation occurs via an enzyme complex composed of NRPS subunits D-lysergyl peptidyl synthetase (Lps2) that activates D-lysergic acid **15** and (Lps1) which in turn activates amino acids alanine, phenylalanine, and proline to form the tripeptide moiety.⁴² The enzyme CloA was also demonstrated to be critical for the oxidation of elymoclavine **16** to yield paspalic acid **17**, which either spontaneously or via an isomerase enzyme rearranges to form D-lysergic acid **15**. Previously, a proposed p450 monooxygenase from a microsomal fraction of *Claviceps* has also been observed to convert agroclavine **10** to elymoclavine **16** (Figure 1.6).^{56, 57}

In contrast, the *A. fumigatus* fumigaclavine C **14** biosynthetic gene cluster carries late ergot pathway genes that have been demonstrated to show acetylation and reverse prenyl transferase activities for the conversion of festuclavine **11** into later pathway

fumigaclavine A **18**, fumigaclavine B **19**, and fumigaclavine C **14**.^{17, 40, 43, 46} Notably, *A. fumigatus* does not carry any genes that encode for NRPS domains that are observed in ergot biosynthetic clusters of *N. lolii* and *C. purpurea* (Figure 1.6).

Figure 1.6. Late step ergot biosynthetic pathway showing agroclavine **10** derived alkaloid ergotamine **12** (*C. purpurea*) and festuclavine **11** derived alkaloid fumigaclavine C **14** (*A. fumigatus*). Enzymes associated with synthesis of ergotamine **12** (red) and fumigaclavine C **14** (blue) that have been identified via gene disruption or *in vitro* characterization. Dashed boxes represent putative enzymes necessary to carry out the respective biosynthetic step.



Research goal and thesis overview

I. Assign function to the conserved genes of the ergot alkaloid biosynthetic pathway that are critical for the cyclization of rings C and D found in all ergot alkaloids.

Divergent ergot producing fungal species share a common set of gene homologues associated with the early pathway biosynthesis of the ergoline ring, the defining feature common to all ergot alkaloids. Yet, at the outset of this research, the genes associated with the critical intramolecular cyclizations to form ergoline ring C and D remained to be identified in the ergot biosynthetic cluster. Chapter 2 describes the systematic disruption of genes associated with early ergot biosynthesis in *A. fumigatus*. The subsequent interpretation of the resulting ergot alkaloid profiles of each *A. fumigatus* mutant yielded valuable insight towards identifying the genes responsible for ring C and D formation. The results from these experiments allowed heterologous expression and functional characterization of enzymes involved in the cyclization of ring D (Chapter 3 and 4) and a putative catalase that facilitates formation of ring C (Chapter 5).

II. Obtain mechanistic insight into the enzymes involved with the intramolecular cyclizations that are essential for formation of the ergoline ring C and D.

Details of ring C and D formation at the enzymatic level have only remained speculative from a combination of previous feeding studies and gene knockout experiments (Figure 1.4). To yield mechanistic insight into the formation of ergoline ring C, Chapter 5 describes our efforts to study enzymes EasC and EasE. Purification of EasC yielded a protein with catalase activity that allowed us to refine our hypothesis regarding ergoline ring C formation.

To gain insight into ring D formation, Chapter 3 describes the cloning, heterologous expression, and characterization of the enzymes EasA and EasG from *A. fumigatus* involved with the formation of ergoline ring D of festuclavine **11**. From this study a mechanism for ergoline ring D cyclization was proposed for the formation of festuclavine **11** from chanoclavine-I-aldehyde **7**. This study also provided new information on how EasA, an Old Yellow Enzyme homologue, plays a biosynthetic role in ergot producing fungi.

III. Investigate the origin of ergot alkaloid structural divergence across different fungal species.

Ergot alkaloid profiles of diverse fungi exhibit either agroclavine **10** derived alkaloids (*C. purpurea*, *N. lolii*) or festuclavine **11** derived alkaloids (*A. fumigatus*). Prior to the cyclization of ring D, the last common precursor across divergent fungi is proposed to be chanoclavine-I-aldehyde **7** (Figure 1.3). In Chapter 4 we describe the study of an EasA homologue from *N. lolii* and its role in the cyclization of ring D to produce agroclavine **10** as opposed to the EasA homologue from *A. fumigatus* which forms festuclavine **11** described in Chapter 3. In addition, by using mutational analysis we investigated the mechanistic rationale behind this critical branch point in ergot alkaloid biosynthesis and created an EasA homologue capable of producing both festuclavine **11** and agroclavine **10** products. This study suggests that the EasA homologue found in diverse ergot producing fungi of different origins exerts control over the formation of festuclavine **11** or agroclavine **10** derived alkaloids. This study provided insight into the mechanistic origin of ergot alkaloid pathway divergence.

References

1. Schardl, C.L., D.G. Panaccione, and P. Tudzynski, *Ergot Alkaloids - Biology and Molecular Biology*, in *The Alkaloids* G. Cordell, Editor. 2006, Elsevier. p. 45-86.
2. Schiff, P., *Ergot and Its Alkaloids*. American Journal of Pharmaceutical Education, 2006. **70**(5): p. 1-10.
3. Dewick, P., *Ergot alkaloids*. 2 ed. Medicinal Natural Products. 2002 John Wiley & Sons, Ltd. 368-376.
4. Kumar, A. and R. Bhansali, *Biotechnology: secondary metabolites*. 2007: Science Publishers. 363-389.
5. Groger, D. and H.G. Floss, *Biochemistry of Ergot Alkaloids-achievements and challenges*, in *The Alkaloids*, G. Cordell, Editor. 1998, Academic Press. p. 171-218.
6. Flaugh, M.E., D.J. Mullen, R.W. Fuller, and N.R. Mason, *6-Substituted 1,3,4,5-tetrahydrobenz[cd]indol-4-amines: potent serotonin agonists*. Journal of Medicinal Chemistry, 1988. **31**: p. 1746.
7. Mukherjee, J. and M. Menge, *Progress and Prospects of Ergot Alkaloid Research*. Advances in Biochemical Engineering / Biotechnology, 2000. **68**: p. 1-18.
8. Martinelli, M.J., W. Bloomquist, B.C. Peterson, and M.L. Cohen, *Amesergide and structurally related nor-D-ergolines: 5HT₂ receptor interactions in the rat*. Journal of Medicinal Chemistry, 1993. **36**(18): p. 2671-2675.
9. Ohno, S., Y. Adachi, M. Koumori, K. Mizukoshi, M. Nagasaka, K. Ichihara, and E. Kato, *Synthesis and Structure-Activity Relationships of New (5R, 8R, 10R)-Ergoline Derivatives with Antihypertensive or Dopaminergic Activity*. Chemical and Pharmaceutical Bulletin, 1994. **42**: p. 1463-1473.
10. Ohno, S., M. Koumori, Y. Adachi, K. Mizukoshi, M. Nagasaka, and K. Ichihara, *Synthesis and Structure-Activity Relationships of New (5R, 8S, 10R)-Ergoline Derivatives with Antihypertensive or Dopaminergic Activity*. Chemical and Pharmaceutical Bulletin, 1994. **42**: p. 2042-2048.
11. Stamos, I.K., E.A. Kelly, H.G. Floss, and J. Cassady, *Synthesis and Analysis of Compounds Having the Skeleton of Ergot Alkaloids with the Nitrogen Atom in the D-Ring Transposed*. Journal of Heterocyclic Chemistry, 1995. **32**: p. 1303-1308.
12. Keller, N., G. Turner, and J. Bennett, *Fungal Secondary Metabolism - From Biochemistry to Genomics*. Nature Reviews Microbiology, 2005. **3**: p. 937-947.
13. Brookman, J. and D. Denning, *Molecular genetics in Aspergillus fumigatus*. Current Opinion in Microbiology, 2000. **3**: p. 468-474.
14. Coyle, C.M. and D.G. Panaccione, *An Ergot Alkaloid Biosynthesis Gene and Clustered Hypothetical Genes from Aspergillus fumigatus*. Applied and Environmental Microbiology, 2005. **71**(6): p. 3112-3118.
15. Coyle, C.M., S. Kenaley, W. Rittenour, and D.G. Panaccione, *Association of ergot alkaloids with conidiation in Aspergillus fumigatus*. Mycologia, 2007. **99**(6): p. 804-811.
16. Cramer, R., E. Shwab, and N. Keller, *Genetic regulation of Aspergillus secondary metabolites and their role in fungal pathogenesis*, in *Aspergillus fumigatus and*

- Aspergillosis*, J. Latge, Steinbach, W., Editor. 2009, ASM Press: Washington, DC. p. 185199.
17. Unsold, I. and S.-M. Li, *Overproduction, purification and characterization of FgaPT2, a dimethylallyltryptophan synthase from Aspergillus fumigatus*. Microbiology, 2005. **151**: p. 1499-1505.
 18. Haarmann, T., C. Machado, Y. Lubbe, T. Correia, C.L. Schardl, D.G. Panaccione, and P. Tudzynski, *The ergot alkaloid gene cluster in Claviceps purpurea: Extension of the cluster sequence and intra species evolution*. Phytochemistry, 2005. **66**: p. 1312-1320.
 19. Tudzynski, P., K. Holter, T. Correia, C. Arntz, N. Grammel, and U. Keller, *Evidence for an ergot alkaloid gene cluster in Claviceps purpurea*. Molecular and General Genetics, 1999. **261**: p. 133-141.
 20. Wang, J., C. Machado, D.G. Panaccione, H.-F. Tsai, and C.L. Schardl, *The determinant step in ergot alkaloid biosynthesis by an endophyte of perennial ryegrass*. Fungal Genetics and Biology, 2004. **41**: p. 189-198.
 21. Fleetwood, D., B. Scott, G. Lane, A. Tanaka, and R. Johnson, *A Complex Ergovaline Gene Cluster in Epichloa Endophytes of Grasses*. Applied and Environmental Microbiology, 2007. **73**(8): p. 2571-2579.
 22. Li, S.-M. and I. Unsold, *Post-genome Research on the Biosynthesis of Ergot Alkaloids*. Planta Medica, 2006. **72**(12): p. 1117-1120.
 23. Schardl, C., D. Panaccione, and P. Tudzynski, *The alkaloids* G. Cordell, Editor. 2006, Elsevier. p. 45-86.
 24. Zhang, Y., N. Keller, D. Tsitsigiannis, and H. Wilkinson, *Secondary metabolite gene clusters*, in *Handbook of Industrial Mycology*, Z. An, Editor. 2005, Marcel Dekker: New York. p. 355-385.
 25. Coyle, C.M., J.Z. Cheng, S.E. O'Connor, and D.G. Panaccione, *An Old Yellow Enzyme Gene Controls the Branch Point between Aspergillus fumigatus and Claviceps purpurea Ergot Alkaloid Pathways*. Applied and Environmental Microbiology, 2010. **76**(12): p. 3898-3903.
 26. Floss, H.G., *Biosynthesis of Ergot Alkaloids and Related Compounds*. Tetrahedron 1976. **32**: p. 873-912.
 27. Floss, H.G., *From Ergot to Ansamycins - 45 Years in Biosynthesis*. Journal of Natural Products, 2006. **69**: p. 158-169.
 28. Floss, H.G., U. Hornemann, N. Schilling, D. Groger, and D. Erge, *Chanoclavines and the biosynthesis of ergot alkaloids*. Chemical Communications, 1967: p. 105-106.
 29. Floss, H.G., U. Hornemann, N. Schilling, K. Kelley, D. Groger, and D. Erge, *Biosynthesis of ergot alkaloids. Evidence for two isomerizations in the isoprenoid moiety during the formation of tetracyclic ergolines*. Journal of the American Chemical Society, 1968. **90**: p. 6500-6507.
 30. Floss, H.G., M. Tcheng-Lin, C. Chang, B. Naidoo, G. Blair, C. Abou-Chaar, and J. Cassidy, *Biosynthesis of ergot alkaloids. Mechanism of the conversion of chanoclavine-I into tetracyclic ergolines*. Journal of the American Chemical Society, 1974: p. 1898-1909.

31. Gebler, J. and C. Poulter, *Purification and characterization of dimethylallyltryptophan synthase from Claviceps purpurea*. Archives of Chemistry and Biophysics, 1992. **296**(1): p. 308-313.
32. Gebler, J., A. Woodside, and C. Poulter, *Dimethylallyltryptophan synthase. An enzyme-catalyzed electrophilic aromatic substitution*. Journal of the American Chemical Society, 1992. **114** (19): p. 7354-7360.
33. Kobayashi, M. and H.G. Floss, *Biosynthesis of ergot alkaloids: origin of the oxygen atoms in chanoclavine-I and elymoclavine*. Journal of Organic Chemistry, 1987. **52**(19): p. 4350-4352.
34. Kozikowski, A., C. Chen, J. Wu, M. Shibuya, C. Kim, and H.G. Floss, *Probing ergot alkaloid biosynthesis: intermediates in the formation of ring C*. Journal of the American Chemical Society, 1993. **115** (6): p. 2482-2488.
35. Kozikowski, A., M. Okita, M. Kobayashi, and H.G. Floss, *Probing ergot alkaloid biosynthesis: synthesis and feeding of a proposed intermediate along the biosynthetic pathway. A new amidomalonate for tryptophan elaboration*. Journal of Organic Chemistry, 1988. **53**(4): p. 863-869.
36. Kozikowski, A., J. Wu, M. Shibuya, and H.G. Floss, *Probing ergot alkaloid biosynthesis: identification of advanced intermediates along the biosynthetic pathway*. Journal of the American Chemical Society, 1988. **110**(6): p. 1970-1971.
37. Robbers, J., H. Otsuka, H.G. Floss, E. Arnold, and J. Clardy, *Clavicipitic acid: its structure, biosynthesis, and role in ergot alkaloid formation*. Journal of Organic Chemistry, 1980. **45**(6): p. 1117-1121.
38. Otsuka, H., F.R. Quigley, D. Groger, J.A. Anderson, and H.G. Floss, *In Vivo and In Vitro Evidence for N-Methylation as the Second Pathway-Specific Step in Ergoline Biosynthesis*. Planta Medica, 1980. **40**: p. 109-119.
39. Correia, T., N. Grammel, I. Ortel, N. Keller, and P. Tudzynski, *Molecular Cloning and Analysis of the Ergopeptine Assembly System in the Ergot Fungus Claviceps purpurea*. Chemistry and Biology, 2003. **10**: p. 1281-1292.
40. Liu, X., L. Wang, N. Steffan, W.-B. Yin, and S.-M. Li, *Ergot Alkaloid Biosynthesis in Aspergillus fumigatus: FgaAT Catalyses the Acetylation of Fumigaclavine B*. Chembiochem, 2009. **10**(14): p. 2325-2328.
41. Panaccione, D.G., R. Johnson, J. Wang, C. Young, P. Damrongkool, B. Scott, and C.L. Schardl, *Elimination of ergovaline from a grass-Neotyphodium endophyte symbiosis by genetic modification of the endophyte*. Proceedings of the National Academy of Sciences of the United States of America, 2001. **98**(22): p. 12820-12825.
42. Riederer, B., M. Han, and U. Keller, *D-Lysergyl Peptide Synthetase from the Ergot Fungus Claviceps purpurea*. The Journal of Biological Chemistry, 1996. **271**(44): p. 27524-27530.
43. Unsold, I. and S.-M. Li, *Reverse Prenyltransferase in the biosynthesis of fumigaclavine C in Aspergillus fumigatus: gene expression, purification, and characterization of fumigaclavineC synthase FGAPT1*. Chembiochem, 2006. **7**: p. 158 - 164.
44. Walzel, B., B. Riederer, and U. Keller, *Mechanism of alkaloid cyclopeptide synthesis in the ergot fungus Claviceps purpurea*. Chemistry and Biology, 1997. **4**(3): p. 223-230.

45. Panaccione, D.G., B.A. Tapper, G.A. Lane, E. Davies, and K. Fraser, *Biochemical Outcome of Blocking the Ergot Alkaloid Pathway of a Grass Endophyte*. Journal of Agricultural and Food Chemistry, 2003. **51**(22): p. 6429-6437.
46. Wallwey, C., M. Matuschek, X.-L. Xie, and S.-M. Li, *Ergot alkaloid biosynthesis in Aspergillus fumigatus: Conversion of chanoclavine-I aldehyde to festuclavine by festuclavine synthase FgaFS in the presence of the old yellow enzyme FgaOx3*. Organic and Biomolecular Chemistry 2010. **8**: p. 3500-3508.
47. Rigbers, O. and S.-M. Li, *Ergot Alkaloid Biosynthesis in Aspergillus fumigatus Overproduction and Biochemical Characterization of a 4-Dimethylallyltryptophan N-Methyltransferase*. The Journal of Biological Chemistry, 2008. **283**(40): p. 26859-26868.
48. Tsai, H.F., H. Wang, J.C. Gebler, C.D. Poulter, and C.L. Schardl, *The Claviceps purpurea Gene Encoding Dimethylallyltryptophan Synthase, the Committed Step for Ergot Alkaloid Biosynthesis* Biochemical and Biophysical Research Communications, 2002. **216**(1): p. 119-125.
49. Lorenz, N., E. Wilson, C. Machado, C.L. Schardl, and P. Tudzynski, *Comparison of Ergot Alkaloid Biosynthesis Gene Clusters in Claviceps Species Indicates Loss of Late Pathway Steps in Evolution of C. fusiformis*. Applied and Environmental Microbiology, 2007. **73**(22): p. 7185-7191.
50. Lorenz, N., J. Olsovska, M. Sulc, and P. Tudzynski, *Alkaloid Cluster Gene ccsA of the Ergot Fungus Claviceps purpurea Encodes Chanoclavine I Synthase, a Flavin Adenine Dinucleotide-Containing Oxidoreductase Mediating the Transformation of N-Methyl-Dimethylallyltryptophan to Chanoclavine I*. Applied and Environmental Microbiology, 2010. **76**(6): p. 1822-1830.
51. Fox, K. and P.A. Karplus, *Old yellow enzyme at 2 Å resolution: overall structure, ligand binding, and comparison with related flavoproteins*. Structure, 1994. **15**(2): p. 1089-1105.
52. Williams, R. and N. Bruce, *'New uses for an old enzyme' – the old yellow enzyme family of flavoenzymes*. Microbiology, 2002. **148**: p. 1607-1614.
53. Kamitori, S., A. Iguchi, A. Ohtaki, M. Yamada, and K. Kita, *X-ray Structures of NADPH-dependent Carbonyl Reductase from Sporobolomyces salmonicolor Provide Insights into Stereoselective Reductions of Carbonyl Compounds*. Journal of Molecular Biology, 2005. **352**: p. 551-558.
54. Price, A., Y.-M. Zhang, C.O. Rock, and S.W. White, *Structure of Beta-Ketoacyl-[acyl carrier protein] Reductase from Escherichia coli: Negative Cooperativity and Its Structural Basis*. Biochemistry, 2001. **40**: p. 12772-12781.
55. Haarmann, T., I. Ortel, P. Tudzynski, and U. Keller, *Bridging the Clavine and Ergoline Alkaloid Pathways*. Chembiochem, 2006. **7**: p. 645-652.
56. Kim, I.-S., S.-U. Kim, and J.A. Anderson, *Microsomal Agroclavine Hydroxylase of Claviceps Species*. Phytochemistry, 1981. **20**(10): p. 2311-2314.
57. Maier, W., B. Schumann, and D. Groger, *Microsomal oxygenases involved in ergoline alkaloid biosynthesis of various Claviceps strains*. Journal of Basic Microbiology, 1988. **28**(1-2): p. 83-93.

Chapter 2 . Assigning Function to Genes Involved in Early Step Ergot Alkaloid Biosynthesis

Part of this chapter has been published in

Coyle, C.M., J.Z. Cheng, S.E. O'Connor, and D.G. Panaccione, *An Old Yellow Enzyme Gene Controls the Branch Point between Aspergillus fumigatus and Claviceps purpurea Ergot Alkaloid Pathways*. Applied and Environmental Microbiology, 2010. **76**(12): p. 3898-3903.

and

Goetz, K.E., C.M. Coyle, J.Z. Cheng, S.E. O'Connor, and D.G. Panaccione, *Ergot cluster-encoded catalase is required for synthesis of chanoclavine-I in Aspergillus fumigatus*. Current Genetics, 2011(accepted).

Introduction

Fungal genes involved in the biosynthesis of secondary metabolites were known to be clustered on a single genetic locus; in contrast, genes associated with primary metabolism were not localized in a cluster.¹ We observe clustering of the ergot biosynthetic genes in *A. fumigatus*^{2,3} as well as Clavicipitaceous fungi such as *C. purpurea*^{4,5} and *N. lolii*^{6,7} (Figure 1.5). Shared homologous genes in the clusters of these divergent fungi were associated with the early steps of ergot alkaloid biosynthesis forming the tetracyclic ergoline ring.

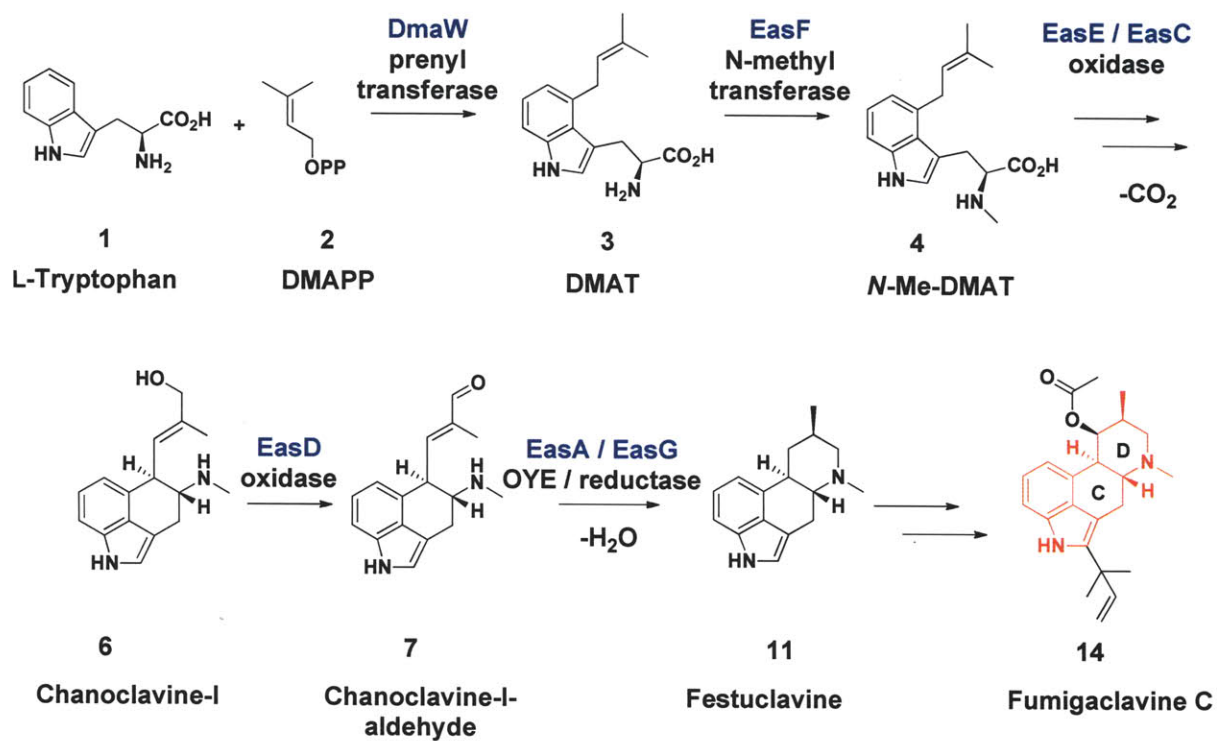
Gene disruption has been a useful *in vivo* approach for assigning functions of clustered ergot biosynthetic genes.⁶⁻⁹ The function of a particular gene is deduced by monitoring accumulation of proposed pathway intermediates along with the disappearance of downstream products in the gene disruption mutant strain. These results were usually reflective of the reaction step catalyzed by the *in vitro* purified gene product, which can be assayed after cloning and heterologous expression of the target gene. For instance, in previous studies, gene disruption of the *dmaW* 4-dimethylallyl prenyltransferase gene in *A. fumigatus* and *N. lolii* eliminated downstream ergot alkaloid products that were observed in the wild type strains.^{7,8} These results complemented the observation that heterologously expressed DmaW was involved in the first determinant step of ergot alkaloid biosynthesis via the prenylation of L-tryptophan **1**.³ Therefore, *in vivo* gene disruption is an important approach toward assigning gene function when used in combination with *in vitro* gene product characterization.

At the outset of this research the only gene of early ergot alkaloid biosynthesis that had been functionally characterized was *dmaW*.^{3,7,8} In contrast, characterization of

the other clustered genes responsible for encoding the enzymes involved with the critical C and D ring cyclizations of ergoline had only been speculative.¹⁰⁻¹² In this chapter we discuss the use of gene disruption upon the ergot alkaloid biosynthetic gene cluster of *A. fumigatus* and analysis of the ergot profiles of the $\Delta easF$, $\Delta easE$, $\Delta easC$, and $\Delta easA$ knockout mutants that were conducted in collaboration with the group of Professor Daniel Panaccione at the University of West Virginia.

Firstly, mutants of *A. fumigatus* disrupted at the *easE* and *easC* alleles ($\Delta easE$ and $\Delta easC$) provided evidence that the *easE* and *easC* gene products were involved in the cyclization of ergoline ring C based on the accumulation of an early biosynthetic intermediate in these disrupted strains (Figure 2.1). Secondly, *A. fumigatus* mutants disrupted at the *easA* allele ($\Delta easA$), along with analysis of the accumulating biosynthetic intermediate, indicated that *easA* is responsible for formation of ring D (Figure 2.1). Augmentation of this *A. fumigatus* disruption mutant with the *easA* allele from *C. purpurea* provided evidence that the *easA* gene product controls a proposed branch point of ergot alkaloid biosynthesis that occurs upon formation of ergoline ring D. These results guided efforts toward the *in vitro* cloning, heterologous expression, and functional characterization of these individual genes to investigate the formation of ergoline rings C and D.

Figure 2.1. Early ergot pathway enzymes and associated functions toward the cyclization of ergoline ring C and D as labeled in fumigaclavine C **14**.



Experimental Methods

***A. fumigatus* Gene Disruption and Complementation**

(Performed by C.M. Coyle and K.E. Goetz in Panaccione Lab)

A. fumigatus gene disrupted mutants were prepared by our collaborators in the Panaccione lab using previously reported protocols.^{8, 13} Gene disruption constructs were made by PCR amplification of an internal fragment of *A. fumigatus* genes *dmaW* (*fgaPTs*) (XM_751048), *easF* (XM_751050), *easC* (XM_751047), *easE* (XM_751049), and *easA* (XM_751040), from *A. fumigatus* genomic DNA prepared following Gene Clean Spin Protocol (Bio 101, Vista, CA). Disruption constructs were prepared by ligating the amplified PCR products into TA cloning vector pCR2.1. Prior to transformation into *A. fumigatus* protoplasts, disruption constructs were linearized by restriction digest that cut once within the internal gene fragment along with a *NotI* linearized hygromycin resistance plasmid pMOcosX (Orbach, 1994).¹⁴ *A. fumigatus* protoplast transformations were performed according to previously reported protocols of Murray et al. with modifications by Coyle et al.^{8, 15} Transformant selection was conducted on regeneration medium plates containing hygromycin B (300µg/mL) as described by Panaccione et al.¹⁶ Transformants were screened using southern blot and by PCR assays amplifying allele junctions resulting from homologous recombination of the native copy of the gene with the disruption construct as previously described by Coyle et al.⁸

Complementation of the gene disrupted *A. fumigatus* mutants was conducted by ectopic insertion of a PCR amplified functional copy of the respective gene with flanking regions into the mutant genome based on the protocol of Coyle et al.¹³ The PCR product

and a phleomycin resistance plasmid, *NotI* linearized pBC-phleo (Fungal Genetics Stock Center, University of Missouri-Kansas City), were transformed into the gene disrupted mutant. Transformants were selected on a regeneration medium (100 µg/mL)¹⁶ and PCR assays were used to verify the presence of the original gene disruption construct along with the introduced functional copy of the wild type gene.⁸

Analysis of Ergot Alkaloid Profiles of *A. fumigatus* by and Gene Disrupted Mutants

(*A. fumigatus* cultures, extracts, and fluorescent HPLC analysis were performed by C.M. Coyle and K.E. Goetz in Panaccione Lab, LC-MS analysis and preparation of N-Me-DMAT 4 standard performed by J.Z. Cheng in O'Connor Lab)

A. fumigatus sporulating cultures were grown on potato dextrose agar (20g dehydrated potato, 20 g glucose, 15 g agar per liter at 37 °C). Culture media was extracted with 80% methanol. HPLC analysis of extracts were conducted via fluorescence detection⁸ with a C18 column Prodigy 5 µm ODS3, 150 mm x 4.6 mm; (Phenomenex Torrance, CA) and a mobile phase multilinear binary gradient from 5:95 to 75:25 (acetonitrile:50 mM aqueous ammonium acetate).¹⁷ Eluting fractions were monitored by fluorescence detection with excitation and emission wavelengths of 272 nm / 372 nm or 310 nm / 410 nm. Peaks correlating to festuclavine **11** and fumigaclavines A **18**, B **19**, and C **14** were identified based on previous mass spectral analysis of *A. fumigatus* extracts.¹⁸ N-Me-DMAT **3** standard was enzymatically prepared using heterologously expressed DmaW prenyltransferase⁷ (see Chapter 5). Chanoclavine-I **6** standard was supplied by B.A. Tapper (AgResearch, Palmerston North, New Zealand). Agroclavine **10** standard was purchased from Sigma (St. Louis, Missouri). Setoclavine **22** isosetoclavine **23** standards were prepared by the oxidation of agroclavine **10** with

horseradish peroxidase and H₂O₂ or with peroxidase-rich plant extract as previously described.^{17, 19-21}

LC-MS analysis of extracts were conducted with an Acquity Ultra Performance BEH C18 column (2.1 x 100 mm; 1.7 µm particle size) and eluted with a flow rate of 0.5 mL/min linear gradient (Acetonitrile:0.1 % formic acid water) of 20:80 to 80:20 over 5 min. Mass detection was conducted on a Micromass LCT Premier TOF MS (Waters, Milford, MA) with an electrospray ionization source set in positive mode.

**Feeding *A. fumigatus easC* Disrupted Mutants with Chanoclavine-I
(Performed by K.E. Goetz and C.M. Coyle in Panaccione Lab)**

Cultures of *A. fumigatus* $\Delta easC$ mutants were fed with chanoclavine-I **6** in order to observe whether the enzyme catalyzed reaction steps downstream of chanoclavine-I **6** were still functional. An *A. fumigatus* $\Delta dmaW$ gene disrupted mutant, which is blocked at the first pathway determinant step toward ergot alkaloid biosynthesis⁸, served as a positive control. Cultures were grown in triplicate starting with 60,000 conidia in 200 µL of lactose-malt extract-arginine broth in culture tubes.²²

Chanoclavine-I **6** (26.7 nmol in 1 µL of methanol) was added to the culture tubes of *A. fumigatus* $\Delta easC$, while 1 µL of methanol was added to the $\Delta dmaW$ control cultures. All cultures were grown at room temperature for three days. Extraction of alkaloids from the cultures were conducted by adding 800 µL of methanol and ten 3-mm diameter glass beads with agitation using a Fast Prep FP120 (Q-biogene, Irving, CA) at 6m per sec for 30 sec. Subsequently extracts were filtered through 0.2 µM nylon filters and analyzed by HPLC.

Results and Discussion

***A. fumigatus* Gene Disruption Mutants and Analysis of Ergot Alkaloid Profiles**

A. fumigatus* Genes *dmaW* and *easF

The *dmaW* gene product had been previously demonstrated to prenylate L-tryptophan **1** to yield DMAT **3** (Figure 2.1). The gene disruption mutant $\Delta dmaW$ (*A. fumigatus*) displayed loss of all ergot alkaloids production when compared to the wild type strain as evidenced by LC-MS analysis (Table 2.1, Figure 2.2-2.3), consistent with previous knockout studies of *dmaW* in *A. fumigatus* and *N. lolii*.^{7, 8} Wild type *A. fumigatus* culture extracts displayed accumulation of downstream ergot alkaloids festuclavine **11** at *m/z* 241 and fumigaclavine C **14** at *m/z* 367 as evidenced by LC-MS analysis, while the $\Delta dmaW$ mutant did not show any trace of either of these compounds.

Table 2.1. *A. fumigatus* wild type gene disrupted mutants and the accumulation of pathway intermediates detected by LC-MS. (•) Indicates accumulation of corresponding mass in LC-MS analysis of *A. fumigatus* wild type and gene disrupted culture extracts. Corresponding LC-MS chromatograms are shown in corresponding Figures 2.2-2.4, 2.6, 2.7, 2.9.

<i>A. fumigatus</i> Culture Description	DMAT 3 [M+H] ⁺ 273	N-Me- DMAT 4 [M+H] ⁺ 287	Chano-I 6 [M+H] ⁺ 257	Chano-I- aldehyde 7 [M+H] ⁺ 255	Festuclavine 11 [M+H] ⁺ 241	Fumigaclavine C 14 [M+H] ⁺ 367
wild type					•	•
$\Delta dmaW$						
$\Delta easF$	•					
$\Delta easE$		•				
$\Delta easC$		•				
$\Delta easA$			•	•		

Figure 2.2. LC-MS trace of *A. fumigatus* wild type culture extract (Peak intensities for this set of chromatograms have been normalized to allow relative comparison of compound masses present).

A. Selected ion monitoring for ergot alkaloids festuclavine **11** $[M+H]^+ = 241$ and fumigaclavine C **14** $[M+H]^+ = 367$. Displays masses corresponding to wild type ergot alkaloids festuclavine **11** $[M+H]^+ = 241$ and fumigaclavine C **14** $[M+H]^+ = 367$. The broad peak at 0.75 to 0.80 min were attributed to compounds extracted from the culture media that are not identifiable as ergot alkaloids or pathway intermediates.

B. Selected ion monitoring for intermediates DMAT **3** $[M+H]^+ = 273$, *N*-Me-DMAT **4** $[M+H]^+ = 287$, chanoclavine-I **6** $[M+H]^+ = 257$, chanoclavine-I-aldehyde **7** $[M+H]^+ = 255$. This trace shows absence of observable pathway intermediates in the ergot alkaloid biosynthetic pathway.

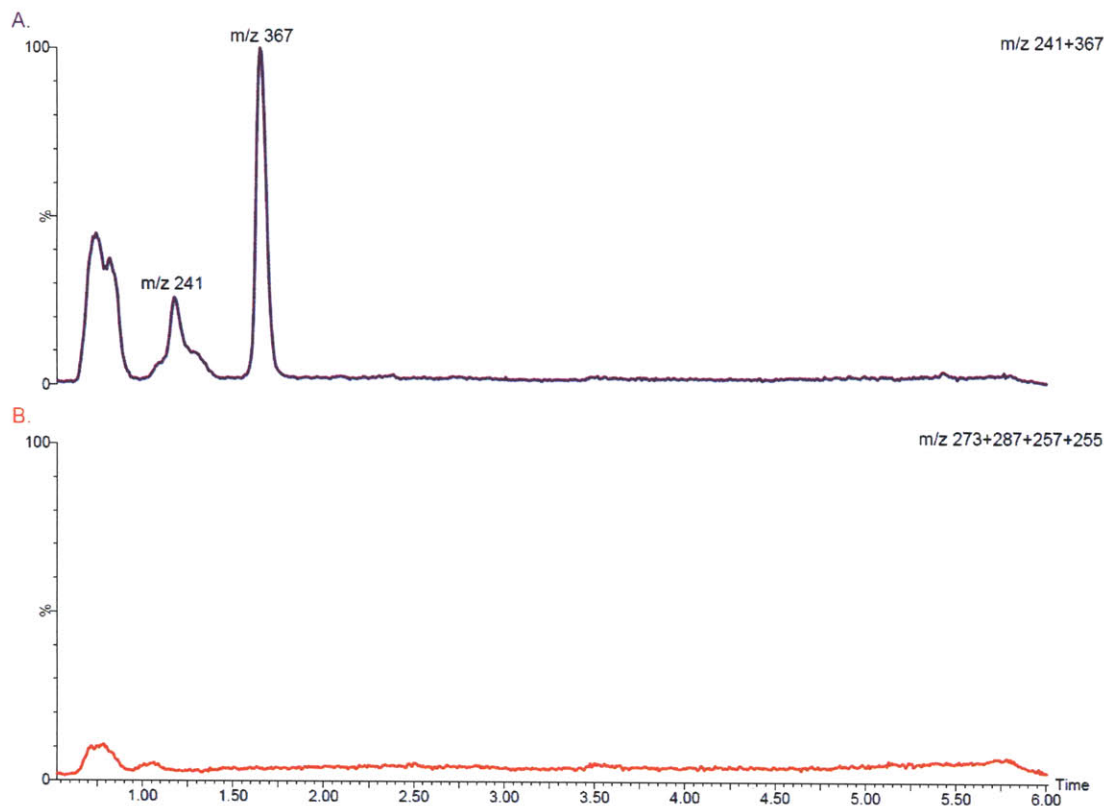
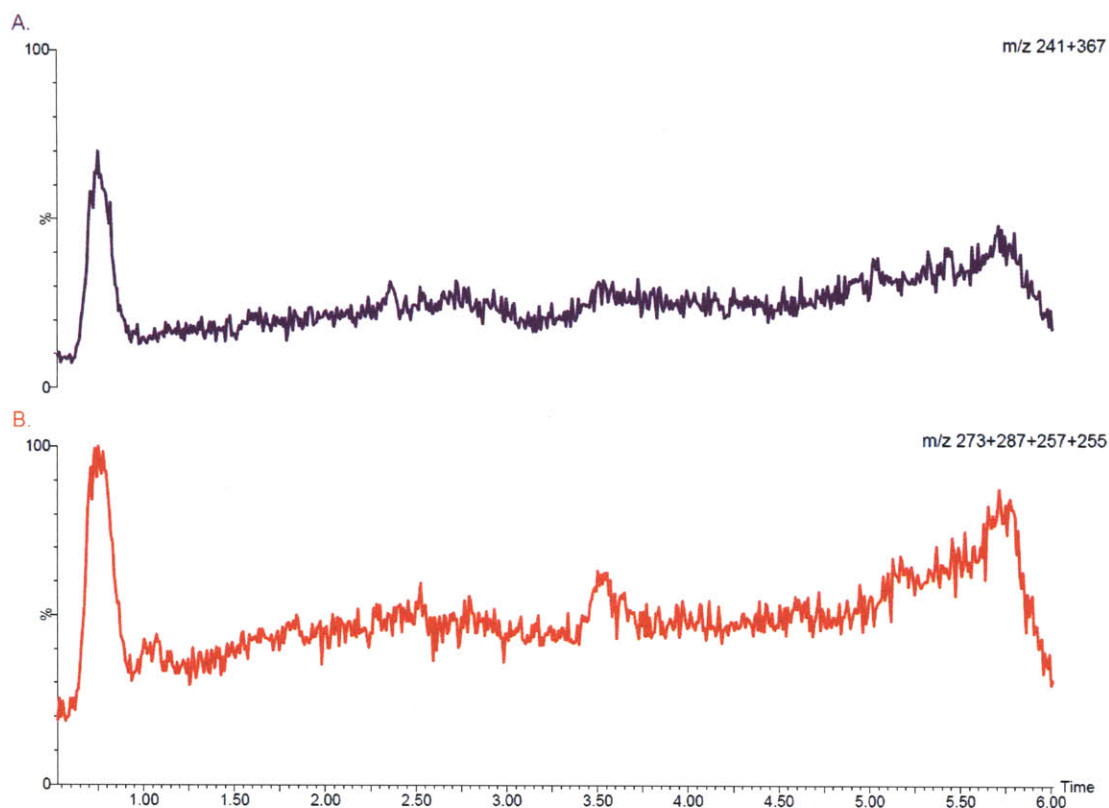
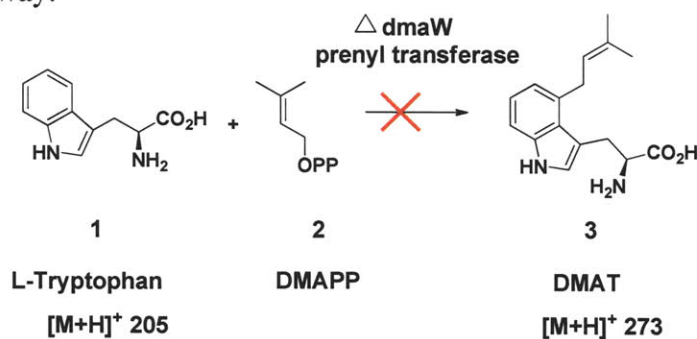


Figure 2.3. LC-MS trace of *A. fumigatus* $\Delta dmaW$ culture extract (Peak intensities for this set of chromatograms have been normalized to allow relative comparison of compound masses present).

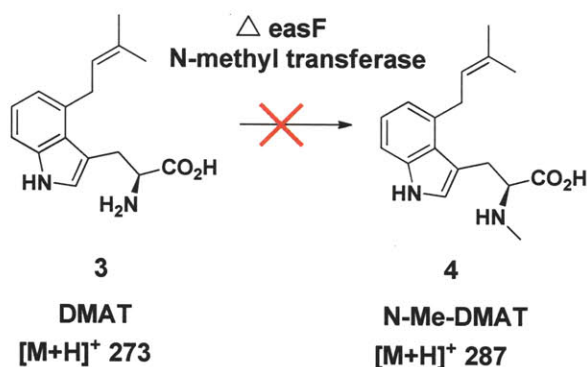
A. Selected ion monitoring for ergot alkaloids festuclavine **11** $[M+H]^+ = 241$ and fumigaclavine C **14** $[M+H]^+ = 367$. This trace shows absence of ergot alkaloids that are observed in wild type *A. fumigatus*.

B. Selected ion monitoring for intermediates DMAT **3** $[M+H]^+ = 273$, *N*-Me-DMAT **4** $[M+H]^+ = 287$, chanoclavine-I **6** $[M+H]^+ = 257$, chanoclavine-I-aldehyde **7** $[M+H]^+ = 255$. This trace shows absence of observable pathway intermediates in the ergot alkaloids biosynthetic pathway.



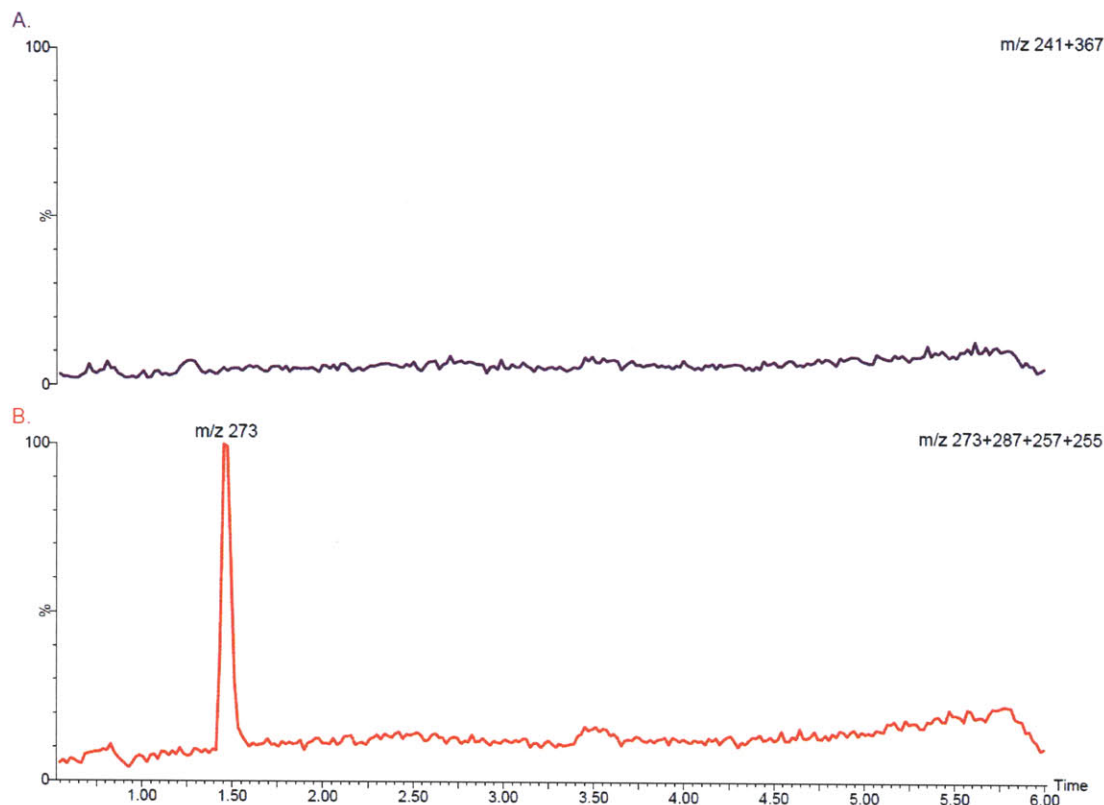
The gene *easF*, proposed to be a S-adenosyl methionine (SAM) dependent *N*-methyltransferase, was similarly disrupted in *A. fumigatus*. This $\Delta easF$ strain displayed accumulation of dimethylallyl tryptophan (DMAT) **3** at m/z 273 (Table 2.1 and Figure 2.4). This result supports the conclusions derived from *Claviceps purpurea* feeding studies conducted by Otsuka et al.²³ These authors proposed that *N*-methylation does not occur after ring C cyclization, but occurs instead on the earlier biosynthetic intermediate DMAT **3** (Figure 2.1).^{23, 24} Our observation that DMAT **3** accumulates in $\Delta easF$ *A. fumigatus* is also consistent with recent enzymology studies using heterologously expressed *A. fumigatus easF* gene product by Rigbers et al.²⁵ Therefore, observations from both our *in vivo* gene disruption data in the $\Delta easF$ mutant, coupled with *in vitro easF* gene product characterization, demonstrates that EasF catalyzes the *N*-methylation of DMAT **3** to yield *N*-Me-DMAT **4** in the second pathway step toward ergot alkaloid biosynthesis.²⁵

Figure 2.4. LC-MS trace of *A. fumigatus* $\Delta easF$ culture extract (Peak intensities for this set of chromatograms have been normalized to allow relative comparison of compound masses present).



A. Selected ion monitoring for ergot alkaloids festuclavine **11** $[M+H]^+ = 241$ and fumigaclavine C $[M+H]^+ = 367$. This trace shows absence of ergot alkaloids that are observed in wild type *A. fumigatus*.

B. Selected ion monitoring for intermediates DMAT **3** $[M+H]^+ = 273$, *N*-Me-DMAT **4** $[M+H]^+ = 287$, chanoclavine-I **6** $[M+H]^+ = 257$, chanoclavine-I-aldehyde **7** $[M+H]^+ = 255$. This trace displays the mass corresponding to DMAT **3** $[M+H]^+ = 273$ pathway intermediate.



***A. fumigatus* genes *easE* and *easC* and the formation of ergoline ring C**

Following the N-methylation by EasF, a set of proposed successive oxidations were required to form the ergoline C ring (Figure 2.1).²⁶ The gene products of *easE* and *easC* were potential candidates to carry out these oxidative steps as they were homologous to FAD oxidoreductase and catalase respectively.^{10, 12} Gene disrupted mutants of *A. fumigatus* $\Delta easE$ and $\Delta easC$ both lose the ability to produce downstream fumigaclavine and festuclavine **11** ergot alkaloids while the pathway intermediate *N*-Me-DMAT **3** accumulates, as evidenced by HPLC and LC-MS analyses (Table 2.1, Figure 2.1).

Fumigaclavines A **18**, B **19**, C **14** and festuclavine **11** that were identified in the HPLC trace of the *A. fumigatus* wild type culture, were not detected in the $\Delta easE$ or $\Delta easC$ mutants (Figure 2.5). Instead the HPLC traces for $\Delta easE$ or $\Delta easC$ mutant cultures showed the accumulation of a peak eluting at 46 min that is not present in the wild type cultures (Figure 2.5). Subsequent LC-MS analysis of the *A. fumigatus* $\Delta easE$ and $\Delta easC$ culture extracts displayed accumulation of a mass at m/z 287 expected for *N*-Me-DMAT **4** (Table 2.1, Figure 2.6-2.7). The *N*-Me-DMAT **4** intermediate that accumulated in both $\Delta easE$ and $\Delta easC$ was further verified by co-elution with an enzymatically prepared *N*-Me-DMAT **4** standard using HPLC (Figure 2.5). This evidence indicates that both gene products of *easE* and *easC* mutants were blocked in ergoline ring C formation and instead accumulated the *N*-Me-DMAT **4** pathway intermediate. These data clearly implicate the role of *easE* and *easC* in ergoline biosynthesis. Moreover, the accumulation of *N*-Me-DMAT **4** suggests that this compound is the immediate precursor to chanoclavine-I **6**, as proposed by early feeding studies.^{12, 23, 26}

Gene disruption of an *easE* homologue in ergot alkaloid producing *Claviceps purpurea* also accumulated the pathway intermediate *N*-Me-DMAT **4**, as well as trace amounts of DMAT **3**.²⁷ These results parallel our observations that *easE* and *easC* in *A. fumigatus* were necessary for the formation of ring C in ergot alkaloid biosynthesis.

Figure 2.5. Fluorescence HPLC ergot alkaloid profiles of cultures wild type (black line), gene disrupted *easE* ($\Delta easE$, blue line), and gene disrupted *easC* ($\Delta easC$, red line). *N*-Me-DMAT **4** standard (green line). Adapted from Goetz et al.²⁸

Wild type displays accumulation of alkaloids (B = fumigaclavine B **19**, Ch = chanoclavine-I **6**, F = festuclavine **11**, A = fumigaclavine A **18**, and C = fumigaclavine C **14**). $\Delta easC$ and $\Delta easE$ gene disrupted mutants display accumulation of intermediate *N*-Me-DMAT **4** with loss of ergot alkaloids that are produced in the wild type. Detection was by fluorescence with excitation at 272 nm and emission at 372 nm.

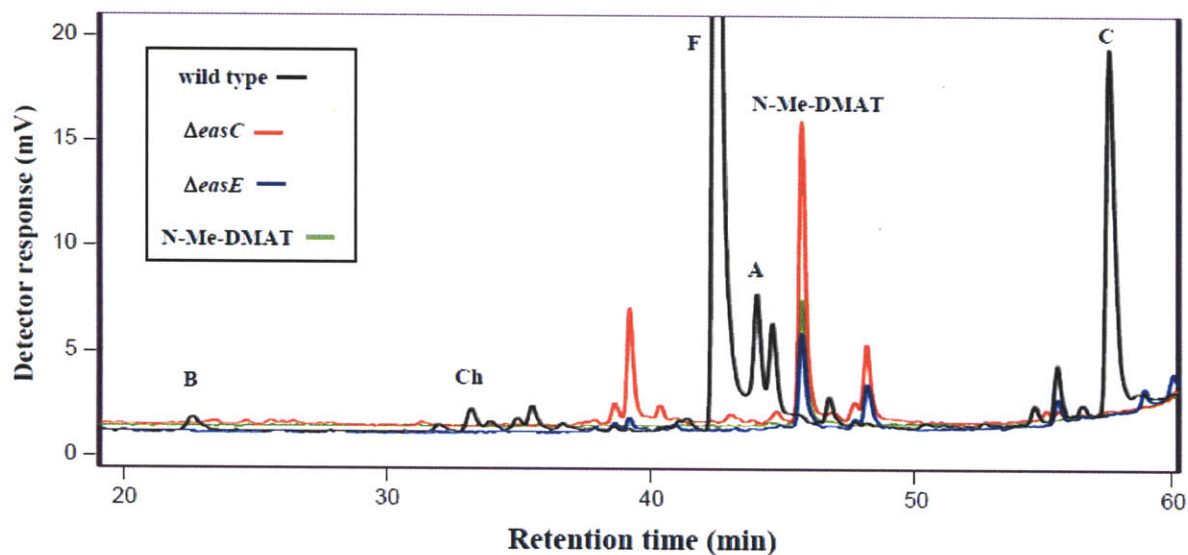
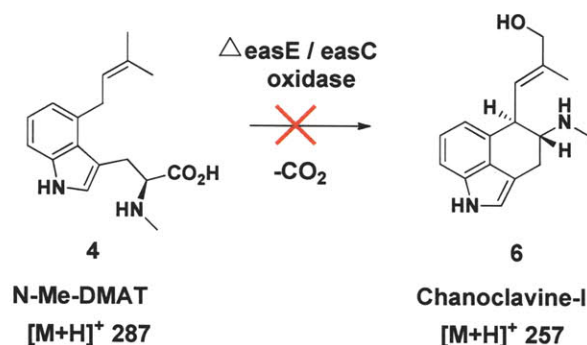


Figure 2.6. LC-MS trace of *A. fumigatus* $\Delta easE$ culture extract (Peak intensities for this set of chromatograms have been normalized to allow relative comparison of compound masses present).



A. Selected ion monitoring for ergot alkaloids festuclavine **11** $[M+H]^+ = 241$ and fumigaclavine C **14** $[M+H]^+ = 367$. This trace shows absence of ergot alkaloids that are observed in wild type *A. fumigatus*.

B. Selected ion monitoring for intermediates DMAT **3** $[M+H]^+ = 273$, *N*-Me-DMAT **4** $[M+H]^+ = 287$, chanoclavine-I **6** $[M+H]^+ = 257$, chanoclavine-I-aldehyde **7** $[M+H]^+ = 255$. This trace displays the mass corresponding to *N*-Me-DMAT **4** $[M+H]^+ = 287$ pathway intermediate.

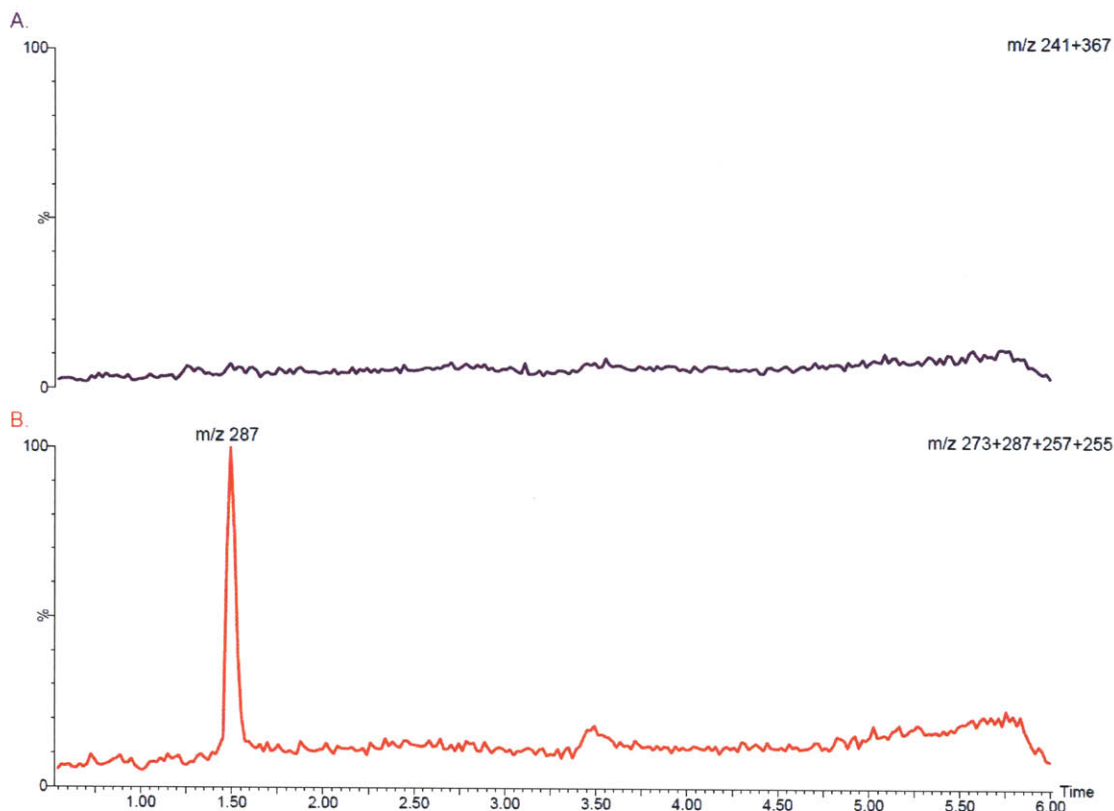
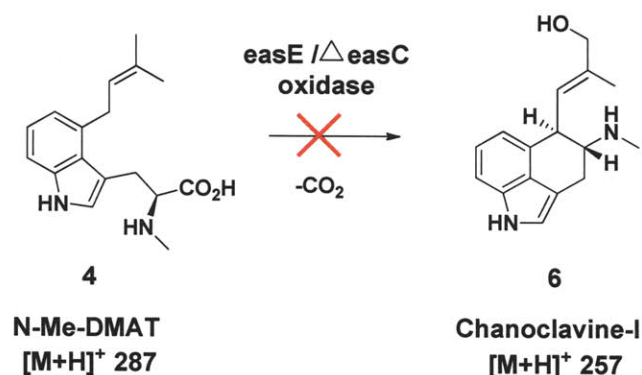
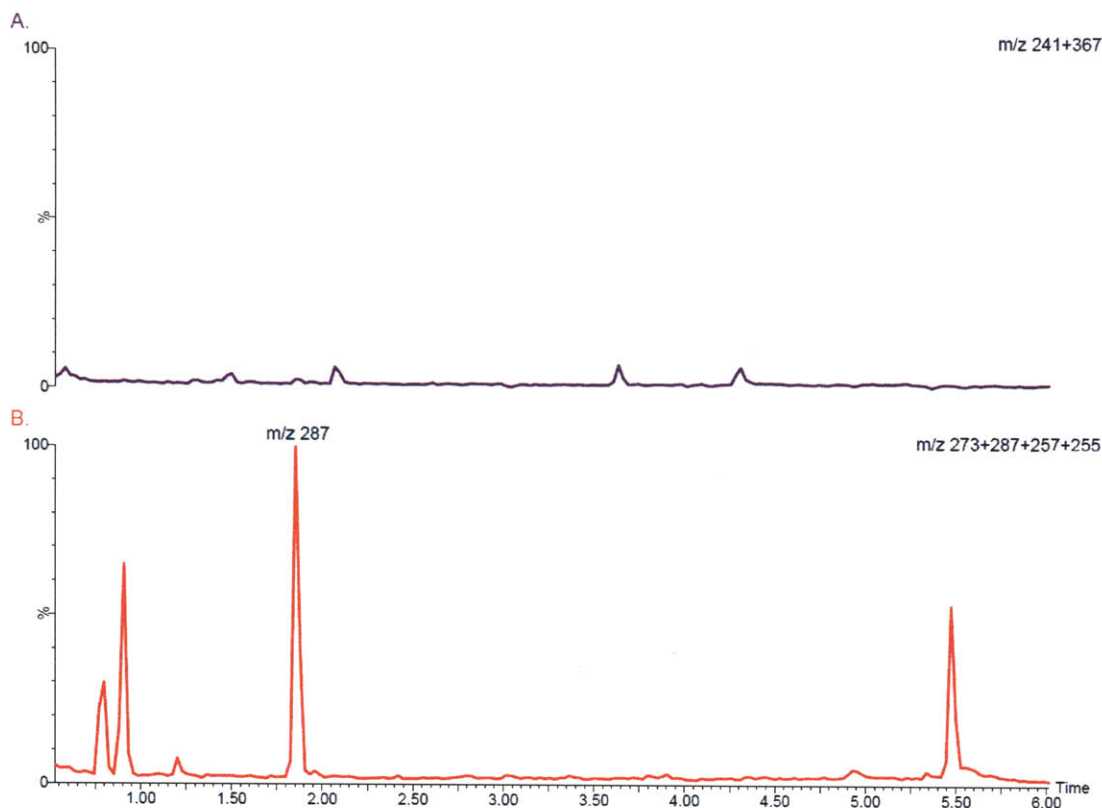


Figure 2.7. LC-MS trace of *A. fumigatus* $\Delta easC$ culture extract (Peak intensities for this set of chromatograms have been normalized to allow relative comparison of compound masses present).



A. Selected ion monitoring for ergot alkaloids festuclavine **11** $[\text{M}+\text{H}]^+ = 241$ and fumigaclavine C **14** $[\text{M}+\text{H}]^+ = 367$. Shows absence of ergot alkaloids that are observed in wild type *A. fumigatus*.

B. Selected ion monitoring for intermediates DMAT **3** $[\text{M}+\text{H}]^+ = 273$, N-Me-DMAT **4** $[\text{M}+\text{H}]^+ = 287$, chanoclavine-I **6** $[\text{M}+\text{H}]^+ = 257$, chanoclavine-I-aldehyde **7** $[\text{M}+\text{H}]^+ = 255$. Displays mass corresponding N-Me-DMAT **4** $[\text{M}+\text{H}]^+ = 287$ pathway intermediate. The peaks at 0.9 min and 5.5 min were attributed to compounds extracted from the culture media that are not identifiable as ergot alkaloids or pathway intermediates.



While the *easE* gene product, homologous to FAD dependent oxidoreductases, could catalyze the 4 electron oxidation necessary for ring C cyclization, the role of the *easC* gene product catalase and its direct involvement in the oxidative transformation to form ring C is not well understood.^{10, 12, 26, 29, 30} The *easC* catalase may serve in a general protective role to *A. fumigatus*, a function that is observed for many other catalases in previous studies.^{4, 31, 32} To further investigate whether the *easC* catalase gene may be necessary for any catalytic steps after ring C cyclization to form chanoclavine-I **6**, an exogenous supply of chanoclavine-I **6** was fed to the $\Delta easC$ mutant to determine if downstream ergot alkaloid production would be restored. To compare levels of downstream ergot alkaloid production, chanoclavine-I **6** was also fed to a $\Delta dmaW$ mutant culture as a positive control.

If the functional role of *easC* was limited only to ring C cyclization, it would be expected that exogenously fed chanoclavine-I **6** would be converted by the downstream pathway enzymes to give festuclavine **11** and fumigaclavine A **18**, B **19**, and C **14** in similar levels to the $\Delta dmaW$ mutant fed with chanoclavine-I **6**. In contrast, if *easC* were acting in a general protective role involved in later steps of the pathway after ring C cyclization, it would be expected that the $\Delta easC$ strain fed with chanoclavine-I **6** would show poor or altered levels of downstream ergot alkaloid production relative to the $\Delta dmaW$ fed with chanoclavine-I **6**. Interestingly, downstream ergot alkaloid production was restored in both $\Delta easC$ and $\Delta dmaW$ cultures to similar levels when fed exogenously supplied chanoclavine-I **6** (Table 2.2). These observations suggested that the *easC* gene product was directly involved in the pathway step toward for the cyclization of ergoline ring C, thus not necessarily functioning as a general protective catalase in other pathway

steps toward ergot alkaloid biosynthesis. These findings also further demonstrate that both EasC and EasE need to be present to catalyze the cyclization of ring C to form chanoclavine-I **6** from *N*-Me-DMAT **4**. Efforts to heterologously express and characterize the functions of *easC* and *easE* gene products *in vitro* were described in Chapter 5.

Table 2.2. Conversion of exogenous chanoclavine-I **6** (26.7 nmol) into downstream ergot alkaloids by cultures of *Aspergillus fumigatus*. Adapted from Goetz et al.²⁸

Ergot Alkaloids (nmol; mean \pm standard error)					
Culture	Chano-I 6	Festoclavine 14	Fumiga B 19	Fumiga A 18	Fumiga C 14
<i>$\Delta easC$</i> control (no Chano-I)	<DL	<DL	<DL	<DL	<DL
<i>$\Delta dmaW$</i> control	<DL	<DL	<DL	<DL	<DL
<i>$\Delta easC$</i> + Chano-I	16.0 \pm 2.7	0.6 \pm 0.08	0.7 \pm 0.03	1.4 \pm 0.03	0.03 \pm 0.01
<i>$\Delta dmaW$</i> + Chano-I	19.4 \pm 1.1	0.3 \pm 0.01	0.6 \pm 0.04	1.4 \pm 0.09	0.04 \pm 0.01
medium + Chano-I (uninoculated)	26.1 \pm 3.7	<DL	<DL	<DL	<DL

Fumiga (Fumigaclavine)

Chano-I (chanoclavine-I)

<DL, below detection limit

***A. fumigatus* gene *easA* and the formation of ergoline ring D**

The *easA* gene, homologous to the Old Yellow Enzyme (OYE) class of flavin dependent oxidoreductases, served as another target for gene disruption experiments. OYE from *Saccharomyces carlsbergensis* had been extensively studied by Massey and co-workers.^{33, 34} OYE enzymes display activity toward the reduction of carbon-carbon double bonds of α,β -unsaturated ketones and aldehydes.^{34, 35} In the early ergot alkaloid biosynthetic pathway, the only proposed intermediate containing an α,β -unsaturated aldehyde was chanoclavine-I-aldehyde **7**; thus the *easA* gene product was likely to play a role in this pathway step to reduce this carbon-carbon double bond to catalyze ring D formation.

When analyzed by fluorescence HPLC (Figure 2.8), the $\Delta easA$ *A. fumigatus* mutant displayed loss of festuclavine **11** and fumigaclavines **A 18**, **B 19**, and **C 14**, but instead accumulated novel peaks at 32 min and 37 min, which were identified as chanoclavine-I **6** and chanoclavine-I-aldehyde **7**, respectively. The peak at 32 min was identified by co-elution with chanoclavine-I **6** standard by HPLC (Figure 2.8) and corresponded to a mass of m/z 257 by LC-MS which is consistent with the mass of chanoclavine-I **6**. Alternatively, the peak at 37 min corresponded to a mass of m/z 255 by LC-MS which is the expected mass of chanoclavine-I-aldehyde **7** (Table 2.1, Figure 2.9). Further analysis by $^1\text{H-NMR}$ resulted in a spectra that matched that previously reported for chanoclavine-I-aldehyde **7** (Figure 3.12).³⁶

These data suggested that the *easA* gene product catalyzed the formation of the ergoline ring D, where the $\Delta easA$ mutant accumulated upstream precursors chanoclavine-I **6** and chanoclavine-I-aldehyde **7**. In Chapter 3, the heterologous expression and

functional characterization of the *A. fumigatus easA* gene product is presented, demonstrating that EasA catalyzes the reduction of chanoclavine-I-aldehyde **7** to cyclize ergoline ring D *in vitro*.

Figure 2.8. Fluorescence HPLC ergot alkaloid profiles of cultures wild type, gene disrupted *easA* ($\Delta easA$), and gene disrupted *easA* complemented with *C. purpurea easA* ($\Delta easA + C.p. easA$). Adapted from Coyle et al.¹³

Wild type displays accumulation of alkaloids (B = fumigaclavine B **19**, F = festuclavine **11**, A = fumigaclavine A **18**, C = fumigaclavine C **14**). $\Delta easA$ gene disrupted mutant displays accumulation of intermediates (Ch = chanoclavine-I **6** and Ald = chanoclavine-I-aldehyde **7**). $\Delta easA + C.p. easA$ gene disrupted mutant complemented with *C. purpurea easA* accumulated alkaloids (Ag = agroclavine **10**, and S/I = setoclavine **22** or isosetoclavine **23**). The relative sequence of elution for the setoclavine **22** and isosetoclavine **23** diastereoisomeric pair remains to be determined. Detection was by fluorescence with excitation and emission (272 nm / 372 nm) and (310 nm / 410 nm).

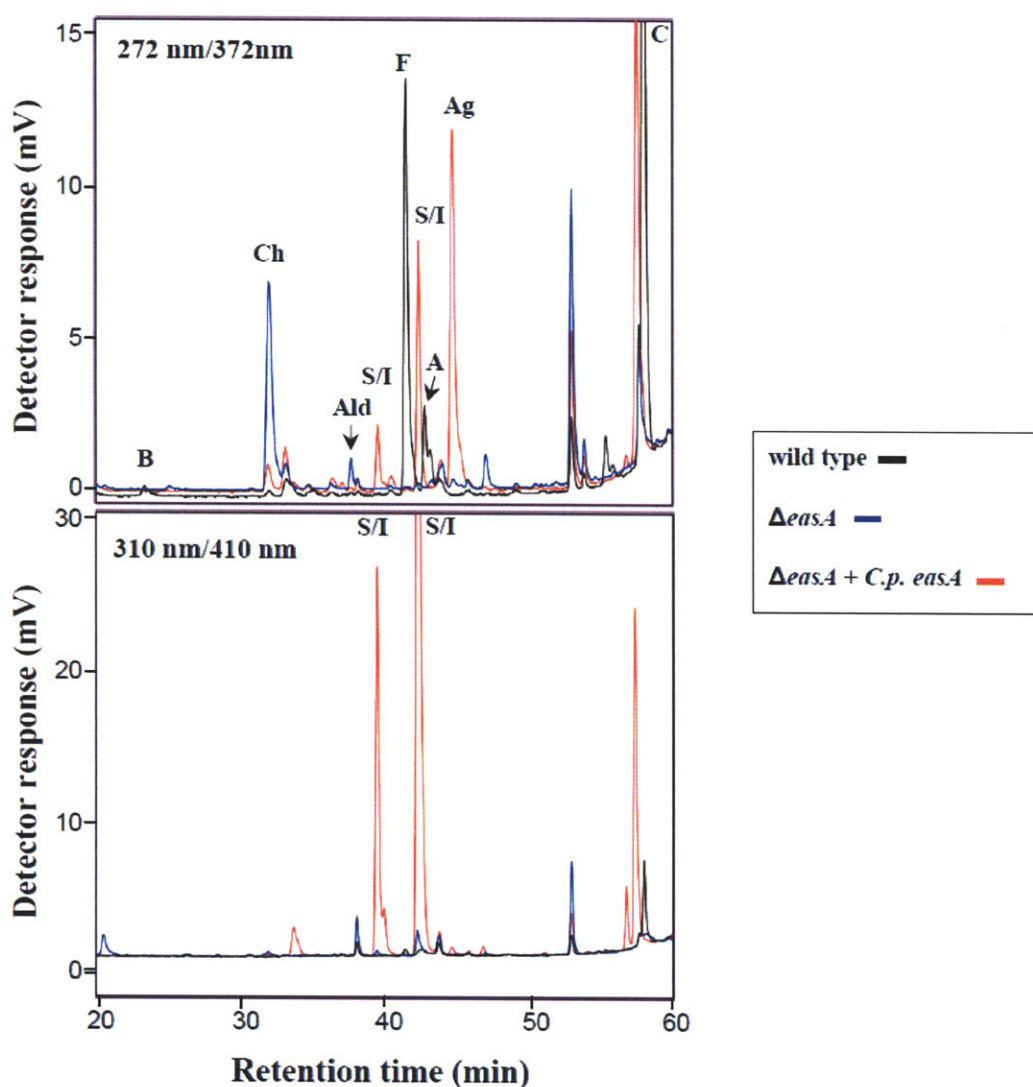
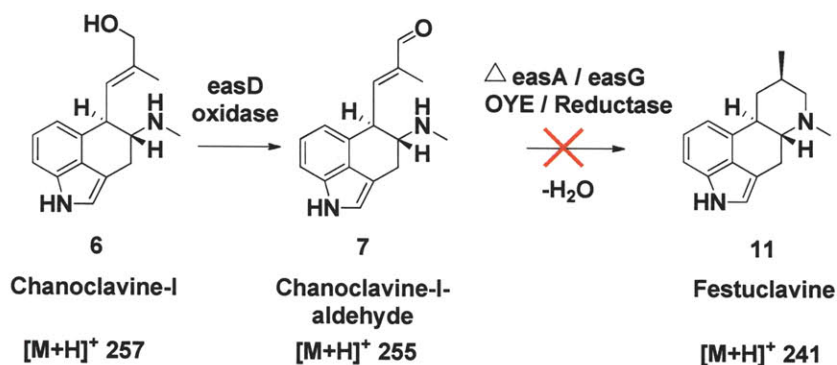
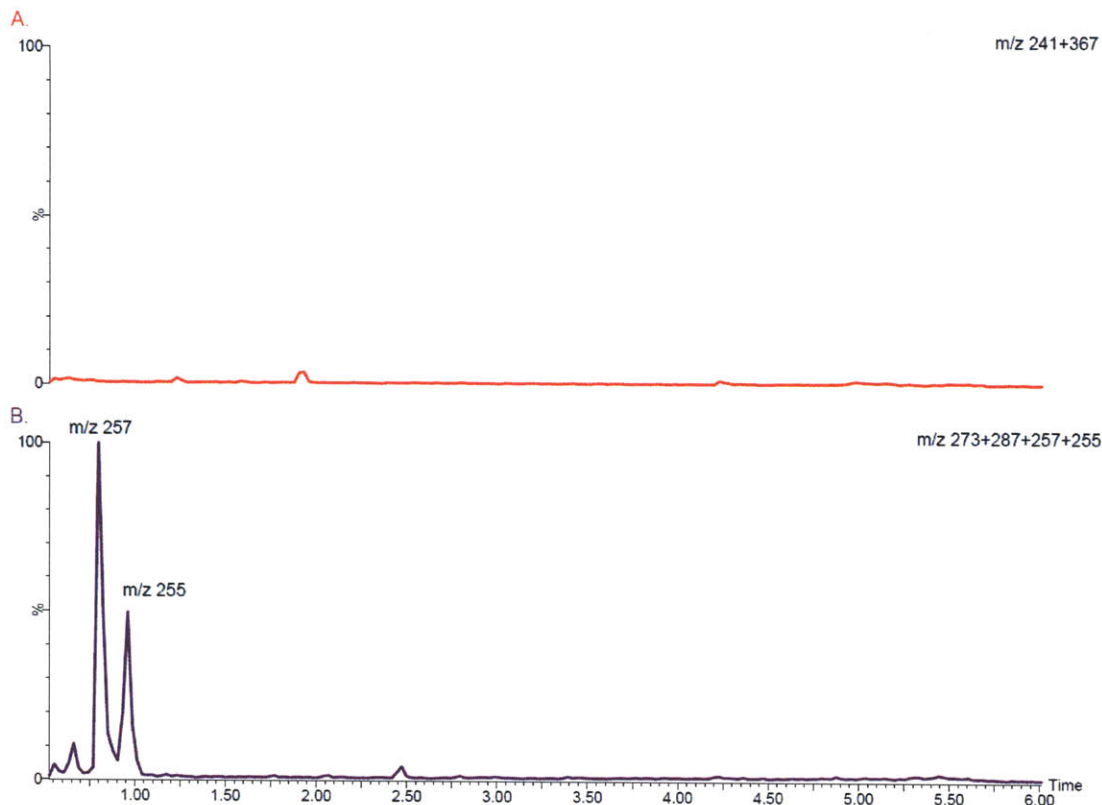


Figure 2.9. LC-MS trace of *A. fumigatus* $\Delta easA$ culture extract (Peak intensities for this set of chromatograms have been normalized to allow relative comparison of compound masses present).



A. Selected ion monitoring for ergot alkaloids festuclavine **11** $[M+H]^+ = 241$ and fumigaclavine C **14** $[M+H]^+ = 367$. This trace shows absence of ergot alkaloids that are observed in wild type *A. fumigatus*.

B. Selected ion monitoring for intermediates DMAT **3** $[M+H]^+ = 273$, *N*-Me-DMAT **4** $[M+H]^+ = 287$, chanoclavine-I **6** $[M+H]^+ = 257$, chanoclavine-I-aldehyde **7** $[M+H]^+ = 255$. Displays masses corresponding to chanoclavine-I **6** $[M+H]^+ = 257$ and chanoclavine-I-aldehyde **7** $[M+H]^+ = 255$ pathway intermediates.



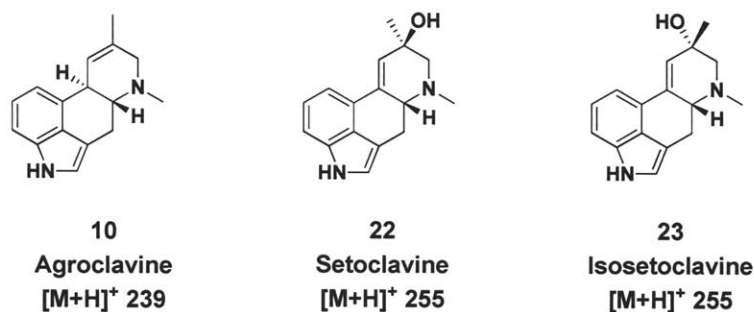
Augmentation of *A. fumigatus* $\Delta easA$ with *C. purpurea easA* and resulting ergot alkaloid structural divergence

The accumulation of chanoclavine-I-aldehyde **7** in $\Delta easA$ suggested that the *easA* gene product plays a catalytic role in the cyclization of ergoline ring D. As presented in Chapter 1, ergot alkaloids with a fully saturated D ring of the ergoline structure such as festuclavine **11** were produced by *A. fumigatus* while ergot alkaloids that have an unsaturated ergoline D ring between the C8 and C9 positions such as agroclavine **10** were produced by Clavicipitaceous fungi *C. purpurea* and *N. lolii*. Due to the shared early steps of ergot alkaloid biosynthesis observed across various fungal species, chanoclavine-I-aldehyde **7** was likely to be the last common precursor prior to pathway divergence at ring D formation, to give either agroclavine **10** or festuclavine **11** derived downstream ergot alkaloids. Therefore, the *easA* gene product was likely to function at the branch point of ergot alkaloid biosynthesis.

To test whether the *easA* gene product functioned at this structural branch point in ergot alkaloid biosynthesis, the *A. fumigatus* $\Delta easA$ mutant was augmented with a wild type allele of *easA* from a *C. purpurea* fungal species that produces agroclavine **10**. HPLC analysis of the *A. fumigatus* $\Delta easA$ + *C. purpurea easA* (*CpeasA*) augmented mutant showed significantly reduced accumulation of peaks identified with chanoclavine-I **6** and chanoclavine-I-aldehyde **7** that were observed in the $\Delta easA$ gene disrupted profile. Peaks that were associated with festuclavine **11** and fumigaclavines produced by wild type *A. fumigatus* were also not present in the augmented *CpeasA* mutant (Figure 2.8). Notably, three novel peaks appeared in the HPLC fluorescence profile for the augmented *CpeasA* mutant, which included peaks eluting at 39 min, 42 min, and 44 min

(Figure 2.8). The peak at 44 min was identified by co-elution with an agroclavine **10** standard on HPLC, and subsequent analysis by LC-MS revealed a compound with m/z 239, which is consistent with the expected mass of agroclavine **10** (Figure 2.10A). Peaks at 39 min and 42 min were similarly identified by co-elution with standards for the diastereoisomeric pair setoclavine **22** and isosetoclavine **23** on HPLC (Figure 2.8), where further analysis by LC-MS demonstrated that these peaks corresponded to a mass of m/z 255, which is the expected mass of setoclavine **22** and isosetoclavine **23** (Figure 2.10. B, C).

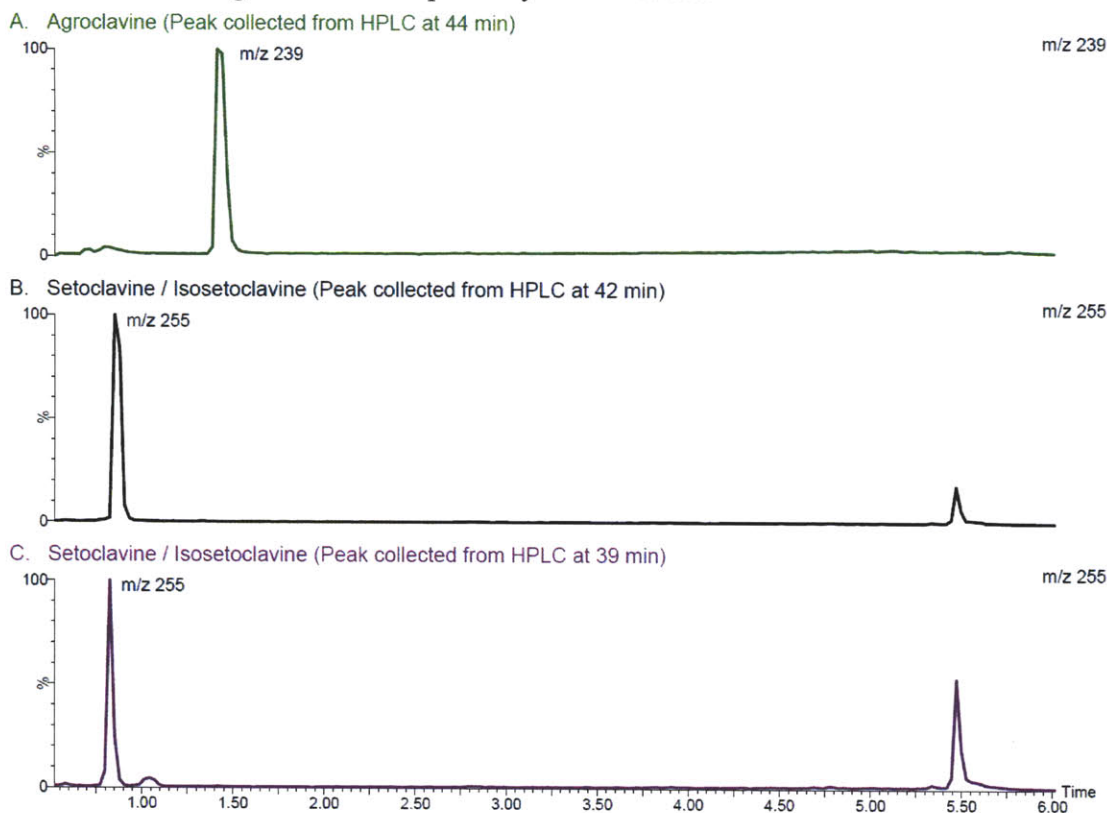
Figure 2.10. LC-MS analysis of peaks collected from HPLC of *A. fumigatus* $\Delta easA$ + *C. purpurea easA* (Figure 2.8) at 39, 42, and 44 min.



A. LC-MS analysis of peak collected at 44 min from HPLC. Selected ion monitoring for m/z 239 displays peak at 1.4 min which corresponds to the expected mass of agroclavine **10** at $[M+H]^+ = 239$.

B. LC-MS analysis of peak collected at 42 min from HPLC. Selected ion monitoring for m/z 255 displays peak at 0.8 min which corresponds to the expected mass of setoclavine **22** / isosetoclavine **23** at $[M+H]^+ = 255$. Peak at 5.5 min was a trace impurity not identifiable as an ergot alkaloid or pathway intermediate.

C. LC-MS analysis of peak collected at 39 min from HPLC. Selected ion monitoring for m/z 255 displays peak at 0.8 min which corresponds to the expected mass of setoclavine **22** / isosetoclavine **23** at $[M+H]^+ = 255$. Peak at 5.5 min was a trace impurity not identifiable as an ergot alkaloid or pathway intermediate.



These results demonstrated that the *A. fumigatus* $\Delta easA$ augmented with *C. purpurea* *easA* allele resulted in a drastically different ergot alkaloid profile where wild type *A. fumigatus* ergot alkaloids festuclavine **11** and fumigaclavine production was not restored. Instead, the production of agroclavine **10** and its oxidation products setoclavine **22** and isosetoclavine **23**, normally produced by *C. purpurea*, was observed. Setoclavine **22** and isosetoclavine **23** were oxidation products derived from agroclavine **10**, and have been previously observed when agroclavine **10** is fed to cultures of *A. fumigatus*,³⁷ so the production of these diastereoisomeric products **22** and **23** provides additional evidence that agroclavine **10** is produced in this *A. fumigatus* strain. The considerable change in ergot profile that is dependent on the individual *easA* gene demonstrates that the *easA* gene product controls the branch point of ergot alkaloid biosynthesis toward the production of either agroclavine **10** or festuclavine **11** derived downstream products. In our efforts to understand the mechanism governing pathway divergence in ergot alkaloids, these findings guided the heterologous expression and functional characterization of the *easA* homologue from the agroclavine **10** producer *N. lolii* described in Chapter 4.

Conclusion

This chapter describes the assignment of function to clustered ergot alkaloid biosynthetic genes. Gene disruption of *dmaW* led to the loss of ergot alkaloid production in *A. fumigatus*, reinforcing the role of *dmaW* in the first committed step of ergot alkaloid biosynthesis. Disruption of *easF* and the resulting accumulation of DMAT **3**, established the role of this gene as an N-methyltransferase at the second step of ergot biosynthesis. The resulting ergot profiles of both of these gene disrupted mutants parallel the results from *in vitro* functional characterization studies that have been reported for *dmaW* and *easF* gene products.^{3, 25}

Knockout mutants of *easE* and *easC*, $\Delta easE$ and $\Delta easC$, show accumulation of common pathway intermediate *N*-Me-DMAT **4**, demonstrating their catalytic role in the formation of ergoline ring C. The chanoclavine-I **6** feeding studies to $\Delta easC$ further demonstrated that the *easC* gene product was essential for the formation of ergoline ring C and that this gene product did not play a role as a general protective catalase in other parts of the ergot pathway for *A. fumigatus*. Efforts to understand the mechanism in which EasE and EasC work to form ergoline ring C were investigated via the heterologous expression and functional characterization of these proteins as detailed in Chapter 5.

Gene disruption of *A. fumigatus easA*, and the resulting accumulation of chanoclavine-I **6** and chanoclavine-I-aldehyde **7** with loss of downstream ergot alkaloids, established the functional role of EasA in the cyclization of ergoline ring D. Augmentation of *A. fumigatus* $\Delta easA$ mutant with the *C. purpurea easA* allele resulted in production of agroclavine **10** and its oxidation products as opposed to festuclavine **11** or

fumigaclavines of wild type *A. fumigatus*. This suggests that subtle catalytic active site differences across *easA* homologues from different fungal species may be responsible for structural divergence of alkaloids across different ergot classes. The mechanistic principle governing such pathway divergence caused by the *easA* gene product is discussed in greater detail in Chapters 3 and 4.

These *in vivo* gene disruption experiments described in this chapter were essential toward guiding our efforts toward the *in vitro* cloning, heterologous expression, and functional characterization of the enzymes responsible for ergoline ring C and D formation.

References

1. Keller, N., G. Turner, and J. Bennett, *Fungal Secondary Metabolism - From Biochemistry to Genomics*. Nature Reviews Microbiology, 2005. **3**: p. 937-947.
2. Coyle, C.M., S. Kenaley, W. Rittenour, and D.G. Panaccione, *Association of ergot alkaloids with conidiation in Aspergillus fumigatus*. Mycologia, 2007. **99**(6): p. 804-811.
3. Unsold, I. and S.-M. Li, *Overproduction, purification and characterization of FgaPT2, a dimethylallyltryptophan synthase from Aspergillus fumigatus*. Microbiology, 2005. **151**: p. 1499-1505.
4. Haarmann, T., C. Machado, Y. Lubbe, T. Correia, C.L. Schardl, D.G. Panaccione, and P. Tudzynski, *The ergot alkaloid gene cluster in Claviceps purpurea: Extension of the cluster sequence and intra species evolution*. Phytochemistry, 2005. **66**: p. 1312-1320.
5. Tudzynski, P., K. Holter, T. Correia, C. Arntz, N. Grammel, and U. Keller, *Evidence for an ergot alkaloid gene cluster in Claviceps purpurea*. Molecular and General Genetics, 1999. **261**: p. 133-141.
6. Fleetwood, D., B. Scott, G. Lane, A. Tanaka, and R. Johnson, *A Complex Ergovaline Gene Cluster in Epichloa Endophytes of Grasses*. Applied and Environmental Microbiology, 2007. **73**(8): p. 2571-2579.
7. Wang, J., C. Machado, D.G. Panaccione, H.-F. Tsai, and C.L. Schardl, *The determinant step in ergot alkaloid biosynthesis by an endophyte of perennial ryegrass*. Fungal Genetics and Biology, 2004. **41**: p. 189-198.
8. Coyle, C.M. and D.G. Panaccione, *An Ergot Alkaloid Biosynthesis Gene and Clustered Hypothetical Genes from Aspergillus fumigatus*. Applied and Environmental Microbiology, 2005. **71**(6): p. 3112-3118.
9. Haarmann, T., I. Ortel, P. Tudzynski, and U. Keller, *Identification of the cytochrome P450 monooxygenase that bridges the clavine and ergoline alkaloid pathways*. ChemBiochem, 2006. **7**: p. 645 - 652.
10. Schardl, C.L., D.G. Panaccione, and P. Tudzynski, *Ergot Alkaloids - Biology and Molecular Biology*, in *The Alkaloids* G. Cordell, Editor. 2006, Elsevier. p. 45-86.
11. Floss, H.G., *From Ergot to Ansamycins - 45 Years in Biosynthesis*. Journal of Natural Products, 2006. **69**: p. 158-169.
12. Floss, H.G. and J. Anderson, *The Biosynthesis of Mycotoxins*, P. Steyn, Editor. 1980, Academic Press. p. 17-67.
13. Coyle, C.M., J.Z. Cheng, S.E. O'Connor, and D.G. Panaccione, *An Old Yellow Enzyme Gene Controls the Branch Point between Aspergillus fumigatus and Claviceps purpurea Ergot Alkaloid Pathways*. Applied and Environmental Microbiology, 2010. **76**(12): p. 3898-3903.
14. Orbach, M.J., *A cosmid with a HyR marker for fungal library construction and screening*. Gene, 1994. **150**: p. 159-162.
15. Murray, F.R., G.C.M. Latch, and D.B. Scott, *Surrogate transformation of perennial ryegrass, Lolium perenne, using genetically modified Acremonium endophyte*. Molecular and General Genetics, 1992. **233**: p. 1-9.
16. Panaccione, D.G., R. Johnson, J. Wang, C. Young, P. Damrongkool, B. Scott, and C.L. Schardl, *Elimination of ergovaline from a grass-Neotyphodium endophyte*

- symbiosis by genetic modification of the endophyte*. Proceedings of the National Academy of Sciences of the United States of America, 2001. **98**(22): p. 12820-12825.
17. Panaccione, D.G., B.A. Tapper, G.A. Lane, E. Davies, and K. Fraser, *Biochemical outcome of blocking the ergot alkaloid pathway of a grass endophyte*. Journal of Agricultural and Food Chemistry, 2003. **51**: p. 6429-6437.
 18. Panaccione, D.G. and C.M. Coyle, *Abundant Respirable Ergot Alkaloids from the Common Airborne Fungus Aspergillus fumigatus*. Applied and Environmental Microbiology, 2005. **71**(6): p. 3106-3111.
 19. Scigelova, M., T. Macek, A. Minghetti, M. Mackova, P. Sedmera, A. Prikrylova, and V. Kren, *Biotransformation of ergot alkaloids by plant cell cultures with high peroxidase activity*. Biotechnology Letters, 1995. **17**: p. 1213-1218.
 20. Taylor, E.H. and H.R. Shough, *Enzymology of ergot alkaloid biosynthesis. II. The oxidation of agroclavine by horseradish peroxidase*. Lloydia, 1967. **30**: p. 197-201.
 21. Taylor, E.H., K.J. Goldner, S.F. Pong, and H.R. Shough, *Conversion of $\Delta^{8,9}$ ergolines to $\Delta^{9,10}$ -8-hydroxyergolines in plant homogenates*. Lloydia, 1966. **29**: p. 239-244.
 22. Spilsbury, J.F. and S. Wilkinson, *The isolation of festuclavine and two new clavine alkaloids from Aspergillus fumigatus Fres*. Journal of the Chemical Society, 1961. **5**: p. 2085-2091.
 23. Otsuka, H., F.R. Quigley, D. Groger, J.A. Anderson, and H.G. Floss, *In Vivo and In Vitro Evidence for N-Methylation as the Second Pathway-Specific Step in Ergoline Biosynthesis*. Planta Medica, 1980. **40**: p. 109-119.
 24. Floss, H.G., *Biosynthesis of Ergot Alkaloids and Related Compounds*. Tetrahedron 1976. **32**: p. 873-912.
 25. Rigbers, O. and S.-M. Li, *Ergot Alkaloid Biosynthesis in Aspergillus fumigatus Overproduction and Biochemical Characterization of a 4-Dimethylallyltryptophan N-Methyltransferase*. The Journal of Biological Chemistry, 2008. **283**(40): p. 26859-26868.
 26. Kozikowski, A., C. Chen, J. Wu, M. Shibuya, C. Kim, and H.G. Floss, *Probing ergot alkaloid biosynthesis: intermediates in the formation of ring C*. Journal of the American Chemical Society, 1993. **115** (6): p. 2482-2488.
 27. Lorenz, N., J. Olsovska, M. Sulc, and P. Tudzynski, *Alkaloid Cluster Gene ccsA of the Ergot Fungus Claviceps purpurea Encodes Chanoclavine I Synthase, a Flavin Adenine Dinucleotide-Containing Oxidoreductase Mediating the Transformation of N-Methyl-Dimethylallyltryptophan to Chanoclavine I*. Applied and Environmental Microbiology, 2010. **76**(6): p. 1822-1830.
 28. Goetz, K.E., C.M. Coyle, J.Z. Cheng, S.E. O'Connor, and D.G. Panaccione, *Ergot cluster-encoded catalase is required for synthesis of chanoclavine-I in Aspergillus fumigatus*. Current Genetics, 2011(accepted).
 29. Haarmann, T., Y. Rolke, S. Giesbert, and P. Tudzynski, *Ergot: from witchcraft to biotechnology*. Molecular Plant Pathology, 2009. **10**(4): p. 563-577.
 30. Wallwey, C. and S.-M. Li, *Ergot alkaloids: structure diversity, biosynthetic gene clusters and functional proof of biosynthetic genes*. Natural Products Reports, 2011. **28**(3): p. 496-510.

31. Zamocky, M., C. Herzog, L. Nykyri, and F. Koller, *Site-directed mutagenesis of the lower parts of the major substrate channel of yeast catalase A leads to highly increased peroxidatic activity*. FEBS Letters, 1995. **367**(241-245).
32. Mate, M., M. Zamocky, L. Nykyri, C. Herzog, P. Alzari, C. Betzel, F. Koller, and I. Fita, *Structure of catalase-A from Saccharomyces cerevisiae*. Journal of Molecular Biology, 1999. **286**(1): p. 135-149.
33. Karplus, P.A., K. Fox, and V. Massey, *Structure-function relations for old yellow enzyme*. The FASEB Journal, 1995. **9**: p. 1518-1526.
34. Williams, R. and N. Bruce, 'New uses for an old enzyme' – the old yellow enzyme family of flavoenzymes. Microbiology, 2002. **148**: p. 1607-1614.
35. Fox, K. and P.A. Karplus, *Old yellow enzyme at 2 Å resolution: overall structure, ligand binding, and comparison with related flavoproteins*. Structure, 1994. **15**(2): p. 1089-1105.
36. Floss, H.G., M. Tchong-Lin, C. Chang, B. Naidoo, G. Blair, C. Abou-Chaar, and J. Cassady, *Biosynthesis of ergot alkaloids. Mechanism of the conversion of chanoclavine-I into tetracyclic ergolines*. Journal of the American Chemical Society, 1974: p. 1898-1909.
37. Béliveau, J. and E. Ramstad, *8-Hydroxylation of agroclavine and elymoclavine by fungi*. Lloydia, 1967. **29**(234-238).

Chapter 3 . Role of Redox Enzymes Involved with the formation of Ergoline Ring D

Parts of this chapter has been published in

Cheng, J.Z., C.M. Coyle, D.G. Panaccione, and S.E. O'Connor, *A Role for Old Yellow Enzyme in Ergot Alkaloid Biosynthesis*. Journal of the American Chemical Society, 2010. **132**(6): p. 1776-1777.

Introduction

The *easA* gene is conserved in ergot alkaloid biosynthetic clusters across divergent fungi including *A. fumigatus*, *C. purpurea*, and *N. lolii*, and is believed to participate in the early pathway formation of the ergoline ring.¹ The gene knockout mutant $\Delta easA$ of *A. fumigatus*, in contrast to the wild type strain, failed to accumulate downstream ergot alkaloids fumigaclavine C **14** but instead displayed accumulation of upstream intermediates chanoclavine-I **6** and chanoclavine-I-aldehyde **7** as discussed in Chapter 2. This finding demonstrated that the *easA* gene product played a catalytic role in the cyclization of ergoline ring D.

The gene product of *A. fumigatus easA* (EasA_Af) was proposed to be a suitable candidate enzyme for turning over the chanoclavine-I-aldehyde **7** substrate, as it displays protein sequence homology to the Old Yellow Enzyme (OYE) family of proteins (Figure 3.1).²⁻⁵ OYE was initially isolated from brewer's bottom yeast and first described by Warburg and Christian in 1932.⁶ In the years following, Theorell purified OYE and demonstrated that OYE consisted of a colorless apoprotein and a yellow co-factor identified as flavin-mononucleotide (FMN).⁷

In later work, Vincent Massey's group extensively characterized an OYE from *S. carlsbergensis* brewer's bottom yeast (designated as OYE1)⁸. In general, substrates for members of the OYE family included oxygen, quinones, and α,β -unsaturated double bonds of aldehydes and ketones (Figure 3.2).^{2, 4, 8-13} While the exact physiological function of OYE1 has only been speculative, other homologues of OYE have been associated with metabolic pathways in bacteria and plants (Figure 3.2).¹⁴⁻¹⁷

Figure 3.1. Protein sequence alignments with EasA_Af and Old Yellow Enzyme homologues. Conserved amino acid residues important to the OYE mechanism are highlighted in red.

```

OYE1_Q02899      MSFVKDFKPKQALGDTNLFKPIKIGNNELLHRAVIPPLTRMRALHPGNI PN 50
OYE2_AAA83386    MPFVKDFKPKQALGDTNLFKPIKIGNNELLHRAVIPPLTRMRALHPGNI PN 50
OYE3_P41816      MPFVKGFEPISLSDTNLFEPKIGNTQLAHRAVMPPLTRMRATHPGNI PN 50
NADPHoxidase_kluyv_AAA98815 MSFMN-FEPKPLADTDIFKPIKIGNTELKHRVMPALTRMRALHPGNVPN 49
easA_afumigatus_XP_756133 -----MREEPSAQLFKPLKVGRCHLQHRMIMAPTTRFRADGQG-VPL 42
                  .:::*.:::*. . * * :. . * : * * * : * : *

OYE1_Q02899      RDWAVEYYTQRAQRPGTMIITEGAFISPGAGGYDNAPGVWSEEQMVWETK 100
OYE2_AAA83386    RDWAVEYYAQRAQRPGTMIITEGTFPSQSGGYDNAPGIWSEEQIKEWTK 100
OYE3_P41816      KEWAAYVYQRAQRPGTMIITEGTFISPGAGGYDNAPGIWSEDEQVAEWKN 100
NADPHoxidase_kluyv_AAA98815 PDWAVEYYRQRSQYPGTMIITEGAFPSAQSGGYDNAPGVWSEEQLAQWRK 99
easA_afumigatus_XP_756133 P-FVQYVYQQRASVPGTLLITEATDITPKAMGYKHVPGIWSPEQREAWRE 91
                  . . * * * : . * : * : * : * : . : . : * : . : * : * : * : *

OYE1_Q02899      IFNAIHEKKSFWVWQLWVLGWAAFPDNLARDGLRYDSASDNVFMDAEQEA 150
OYE2_AAA83386    IFKAIHENKSAFWVQLWVLGWAAFPDNLARDGLRYDSASDNVFMNAEQEE 150
OYE3_P41816      IFLAIHDCQSAFWVQLWSLGWASFPDVLARDGLRYDCASDRVYMNATLQE 150
NADPHoxidase_kluyv_AAA98815 IFKAIHDNKSFWVWQLWVLGRQAFADNLARDGLRYDSASDEVYMGDEKE 149
easA_afumigatus_XP_756133 IVSRVHSHKCFIFCQLWATGRAADPDVLA--DMKDLISSAVPVEEK--- 136
                  * . : * . : * : * * * : . * * * . : : : * : . : * :

OYE1_Q02899      KAKKANNPQHSLTKDEIKQYIKEYVQAAKNSIAAGADGVEIHSANGYLLN 200
OYE2_AAA83386    KAKKANNPQHSITKDEIKQYVKEYVQAAKNSIAAGADGVEIHSANGYLLN 200
OYE3_P41816      KAKDANNLEHSLTKDDIKQYIKDYIHAAKNSIAAGADGVEIHSANGYLLN 200
NADPHoxidase_kluyv_AAA98815 RAIRSNNPQHSGITKDEIKQYIRDYVDAAKKCIDAGADGVEIHSANGYLLN 199
easA_afumigatus_XP_756133 -----GPLPRALTEDEIQCCIADFAQAARNAINAGFDGVEIHGANGYLID 181
                  . : . : * : * : * : : : . * : . : * * * * * : * : * : * :

OYE1_Q02899      QFLDPHSNTRTDEYGGSIENRARFTLEVVDALVEAIGHEKVGLRLSPYGV 250
OYE2_AAA83386    QFLDPHSNTRTDEYGGSIENRARFTLEVVDADVDAIGPEKVGLRLSPYGV 250
OYE3_P41816      QFLDPHSNKRTRDEYGGTIENRARFTLEVVDALITETIGPERVGLRLSPYGT 250
NADPHoxidase_kluyv_AAA98815 QFLDPI SNKRTDEYGGSIENRARFVLEVVDADVDAVGAERTSIRFSPYGV 249
easA_afumigatus_XP_756133 QFTQKSCNHRQDRWGGSIENRARFAVEVTRAVIEAVGADRVGVKLSYPSQ 231
                  * * : . * * * : * : * : * : * : * : * : * : * : * : * : * : * :

OYE1_Q02899      FNSMSGGAETGIVAQYAYVAGELEKRAKAGKRLAFVHLVEPRVTNPFLTE 300
OYE2_AAA83386    FNSMSGGAETGIVAQYAYVLGELEKRAKAGKRLAFVHLVEPRVTNPFLTE 300
OYE3_P41816      FNSMSGGAEPGIIAQYSYVLGELEKRAKAGKRLAFVHLVEPRVTNPFLTE 300
NADPHoxidase_kluyv_AAA98815 FGTMSGVSDPVLVAQFAYVLAELKRAKAGKRLAYVDLVEPRVTSFPQPE 299
easA_afumigatus_XP_756133 YLGMG--TMDELVPQFEYLIAQMRR----LDVAYLHLANSRWLD----- 269
                  : * . : : . : * : * : : : : : : : * : . : . : * .

OYE1_Q02899      GEGEYEGGSNDFVYSIWKG--PVIRAGNF-ALHPEVVREEVKDK---RTL 344
OYE2_AAA83386    GEGEYNGGSNKFAYSIWKG--PIIRAGNF-ALHPEVVREEVKDP---RTL 344
OYE3_P41816      GEGEYSEGTNDFAYSIWKG--PIIRAGNY-ALHPEVVREQVKDP---RTL 344
NADPHoxidase_kluyv_AAA98815 FEGWYKGTNEFVYSVWKG--NVLRVGNY-ALDPDAAITDSKNP---NTL 343
easA_afumigatus_XP_756133 EEKPHDPDPNHEVFRVWVGQSSPILLAGGYDAASAEKVTEQMAAATYTNVA 319
                  * : : . . . : * : : . : * : * . . : . .

OYE1_Q02899      IGYGRFFISNPDLVDRLEKGLPLNKYDRDTFY-QMSAHGYIDYPTYEEAL 393
OYE2_AAA83386    IGYGRFFISNPDLVDRLEKGLPLNKYDRDTFY-KMSAEGYIDYPTYEEAL 393
OYE3_P41816      IGYGRFFISNPDLVYRLEELPLNKYDRSTFY-TMSAEGYIDYPTYEEAV 393
NADPHoxidase_kluyv_AAA98815 IGYGRAFIANPDLVERLEKGLPLNKYDRPSFY-KMSAEGYIDYPTYEEAV 392
easA_afumigatus_XP_756133 IAFGRYFISTPDLFPRVMAGIQLQKYDRASFYSTLSREGYLDYPFSAEYM 369
                  * : * * * : * * * : * : * : * : * : * : * : * : * : * :

OYE1_Q02899      KLGWDKK 400
OYE2_AAA83386    KLGWDKN 400
OYE3_P41816      DLGWNKN 400
NADPHoxidase_kluyv_AAA98815 AKGYKK- 398
easA_afumigatus_XP_756133 ALHNFFV 376

```

Protein Sequence Alignments with *A. fumigatus* EasA

OYE1 ID = 40% Positives = 58%
 OYE2 ID = 41% Positives = 58%
 OYE3 ID = 40% Positives = 57%
 Kluyveromyces ID = 39% Positives = 55%

Defining characteristics of OYE include a non-covalently bound FMN as a cofactor and the requirement of NADPH as a reducing agent. The reduction of the carbon-carbon double bonds of α,β -unsaturated aldehydes or ketones by OYE involves two half reactions (Figure 3.3). First, in the reductive half reaction for OYE, one molecule of NADPH binds to the OYE active site, where a hydride is transferred from NADPH to reduce the FMN cofactor of OYE. Subsequently, NADP^+ leaves the active site.^{4, 18} In the oxidative half reaction, the hydride on the reduced FMN cofactor of OYE reduces a substrate such as 2-cyclohexenone to yield cyclohexanone.^{12, 19} The catalytic cycle of OYE has been previously demonstrated to function in a ping-pong bi-bi mechanism.^{2, 10, 11, 19-21}

Figure 3.2. Representative substrates of various OYE homologues. A. 2-cyclohexenone to 2-cyclohexanone (*Saccharomyces carlsbergensis*)²; B. Acrolein to Propionaldehyde (*Saccharomyces carlsbergensis*, *Saccharomyces cerevisiae*)^{9, 17}; C. Morphinone to Hydromorphone (*Pseudomonas putida*)^{16, 22}; D. 9S,13S-12-oxophytodienoate to 1S,2S-3-oxo-2(2'[Z]-pentenyl)-cyclopentane-1-octanoate (*Lycopersicon esculentum*, *Arabidopsis thaliana*)¹⁵; E. Chanoclavine-I-aldehyde **7** to Dihydrochanoclavine-I-aldehyde **24** (*Aspergillus fumigatus*)^{23, 24}

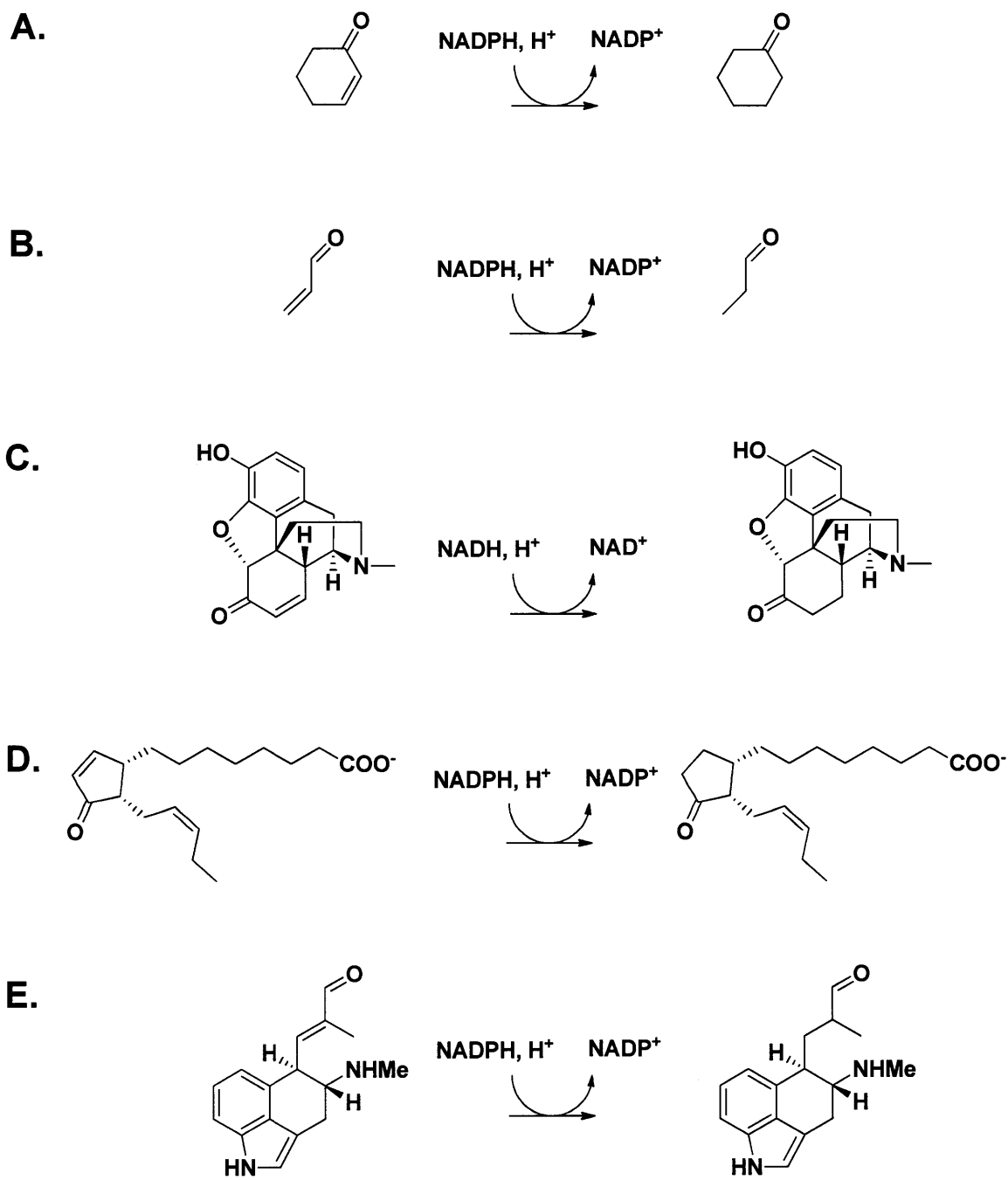
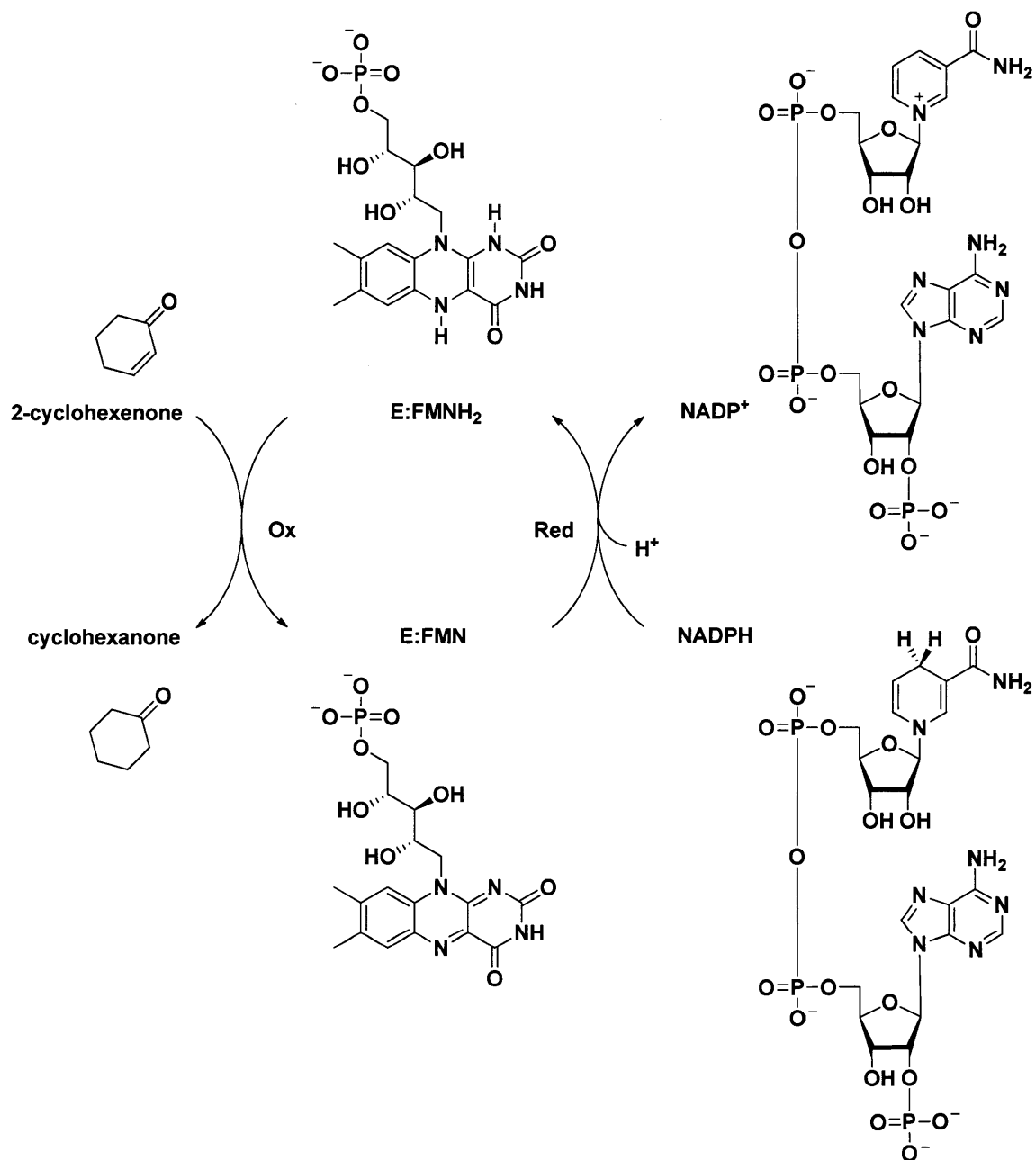


Figure 3.3. Illustrated catalytic cycle for OYE with NADPH and 2-cyclohexenone substrate (Ox = oxidative half reaction, Red = reductive half reaction, E:FMNH₂ = OYE with reduced FMN co-factor, E:FMN = OYE with oxidized FMN co-factor).



Previous mechanistic studies by the Massey group and the elucidation of the OYE1 crystal structure by Fox et al., have identified catalytic residues that were important in the reduction of α,β -unsaturated ketones and aldehydes.^{2, 4, 9-11, 25} In protein sequence alignments, *A. fumigatus* EasA (EasA_Af) shares identical residues to OYE1 that were involved in the binding and oxidation of NADPH and reduction of α,β -unsaturated ketone or aldehyde substrates (Figure 3.1). The catalytic residues in the active site of OYE1 have been identified as T37, Q114, H191, N194, and Y196, which correspond to T31, Q106, H173, N176, and Y178 in the EasA_Af protein sequence (Figures 3.1, 3.4-3.6).^{2, 4, 10, 11} Based on the crystal structure of OYE1 with an NADPH analogue, H191 and N194 of OYE1 were believed to be hydrogen bond donors that interact with the amide oxygen of NADPH (Figure 3.4), thus positioning the C4 of the nicotinamide moiety adjacent with the N5 of flavin.^{2, 3, 19} It has also been suggested that H191 and N194 play a role in reducing α,β -unsaturated aldehyde substrates by hydrogen bonding to the carbonyl oxygen, thus stabilizing the transition state after a hydride is transferred to the β carbon double bond. Y196 acts as a general acid for the substrate either concurrently with or after hydride transfer from FMN.⁴ Q114 of OYE1 has been shown to facilitate hydrogen bond interactions with the O2 and N3 of the FMN structure.¹⁰ The hydroxyl group of T37 forms a hydrogen bond with the O4 of FMN (Figure 3.4).¹¹

Figure 3.4. Catalytic active site residues of OYE1 and the proposed mechanism for the reduction of 2-cyclohexenone to yield cyclohexanone.^{2-4, 10, 11, 19}

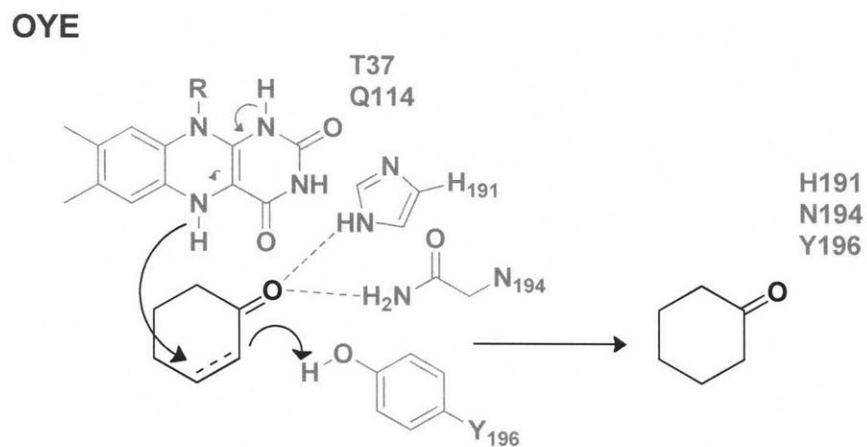
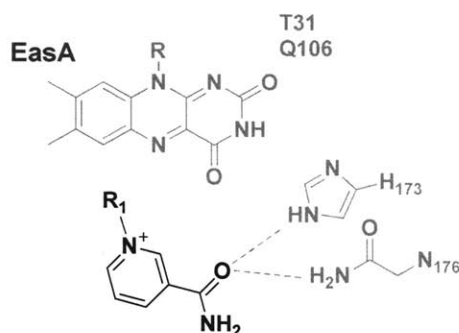


Figure 3.5. A. H173 and N176 hydrogen bonding interactions with the amide nicotinamide moiety of NADPH. B. Conserved active site residues of *A. fumigatus* EasA homologue and proposed mechanism for the reduction of chanoclavine-I-aldehyde **7** to yield a cyclic iminium intermediate **9**. EasG serves as the NADPH dependent reductase in the final step to yield festuclavine **11**.

A.



B.

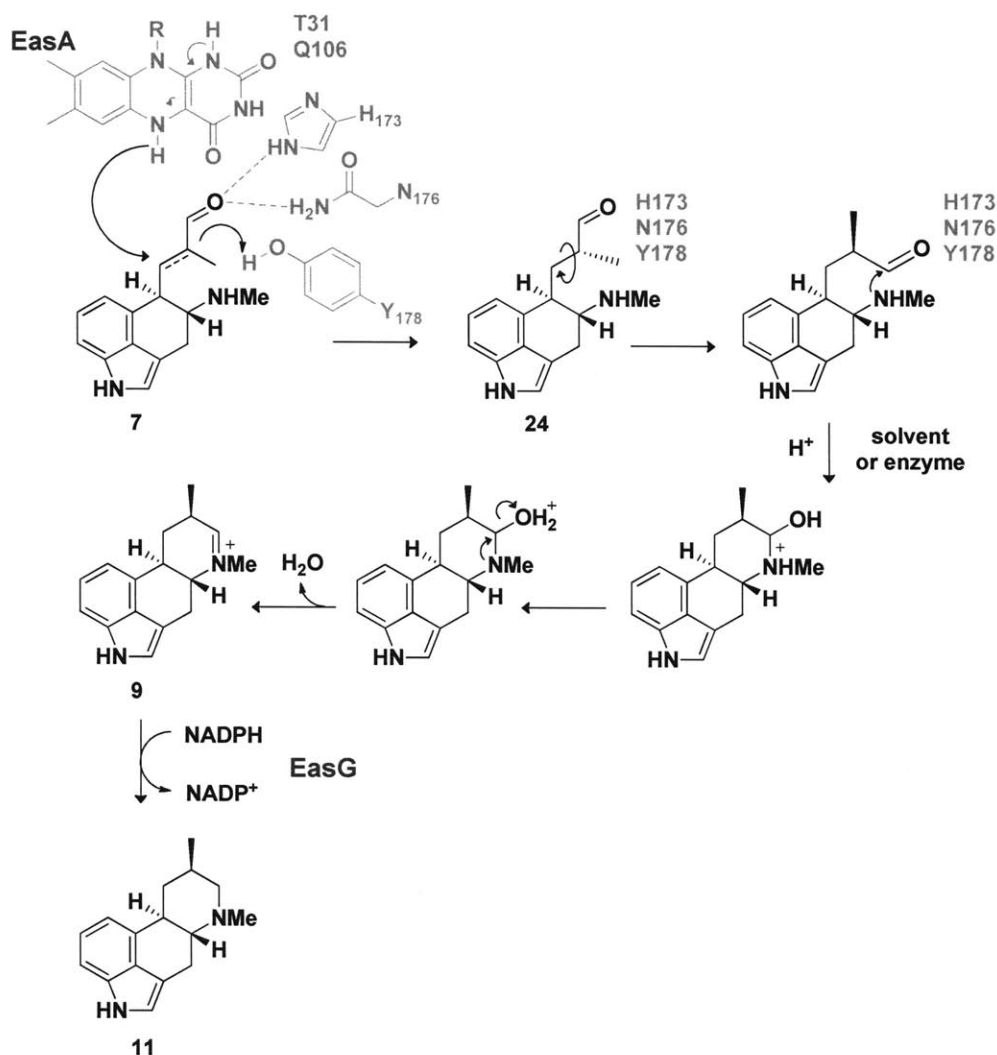
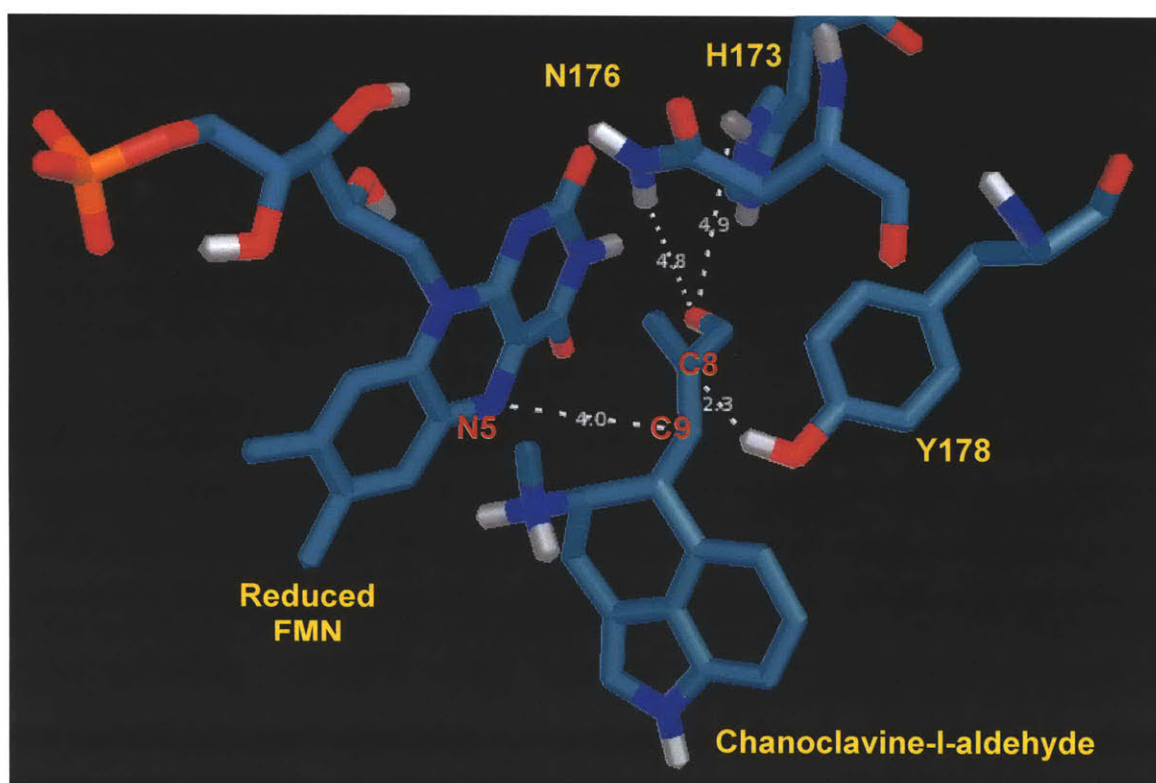


Figure 3.6. Homology model of EasA_Af with chanoclavine-I-aldehyde **7** in active site, estimated distances are in angstroms. Residues H173 and N176 are believed to be hydrogen bond donors to the carbonyl oxygen while the Y178 residue acts as a proton donor to the C8 position of chanoclavine-I-aldehyde **7**. The reduced flavin N5 position transfers a hydride to the C9 position of the substrate.

The homology model of EasA_Af and estimated docking distance of chanoclavine-I-aldehyde **7** in the active site were obtained using programs SWISS-MODEL Workspace^{26, 27} and DockingServer²⁸. Modeling and estimated docking distances utilized the structure of *S. carlsbergensis* OYE (PDB:1OYC) as a template, which shares 40% identity and 58% similarity in protein sequence to EasA_Af.



Based on the protein sequence homology of EasA_Af to the OYE like family of enzymes, it was hypothesized that EasA_Af could reduce the α,β -unsaturated aldehyde substrate chanoclavine-I-aldehyde **7** in the ergot alkaloid biosynthetic pathway to form a proposed cyclic iminium intermediate **9** (Figure 3.5B). It was further proposed that the resultant cyclic iminium intermediate **9** of EasA_Af would require a downstream reductase to form festuclavine **11** (Figure 3.5B).

While comparing conserved genes across ergot alkaloid biosynthetic clusters of different fungi, our attention focused on a putative NADPH-dependent oxidoreductase EasG. This candidate enzyme consisted of a domain homologous to the Rossmann fold NAD(P)H/NAD(P)⁺ binding domains found in dehydrogenases.²⁹⁻³² Therefore, it seemed likely that EasG could facilitate the reduction of the proposed cyclic iminium intermediate **9** to yield festuclavine **11**.

This chapter describes the functional characterization of EasA_Af, an OYE homologue, and EasG, an NADPH dependent reductase, that catalyze the critical cyclization of ring D in ergot alkaloid biosynthesis. Gene products of *easA* and *easG* enzymes from *A. fumigatus* were cloned and heterologously expressed in *E. coli* and shown to catalyze the formation of festuclavine **11** from substrate precursor chanoclavine-I-aldehyde **7**.

Experimental Methods

General materials and methods

Recombinant DNA cloning procedures were performed using pGEM-T vector (Promega) propagated in *E. coli* Top10 (Invitrogen). Protein expression was conducted in *E. coli* BL-21(DE3) (Invitrogen). PCR amplification utilized Platinum Taq DNA Polymerase (Invitrogen). Recombinant DNA plasmids were prepared using Qiaprep Spin Miniprep and Qiaquick Gel Extraction kits (Qiagen). Restriction enzymes and T4 DNA ligase were purchased from New England Biolabs. Primers for cloning were synthesized by Integrated DNA Technologies and DNA sequencing was conducted by the MIT Biopolymers Laboratory (Cambridge, MA).

LC-MS analysis was conducted using an Acquity Ultra Performance BEH C18 column with a 1.7 mm particle size, 2.1 x 100 mm dimension, with an acetonitrile/0.1% trifluoroacetic acid in water mobile phase. The column elution was coupled to MS analysis carried out using a Micromass LCT Premier TOF Mass Spectrometer with an ESI source (Waters).

Exact mass data were acquired on a Bruker Daltonics APEXIV 4.7 Tesla Fourier Transform Ion Cyclotron Resonance Mass Spectrometer (FT-ICR-MS). ¹H-NMR was taken using a 500MHz Varian Inova NMR Spectrometer. A Varian Cary 50 Bio Scanning Spectrometer was used to acquire UV-Vis spectra.

HPLC analysis was conducted on a Beckman Coulter System Gold 125 HPLC with a model 168 photodiode array detector using a Hibar RT 250-4LiChrosorb C18 column (Merck). Preparative HPLC was performed with a Grace Vydac C18 column.

Preparation of cDNA from Total RNA Extraction of *A. fumigatus* Mycelia

To clone the desired genes from *A. fumigatus*, total RNA was first extracted from mycelia tissue using the Trizol RNA extraction procedure (Invitrogen). The purity of the extracted total RNA was checked by spectrophotometer giving an absorbance A_{260}/A_{280} of 2.1, which indicated sufficient RNA quality for the subsequent steps.³³ Using the Creator SMART MMLV reverse transcriptase (Clontech) cDNA was constructed from the extracted total RNA from *A. fumigatus* using PCR.

Cloning, overexpression, and purification of EasA_Af

The *A. fumigatus easA* gene was PCR amplified using *A. fumigatus* cDNA. Primers were designed based on the nucleotide sequence of *easA* from the NCBI database (XM_751040). A pair of oligonucleotide primers were used to amplify the *easA* gene from cDNA: forward primer 5'-TTAGATCTGGCGAATTCGGCC**ATATGCGAGAAG**AACCGTCCTCTGCTCAGC-3' (with NdeI restriction site in bold) and reverse primer 5'-G**ACTCGAG**TTAAAGCTTGCCGCTAGCGACGGGGAAATTATGCAATGC**CATA**-3' (XhoI restriction site in bold). (Additional restriction sites were incorporated into the primers to allow for cloning of *easA* as either an N-His₆ or C-His₆ construct.) The PCR amplified *easA* gene was inserted into pGEM-T vector (Promega) for propagation and sequencing. Subsequently, the *easA* sequence was excised from pGEM-T by restriction digest and ligated into the NdeI/XhoI site of pET-28a(+) (Novagen) expression vector as an N-His₆ construct.

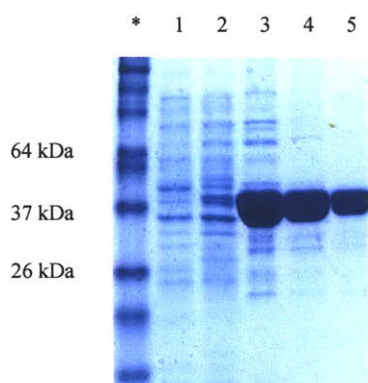
Expression was carried out in LB media with Kanamycin (50 µg/mL). *E. coli* BL-21(DE3) cells were grown to an OD₆₀₀ of 0.7 prior to induction with IPTG (5 µM) and grown for 60 hours at 15 °C prior to harvesting. Cells were resuspended in buffer (20 mM

Tris-HCl, 300 mM NaCl, 10% (v/v) glycerol, pH = 8.0) and incubated on ice for 30 min with added lysozyme (1 mg/mL) and DNaseI (10 µg/mL) and lysed by sonication.

Cellular debris was pelleted by centrifugation (15,000 x g for 1 hour).

EasA_Af enzyme was purified by Ni-NTA agarose (Qiagen). The yield of active (holo) EasA_Af was estimated to be 2.5 mg per liter of culture as measured by UV absorbance of flavin at 446 nm. Fractions containing pure EasA_Af, as demonstrated by SDS-PAGE, were collected and exchanged with dialysis buffer (50 mM K₂HPO₄, 100 mM NaCl, 10% (v/v) glycerol, pH = 7.0) (Figure 3.7). Total purified EasA_Af from each expression (holo plus apoenzyme) was determined by Bradford Assay. Holoenzyme concentration was determined using flavin absorption, where the final stock concentration was 30 µM.

Figure 3.7. SDS-PAGE of *A. fumigatus* EasA (EasA_Af) (42 kDa).



*. Invitrogen BenchMark Pre-Stained Protein Ladder.

1. buffer wash with 10 mM imidazole

2. 25 mM imidazole

3. 50 mM imidazole

4. 100 mM imidazole

5. 150 mM imidazole elution

Characterization of the bound EasA_Af flavin

The bound FMN was readily released from EasA_Af by denaturation of the enzyme solution with 0.2% sodium dodecyl sulfate (SDS).³⁴ Precipitated protein was removed by centrifugation at 17,000 x g, and a UV-visible spectra from 250 nm to 550 nm was taken of the free flavin in solution and compared to the spectra of FMN standard (Figure 3.8). The released flavin from EasA_Af exhibits the same absorbance maxima at 373 nm and 446 nm as the FMN standard.

The identity of the released flavin was further verified by co-migration with FMN standard by HPLC (Figure 3.9). The samples were chromatographed using a Hibar 250-4 LiChrosorb RP-Select B 5µm column (Merck) with an acetonitrile/0.1% trifluoroacetic acid in water mobile phase (12:88 to 95:5 from 0-15 min, 95:5 to 12:88 from 15–23 min, at a constant flow rate of 1 mL/min) with the UV detection range set at 280 nm.

Figure 3.8. Characteristic flavin absorbance spectrum (300 nm to 550 nm).

A. Native EasA_Af

B. Supernatant from EasA_Af denatured with 0.2% SDS

C. FMN Standard

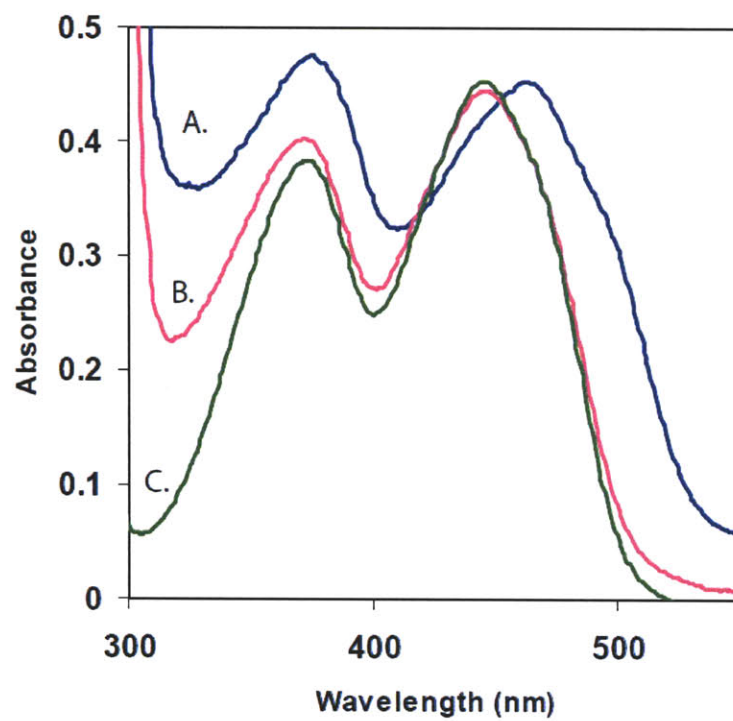
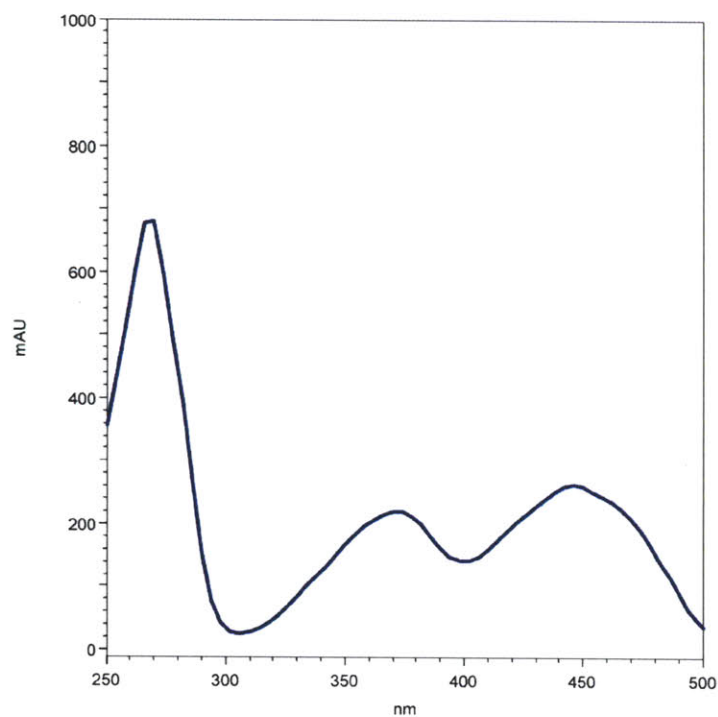
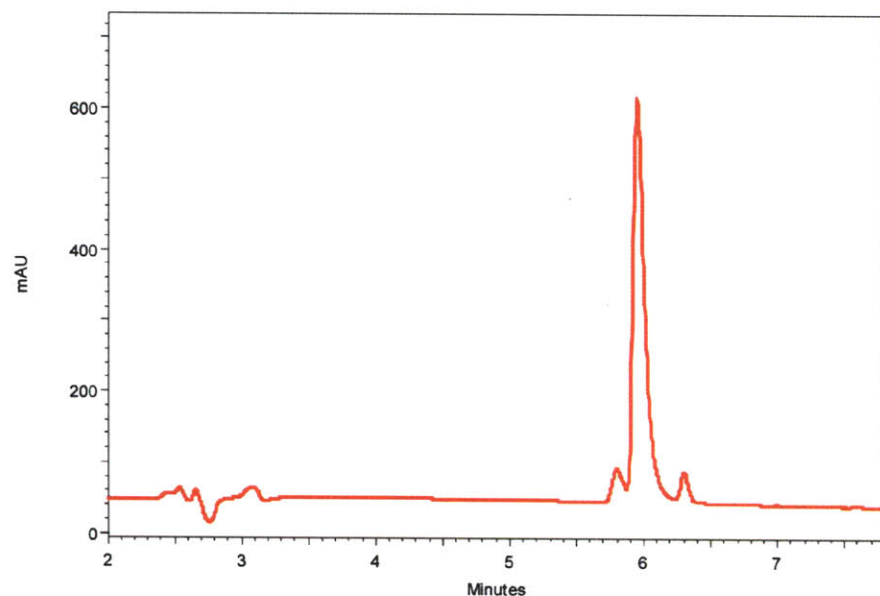


Figure 3.9. Released flavin from EasA_Af identified as FMN by HPLC. HPLC chromatogram (280 nm) of supernatant from denatured EasA_Af with FMN standard. FMN elutes at 5.95 min (top). UV-Vis spectrum of peak maxima at 5.95 min characteristic of FMN (bottom).



Isolation and HPLC purification of chanoclavine-I-aldehyde 7

Chanoclavine-I-aldehyde 7 was purified from crude extracts of 14 day old surface cultures of *A. fumigatus easA* knockout strain. This *easA* disrupted strain accumulated higher amounts of chanoclavine-I-aldehyde 7 than the wild type *A. fumigatus* strain as presented in Chapter 2. The Panaccione lab prepared and extracted cultures with a 4:1 mixture of methanol:water according to their previously published methods.³⁵

Chanoclavine-I-aldehyde 7 was identified in the crude extracts by LC-MS analysis (gradient of acetonitrile/0.1% trifluoroacetic acid in water mobile phase, 10:90 to 90:10 from 0-9 min, 90:10 to 10:90 from 9-10 min, at a constant flow rate of 0.5 mL/min). A preparative HPLC method, based on the polarity of chanoclavine-I-aldehyde 7 exhibited on the LC-MS gradient, was optimized to isolate this compound.

Chanoclavine-I-aldehyde 7 was isolated on a Grace Vydac preparative C18 column with an isocratic elution (15:85 acetonitrile/0.1% trifluoroacetic acid in water, constant flow rate at 4.0 mL/min, 228 nm detection). Under these conditions, pure chanoclavine-I-aldehyde 7 eluted at 25-26 min (Figure 3.10). Subsequent LC-MS analysis of the preparative HPLC purified compound demonstrated that chanoclavine-I-aldehyde 7 was not contaminated with any other compounds from the extract (Figure 3.11 and 3.12).

Figure 3.10. Isolation and purification of chanoclavine-I-aldehyde **7** EasA_Af substrate. Preparative HPLC chromatogram of crude *A. fumigatus* organic extract. Chanoclavine-I-aldehyde **7** elutes at 25 minutes (225 nm detection) (top). UV-Vis spectrum of chanoclavine-I-aldehyde **7** (17 μ M) in methanol (bottom).

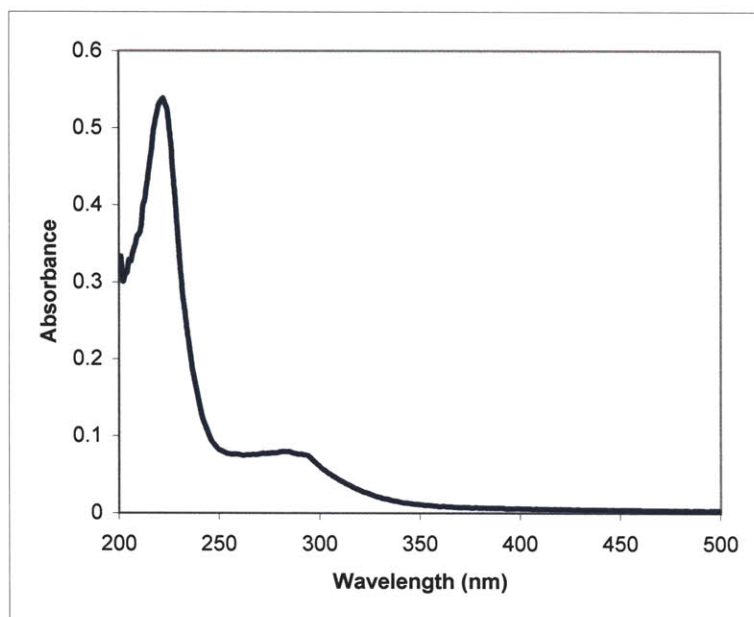
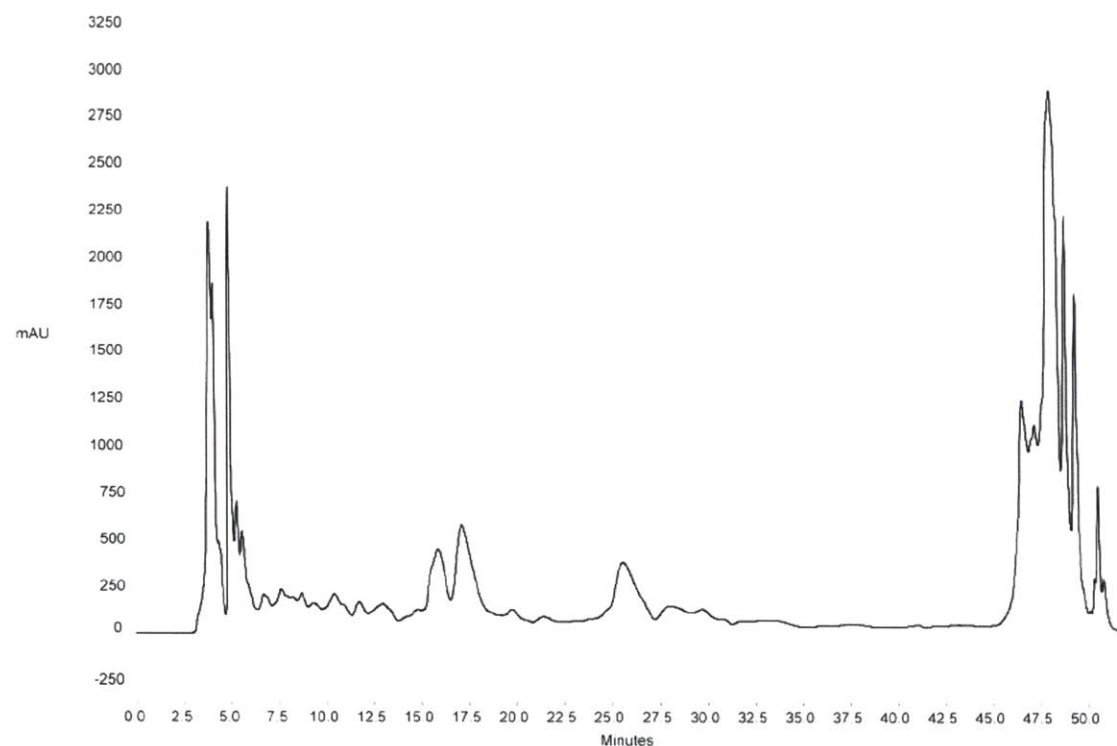


Figure 3.11. Total ion counts of LC-MS chromatograms of crude *A. fumigatus* extract (top) and purified chanoclavine-I-aldehyde **7** (bottom).

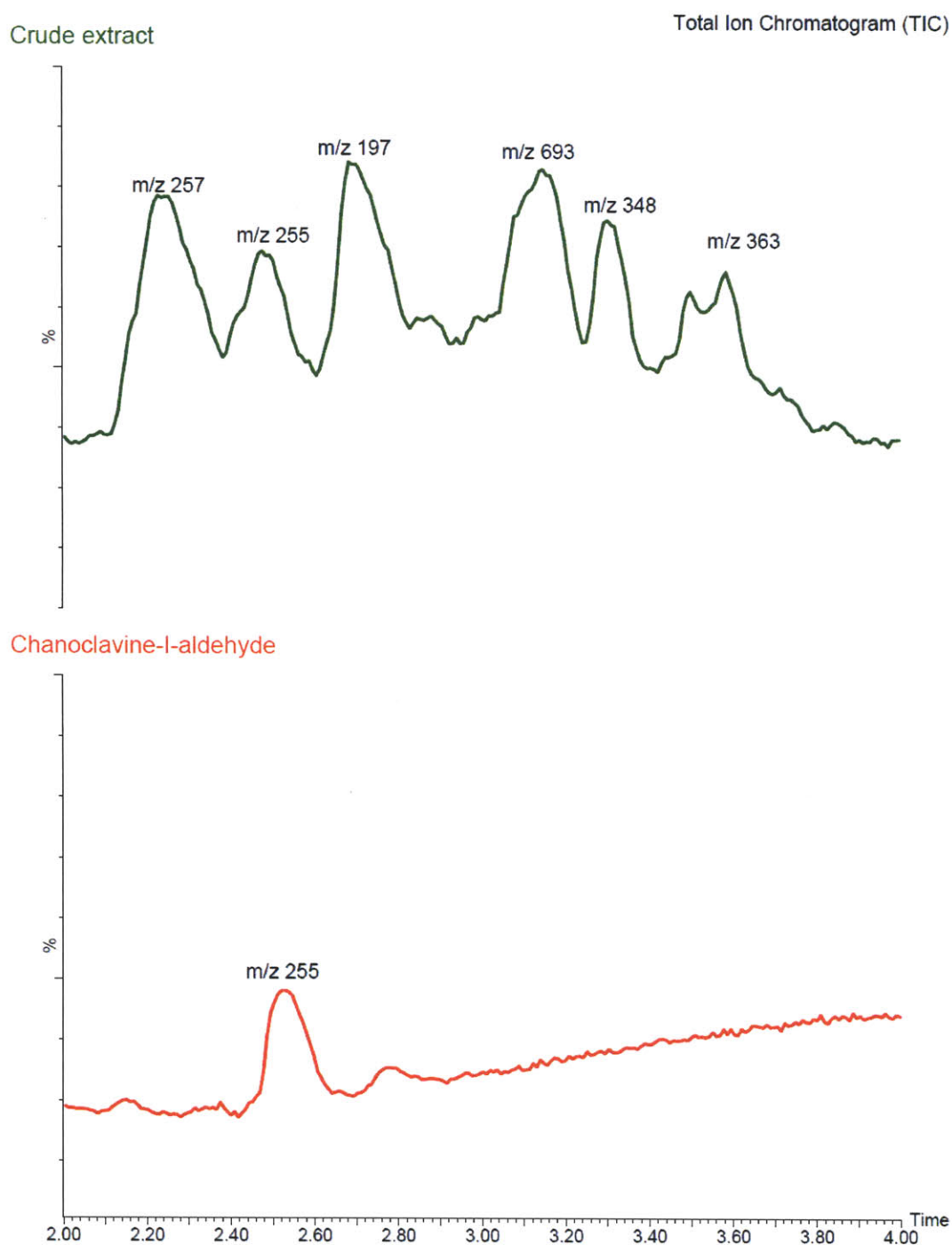
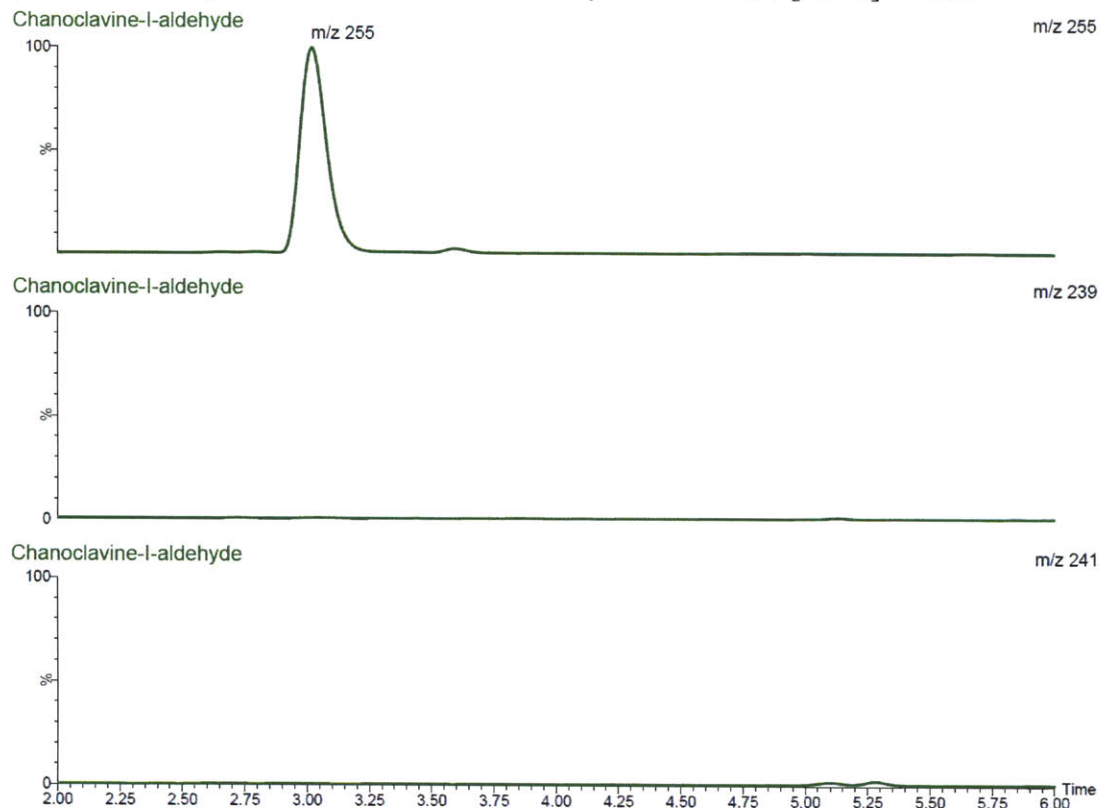


Figure 3.12. LC-MS chromatograms with selected ion monitoring of chanoclavine-I-aldehyde **7** substrate. Peak intensities for this set of chromatograms have been normalized to allow relative comparison of compound masses present.

Selected ion monitoring of substrate chanoclavine-I-aldehyde **7** for m/z 255, m/z 239, and m/z 241, demonstrates that there are no contaminants with masses $[M]^+ = 239$ and $[M+H]^+ = 241$ in the purified chanoclavine-I-aldehyde **7** substrate $[M+H]^+ = 255$.



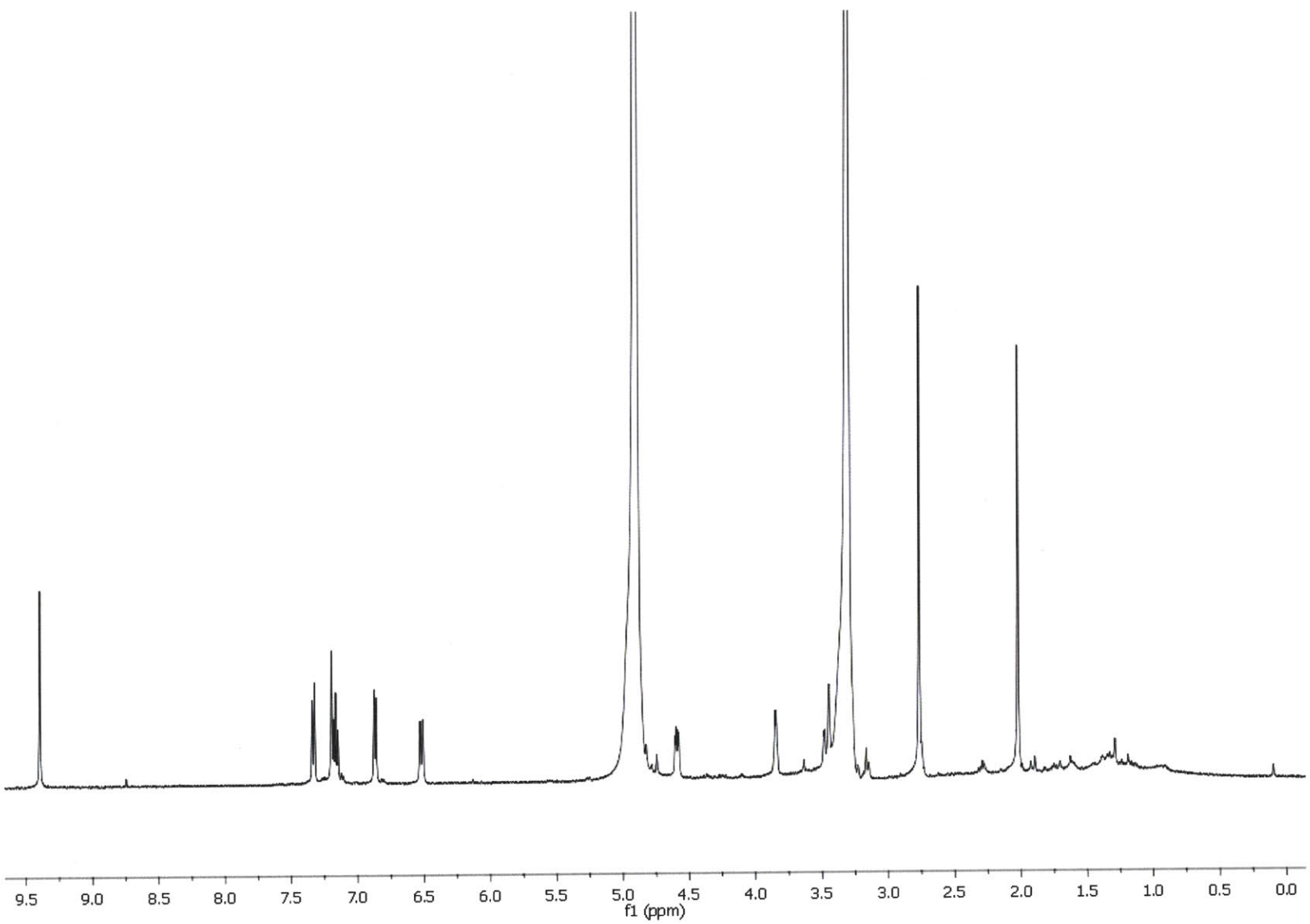
Purified chanoclavine-I-aldehyde **7** was analyzed by ^1H -NMR (500MHz Varian Inova).

The spectra matched the ^1H -NMR data previously reported by Floss and co-workers (Figure 3.13).³⁶

Purified Chanoclavine-I-aldehyde **7** (Figure 3.13):

^1H -NMR (500 MHz, CD_3OD) 2.03 (s, 3H), 2.77 (s, 3H), 3.45-3.49 (m, 2H), 3.84 (d, J = 4.5Hz, 1H), 4.58 (dd, J = 4.5, 10Hz, 1H), 6.52 (d, J = 10Hz, 1H), 6.87 (d, J = 7.0Hz, 1H), 7.16 (d, J = 8.0Hz, 1H), 7.19 (d, J = 8.5Hz, 1H), 7.34 (d, J = 8.0 Hz, 1H), 9.40 (s, 1H).

Figure 3.13. Chanoclavine-I-aldehyde 7



Catalytic hydrogenation of agroclavine **10 to yield festuclavine **11****

Festuclavine **11** was prepared from agroclavine **10** following a previously published protocol. The identity of the starting material agroclavine **10** was verified using LC-MS and ^1H -NMR (Figure 3.14 and 3.16). Agroclavine **10** (1 mg, 4.2 μmol) in 2 mL of methanol was placed over 1 mg of Pt-black at 1 atm of hydrogen at 25 $^\circ\text{C}$.^{37, 38} After 2 hours, the catalyst was filtered and the filtrate was evaporated under vacuum. The resulting festuclavine **11** product was verified by LC-MS and ^1H -NMR. (Figure 3.15 and 3.17).

Figure 3.14. LC-MS chromatograms with selected ion monitoring of agroclavine standard **10**. Peak intensities for this set of chromatograms have been normalized to allow relative comparison of compound masses present.

Selected ion monitoring at m/z 239 shows that only the agroclavine standard **10** with mass of $[M+H]^+ = 239$ is present. Mass monitoring at m/z 241 shows that there are no contaminants with this mass in the standard. Agroclavine **10** was also incubated with NaCNBH_3 and as expected does not react with this reducing agent.

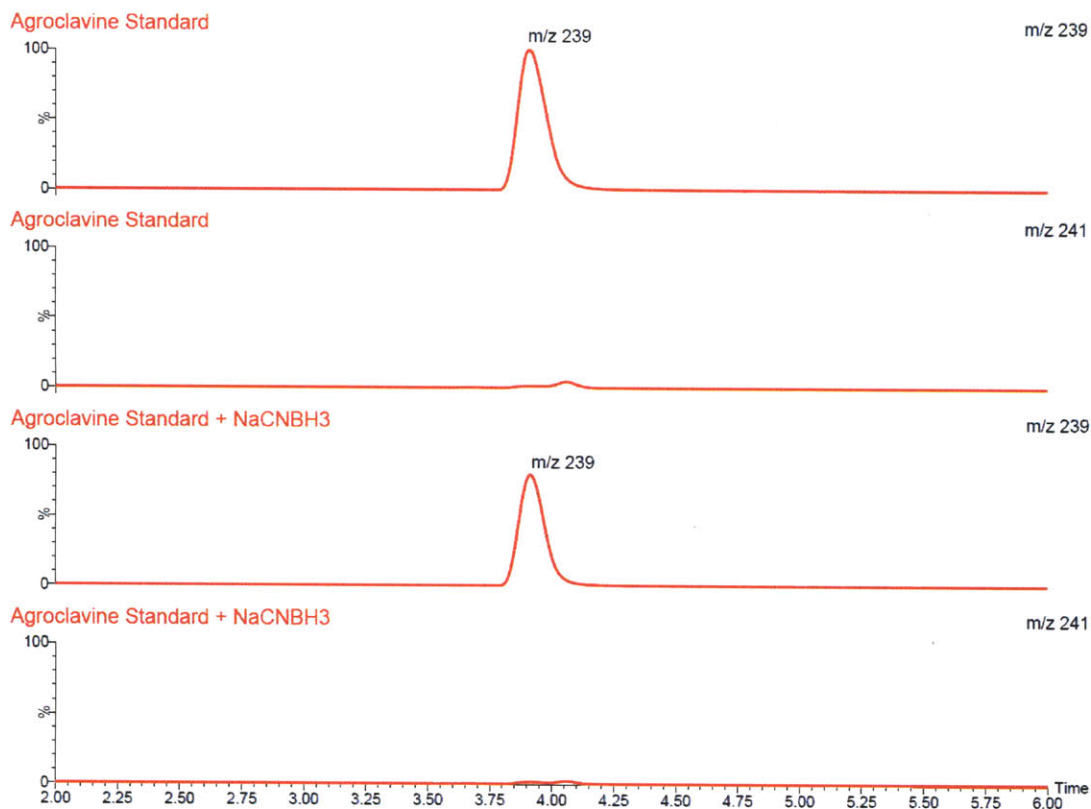
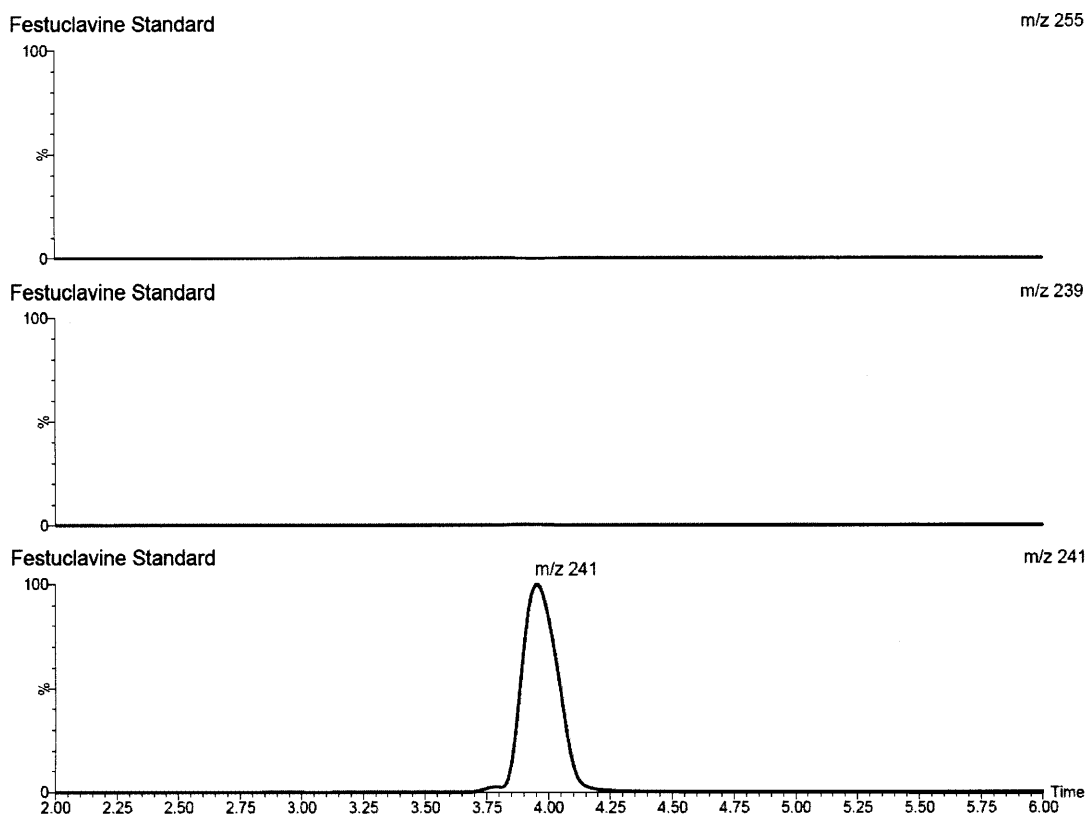


Figure 3.15. LC-MS chromatograms with selected ion monitoring of festuclavine standard **11**. Peak intensities for this set of chromatograms have been normalized to allow relative comparison of compound masses present.

Selected ion monitoring at m/z 241 shows that only the festuclavine **11** mass $[M+H]^+ = 241$ is present. Selected ion monitoring at m/z 255 and m/z 239 shows that there are no contaminants with these masses in the festuclavine standard **11**.



¹H-NMR analysis of the hydrogenated product indicated the presence of only one major diastereomer (Figure 3.17). Previous reports have demonstrated that festuclavine **11** is the major diastereomer resulting from hydrogenation of agroclavine **10** under these conditions.³⁷

Agroclavine **10** starting material (Sigma) (Figure 3.16):

¹H-NMR (500 MHz, CD₃OD) 1.80 (s, 3H), 2.49 (s, 3H), 2.73 (t, *J*=13.7Hz, 1H), 2.98 (d, *J*=16.3Hz, 1H), 3.26 (d, *J*=16.2Hz, 1H), 3.36 (dd, *J*=4.10, 14.2Hz, 2H), 3.68 (d, *J*=8.50Hz, 1H), 6.23 (s, 1H), 6.89-6.92(m, 2H), 7.05 (t, *J*=7.10Hz, 1H), 7.13 (d, 1.6Hz, 1H)

Festuclavine **11** product (Figure 3.17):

¹H-NMR (500 MHz, CD₃OD) 1.17 (d, *J*=6.5Hz, 3H), 1.38 (m, 1H), 2.21 (m, 1H), 2.83-2.95 (m, 3H), 3.09 (s, 3H), 3.27 (m, 2H), 3.60 (dd, *J*=2.0, 12.5Hz, 1H), 3.70 (dd, *J*=3.5, 14.5Hz, 1H), 6.94 (d, *J*=7.0Hz, 1H), 7.04 (d, *J*=1.5Hz, 1H), 7.12 (t, *J*=7.0Hz, 1H), 7.21 (d, *J*=8.0Hz, 1H)

Figure 3.17. Festuclavine 11

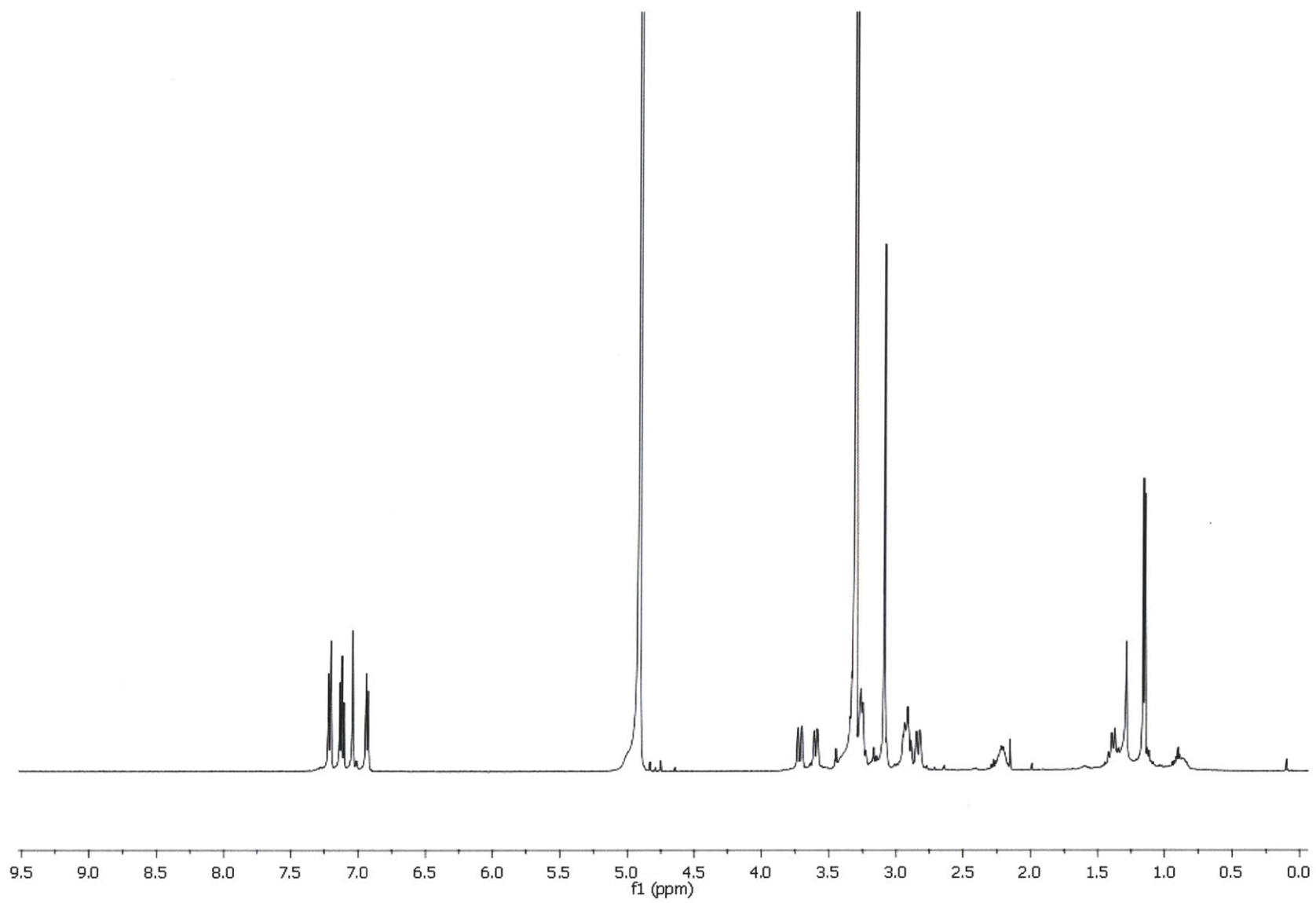
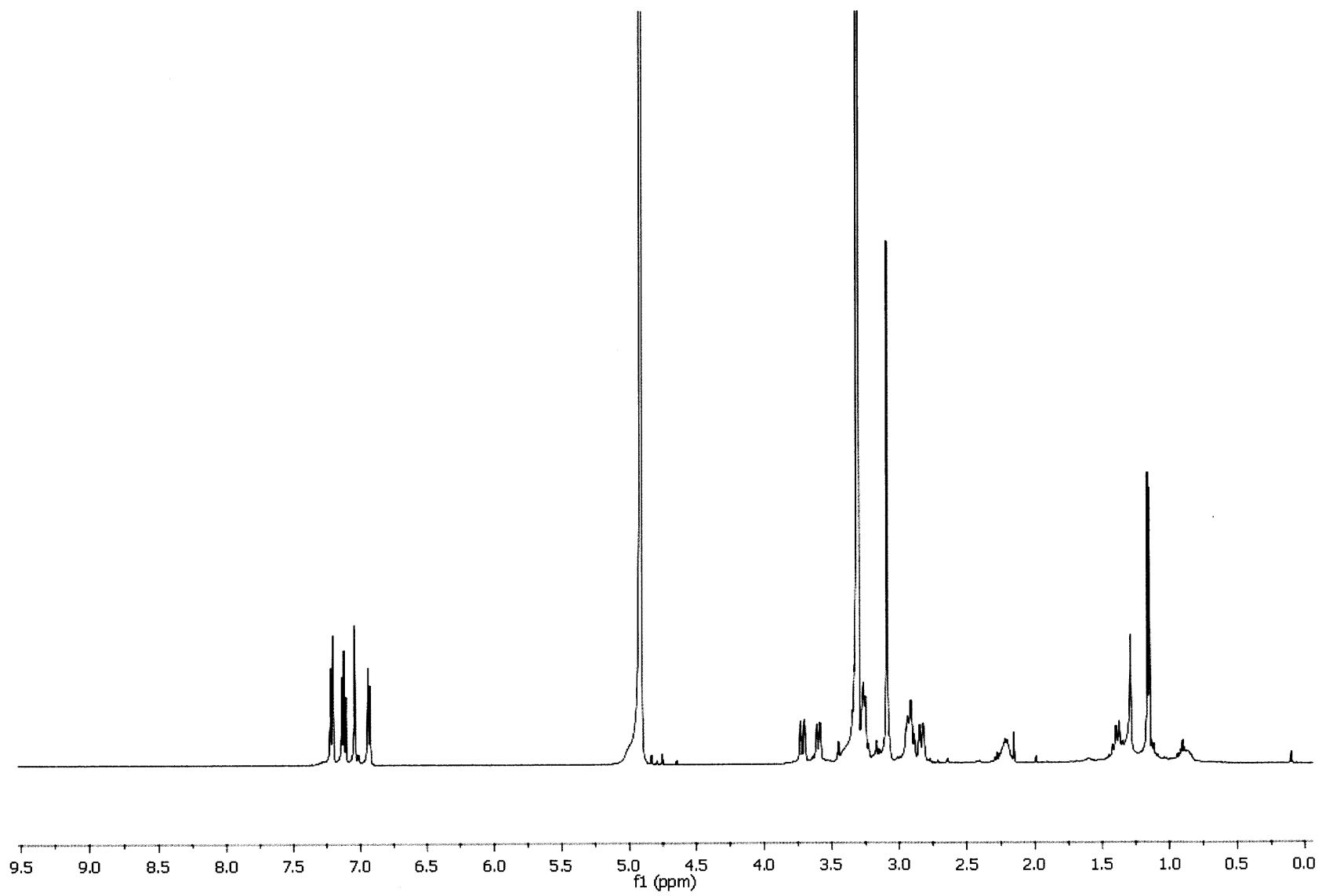


Figure 3.17. Festuclavine 11



End Point Assay of EasA_Af for the conversion of chanoclavine-I-aldehyde 7 to cyclic iminium intermediate 9

To test for substrate turnover, purified EasA_Af (1.5 μ M) was incubated with chanoclavine-I-aldehyde 7 (1 mM) and NADPH (1.5 mM) in 100 mM K_2HPO_4 (pH = 7.0)² buffer at 25 °C for 1 hour. The product identity was confirmed by LC-MS analysis (gradient of acetonitrile/0.1% trifluoroacetic acid in water mobile phase, 10:90 to 90:10 from 0-9 min, 90:10 to 10:90 from 9-10 min, at a constant flow rate of 0.5 mL/min) and high resolution mass spectrometry.

Steady state kinetic analysis of EasA_Af

The k_{cat} and K_m values for chanoclavine-I-aldehyde 7 and NADPH were obtained by LC-MS, monitoring the initial rate of chanoclavine-I-aldehyde 7 consumption over time. Mass spectrometry using electrospray ionization has been previously used as an assay method for kinetic characterization of a variety of enzymes.^{39, 40} Chanoclavine-I-aldehyde 7 was quantified with a standard curve of chanoclavine-I-aldehyde 7 plotted against peak response area for mass $[M+H]^+$ 255 (Figure 3.18). Aliquots of the reaction were quenched in 0.1% formic acid (containing 500 nM yohimbine as an internal standard) over a 3 min time course at 30 sec intervals. Reactions contained varying substrate ranges of chanoclavine-I-aldehyde 7 (0.5-10 μ M) and NADPH (10-500 μ M) and EasA_Af at (2.5 nM), and were incubated in 100 mM K_2HPO_4 at pH = 7.0 buffer in 50 μ L volumes at 25°C under aerobic conditions.

Enzyme concentration was calculated using flavin absorption, ensuring that only holoenzyme was considered in the protein concentration measurement. Linear regression

analysis was used to determine the initial rate of each assay. Experiments were repeated in triplicate and data were fit using software SigmaPlot 9.0. A control to check for the stability of chanoclavine-I-aldehyde **7** under assay conditions was conducted by setting up a reaction containing boiled (inactive) EasA_Af (2.5 nM), chanoclavine-I-aldehyde **7** (5 μ M), and NADPH (500 μ M). Aliquots of the reaction were quenched in 0.1% formic acid (plus yohimbine internal standard) over time and analyzed by LC-MS. The concentration of chanoclavine-I-aldehyde **7** was maintained over a 60 min time course, suggesting that the disappearance of chanoclavine-I-aldehyde **7** in the EasA_Af assay is solely due to enzyme turnover (Figure 3.19).

Figure 3.18. Chanoclavine-I-aldehyde **7** standard curve on LC-MS displaying concentration and peak area response. The concentration of the chanoclavine-I-aldehyde **7** standard was determined based on UV absorbance at 225 nm using the extinction coefficient ($30,900 \text{ M}^{-1} \text{ cm}^{-1}$ at 225 nm). The concentrations 100-500 nM represent the full range of chanoclavine-I-aldehyde **7** substrate that was analyzed by mass spectrometry, after quenching and dilution of the enzyme assay reaction.

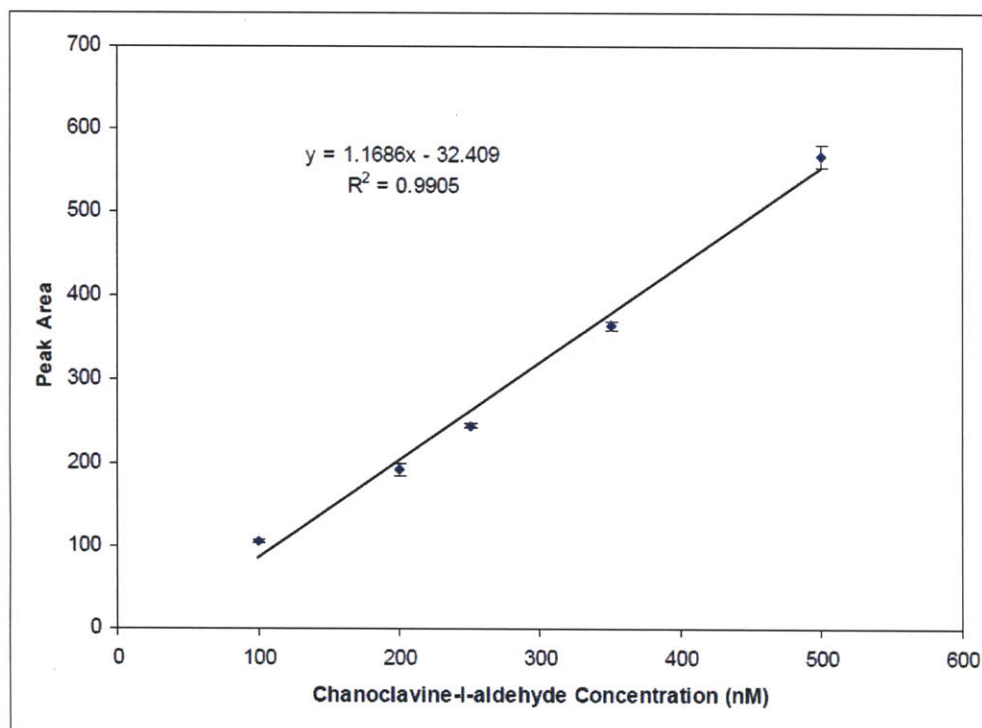
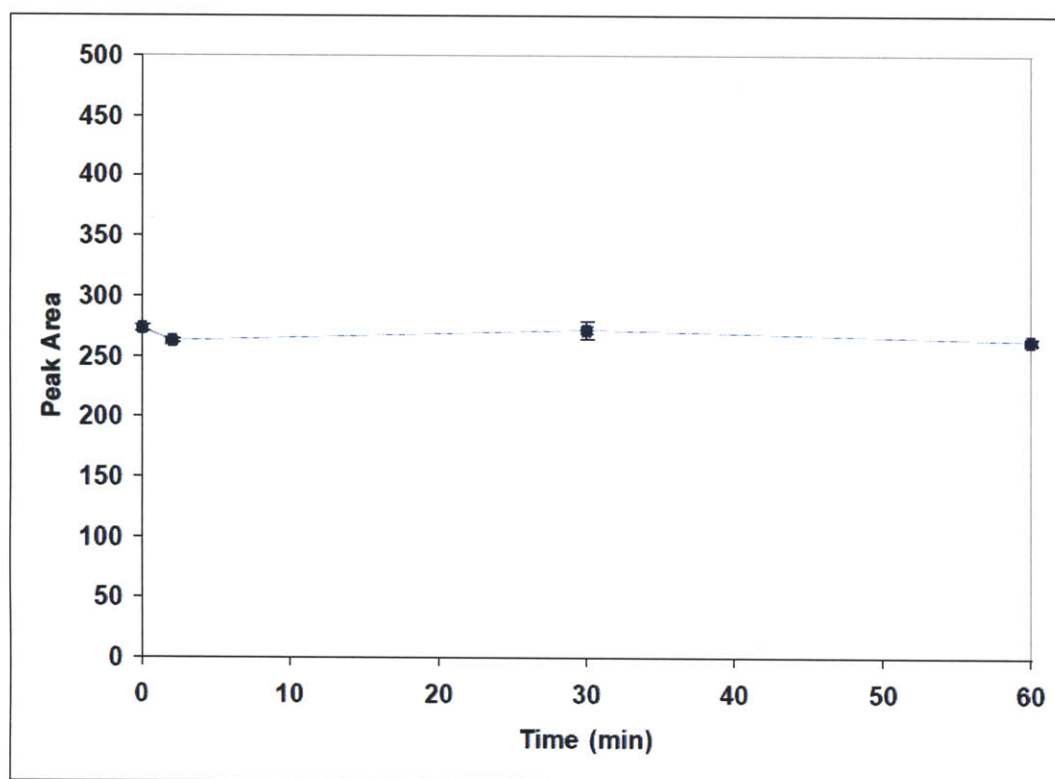


Figure 3.19. Stability of chanoclavine-I-aldehyde **7** (5 μ M) under assay conditions with boiled inactive EasA_Af (2.5 nM) and NADPH (500 μ M) over a time course.



Large scale enzymatic preparation of EasA_Af product cyclic iminium product **9 and subsequent synthetic reduction to yield festuclavine **11****

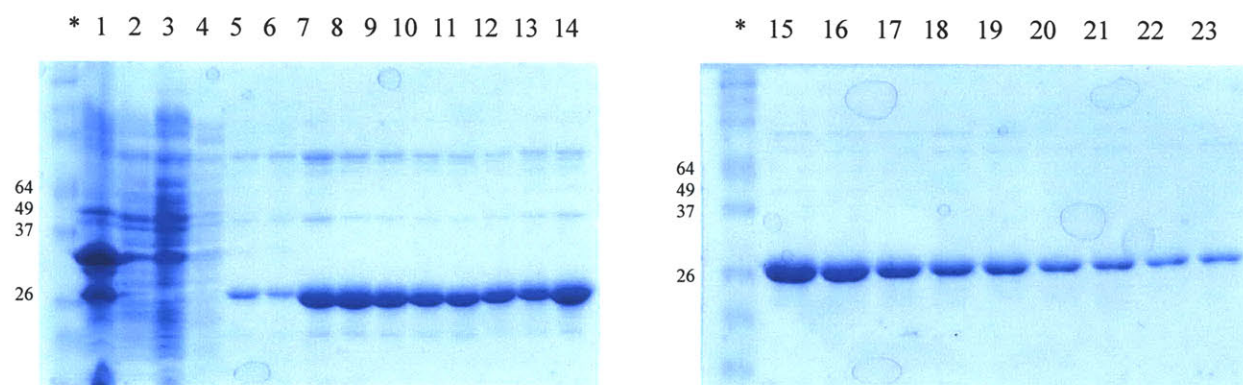
A total of 7 x 1 mL reactions of chanoclavine-I-aldehyde **7** (1 mM), NADPH (5 mM), and EasA_Af (6 μ M) were allowed to react for 10 minutes prior to quenching with NaCNBH₃ (5 mM). The reaction solutions were combined and extracted three times with ethyl acetate 1:1 (v/v), then centrifuged at 17,000 x g for 15 min to pellet protein precipitates. The combined organic fractions were filtered and evaporated to dryness. The concentrated reduced enzymatic product festuclavine **11** was purified by preparative HPLC.

Cloning, overexpression, and purification of *Aspergillus fumigatus* EasG

The *easG* gene from *A. fumigatus* was PCR amplified using *A. fumigatus* cDNA. Primers were designed based on the nucleotide sequence of *easG* from the NCBI database (XM_751041). A pair of oligonucleotide primers were used to amplify the *easG* gene: forward primer 5'- TTGGCC**ATATG**ACTATCCTCGTGCTGGGTGGCCGCG-3' (with NdeI restriction site in bold) and reverse primer 5'- GAAAGC**TTATG**CCGCATCCAGCGCGCTTTTTC -3' (HindIII restriction site in bold). The PCR amplified *easG* gene was inserted into pGEM-T vector (Promega) for propagation and sequencing. Subsequently, the *easG* sequence was excised from pGEM-T by restriction digest and ligated into the NdeI/HindIII site of pET-24a(+) (Novagen) expression vector as a C-His₆ tagged construct.

Expression was carried out in *E. coli* BL-21(DE3) cells grown in LB medium supplemented with kanamycin (50 µg/mL). Cells were grown to an OD₆₀₀ of 0.7 prior to induction with IPTG (5 µM) and grown for 60 hours at 15 °C prior to harvesting. Cells were resuspended in buffer (20 mM Tris-HCl, 300 mM NaCl, 10% (v/v) glycerol, pH = 8.0) and incubated on ice for 30 minutes with added lysozyme (1 mg/mL) and DNaseI (10 µg/mL) then lysed by sonication. Cellular debris was pelleted by centrifugation (15,000 x g for 1 hour). Crude EasG enzyme was purified by incubating with Ni-NTA agarose (Qiagen). Fractions containing pure EasG, as demonstrated by SDS-PAGE (Figure 3.19), were collected and buffer exchanged (50 mM K₂HPO₄, 100 mM NaCl, 10% (v/v) glycerol, pH = 7.0). The yield of EasG was estimated by Bradford assay as 6 mg/L culture. Final purified EasG enzyme stock concentration was 20 µM.

Figure 3.20. SDS-PAGE of EasG (*A. fumigatus*) (32 kDa)



*. Invitrogen BenchMark Pre-Stained Protein Ladder

- 1. column flow-through
- 2-3. buffer wash 10 mM imidazole
- 4. 25 mM imidazole
- 5-11. 50 mM imidazole
- 12-19. 100 mM imidazole
- 20-23. 150 mM imidazole

Endpoint assays for EasA_Af and EasG

Endpoint assays involved incubating EasA_Af (0.1 μ M), EasG (0.1 μ M), chanoclavine-I-aldehyde **7** (10 μ M), and NADPH (500 μ M) in 100 mM K₂HPO₄ buffer (pH = 7.0) at 25 °C for 30 min. Aliquots (3 μ L) were quenched by dilution in 0.1% formic acid in water and analyzed by LC-MS.

Results and Discussion

Heterologous expression of EasA_Af and characterization of the bound flavin

The putative flavin dependent oxidoreductase OYE homologue *easA* of the *A. fumigatus* ergot gene cluster was successfully cloned and heterologously expressed in *E. coli*. Soluble EasA_Af protein was obtained at a concentration of 2.5 mg/L culture and purified by Ni-NTA affinity chromatography (Figure 3.7). Purified EasA_Af appears yellow in color indicating that it co-purifies with a flavin.

The flavin co-factor was identified as non-covalently bound flavin mononucleotide (FMN). The released flavin from EasA_Af exhibits the same absorbance maxima at 373 nm and 446 nm as the FMN standard (Figure 3.8). The identity of the released flavin was further verified by co-migration with FMN standard by HPLC (Figure 3.9). The extinction coefficient of the purified FMN bound EasA_Af was calculated by comparing the absorbance of the bound EasA_Af flavin versus the absorbance of the flavin released after denaturation at 446 nm.³⁴ Using the known extinction coefficient of 12,200 M⁻¹cm⁻¹ for free FMN at 446 nm, the extinction coefficient for the EasA_Af bound FMN was determined to be 11,500 M⁻¹cm⁻¹. Typically, 20 to 25% of heterologously expressed EasA_Af protein co-purified with the flavin cofactor. Attempts at reconstitution, by adding FMN to the protein followed by dialysis, perturbed the flavin spectra when the protein was re-isolated and did not result in greater catalytic activity. The concentration of holoenzyme EasA_Af bound with FMN used in subsequent experiments was determined using flavin absorption. These results demonstrated that the bound flavin of EasA_Af was FMN, a defining characteristic of OYE homologues observed in previous studies.^{3, 11, 14, 19, 25}

Isolation of chanoclavine-I-aldehyde the proposed substrate of EasA_Af

Chanoclavine-I-aldehyde **7** was successfully isolated from a culture of *A. fumigatus easA* disrupted strain, which accumulated pathway intermediate chanoclavine-I-aldehyde **7** as described in Chapter 2. Chanoclavine-I-aldehyde **7** was purified and isolated by HPLC (Figure 3.10). LC-MS analysis displayed a corresponding mass of m/z 255 which is the expected $[M+H]^+$ mass of chanoclavine-I-aldehyde **7** (Figure 3.12). The identity of the isolated product was further substantiated by ^1H -NMR and High Resolution MS to be chanoclavine-I-aldehyde **7** (Figure 3.13, Table 3.1).

Functional role of EasA_Af in the reduction and cyclization of ergot pathway intermediate chanoclavine-I-aldehyde **7 to yield a cyclic iminium intermediate **9****

The conversion of chanoclavine-I-aldehyde **7** $[M+H]^+$ 255 to a compound with $[M]^+$ 239 with a retention time at 3.4 min was observed upon the addition of EasA_Af enzyme and NADPH (Figure 3.21A, B). The mass of this peak corresponded with mass of the hypothetical downstream cyclized iminium ion intermediate **9** (Figure 3.5).

Steady state kinetic constants for EasA_Af were measured by monitoring the disappearance of chanoclavine-I-aldehyde **7** $[M+H]^+$ 255 by LC-MS, where data were fit to a ping-pong bi-bi kinetic model, which is typical for OYE.^{2, 10, 21} The resulting K_m value of chanoclavine-I-aldehyde **7** and NADPH was $4.8 \pm 1.1 \mu\text{M}$ and $192 \pm 40.1 \mu\text{M}$, respectively, with a k_{cat} value of $2,310 \pm 282 \text{ min}^{-1}$. Control experiments performed with either boiled EasA_Af or in the absence of NADPH displayed no formation of $[M]^+$ 239 (Figure 3.22).

High resolution mass spectrometry of the enzymatic product also corresponded to the expected theoretical formula of compound **9** (Table 3.1). These assays demonstrated that upon the addition of EasA_Af enzyme and NADPH, the alkene of chanoclavine-I-aldehyde **7** $[M+H]^+$ 255 was reduced and yielded a product with a mass corresponding to the proposed cyclic iminium intermediate **9** $[M]^+$ 239 (Figure 3.21B).

Furthermore, our genetic studies in Chapter 2 demonstrated that the $\Delta easA$ disruption mutant of *A. fumigatus* failed to accumulate downstream ergot alkaloids, while upstream pathway intermediates chanoclavine-I **6** and chanoclavine-I-aldehyde **7** accumulated.³⁵ Therefore, the biochemical properties observed for purified EasA_Af *in vitro* is consistent with the proposed function of the *easA* gene product *in vivo*, and demonstrated that chanoclavine-I-aldehyde **7** is the substrate of EasA_Af.

Figure 3.21. LC-MS chromatograms with selected ion monitoring.

- A. Starting substrate chanoclavine-I-aldehyde **7** with expected mass of $[M+H]^+ = 255$.
B. Product resulting from incubation of EasA_Af with NADPH and chanoclavine-I-aldehyde **7** is proposed to be cyclic iminium intermediate $[M]^+ = 239$ major product **9** at 3.4 min and minor product **25** at 3.2 min. Peaks observed are hypothetical diastereoisomers .
C. Product in chromatogram B (cyclic iminium intermediate **9**) reduced with NaCNBH_3 to yield festuclavine **11** with an expected $[M+H]^+ = 241$.
D. Festuclavine **11** standard with an expected $[M+H]^+ = 241$.

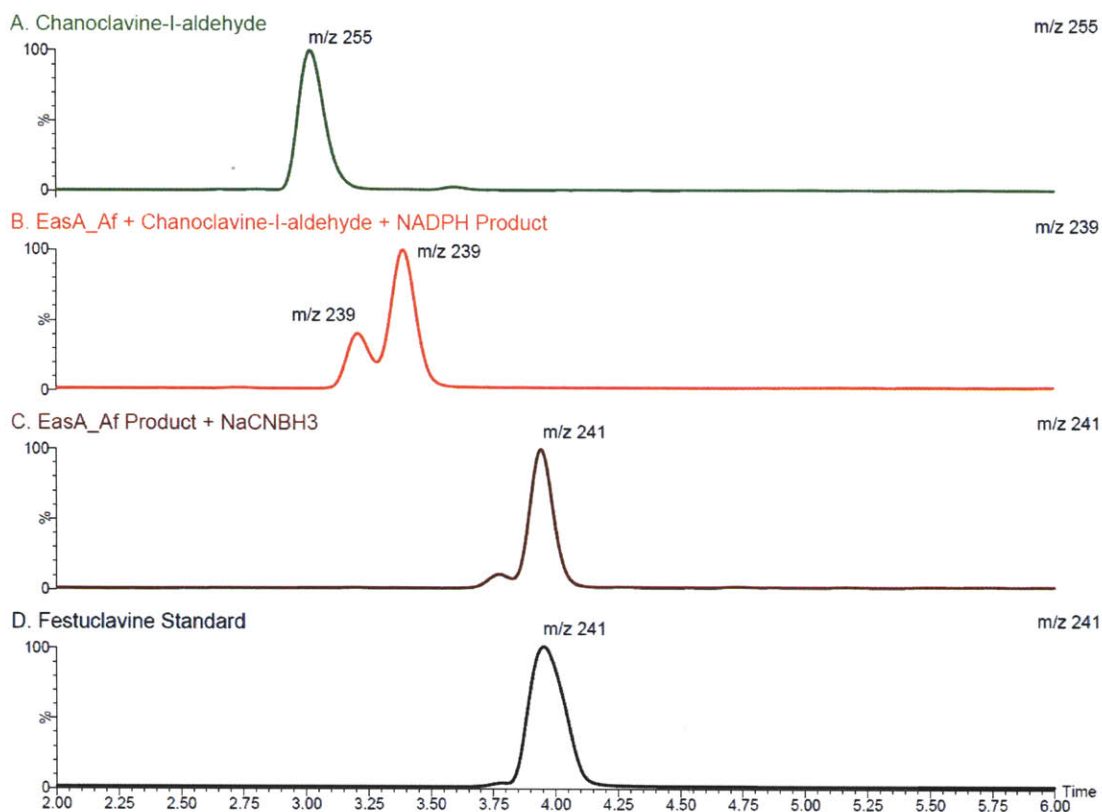
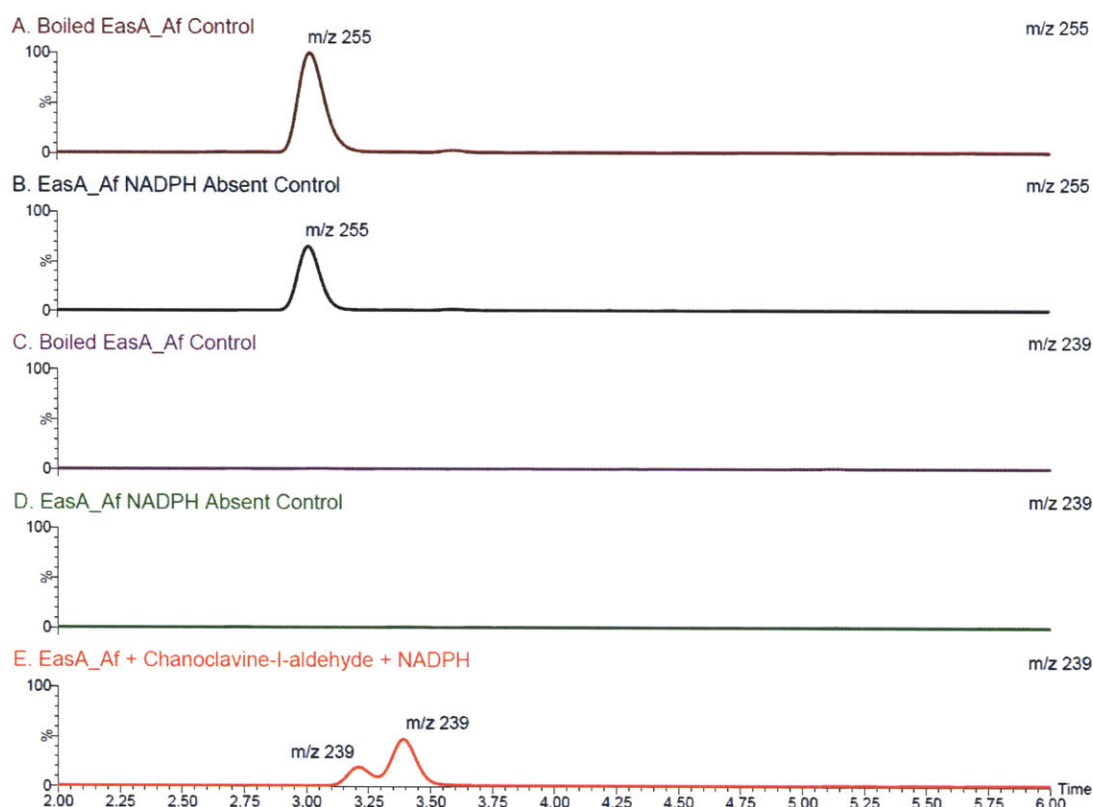


Table 3.1. Exact Mass of Compounds Determined by High Resolution MS

Compound	Observed Mass	Theoretical Mass	Deviation of Theoretical from Observed (ppm)	Molecular Formula
Chanoclavine-I-aldehyde 7 [M+H] ⁺	<i>m/z</i> 255.1500	<i>m/z</i> 255.1497	1.2	C ₁₆ H ₁₉ N ₂ O
Cyclized iminium intermediate 9 [M] ⁺	<i>m/z</i> 239.1551	<i>m/z</i> 239.1548	1.3	C ₁₆ H ₁₉ N ₂
Festoclavine 11 [M+H] ⁺	<i>m/z</i> 241.1704	<i>m/z</i> 241.1705	- 0.4	C ₁₆ H ₂₁ N ₂

Figure 3.22. LC-MS chromatograms with selected ion monitoring comparing active EasA_Af with controls. Peak intensities for this set of chromatograms have been normalized to allow relative comparison of compound masses present.

- A. Starting material chanoclavine-I-aldehyde **7** $[M+H]^+ = 255$ remains in enzyme assays with boiled, denatured EasA_Af enzyme.
- B. Starting material chanoclavine-I-aldehyde **7** $[M+H]^+ = 255$ remains in enzyme assays with active EasA_Af with no NADPH present.
- C. The cyclized iminium ion enzymatic product **9** $[M]^+ = 239$ is not observed with boiled, denatured EasA_Af enzyme.
- D. The cyclized iminium ion enzymatic product **9** $[M]^+ = 239$ is not observed with active EasA_Af with no NADPH present
- E. The cyclized iminium ion enzymatic major product **9** $[M]^+ = 239$ and minor product **25** $[M]^+ = 239$ is observed with active EasA_Af enzyme and NADPH present.



The immediate product of the chanoclavine-I-aldehyde **7** reduction was expected to be dihydrochanoclavine aldehyde **24** $[M+H]^+$ 257 (Figure 3.5); however, accumulation of this mass was not observed at significant levels relative to the $[M]^+$ 239 peak. This led us to speculate that the $[M]^+$ 239 was the cyclized iminium **9** form of dihydrochanoclavine aldehyde $[M+H]^+$ 257 formed after free rotation about the C8-C9 bond to allow condensation of the secondary amine and aldehyde (Figure 3.5). Therefore, the reaction of the aldehyde and amine moieties of dihydrochanoclavine aldehyde **24** was rapid and favored the formation of the cyclized iminium ion **9**. Consistent with our findings, in a later study on *A. fumigatus* EasA (orthologue FgaOx3) by Wallwey et al., an $[M]^+$ 239 intermediate was observed in trace amounts by ESI-MS and also proposed to be the cyclic iminium intermediate from EasA_Af reduction of chanoclavine-I-aldehyde **7**.²⁴

Notably, we also observed that a minor $[M]^+$ 239 peak at a retention time of 3.2 min forms over the time course of the assay relative to the major $[M]^+$ 239 more hydrophobic peak at 3.4 min (Figure 3.23). Although these compounds could not be isolated in quantities sufficient for structural characterization, the observation of the two $[M]^+$ 239 peaks provided us with a new working hypothesis. We speculate that the peaks were diastereoisomers **9** and **25** resulting from the possible imine-enamine tautomerization that could occur in aqueous conditions once the major cyclic iminium product is formed and no downstream reductase is present to reduce the intermediate to yield festuclavine **11** (Figure 3.24). The dihydrochanoclavine aldehyde **24** $[M+H]^+$ 257, which can undergo keto-enol tautomerization, may also be another source of the proposed diastereotopic peaks for $[M]^+$ 239. It remains to be determined whether the

cyclization of the major $[M]^+$ 239 intermediate is spontaneous or enzymatically catalyzed. Possible scenarios to explain how EasA_Af may work with a downstream reductase to facilitate reduction of the correct diastereoisomer to form festuclavine **11** are discussed later in this chapter.

Figure 3.23. LC-MS chromatograms with selected ion monitoring of enzyme product of EasA_Af and chanoclavine-I-aldehyde **7** substrate in presence of NADPH. Peak intensities for this set of chromatograms have been normalized to allow relative comparison of compound masses present.

Selected ion monitoring at m/z 255 to shows complete consumption of substrate chanoclavine-I-aldehyde **7** $[M+H]^+ = 255$. Selected ion monitoring at m/z 239 shows formation of cyclized iminium intermediate $[M]^+ = 239$. Selected ion monitoring at m/z 241 demonstrates that the reduced product festuclavine **11** $[M+H]^+ = 241$ only forms upon addition of NaCNBH_3 .

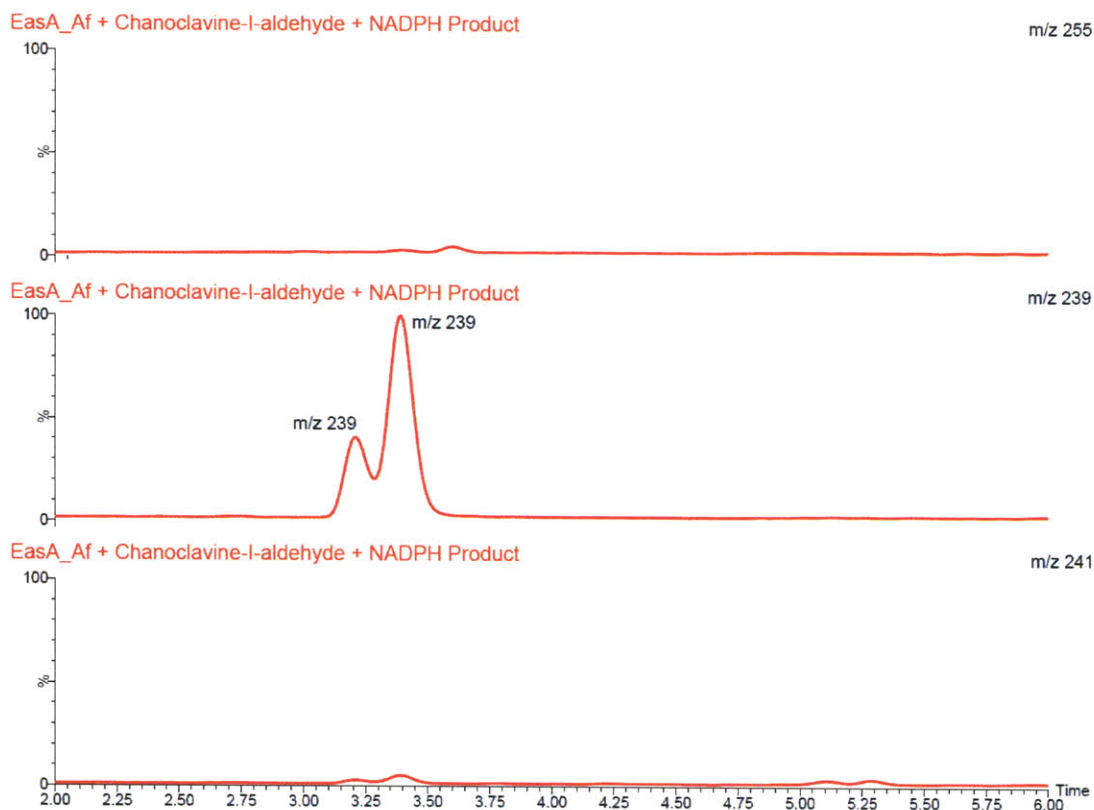
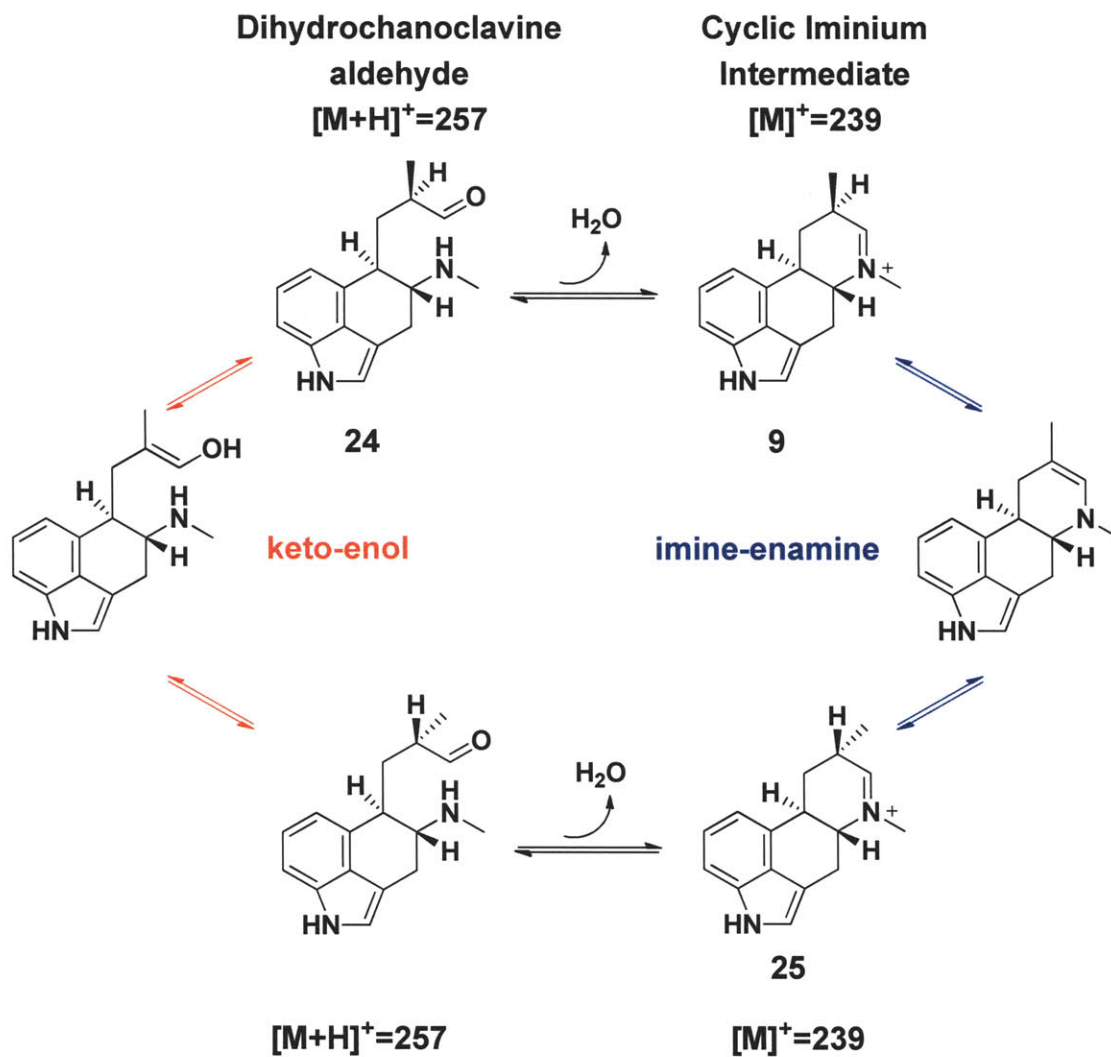


Figure 3.24. Racemization of the dihydrochanoclavine aldehyde **24** via keto-enol or imine-enamine tautomerization producing the major **9** and minor **25** diastereoisomers of the cyclized iminium intermediate.



The cyclic iminium EasA_Af product as the precursor of festuclavine

To yield further insight into the identity of this cyclic iminium intermediate $[M]^+$ 239 and to further substantiate the enzymatic activity of EasA_Af, we attempted to trap the enzyme product via synthetic reduction with sodium cyanoborohydride (NaCNBH_3). Addition of NaCNBH_3 to the assay mixture, after EasA_Af catalyzed complete consumption of chanoclavine-I-aldehyde **7**, resulted in the conversion of the major cyclic iminium intermediate **9** $[M]^+$ 239 to the expected reduction product festuclavine **11** $[M+H]^+$ 241 (Figure 3.21C). The reduced enzymatic product co-migrated with the festuclavine **11** standard (Figure 3.21D). The identity of the reduced enzymatic product was further confirmed by $^1\text{H-NMR}$ (Figure 3.26-3.28). Furthermore, high resolution MS of the reduced cyclic iminium intermediate was in agreement with the expected mass of festuclavine **11** (Table 3.1). These results further substantiated that the product observed of EasA_Af reduction of chanoclavine-I-aldehyde **7** was the cyclic iminium intermediate **9**.

Figure 3.25. LC-MS chromatograms with selected ion monitoring of NaCNBH₃ trapped cyclic iminium intermediate **9** (enzyme product of EasA_Af + chanoclavine-I-aldehyde **7** + NADPH) to yield festuclavine **11**. Peak intensities for this set of chromatograms have been normalized to allow relative comparison of compound masses present.

Selected ion monitoring at m/z 255 displays complete turnover of chanoclavine-I-aldehyde substrate **7** [$M+H$]⁺ = 255 by EasA_Af. Mass monitoring at m/z 239 displays complete reduction of cyclic iminium intermediate **9** [$M+H$]⁺ = 239. Mass monitoring at m/z 241 shows formation of the reduced product festuclavine **11** [$M+H$]⁺ = 241.

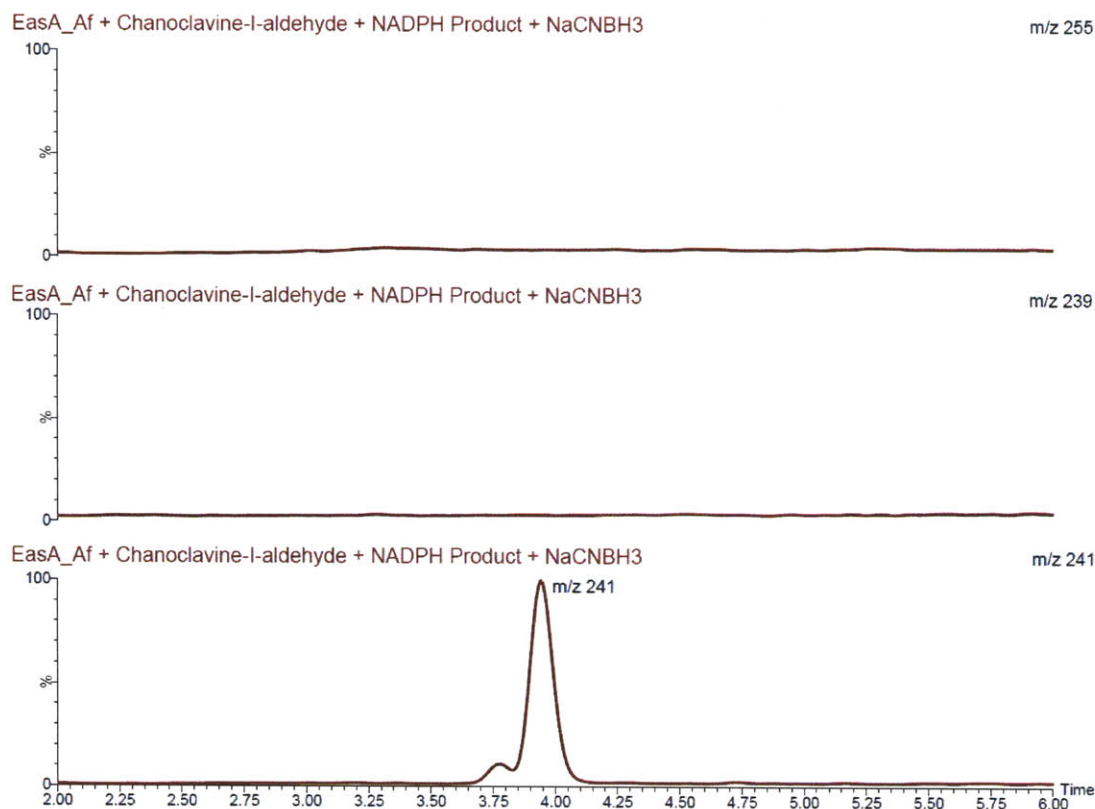


Figure 3.26. ^1H -NMR Easa_Af Enzyme product reduced with NaCNBH_3

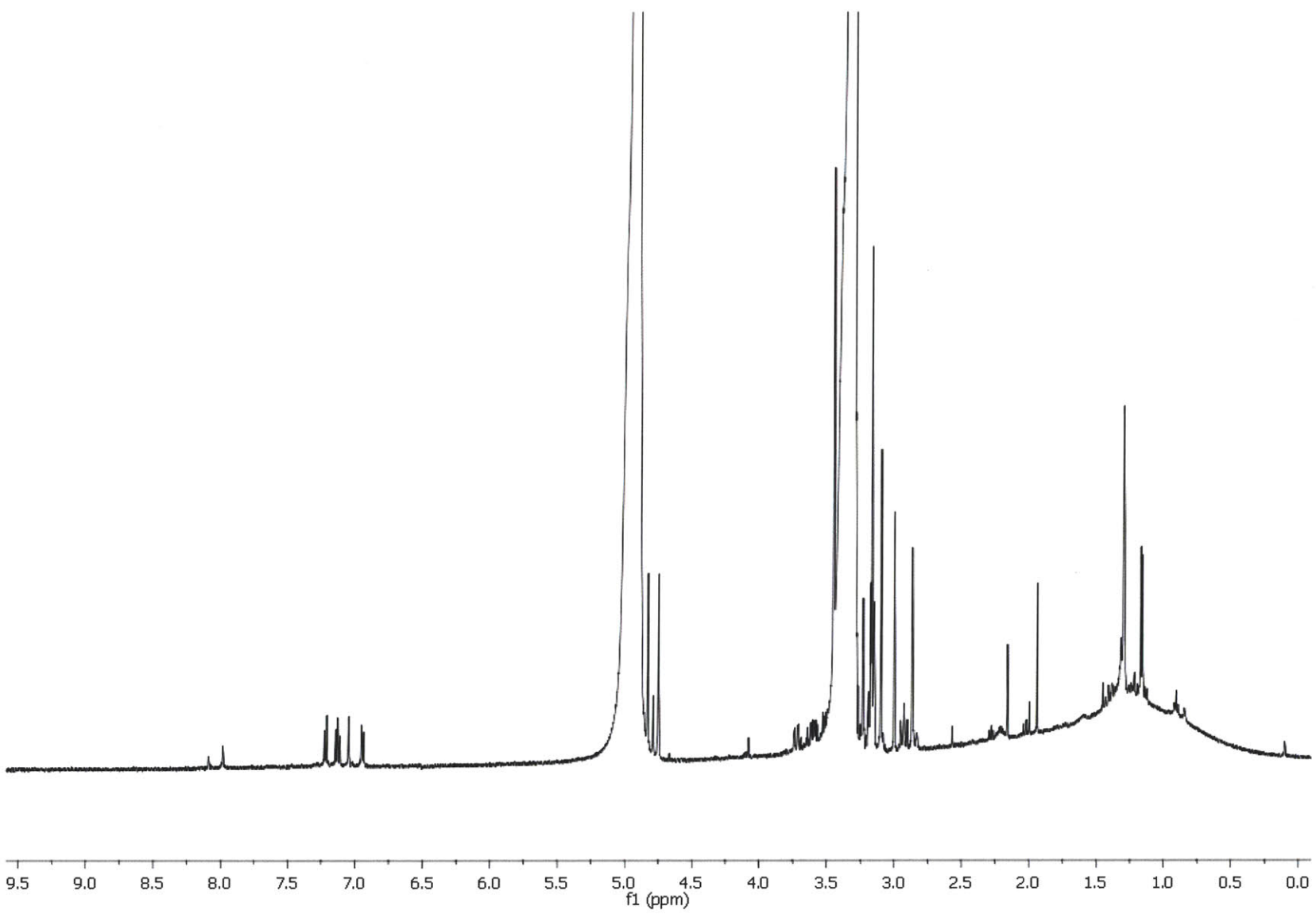


Figure 3.27. ^1H -NMR spectra of compounds used in this study. Full spectra A. EasA_Af Enzyme product reduced with NaCNBH_3 , B. Festuclavine **11**, C. Chanoclavine-I-aldehyde **7**, D. Agroclavine **10**

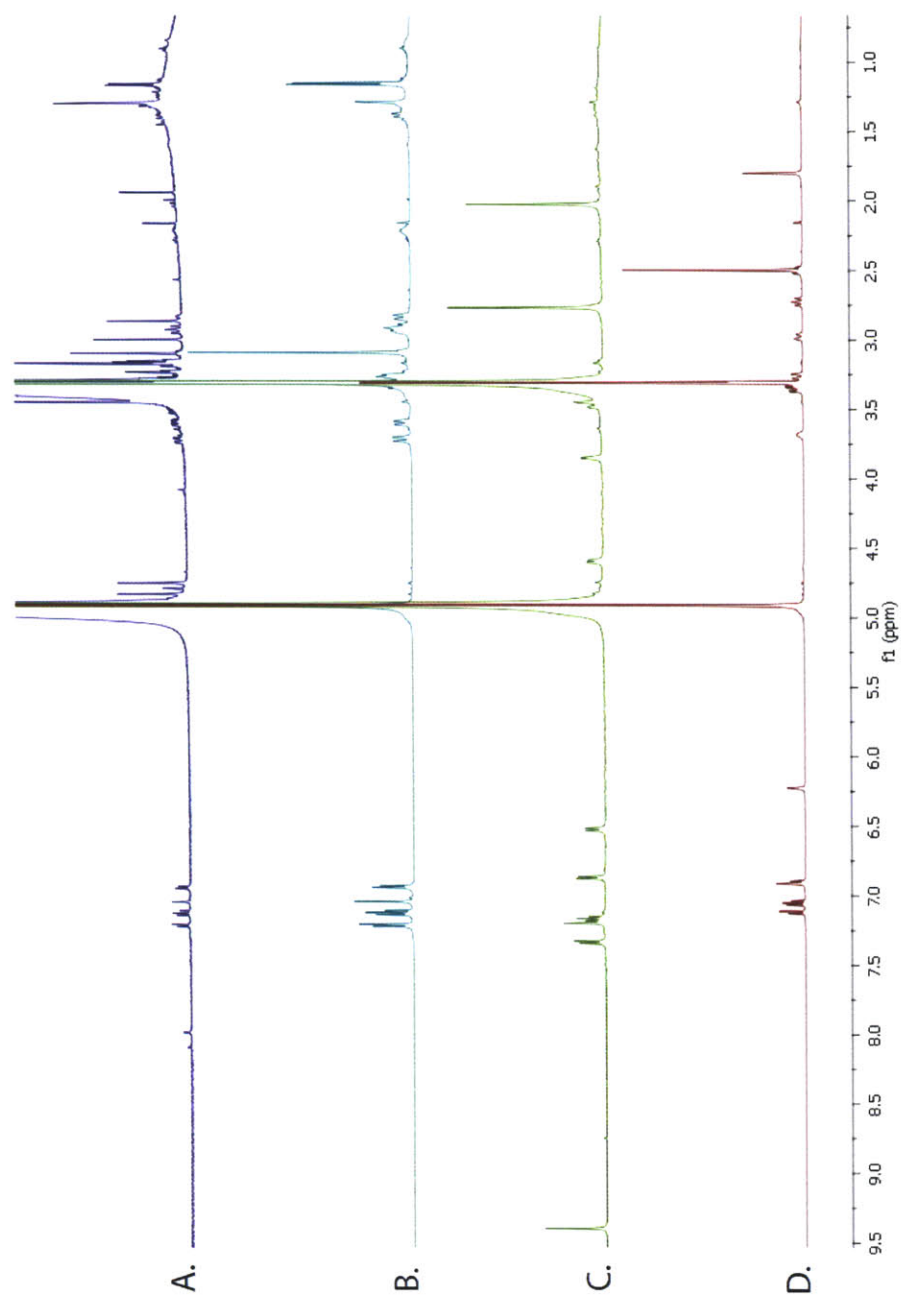
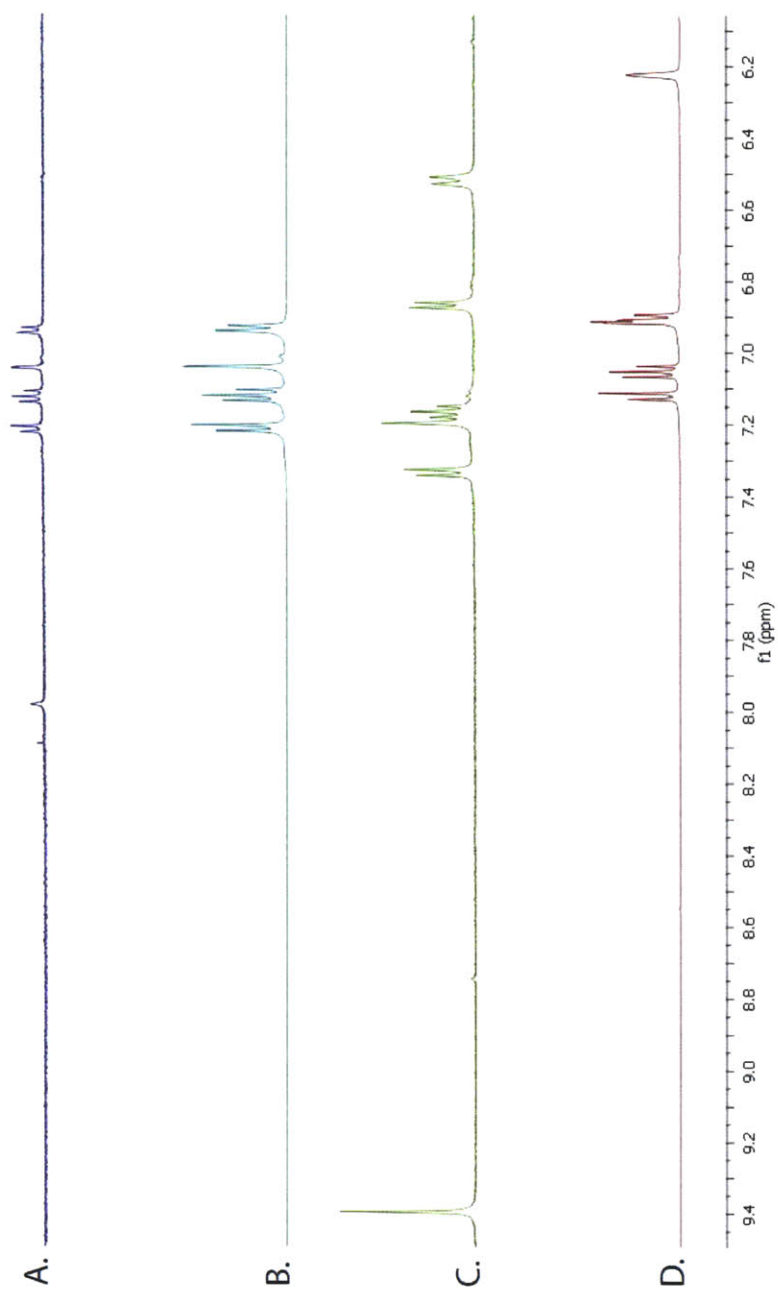


Figure 3.28. ^1H -NMR Aromatic region A. EasA_Af enzyme product reduced with NaCNBH_3 , B. Festuclavine **11**, C. Chanoclavine-I-aldehyde **7**, D. Agroclavine **10**



EasA_Af proposed mechanism of ring D formation based on Old Yellow Enzyme

EasA_Af was compared to the Old Yellow Enzyme homologue from *Saccharomyces carlsbergensis*, OYE1, which has been extensively studied and structurally characterized.⁷ Mechanistic studies of OYE1 suggest that T37¹¹ and Q114¹⁰ residues were critical for flavin binding²⁵, while H191 and N194 interact with NADPH.² Collectively, active site residues H191 and N194, and Y196 were involved in reduction of the substrate alkene.^{2, 4} Protein sequence alignments demonstrate that these OYE1 residues align with T31, Q106, H173, N176, and Y178 of the EasA_Af protein sequence (Figure 3.1). Based on the high sequence identity of EasA_Af with OYE1 (40%), a mechanism for chanoclavine-I-aldehyde **7** reduction that is analogous to the OYE1 mechanism for reduction of α , β -unsaturated ketones and aldehydes can be proposed (Figure 3.4 and 3.5).

Initially, binding and transfer of a hydride from NADPH to reduce the FMN of EasA_Af occurs, followed by release of NADP⁺ to allow for binding of chanoclavine-I-aldehyde **7** (Figure 3.5A). Subsequently, the hydride from reduced FMN is transferred to the β carbon of chanoclavine-I-aldehyde **7**, where H173 and N176 of EasA_Af would act as hydrogen bond donors and polarize the carbonyl oxygen of chanoclavine-I-aldehyde **7**.² The Y178 residue of EasA_Af serves as a proton donor to the α carbon either concurrently with or after transfer of the hydride to the β carbon, as in OYE1 (Figure 3.5B).⁴

In the EasA_Af catalyzed reaction, the immediate reduction product dihydrochanoclavine aldehyde **24** is believed to cyclize and form the cyclic iminium intermediate **9**, it remains an area of our future research efforts to determine whether this

cyclization is spontaneous or enzymatically catalyzed. Some preliminary studies on site directed mutations targeting mechanistically important EasA_Af catalytic active site residues were discussed in Chapter 6.

EasG reductase and its functional role in Ergoline Ring D formation

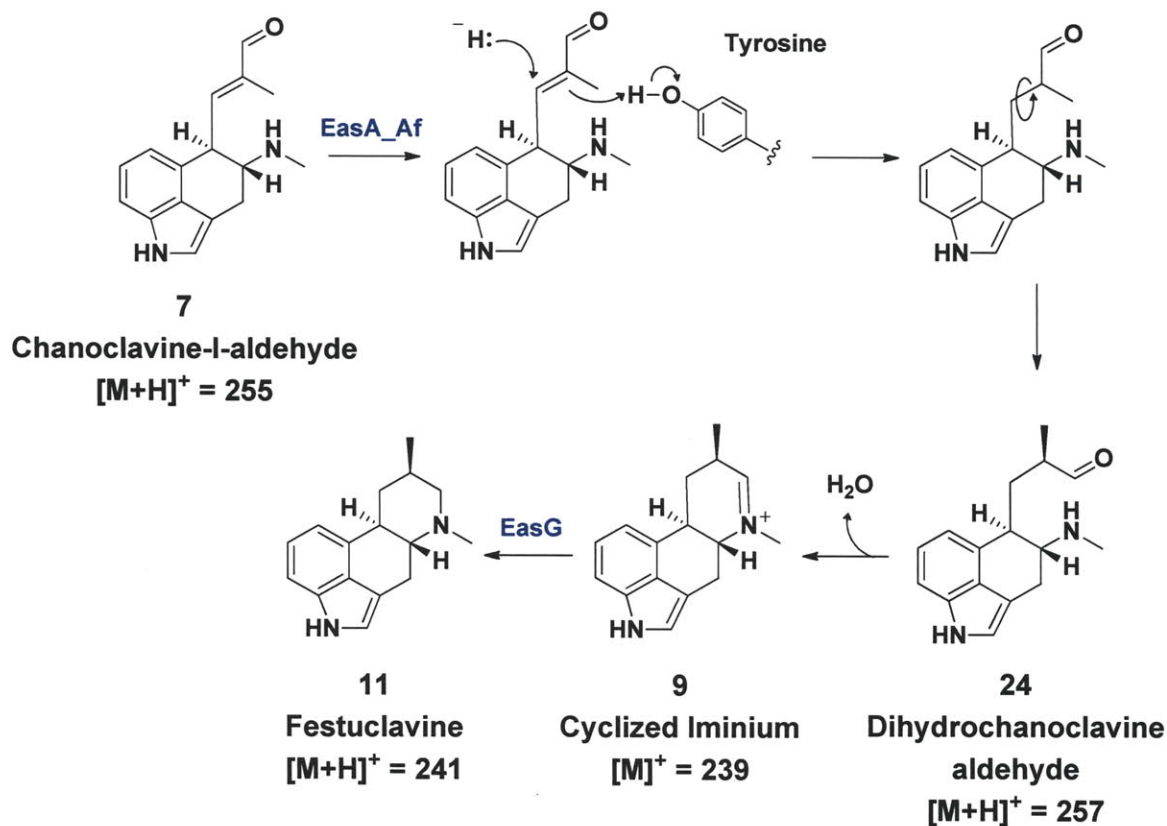
The putative NADPH dependent reductase *easG* of the *A. fumigatus* ergot gene cluster was successfully cloned and heterologously expressed in *E. coli*. Soluble EasG protein was obtained at 6 mg/L of culture and purified by Ni-NTA affinity chromatography (Figure 3.19).

Assay of purified *A. fumigatus* EasG with chanoclavine-I-aldehyde **7**, NADPH, and EasA_Af enzyme yielded a product with a mass and retention time identical to the festuclavine standard **11** $[M+H]^+$ 241 (Figure 4.6). Identity of the festuclavine product **11** was further substantiated by high resolution MS (Table 4.1). A control experiment consisting of heat inactivated EasG with chanoclavine-I-aldehyde **7**, NADPH, and EasA_Af displayed production of the cyclic iminium intermediate **9** with mass of $[M]^+$ 239 as expected (Figure 4.6). It follows from these observations that EasG facilitates the transfer of a hydride to reduce the cyclic iminium intermediate that is produced by EasA_Af demonstrating that EasA_Af and EasG were required in order to form festuclavine **11**. Recent work by Wallwey et al. to characterize the EasG orthologue (fgaFS) from *A. fumigatus* further substantiates that this NADPH dependent reductase is needed to facilitate the conversion of the EasA_Af product, cyclic iminium intermediate **9**, to festuclavine **11** (Figure 3.29).²⁴

From our studies, two scenarios relating to the *in vivo* function of EasA_Af toward producing festuclavine **11** may be inferred. If the cyclization were enzymatically catalyzed, the released cyclized iminium ion **9** would be efficiently incorporated and reduced by a downstream reductase EasG enzyme to create festuclavine **11**. If the cyclization were not enzymatically driven, the released EasA_Af product would be dihydrochanoclavine aldehyde **24**, which could undergo subsequent tautomerization and cyclization under equilibrium conditions producing two diastereoisomers (Figure 3.23). In this scenario, the downstream iminium reductase EasG that forms festuclavine **11** would presumably only recognize the correct diastereomer of the cyclized iminium ion **9**.

It also remains a possibility that EasA_Af and EasG were associated with one another to foster the delivery of intermediate **9** from the active site of EasA to EasG, so that racemization is minimized. Approaches to study possible protein-protein interaction between EasA_Af and EasG enzymes will be further discussed in Chapter 6.

Figure 3.29. Proposed functional roles of EasA_Af and EasG in the conversion of chanoclavine-I-aldehyde **7** to festuclavine **11**. Expected $[M+H]^+$ masses of pathway intermediates are displayed.



Conclusion

This chapter describes the functional characterization of *A. fumigatus* enzymes EasA and EasG that were involved in the formation of ring D in ergot alkaloid biosynthesis. This study demonstrated that EasA_Af facilitates the reduction of the alkene in chanoclavine-I-aldehyde **7** allowing for free rotation about the C8 and C9 bond followed by the intramolecular condensation of the secondary amine and aldehyde moieties to form the cyclic iminium intermediate **9** (Figure 3.5B, Figure 3.29). However, it remains a point of interest to study whether the cyclization of dihydrochanoclavine aldehyde **24**, the immediate product expected of EasA_Af reduction, into the cyclic iminium intermediate **9** is spontaneous or enzyme catalyzed.

Our results from the *in vitro* biochemical characterization of EasA_Af enzyme coincided with our observations from our *in vivo* study on the accumulation of chanoclavine-I **6** and chanoclavine-I-aldehyde **7** in the *easA* gene disrupted *A. fumigatus* mutant in Chapter 2, thereby further substantiating that chanoclavine-I-aldehyde **7** is the substrate of EasA_Af.

This study also demonstrated that EasG, an NADPH dependent oxidoreductase, along with EasA_Af were required to form festuclavine **11** from substrate chanoclavine-I-aldehyde **7**. Therefore, EasG acts directly after the reduction of chanoclavine-I-aldehyde **7** by EasA_Af (Figure 3.29). It remains a point of interest to study how and whether EasA_Af and EasG interact to form festuclavine. Furthermore, the successful cloning and expression of active EasG from *A. fumigatus* proved to be instrumental toward our efforts in studying the origins of structural divergence in ergot alkaloid biosynthesis.

The work in this chapter highlights a new role for an OYE homologue in natural product biosynthesis. This work provided functional insight into enzymes EasA_Af and EasG, and their role in catalyzing the critical D ring cyclization of festuclavine **11** in ergot alkaloid producing fungi.

References

1. Schardl, C.L., D.G. Panaccione, and P. Tudzynski, *Ergot Alkaloids - Biology and Molecular Biology*, in *The Alkaloids* G. Cordell, Editor. 2006, Elsevier. p. 45-86.
2. Brown, B., Z. Deng, P.A. Karplus, and V. Massey, *On the Active Site of Old Yellow Enzyme Role of Histidine 191 and Asparagine 194*. The Journal of Biological Chemistry, 1998. **273**(49): p. 32753-32762.
3. Fox, K. and P.A. Karplus, *Old yellow enzyme at 2 Å resolution: overall structure, ligand binding, and comparison with related flavoproteins*. Structure, 1994. **15**(2): p. 1089-1105.
4. Kohli, R. and V. Massey, *The Oxidative Half-reaction of Old Yellow Enzyme The Role of Tyrosine 196*. The Journal of Biological Chemistry, 1998. **273**(49): p. 32763-32770.
5. Jo Brown, B., J. Hyun, S. Duwuri, A. Karplus, and V. Massey, *The Role of Glutamine 114 in Old Yellow Enzyme*. The Journal of Biological Chemistry, 2002. **277**(3): p. 2138-2145.
6. Warburg, O. and W. Christian, *Ein zweites sauerstoffübertragendes Ferment und sein Absorptionsspektrum*. Naturwissenschaften, 1932. **20**: p. 688.
7. Theorell, H. and A. Akeson, *Molecular weight and FMN content of crystalline "old yellow enzyme"*. Archives of Biochemistry and Biophysics, 1956. **65**(1): p. 439-448.
8. Saito, K., D. Thiele, M. Davio, O. Lockridge, and V. Massey, *The Cloning and Expression of a Gene Encoding Old Yellow Enzyme from Saccharomyces carlsbergensis*. The Journal of Biological Chemistry, 1991. **266**(31): p. 20720-20724.
9. Vaz, A., S. Chakraborty, and V. Massey, *Old Yellow Enzyme: Aromatization of Cyclic Enones and the Mechanism of a Novel Dismutation Reaction*. Biochemistry, 1995. **34**: p. 4246-4256.
10. Brown, B.J., J. Hyun, S. Duwuri, P.A. Karplus, and V. Massey, *The Role of Glutamine 114 in Old Yellow Enzyme*. The Journal of Biological Chemistry, 2002. **277**(3): p. 2138-2145.
11. Xu, D., R. Kohli, and V. Massey, *The Role of Threonine 37 in Flavin Reactivity of the Old Yellow Enzyme*. Proceedings of the National Academy of Sciences of the United States of America, 1999. **96**: p. 3556-3561.
12. Stott, K., K. Saito, D. Thiele, and V. Massey, *Old Yellow Enzyme The Discovery of Multiple Isozymes and a Family of Related Proteins*. The Journal of Biological Chemistry, 1993. **268**(9): p. 6097-6106.
13. Meah, Y. and V. Massey, *Old Yellow Enzyme: Stepwise reduction of nitro-olefins and catalysis of aci-nitro tautomerization*. Biochemistry, 2000. **97**(20): p. 10733-10738.
14. Williams, R. and N. Bruce, *'New uses for an old enzyme' – the old yellow enzyme family of flavoenzymes*. Microbiology, 2002. **148**: p. 1607-1614.
15. Breithaupt, C., R. Kurzbauer, H. Lilie, A. Schaller, J. Strassner, R. Huber, P. Macheroux, and T. Clausen, *Crystal structure of 12-oxophytodienoate reductase 3 from tomato: Self-inhibition by dimerization*. Proceedings of the National

- Academy of Sciences of the United States of America, 2006. **103**(39): p. 14337-14342.
16. French, C.E. and N.C. Bruce, *Bacterial morphinone reductase is related to Old Yellow Enzyme*. Biochemical Journal, 1995. **312**: p. 671-678.
 17. Trotter, E.W., E.J. Collinson, I.W. Dawes, and C.M. Grant, *Old Yellow Enzymes Protect against Acrolein Toxicity in Yeast *Saccharomyces cerevisiae**. Applied and Environmental Microbiology, 2006. **72**(7): p. 4885-4892.
 18. Massey, V. and L. Schopfer, *Reactivity of Old Yellow Enzyme with alpha-NADPH and Other Pyridine Nucleotide Derivatives*. The Journal of Biological Chemistry, 1986. **261**(3): p. 1215-1222.
 19. Karplus, P.A., K. Fox, and V. Massey, *Structure-function relations for old yellow enzyme*. The FASEB Journal, 1995. **9**: p. 1518-1526.
 20. Meah, Y., B. Brown, S. Chakraborty, and V. Massey, *Old yellow enzyme: Reduction of nitrate esters, glycerin trinitrate, and propylene 1,2-dinitrate*. Proceedings of the National Academy of Sciences of the United States of America, 2001. **98**(15): p. 8560-8565.
 21. Brige, A., D. Van Den Hemel, W. Carpentier, L. De Smet, and B. J., *Comparative characterization and expression analysis of the four old yellow enzyme homologues from *Shewanella oneidensis* indicate differences in physiological function*. Biochemical Journal, 2006. **394**: p. 335-344.
 22. Barna, T., H. Messiha, C. Petosa, N. Bruce, N. Scrutton, and P. Moody, *Crystal Structure of Bacterial Morphinone Reductase and Properties of the C191A Mutant Enzyme*. The Journal of Biological Chemistry, 2002. **277**: p. 30976-30983.
 23. Cheng, J.Z., C.M. Coyle, D.G. Panaccione, and S.E. O'Connor, *A Role for Old Yellow Enzyme in Ergot Alkaloid Biosynthesis*. Journal of the American Chemical Society, 2010. **132**(6): p. 1776-1777.
 24. Wallwey, C., M. Matuschek, X.-L. Xie, and S.-M. Li, *Ergot alkaloid biosynthesis in *Aspergillus fumigatus*: Conversion of chanoclavine-I aldehyde to festuclavine by festuclavine synthase FgaFS in the presence of the old yellow enzyme FgaOx3*. Organic and Biomolecular Chemistry 2010. **8**: p. 3500-3508.
 25. Fox, K. and P. Karplus, *The Flavin Environment in Old Yellow Enzyme*. The Journal of Biological Chemistry, 1999. **274**(14): p. 9357-9362.
 26. Arnold, K., L. Bordoli, J. Kopp, and T. Schwede, *The SWISS-MODEL Workspace: A web-based environment for protein structure homology modelling*. Bioinformatics, 2006. **22**: p. 195-201.
 27. Bordoli, L., F. Kiefer, K. Arnold, P. Benkert, J. Battey, and T. Schwede, *Protein structure homology modeling using SWISS-MODEL workspace*. Nature Protocols, 2009. **4**: p. 1-13.
 28. Bikadi, Z. and E. Hazai, *Application of the PM6 semi-empirical method to modeling proteins enhances docking accuracy of AutoDock*. Journal of Cheminformatics, 2009. **1**(15): p. 1-16.
 29. Price, A., Y.-M. Zhang, C.O. Rock, and S.W. White, *Structure of Beta-Ketoacyl-[acyl carrier protein] Reductase from *Escherichia coli*: Negative Cooperativity and Its Structural Basis*. Biochemistry, 2001. **40**: p. 12772-12781.

30. Kamitori, S., A. Iguchi, A. Ohtaki, M. Yamada, and K. Kita, *X-ray Structures of NADPH-dependent Carbonyl Reductase from Sporobolomyces salmonicolor Provide Insights into Stereoselective Reductions of Carbonyl Compounds*. Journal of Molecular Biology, 2005. **352**: p. 551-558.
31. Phillips, R.S., *NAD(P) dependent dehydrogenases*, in *Wiley Encyclopedia of Chemical Biology*. 2009. p. 200-209.
32. Weiner, H. and D. Thomas, *NADP⁺ binding to dehydrogenases* in *Handbook of Proteins*, M.M.P. Cox, George N Editor. 2007. p. 626-632.
33. Chomczynski, P. and N. Sacchi, *The single-step method of RNA isolation by acid guanidinium thiocyanate-phenol-chloroform extraction: twenty-something years on*. Nature Protocols, 2006. **1**(2): p. 581-585.
34. Macheroux, P., *UV-visible spectroscopy as a tool to study flavoproteins*, in *Methods in Molecular Biology: Flavoprotein Protocols*, S. Chapman and G. Reid, Editors. 1999, Humana Press Inc.: Totowa, NJ.
35. Coyle, C.M., J.Z. Cheng, S.E. O'Connor, and D.G. Panaccione, *An Old Yellow Enzyme Gene Controls the Branch Point between Aspergillus fumigatus and Claviceps purpurea Ergot Alkaloid Pathways*. Applied and Environmental Microbiology, 2010. **76**(12): p. 3898-3903.
36. Floss, H.G., M. Tcheng-Lin, C. Chang, B. Naidoo, G. Blair, C. Abou-Chaar, and J. Cassady, *Biosynthesis of ergot alkaloids. Mechanism of the conversion of chanoclavine-I into tetracyclic ergolines*. Journal of the American Chemical Society, 1974: p. 1898-1909.
37. Nakahara, Y., T. Niwaguchi, and H. Ishii, *Studies on Lysergic Acid Diethylamide and Related Compounds*. Chemical and Pharmaceutical Bulletin, 1977. **25**(7): p. 1756-1763.
38. Yokoyama, Y., K. Kondo, M. Mitsuhashi, and Y. Murakami, *Total Synthesis of Optically Active Chanoclavine-I*. Tetrahedron Letters, 1996. **37**(52): p. 9309-9312.
39. Greis, K., *Mass Spectrometry For Enzyme Assays and Inhibitor Screening: An Emerging Application In Pharmaceutical Research*. Mass Spectrometry Reviews, 2007. **26**: p. 324-339.
40. Zea, C. and N. Pohl, *General Assay for Sugar Nucleotidyltransferases Using Electrospray Ionization Mass Spectrometry*. Analytical Biochemistry, 2004. **328**: p. 196-202.

Chapter 4 . Controlling Pathway Divergence in Ergot Alkaloid Biosynthesis

Part of this chapter has been published in

Cheng, J.Z., C.M. Coyle, D.G. Panaccione, and S.E. O'Connor, *Controlling a Structural Branch Point in Ergot Alkaloid Biosynthesis*. Journal of the American Chemical Society, 2010. **132**(37): p. 12835-12837.

Introduction

The ergot biosynthetic gene clusters of *A. fumigatus* and Clavicipitaceous fungi *C. purpurea* and *N. lolii* share a set of homologous genes that were associated to early pathway of ergot alkaloid biosynthesis (Figure 1.5). This shared set of homologous genes across the divergent fungal species were attributed to the early steps of ergoline biosynthesis up to the cyclization of the ring D (Figure 1.4).¹ The *A. fumigatus* EasA_Af and EasG ergot alkaloid biosynthetic enzymes were functionally characterized and shown to play a key role in the formation of ring D, producing festuclavine **11** from the chanoclavine-I-aldehyde **7** as described in Chapter 3.^{2,3} These findings correlate with the observation that *A. fumigatus* produces festuclavine **11** and its derivatives the fumigaclavines A **18**, B **19**, and C **14**. Whereas Clavicipitaceous fungi *C. purpurea* and *N. lolii* produce only agroclavine **10** derived lysergic acid amides and ergopeptides (Figure 1.3).⁴⁻⁷

From a mechanistic standpoint, in order to produce the downstream ergot alkaloids unique to each fungal species, *A. fumigatus* EasA_Af functions as a reductase in which the C8-C9 alpha beta double bond of chanoclavine-I-aldehyde **7** is reduced and remains a single bond in the cyclized festuclavine **11** ring D (Figure 4.1). In contrast, the *C. purpurea* or *N. lolii* EasA would be expected to function as an isomerase, where the C8-C9 double bond of chanoclavine-I-aldehyde **7** is preserved but displays the opposite geometrical configuration in the cyclized agroclavine **10** ring D (Figure 4.1).

The cyclization of chanoclavine-I-aldehyde **7** to agroclavine **10** via the isomerization of the C8-C9 alkene has been previously suggested based on isotope feeding studies to cultures of *Claviceps* (Figure 4.2).⁸⁻¹³ The results of these studies

demonstrated that the conversion of chanoclavine-I-aldehyde **7** to agroclavine **10** involved a cis-trans isomerization. Yet the exact mechanism by which agroclavine **10** was formed from chanoclavine-I-aldehyde **7** remained speculative.

Protein sequence alignments for homologues of reductase type EasA (festuclavine producers) and isomerase type EasA (agroclavine producers), displays a significant trend. Reductase type EasA enzymes such as *A. fumigatus* EasA_Af described in Chapter 3 has a catalytic active site tyrosine, whereas isomerase type EasA such as *N. lolii* EasA_Nl has a phenylalanine in the same position (Figure 4.3). Notably, other catalytically important active site residues were generally well conserved between the two enzymes.³

Given the proposed role of the catalytic tyrosine to protonate C8 upon hydride transfer to the C9 position in reductase type EasA, we speculated that for isomerase EasA the lack of this proton donating tyrosine would allow enolate formation followed by bond rotation, and finally re-oxidation of the C8-C9 double bond prior to ring D formation (Figure 4.1).

Further evidence regarding the importance of these tyrosine and phenylalanine residues in the active site comes from our augmentation of reductase type *easA* with isomerase type *easA* from *C. purpurea in vivo* as presented in Chapter 2. Replacement of the reductase with isomerase *easA* in *A. fumigatus*, demonstrated a switch in ergot profile from the production of festuclavine **11** to agroclavine **10** derived alkaloids.³

Figure 4.1. Proposed pathway branch point of ergot alkaloid biosynthesis in divergent fungal species. Common intermediate chanoclavine-I-aldehyde **7** is converted via *N. lolii* EasA (EasA_Nl) by isomerization of the C8-C9 alkene to eventually yield agroclavine **10**. Alternatively chanoclavine-I-aldehyde **7** is converted in *A. fumigatus* EasA (EasA_Af) by reduction of the C8-C9 alkene to eventually yield festuclavine **11**.

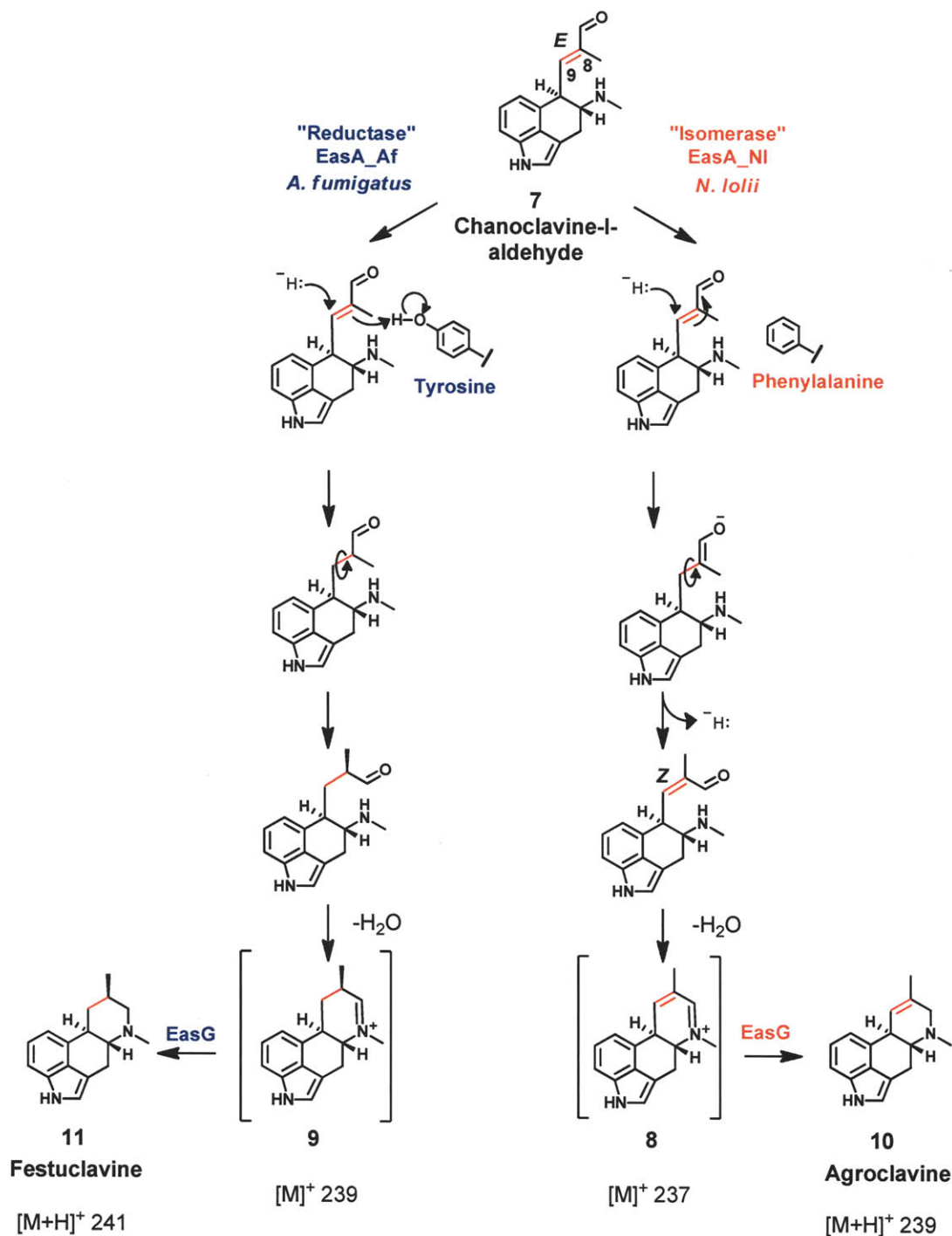
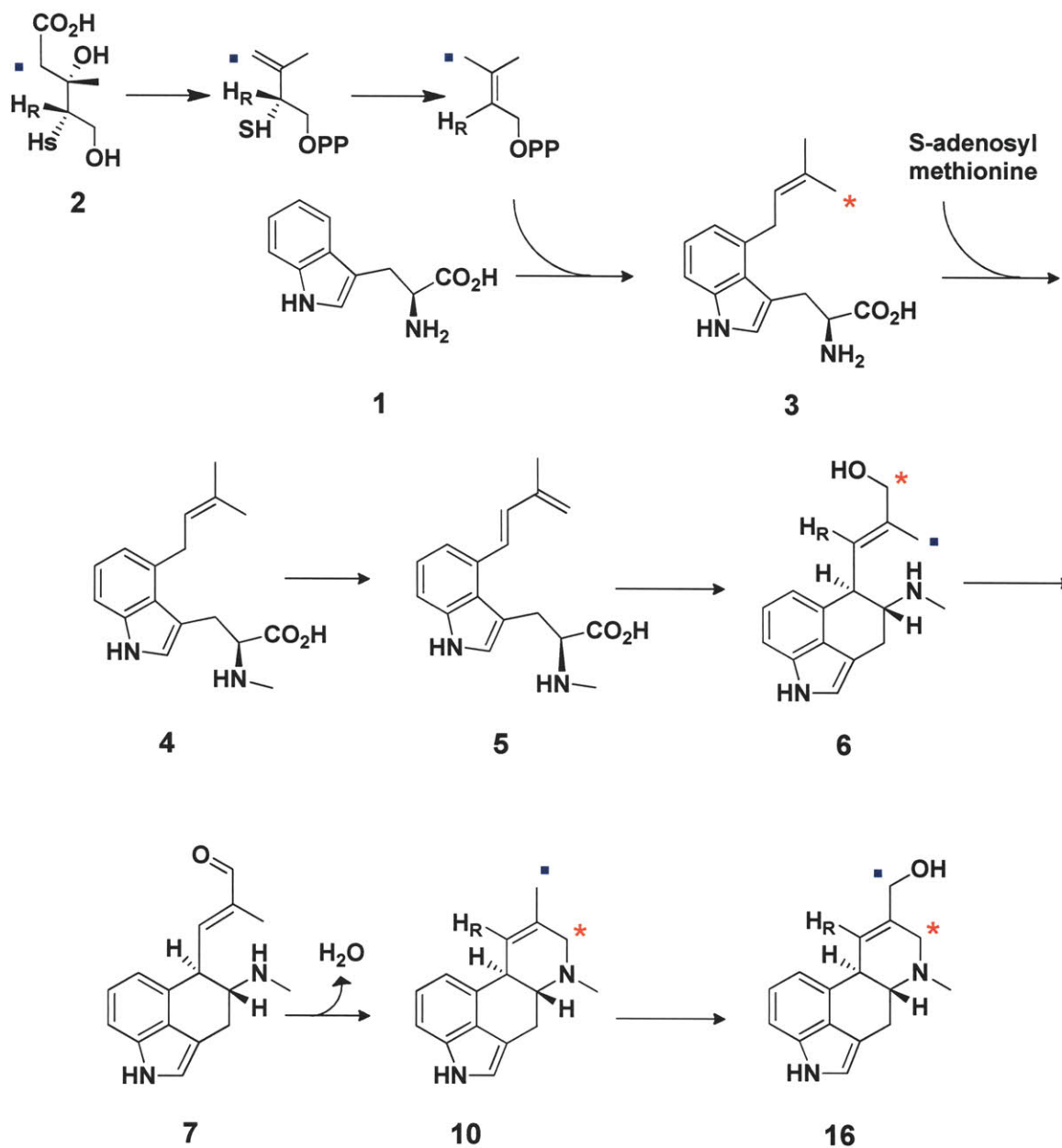


Figure 4.2. Early isotope feeding studies suggest that two cis-trans isomerizations occurring, the first between DMAT **3** and chanoclavine-I⁸ **6** and second between chanoclavine-I **6** and agroclavine **10**.^{5, 6, 9-13}

(●) indicates ¹⁴C label of [2-¹⁴C] mevalonate feeding study conducted by Fehr et al.⁹

(*) indicates ¹⁴C label of [Z-¹⁴CH₃] DMAT feeding study conducted by Pachlatko et al.⁸

Note: Molecules drawn with double labels represent the superposition of two individual single labeled downstream molecules that were observed in separate feeding studies. They indicate where the upstream labeled precursor were incorporated into the downstream products.



C_purpureaP1	DDLVPQFEHFITCLREMDIAYLHLANSRWVEEEDPSIRTHPDFHNQTFVQMWGKKRPILL	296
C_purpureaA2	DDLVPQFEHFITCLREMDIAYLHLANSRWVEEEDPSIRTHPDFHNQTFVQMWGKKRPILL	296
C_fusiformis	DDLVAQFEHFISRLREMDIAYIHLVNTRWLEEEEPGIKTHPDVDNQTFFVRMWGNKTPILL	296
<u>C_africana</u>	DDLVPQFQHFISSLREMDVAYLHLTNSRWLQEEQPGIKIHPDVHNATFVRMWGREKPIVL	278
<u>C_gigantea</u>	VDLLPQFQHFITCLREMDIAYLHLTNSRWLQEEQPGVKIHPDVNNATFVRMWGLEKPIVL	278
N_lolii	DDLIPQFEHFIMRLREIGIAYLHLANSRWVEEEDPTIRTHPDIHNETFVRMWGKEKPVLL	296
E_festuceae	DDLIPQFEHFIMRLREIGIAYLHLANSRWVEEEDPTIRTHPDIHNETFVRMWGKEKPVLL	296
<u>A_fumigatus</u>	DELVPQFEYLIAQMRRLDVAYLHLANSRWLDEEKP---HPDPNHEVFVRVWGQSSPILL	294
	:*:.**::* :*:.:***:**.*:***:***.* *** .: .**::** . *::*	
C_purpureaP1	AGGYDPDSARRLVDQTYSD-RNNVLVVFGRHYISNPDLPFRLRMGIACRSTIETHSIFPA	355
C_purpureaA2	AGGYDPDSARRLVDQTYSD-RNNVLVVFGRHYISNPDLPFRLRMGIALQKYNRDTFYIPC	355
C_fusiformis	AGGYDADSARRLVDETYSD-QNNIMVVFGGRHYISNPDLPFRLRLGIPLQKYNRDTFYIPF	355
<u>C_africana</u>	AGGYDADSAKRLVDETYSD-QNNVLVAFGRHYISNPDLPFRLKMGIALQKYNRDT-----	332
<u>C_gigantea</u>	AGGYDADSAKRLVDETYSE-HNNVLVAFGRHYISNPDLPFRLKMGIALQKYNRDT-----	332
N_lolii	AGGYGPESAKLVVDETYSD-HKNIGVVFGGRHYISNPDLPFRLKMGLPLQKYNRETIFYIPF	355
E_festuceae	AGGYGPESAKLVVDETYSD-HKNIGVVFGGRHYISNPDLPFRLKMGLPLQKYNRETIFYIPF	355
<u>A_fumigatus</u>	AGGYDAASAEKVTEQMAAATYTNVAIAFGRYFISTPDLPFVRVMAGIQLQKYDRASFYSTL	354
	.. ** .:..: : .*: :.:***.*****: *: :. .	

In this chapter we describe the cloning, expression, and functional characterization of *N. lolii* isomerase type EasA (EasA_Nl) and its catalytic role in the cyclization of ring D in the presence of *A. fumigatus* EasG NADPH dependent reductase (described in Chapter 3) to produce agroclavine **10**. This set of *in vitro* experiments served to complement our study in Chapter 2, where the augmentation of the reductase type *easA* gene in *A. fumigatus* by isomerase type *easA* from *C. purpurea* *in vivo* provided a switch from festuclavine **11** to agroclavine **10** derived alkaloid production in cultures.³ To gain further insight into the distinct functional roles of reductase versus isomerase type EasA, we used mutational analysis to provide a mechanistic rationale to explain how EasA can control this critical branch point in ergot alkaloid biosynthesis.

Experimental Methods

General Materials and Methods

General recombinant DNA cloning procedures were performed using pGEM-T vector (Promega) and propagated in *E. coli* Top10 (Invitrogen). Protein expression for *N. lolii* EasA was conducted in *E. coli* Rosetta (DE3) pLysS (Novagen). Protein expression for EasG was conducted in *E. coli* BL-21(DE3) (Invitrogen). PCR amplification utilized Platinum Taq DNA Polymerase (Invitrogen). Recombinant DNA plasmids were prepared using Qiaprep Spin Miniprep and Qiaquick Gel Extraction kits (Qiagen). Restriction enzymes and T4 DNA ligase were purchased from New England Biolabs. Primers for cloning were synthesized by Integrated DNA Technologies and DNA sequencing was conducted by the MIT Biopolymers Laboratory (Cambridge, MA).

LC-MS analysis was conducted using an Acquity Ultra Performance BEH C18 column with a 1.7 mm particle size, 2.1 x 100 mm dimension, with a gradient of acetonitrile/0.1% formic acid in water mobile phase (10:90 to 20:80 from 0-5 min, 20:80 to 90:10 from 5-6 min, and 90:10 to 10:90 from 6-7 min at a constant flow rate of 0.5 mL/min). The column elution was coupled to MS analysis carried out using a Micromass LCT Premier TOF Mass Spectrometer with an ESI source (Waters). Accurate mass data were acquired using reference compound leucine enkephalin for lock mass correction. A Varian Cary 50 Bio Scanning Spectrometer was used to acquire UV-Vis spectra. The chanoclavine-I-aldehyde **7** substrate was isolated from the $\Delta easA$ deletion strain of *A. fumigatus* in Chapter 3 and as previously described.¹

Cloning, overexpression, and purification of *Neotyphodium lolii* EasA

The *N. lolii easA* gene was PCR amplified using *N. lolii* genomic DNA supplied by Daniel Panaccione. Primers were designed based on the nucleotide sequence of *N. lolii easA* from the NCBI database (EF125025.1). The following pair of oligonucleotide primers were used to amplify the *easA* gene: forward primer 5'-**TTGGCCATATGTCAACTTCAAATCTTTT**CACGCCGC-3' (with NdeI restriction site in bold) and reverse primer 5'-**GACTCGAGT**GCTAGAACTGCCTGCTTCTTGTTCC-3' (XhoI restriction site in bold). The PCR amplified *easA* gene was inserted into pGEM-T vector (Promega) for propagation and sequencing. Subsequently, the *easA* sequence was excised from pGEM-T by restriction digest then ligated into the NdeI/XhoI site of pET-24a(+) (Novagen) expression vector as a C-His₆ tagged construct.

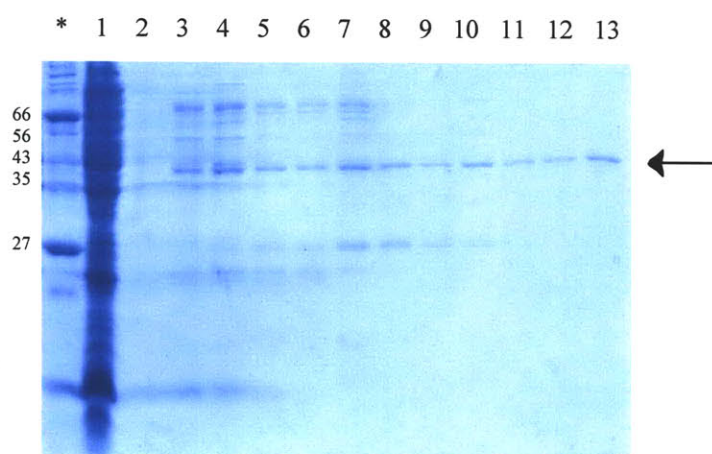
The F176Y mutant of *N. lolii easA* was constructed using the Quickchange II Site Directed Mutagenesis Kit (Stratagene). The following pair of oligonucleotide primers were used: forward primer 5'-**TCCACGGTGCCAATGGATATCTCATCGATCAGTTT**-3' and reverse primer 5'-**AAACTGATCGATGAGATATCCATTGGCACCGTGGA**-3'.

EasA_Af_Y178F expression was conducted according to the method described in Chapter 3 for expression of EasA_Af.¹ The Y178F mutant of *A. fumigatus easA* was constructed using the Quickchange II Site Directed Mutagenesis Kit (Stratagene). The following pair of oligonucleotide primers were used: forward primer 5'-**CATGGTGCCAATGGGTTCTCATCGACCAGT**-3' and reverse primer 5'-**ACTGGTCGATGAGGAACCCATTGGCACCATG**-3'.

Expression for both wild type and mutant *N. lolii* EasA was carried out in LB medium supplemented with kanamycin (50 µg/mL) and chloramphenicol (34 µg/mL). Rosetta (DE3) pLysS cells were grown to an OD₆₀₀ of 0.7 prior to induction with IPTG (1 mM) and grown for 30 hours at 15 °C prior to harvesting. Cells were resuspended in buffer (20 mM Tris-HCl, 300 mM NaCl, 10% (v/v) glycerol, pH = 8.0) and incubated on ice for 30 mins with added lysozyme (1 mg/mL) and DNaseI (10 µg/mL) and lysed by sonication. Cellular debris were pelleted by centrifugation (15,000 x g for 1 hr). EasA enzyme was purified using Ni-NTA agarose (Qiagen).

Previous work established that all OYE homologs as well as EasA from *A. fumigatus* co-purifies with an FMN flavin cofactor as discussed in Chapter 3.¹⁻⁸ The yield of active holoenzyme EasA from *N. lolii* wild type EasA (EasA_Nl) and *N. lolii* EasA F176Y mutant (EasA_Nl_F176Y) were both estimated to be 0.3 mg/L culture by measuring the UV absorbance of flavin at 446 nm (FMN extinction coefficient of 12,200 M⁻¹cm⁻¹).¹⁹ Assays were conducted with enzyme that eluted in the 50 mM imidazole fractions from the Ni-NTA agarose column (Figure 4.4). The enzyme in these fractions co-purified with flavin cofactor. Final EasA_Nl holoenzyme stock concentration was at 6 µM. Enzyme eluted in the 150-300 mM imidazole fractions lacked the flavin cofactor as evidenced by UV-Vis spectra (Figure 4.5). These fractions were also shown to convert chanoclavine-I-aldehyde **7** to agroclavine **10** when assayed with added FMN (1 µM) and apoenzyme EasA_Nl (0.1 µM).

Figure 4.4. SDS-PAGE of EasA (*N. loli*) (42 kDa)

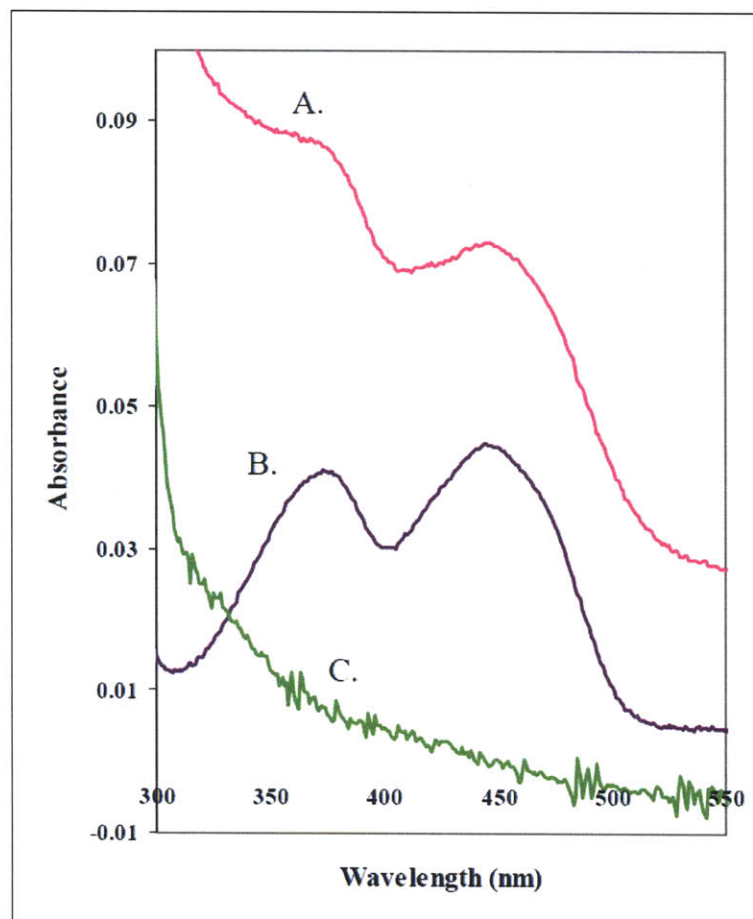


*. NEB Broad Range Protein Ladder (2-212 kDa)

1. column flow-through
2. buffer wash 10 mM imidazole
3. 25 mM imidazole
- 4-6. 50 mM imidazole
7. 100 mM imidazole
- 10-12. 150 mM imidazole
13. 300 mM imidazole

Figure 4.5. Flavin absorbance spectrum (300 nm to 550 nm).

- A. EasA_Nl co-purified with FMN
- B. Free FMN
- C. EasA_Nl apoenzyme



Cloning, overexpression, and purification of *Aspergillus fumigatus* EasG

The *easG* gene from *A. fumigatus* was cloned and heterologously expressed according to the methods and materials section in Chapter 3.

Endpoint assays for EasA and EasG

Endpoint assays incubated EasA_Af, EasA_Nl, and EasA mutants (0.1 μ M, final concentration) with EasG (0.1 μ M, final concentration), chanoclavine-I-aldehyde **7** (10 μ M, final concentration), and NADPH (500 μ M, final concentration) in 100 mM K₂HPO₄ buffer (pH = 7.0) at 25 °C for 30 min. Aliquots (3 μ L) were quenched by dilution in 0.1% formic acid in water and analyzed by LC-MS.

Results and Discussion

Heterologous expression of EasA_Nl and characterization of the bound flavin

The putative flavin dependent oxidoreductase OYE homologue *easA* of the *N. lolii* ergot gene cluster was successfully cloned and heterologously expressed in *E. coli*. Crude EasA_Nl was purified by Ni-NTA affinity chromatography to yield holoenzyme EasA_Nl at 0.3 mg/L culture (Figure 4.4). EasA_Nl, which eluted in the 50mM imidazole fractions from the Ni-NTA agarose column, appeared yellow in color while enzyme eluting in the 150-300 mM imidazole fractions appeared colorless. UV-Vis spectrophotometry demonstrated that the yellow fractions contained EasA_Nl that co-purified with flavin cofactor, while colorless enzyme, eluting in the 150-300 mM imidazole fractions, lacked flavin. The flavin that co-purified with EasA_Nl was identified as flavin mononucleotide (FMN) and exhibited the same absorbance maxima at 373 nm and 446 nm as the FMN standard (Figure 4.5). Active EasA_Nl holoenzyme concentration was measured by UV absorbance of flavin at 446 nm based on the FMN extinction coefficient of $12,200 \text{ M}^{-1}\text{cm}^{-1}$.¹⁹ Assays were conducted with EasA_Nl enzyme that co-purified with FMN (50 mM imidazole fractions). EasA_Nl that did not co-purify with FMN (100-300 mM) was also active toward the conversion of chanoclavine-I-aldehyde **7** to agroclavine **10** when assayed along with added FMN (1 μM) to apoenzyme EasA_Nl (0.1 μM), though displayed a much slower rate of turnover qualitatively.

The functional role of EasA_Nl isomerase

When assayed with EasA_Nl and NADPH, the chanoclavine-I-aldehyde **7** $[M+H]^+$ 255 peak decreased over time. Unlike EasA_Af that accumulated the cyclic iminium intermediate **9** with a peak corresponding to $[M]^+$ 239 (Figure 4.6), the EasA_Nl did not accumulate any intermediate species in significant yield as evidenced by LC-MS (Figure 4.7). It was expected that EasA_Nl would accumulate the proposed intermediate **8** $[M]^+$ 237 with its expected isomerase type activity (Figure 4.1), however the chromatograms of EasA_Nl, inactive boiled EasG, NADPH, and chanoclavine-I-aldehyde **7** did not show significant accumulation of this selected ion mass (Figure 4.8). We hypothesized that the $[M]^+$ 237, if formed, may not have accumulated in adequate amounts to allow for detection by LC-MS. The instability of the $[M]^+$ 237 hypothetical cyclized iminium intermediate may arise from its reactivity as a Michael acceptor to undergo possible 1,4 addition with nucleophiles such as protein side chains.

Synthetic reduction with NaCNBH₃ and NaCNBD₃ of assays consisting of the immediate product of EasA_Nl turnover of chanoclavine-I-aldehyde **7** did not yield any trapped product in significant amounts that were identifiable by mass spectrometry (Figure 4.9). This provided additional evidence that the immediate product of EasA_Nl was unique from the cyclized iminium produced by EasA_Af intermediate catalyzed reduction of chanoclavine-I-aldehyde **7**.

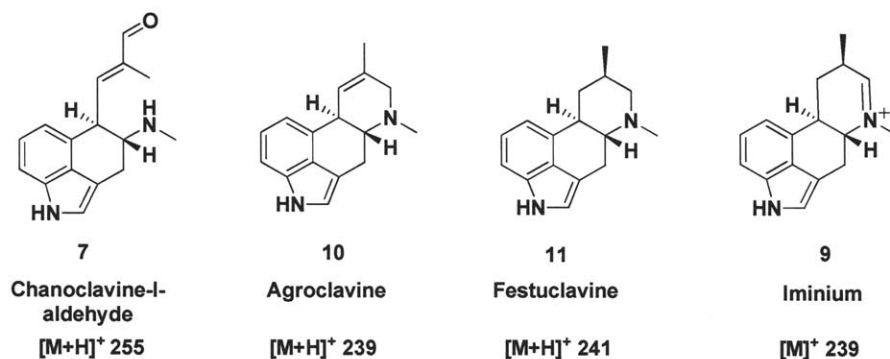
To further investigate the functional role of EasA_Nl, we assayed this enzyme with NADPH dependent reductase from *A. fumigatus* EasG (65% amino acid similarity to *N. lolii* EasG, Figure 4.10), in the presence of chanoclavine-I-aldehyde **7**, and NADPH. Gratifyingly, these assays demonstrated the conversion of chanoclavine-I-aldehyde **7**

detected at m/z 255 to a compound with a mass m/z 239 and retention time that was identical to the agroclavine standard **10** (Figure 4.11). High resolution mass data of the EasA_Nl and EasG product were also identical to the expected theoretical mass of agroclavine **10** (Table 4.1).

Additionally we noted that the product with $[M+H]^+$ 239, resulting from EasA_Nl and EasG, was different from the proposed cyclic iminium intermediate **9** of EasA_Af with the same mass $[M]^+$ 239, as these two compounds display different retention times (Figure 4.6 and 4.7). The EasA_Nl and EasG agroclavine product also showed no decrease in product intensity over prolonged incubation of 12 hours, as opposed to the gradual degradation of the cyclic iminium intermediate **9** produced by EasA_Af over the same time interval.

To further substantiate the identity of agroclavine **10** from the cyclized iminium intermediate **9**, we subjected the product of EasA_Nl and EasG to synthetic reduction with NaCNBH₃ or NaCNBD₃, which resulted in no change in mass (Figure 4.12). In contrast, synthetic reduction using NaCNBH₃ or NaCNBD₃ of the immediate product of EasA_Af, the cyclic iminium intermediate **9** with m/z 239, resulted in formation of products with masses consistent with festuclavine **11** at m/z 241 and singly deuterated festuclavine at m/z 242 (Figure 4.9).

Figure 4.6. LC-MS chromatograms with selected ion monitoring comparing active EasA_Af + EasG with controls. Peak intensities for this set of chromatograms have been normalized to allow relative comparison of compound masses present.



- A. Substrate chanoclavine-I-aldehyde **7** $[M+H]^+ = 255$ remains in enzyme assays with boiled EasA_Af enzyme and active EasG.
- B. The cyclized iminium ion enzymatic product **9** $[M]^+ = 239$ was observed in the presence of active EasA_Af + boiled EasG.
- C. Festuclavine **11** with $[M+H]^+ = 241$ was observed with active EasA_Af and EasG.
- D. Agroclavine standard **10** $[M+H]^+ = 239$
- E. Festuclavine standard **11** $[M+H]^+ = 241$

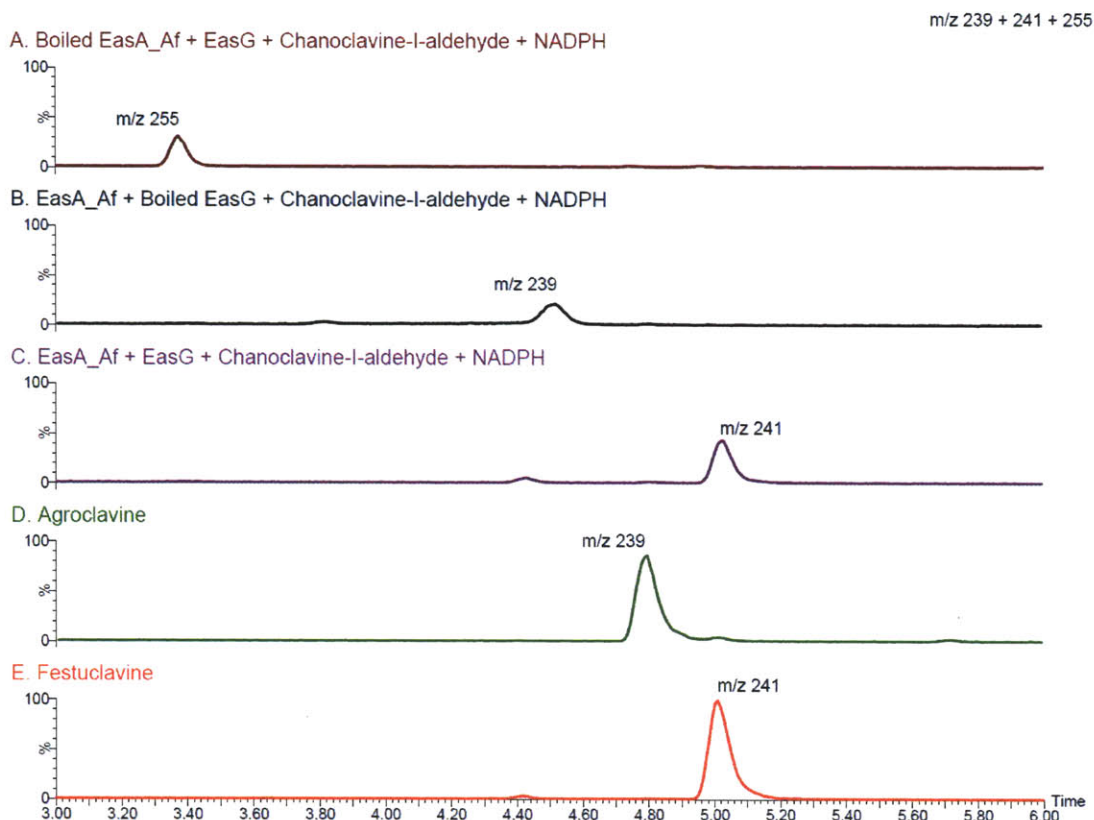


Figure 4.7. LC-MS chromatograms with selected ion monitoring comparing active EasA_NI + EasG with controls. Peak intensities for this set of chromatograms have been normalized to allow relative comparison of compound masses present.

- A. Substrate chanoclavine-I-aldehyde **7** $[M+H]^+ = 255$ remains in enzyme assays with boiled EasA_NI enzyme and active EasG
 B. Negligible products observed. Also see Figure 4.8C, D traces $[M]^+ = 237$ and 239
 C. Agroclavine **10** with $[M+H]^+ = 239$ was observed with active EasA_NI and EasG.
 D. Agroclavine **10** standard $[M+H]^+ = 239$
 E. Festuclavine **11** standard $[M+H]^+ = 241$

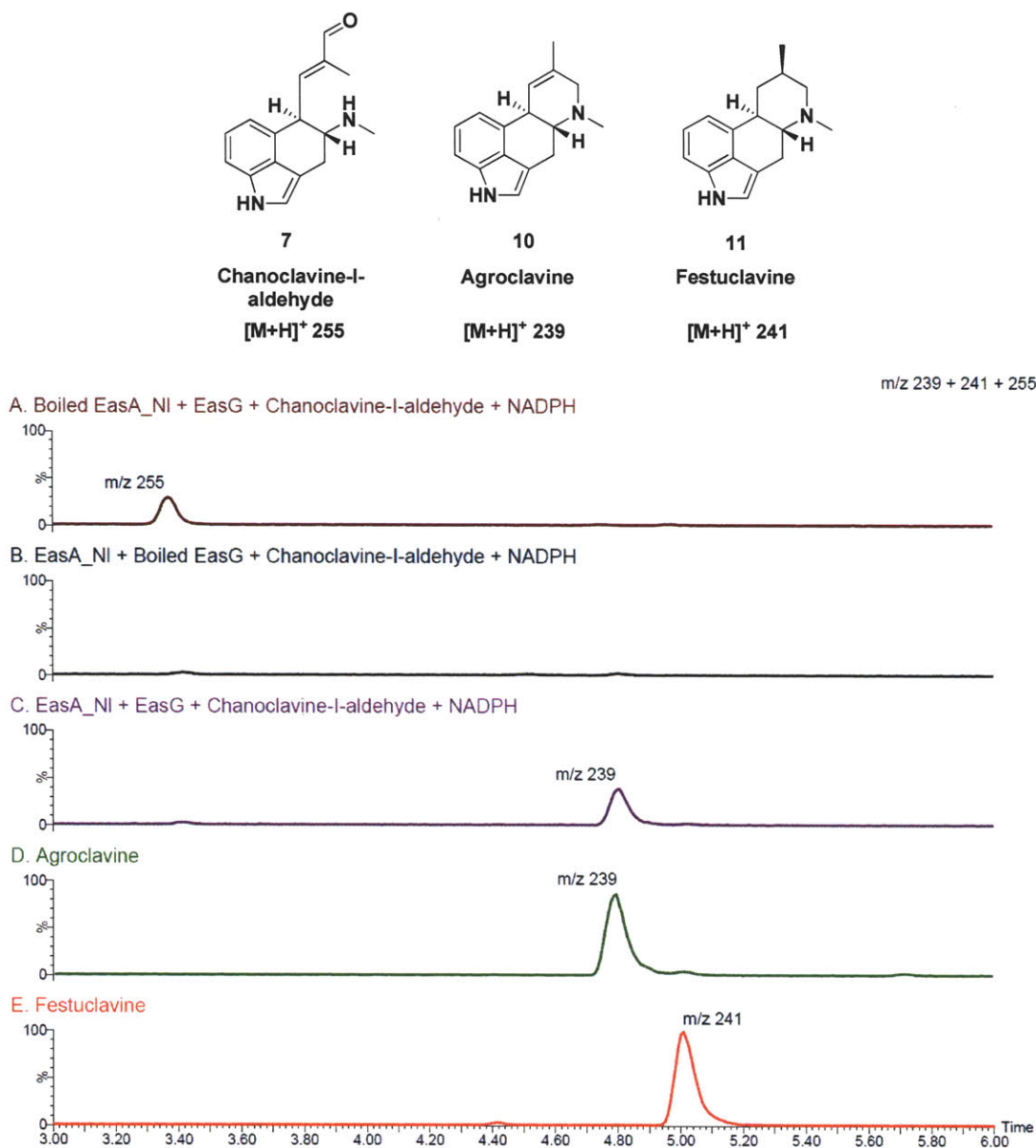
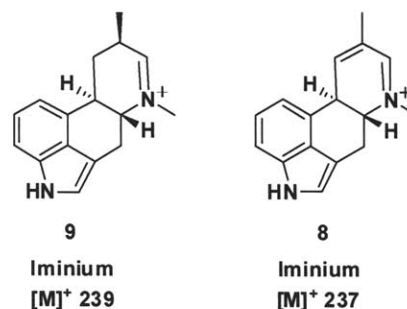


Figure 4.8. LC-MS chromatograms with selected ion monitoring for comparison of intermediates produced exclusively by EasA_Af, EasA_Nl, or EasA_Nl_F176Y with boiled EasG. Selected ion monitoring of iminium intermediates with expected masses $[M]^+ = 239$ and $[M]^+ = 237$. Peak intensities for this set of chromatograms have been normalized to allow relative comparison of compound masses present.



- A. Selected ion monitoring at m/z 239 of EasA_Af + boiled EasG. Observed cyclic iminium intermediate **9** with mass $[M]^+ = 239$.
- B. Selected ion monitoring at m/z 237 of EasA_Af + boiled EasG. Cyclic iminium intermediate **8** with mass $[M]^+ = 237$ not observed.
- C. Selected ion monitoring at m/z 239 of EasA_Nl + boiled EasG. Cyclic iminium intermediate **9** with mass $[M]^+ = 239$ not observed.
- D. Selected ion monitoring at m/z 237 of EasA_Nl + boiled EasG. Cyclic iminium intermediate **8** with mass $[M]^+ = 237$ not observed.
- E. Selected ion monitoring at m/z 239 of EasA_Nl_F176Y mutant + boiled EasG. Observed cyclic iminium intermediate **9** with mass $[M]^+ = 239$.
- F. Selected ion monitoring at m/z 237 of EasA_Nl_F176Y mutant + boiled EasG. Cyclic iminium intermediate **8** with mass $[M]^+ = 237$ not observed.

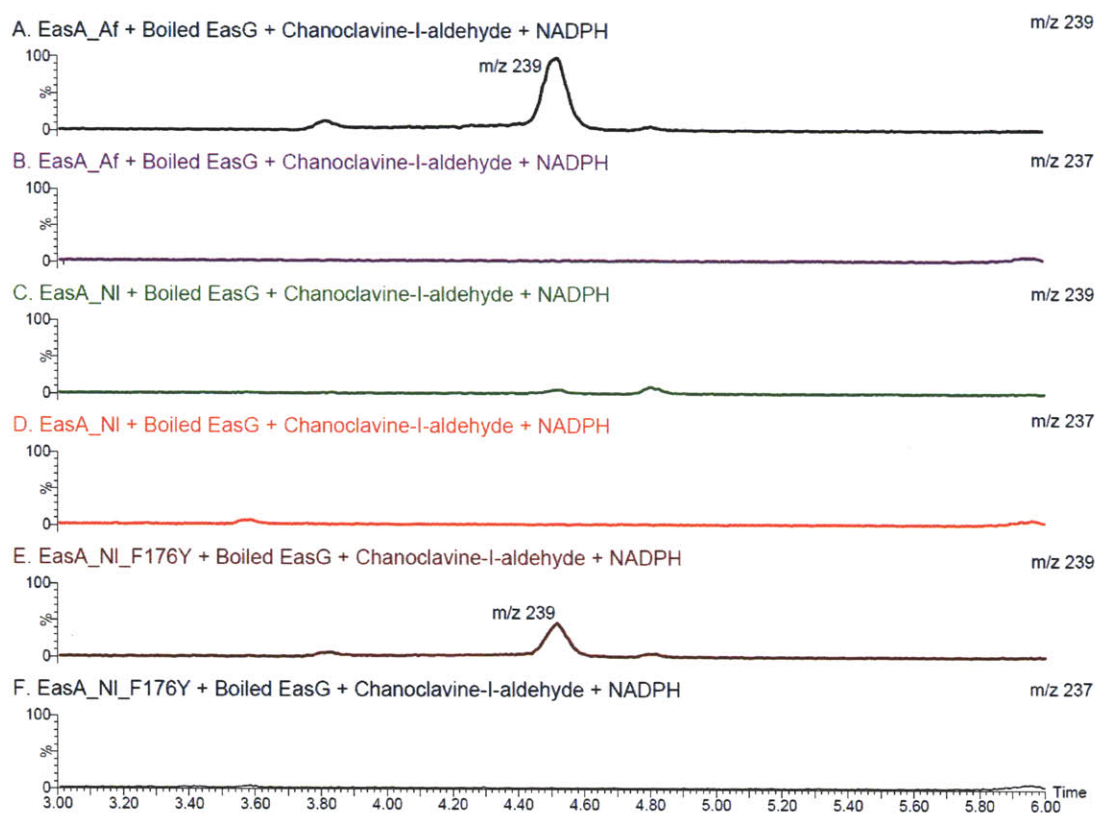
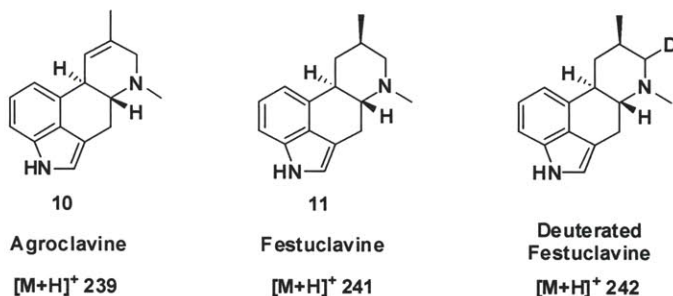


Figure 4.9. LC-MS

chromatograms with selected ion monitoring comparing active EasA_Af, EasA_NI, and EasA_NI_F176Y with boiled EasG with added NaCNBH₃ or NaCNBD₃ to observe reduced intermediate masses. Peak intensities for this set of chromatograms have been normalized to allow relative comparison of compound masses present.



- A. Festuclavine **11** [M+H]⁺ = 241 was observed, consistent with the NaCNBH₃ reduction of the cyclic iminium intermediate at mass [M]⁺ = 239.
- B. Singly deuterated festuclavine [M+H]⁺ = 242 was observed, consistent with the NaCNBD₃ reduction of the cyclic iminium intermediate **9** at mass [M]⁺ = 239.
- C. Negligible products observed.
- D. Negligible products observed.
- E. Festuclavine **11** [M+H]⁺ = 241 was observed, consistent with the NaCNBH₃ reduction of the cyclic iminium intermediate at mass [M]⁺ = 239.
- F. Singly deuterated festuclavine [M+H]⁺ = 242 was observed, consistent with the NaCNBD₃ reduction of the cyclic iminium intermediate **9** at mass [M]⁺ = 239.
- G. Festuclavine standard [M+H]⁺ = 241

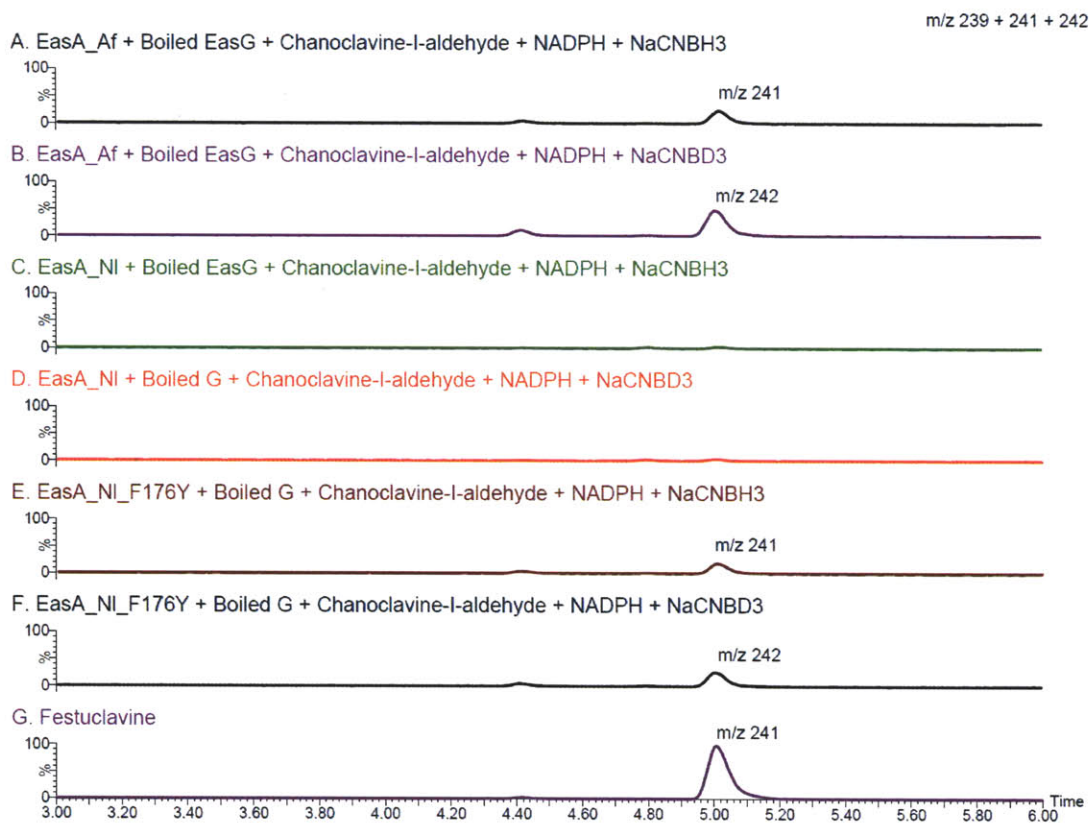


Figure 4.10. Alignment of EasG sequences.
Accessions: *A. fumigatus* EasG, XM_751041; *N. lolii* EasG, EF125025.1.

```

EasG_Af_XM_751041      -----MTILVLGGRGKTASRLSLLLDNAGVPFLVGSSST--SYV 37
EasG_Nl_EF125025.1    MVQIYLPRLSMRLGYHDKNNKMTILLTGGRGKTASHIASLLQAAKVPFIVASRSSDPSSS 60
                        *****::: **: * **:*.* *: *

EasG_Af_XM_751041      GPYKMTHTFDWLNEDTWTNVFLRASLDGIDPISAVYLVGGHAPELVDPGIRFINVARAQGV 97
EasG_Nl_EF125025.1    SPYYQNCFDWLDEKTYGDVLT--SKDSMQPISTIWLVPPIFDLAPLMIKFVDFASRKGV 118
                        .** . *****:.*: **: * *.:***::** :. *:*:.* **:

EasG_Af_XM_751041      NRFVLLSASNIAGTHSMGILHAHLDSELDVQYVVLRPWFWMENLLEDPHVS--WIKKED 155
EasG_Nl_EF125025.1    KRFVLLSASTIKKGGPAMGQVHEYLASLGGIEYAVLRPTWFWMENFSYPQELQRLAIKNEN 178
                        :*****.* ** **: * * * *.:*.*****: .. **:*:

EasG_Af_XM_751041      KIYSATGDGKIPFISADDIARVAFSVLTEWKSQRAQEYFVLGPELLSYDQVADILTTLVLG 215
EasG_Nl_EF125025.1    KIYSAAGDGKLPFVSVADIARVAFRTLDEKS-HNTDYVLLGPELITYDQVAETLSTVLG 237
                        *****:***:*. ***** .*: * : :*.*****:*****: *.***

EasG_Af_XM_751041      RKITHVSLAEADLARLLRDDVGLPPDFAAMLASMETDVKHGTEVRNSHDVKKVTGSLPCS 275
EasG_Nl_EF125025.1    RTITHIKLTEEELVKRL-ENSGMPAEDAKMLAGMDTSISDGAEDRLNNVVKHVTGADPRT 296
                        *.***:.*:* :*: * :*: **: * **.*:*.***:* * :*:***: * :

EasG_Af_XM_751041      FLDFAEQEKAQWMMRH 290
EasG_Nl_EF125025.1    FLDFATHQKATWG-- 309
                        ***** :*: *

```

Figure 4.11. LC-MS chromatograms with select ion monitoring at m/z 239 and 241 displays products of EasA_Af, EasA_Nl, and EasA_Nl_F167Y with EasG.

- A. EasA_Af + EasG + Chanoclavine-I-aldehyde **7** + NADPH
- B. EasA_Nl + EasG + Chanoclavine-I-aldehyde **7** + NADPH
- C. EasA_Nl_F176Y + EasG + Chanoclavine-I-aldehyde **7** + NADPH
- D. Agroclavine standard **10** $[M+H]^+ = 239$
- E. Festuclavine standard **11** $[M+H]^+ = 241$

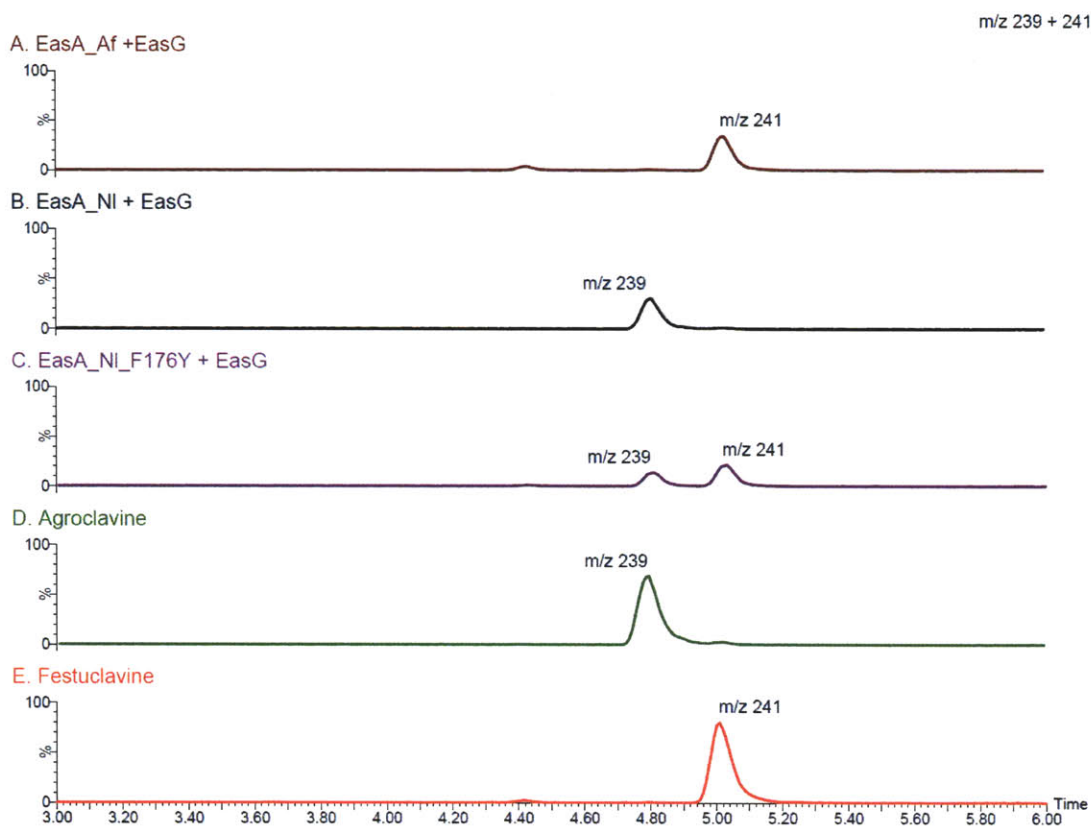
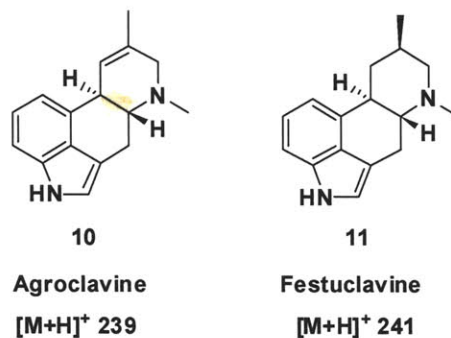
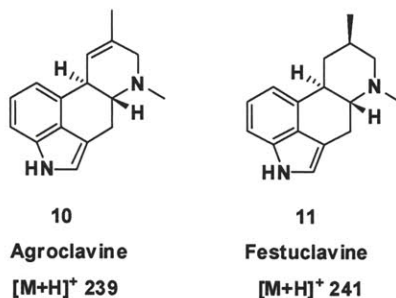


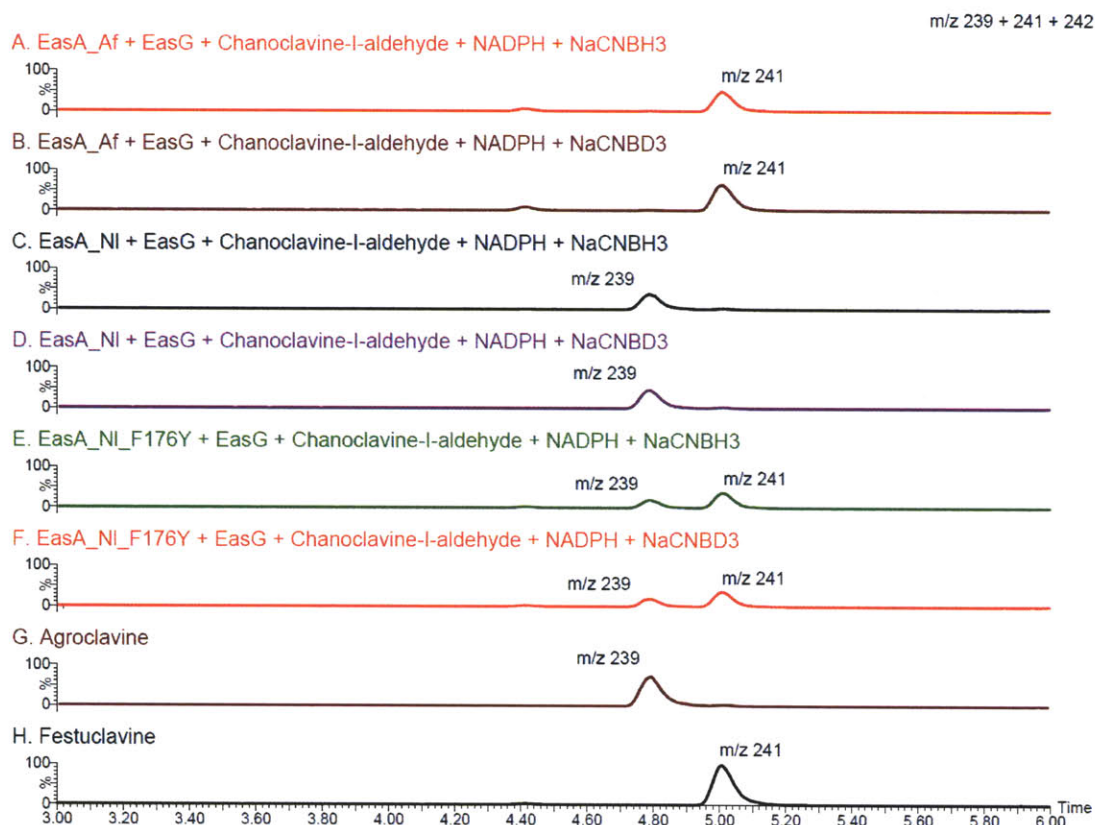
Table 4.1. Exact Mass of Compounds Determined by High Resolution MS

Compound	Observed Mass	Theoretical Mass	Deviation of Theoretical from Observed Mass (ppm)	Molecular Formula
EasA_Af + EasG Product Festoclavine 11 [M+H] ⁺	<i>m/z</i> 241.1695	<i>m/z</i> 241.1705	-4.1	C ₁₆ H ₂₁ N ₂
EasA_Nl + EasG Product Agroclavine 10 [M+H] ⁺	<i>m/z</i> 239.1541	<i>m/z</i> 239.1548	-2.9	C ₁₆ H ₁₉ N ₂
EasA_Nl_F176Y + EasG Product Agroclavine 10 [M+H] ⁺	<i>m/z</i> 239.1556	<i>m/z</i> 239.1548	3.3	C ₁₆ H ₁₉ N ₂
EasA_Nl_F176Y + EasG Product Festoclavine 11 [M+H] ⁺	<i>m/z</i> 241.1708	<i>m/z</i> 241.1705	1.2	C ₁₆ H ₂₁ N ₂

Figure 4.12. LC-MS chromatograms with selected ion monitoring comparing active EasA_Af, EasA_Nl, and EasA_Nl_F176Y with EasG with added NaCNBH₃ or NaCNBD₃ to display no reaction with enzyme products. Peak intensities for this set of chromatograms have been normalized to allow relative comparison of compound masses present.



- A.) Festuclavine **11** [M+H]⁺ = 241 was observed.
 B.) Festuclavine **11** [M+H]⁺ = 241 was observed.
 C.) Agroclavine **10** [M+H]⁺ = 239 was observed.
 D.) Agroclavine **10** [M+H]⁺ = 239 was observed.
 E.) Festuclavine **11** [M+H]⁺ = 241 and agroclavine [M+H]⁺ = 239 was observed.
 F.) Festuclavine **11** [M+H]⁺ = 241 and agroclavine [M+H]⁺ = 239 was observed.
 G.) Festuclavine standard **11** [M+H]⁺ = 241
 H.) Agroclavine standard **10** [M+H]⁺ = 239



Observing the production of agroclavine **10** only in the presence of added EasG in assays suggested a role for this enzyme in reducing the proposed iminium intermediate **8**. Thus, we speculated that EasG may work after or in conjunction with EasA_Nl. It remains a focus of our research efforts to understand the nature of this potential interaction between EasA_Nl and EasG, and the details regarding how the proposed cyclic iminium intermediate **8** [M]⁺ 237 of EasA_Nl was stabilized or rapidly reduced by EasG.

The collective results of these experiments supported the hypothesis that EasA_Nl functions as an isomerase as opposed to the EasA_Af reductase. Interestingly, the function demonstrated by EasA_Nl in these *in vitro* assays parallel the ergot alkaloid production profile of the *N. lolii* species. These results further validate that homologues of EasA exert control over the production of either festuclavine **11** (EasA_Af + EasG) or agroclavine **10** (EasA_Nl + EasG) derived ergot alkaloids from the common pathway intermediate chanoclavine-I-aldehyde **7**.

EasA at the branch point of ergot alkaloid biosynthesis and the mechanistic control over pathway divergence

To achieve a better understanding of the mechanistic difference that accounted for the production of festuclavine **11** or agroclavine **10** by the two homologues of EasA, we compared the sequences of EasA_Nl with EasA_Af as well as other EasA homologs from both festuclavine **11** and agroclavine **10** producing fungal species (Figure 4.3). The most intriguing trend between these sets of ergot alkaloid producers were that EasA homologues, in fungal species which produce agroclavine **10**, consisted of an active site phenylalanine such as seen in the EasA_Nl protein sequence. In contrast, fungal species that produce festuclavine **11** have an active site tyrosine instead, such as observed in the protein sequence of EasA_Af reductase and other OYE homologues (Figures 4.1 and 4.3).

In previous mechanistic studies of OYE, this catalytic active site tyrosine acts as a general acid to protonate the alpha carbon position either with or after hydride donation to the beta position of an alkene substrate, thus allowing the enzyme to function as a reductase.^{16, 20} In the EasA_Af reduction of chanoclavine-I-aldehyde **7**, this catalytic tyrosine was proposed to act in an analogous fashion to the OYE tyrosine residue, as discussed in Chapter 3.² We hypothesized that due to the substitution of this tyrosine for a phenylalanine residue in the active site of EasA_Nl, this enzyme was not be able to protonate the alpha position of chanoclavine-I-aldehyde **7** after transfer of a hydride from FMN to the C9 position; this would allow enolization of the substrate (Figure 4.1). Subsequent rotation of the enolate around the C8-C9 position followed by tautomerization and re-oxidation by transfer of the hydride back to the flavin would result

in the formation of the Z alkene geometry required for D ring cyclization. The condensation between the aldehyde and secondary amine moieties would result in the formation of a cyclic iminium ion intermediate **8** that was a unique product of the isomerase type EasA_Nl catalyzed reaction (Figure 4.1).

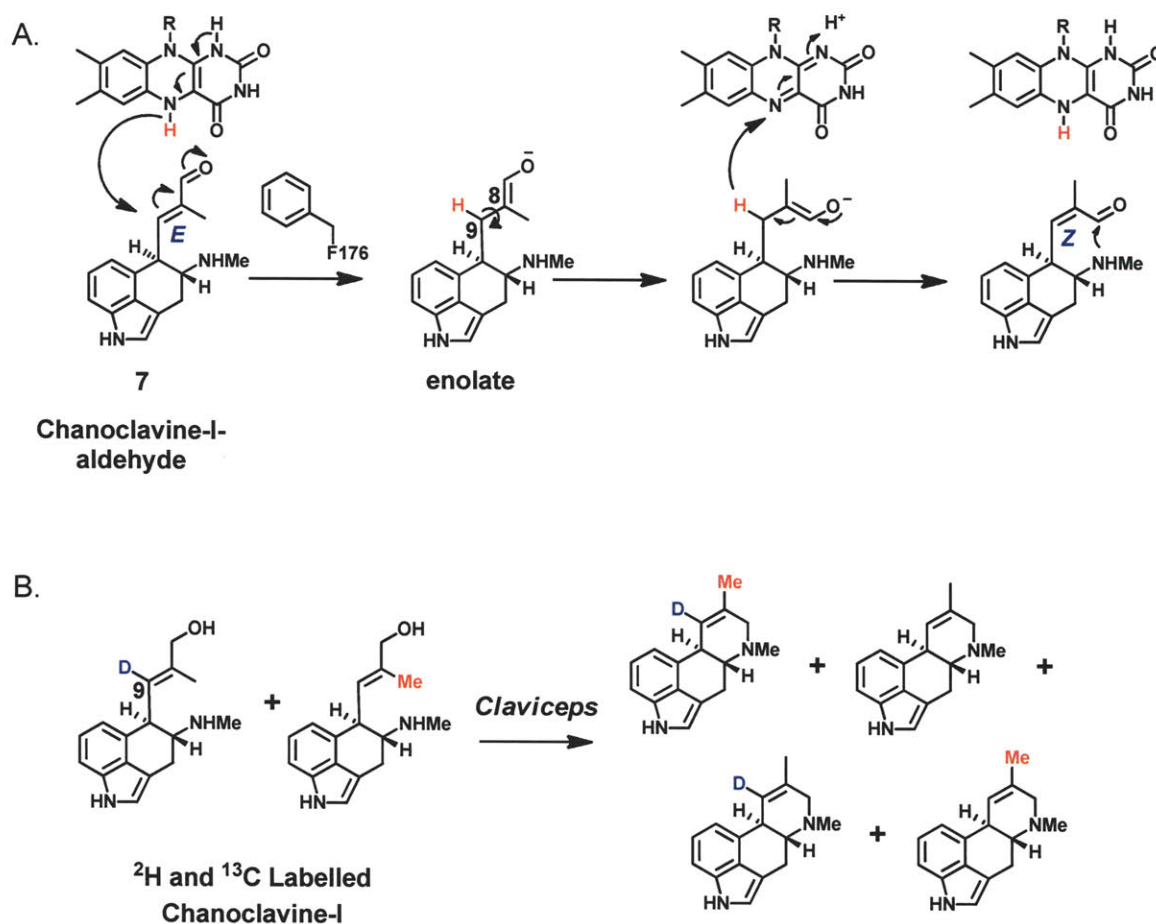
Precedence for our proposed isomerase type EasA_Nl mechanism was found in previous isotope labeled pre-cursor feeding studies to cultures of *C. purpurea* an agroclavine producer (Figure 4.13A.).²¹ The outcome of the numerous feeding experiments by Floss and co-workers supported a mechanism that involved the intermolecular transfer of the hydrogen at C9.^{5, 10, 21} One of the feeding experiments that provided the most compelling evidence to support intermolecular hydrogen transfer involved feeding separately labeled ²H and ¹³C chanoclavine-I **6**, the direct precursor to chanoclavine-I-aldehyde **7**, to *Claviceps* culture which transformed this substrate to doubly labeled agroclavine derived ergot alkaloids (Figure 4.13B).²¹

The double labeled end product was supportive of a mechanism where the hydrogen at C9 undergoes an intermolecular transfer from one substrate to the next. Floss and co-workers accounted for this observation by proposing that this transfer occurs by addition of a hydrogen at C9 followed by removal of a hydrogen, and suggesting that one of these steps may be non-stereoselective (Figure 4.13B).^{5, 11, 21} Likewise, we hypothesize that EasA_Nl could act in an analogous manner (Figure 4.13A). The details of intermolecular transfer and sequence of events of the isomerization of EasA_Nl cyclization remain a point of focus in our future research efforts.

Figure 4.13. Chanoclavine-I-aldehyde **7** and the isomerization of the C8-C9 alkene.

A. Proposed mechanism for isomerization of the chanoclavine-I-aldehyde **7** C8-C9 alkene by *N. lolii* EasA (EasA_{Nl}) involving reoxidation of the C8-C9 bond. Intermolecular hydrogen transfer occurs when the reduced FMN binds another molecule of chanoclavine-I-aldehyde **7**.

B. Whole cell labeling studies conducted by the group of Floss^{5, 11, 21} displayed a mixture of double, single, and unlabelled downstream products when labeled chanoclavine-I (direct precursor of chanoclavine-I-aldehyde **7**) was fed to cultures of *Claviceps*. These feeding studies suggested that the H of C9 undergoes intermolecular transfer.



Switching the activity of EasA from isomerase to reductase

To test our hypothesis regarding the association of an EasA_Nl isomerase type mechanism with an active site phenylalanine as opposed to tyrosine, we produced an EasA_Nl mutant with F176Y substitution (EasA_Nl_F176Y) to see if we could switch the activity from isomerase to reductase. Upon assay of EasA_Nl_F176Y with EasG, NADPH, and chanoclavine-I-aldehyde **7** we observed substrate disappearance along with the production of peaks with identical mass and retention time to the festuclavine **11** $[M+H]^+$ 241 and agroclavine **10** $[M+H]^+$ 239 standards (Figure 4.11). High resolution MS of these products were consistent with theoretical masses for agroclavine **10** and festuclavine **11** (Table 4.1). The EasA_Nl_F176Y mutant production of both festuclavine **11** and agroclavine **10**, contrasted the production of only agroclavine **10** by wild type EasA_Nl (Figure 4.11).

Further substantiating evidence that EasA_Nl_F176Y could produce festuclavine **11** was observed in the control assay of EasA_Nl_F176Y with heat inactivated EasG. Accumulation of the proposed cyclic iminium intermediate **9** $[M]^+$ 239 occurred in this assay (Figure 4.14), with an identical mass and retention time to those of the EasA_Af product. Trapping the cyclic iminium intermediate of the EasA_Nl_F176Y of the reaction by synthetic reduction using NaCNBH₃ or NaCNBD₃ resulted in masses consistent with festuclavine **11** at $[M+H]^+$ 241 and singly deuterated festuclavine at $[M+H]^+$ 242 (Figure 4.9). The products of synthetic reduction were identical in mass and retention time to the synthetically reduced product of EasA_Af.

To investigate whether a similar switch in activity from reductase to isomerase would be observed for EasA_Af, we created a mutant EasA_Af with Y178F substitution

(EasA_Af_Y178F) to determine if we could observe agroclavine **10** production in addition to festuclavine **11**. Interestingly, the EasA_Af_Y178F mutant when assayed along with EasG, NADPH, and chanoclavine-I-aldehyde **7** did not accumulate agroclavine **10** but only festuclavine **11**. The overall reaction of the EasA_Af_Y178F mutant was qualitatively similar to the wild type EasA_Af as they both produce festuclavine **11** (Figure 4.15).

The results of these experiments demonstrated that the active site phenylalanine in EasA_Nl played an important role in the production of agroclavine **10**. Furthermore, this experiment substantiated that a tyrosine in this position serves as a general acid to protonate the alpha position of chanoclavine-I-aldehyde **7** following transfer of a hydride to the beta position, as we observe in the wild type EasA_Af reductase.² This suggested that the tyrosine in the active site of EasA homologues plays a similar role as a general acid like the conserved tyrosine in OYE homologues and EasA_Af.¹⁶ These results were also consistent with the *in vivo* augmentation of the reductase type *easA* of *A. fumigatus* with isomerase type *easA* from *C. purpurea*, as detailed in Chapter 2, resulting in a switch in ergot alkaloid production profile from festuclavine **11** to agroclavine **10** derived alkaloids.³

Notably, the observation that the EasA_Nl_F176Y mutant still produces agroclavine **10** in addition to festuclavine **11** suggested that other residues in the active site still contribute toward the isomerization of the C8-C9 double bond. We speculated that this may occur in EasA_Nl by exclusion of outside proton donors such as water into the active site or by residues that contribute to the thermodynamic accessibility of the proposed enolate intermediate.

Likewise, the failure of the EasA_Af_Y178F to show isomerase activity also allowed us to speculate on the general active site differences between isomerase EasA_Nl and reductase EasA_Af. We propose that the EasA_Af active site may be more exposed to proton donors such as water that can protonate the C8 position, thus still allowing the cyclic iminium intermediate **9** to form even in the absence of the tyrosine residue. Moreover, other residues that may stabilize the proposed enolate intermediate in the isomerase pathway (Figure 4.1) may not be present in EasA_Af_Y178F, resulting in reductase activity being favored over isomerase activity.

These results suggest that more extensive mutational analysis of the active site of both isomerase and reductase type EasA were required in order to observe a complete switch in activity. Mutational analysis and further structural characterization of product stereochemistry will allow us to reconcile the mechanistic differences of isomerase versus reductase EasA. Experiments to detail these mechanistic differences are discussed in future directions Chapter 6.

Collectively, these findings demonstrated that critical active site presence of a phenylalanine in place of a tyrosine in isomerase type EasA_Nl was responsible for its isomerase activity, thus producing agroclavine **10** derived ergot alkaloids with an unsaturated ring D. This finding was in contrast to the reductase type EasA_Af described in Chapter 3, where the critical active site tyrosine facilitated the production of festuclavine **11** derived ergot alkaloids with a saturated ring D.

Figure 4.14. LC-MS chromatograms with selected ion monitoring comparing active EasA_Nl_F176Y + EasG with controls. Peak intensities for this set of chromatograms have been normalized to allow relative comparison of compound masses present.

- A.) Substrate chanoclavine-I-aldehyde **7** $[M+H]^+ = 255$ remained in enzyme assays with boiled EasA_Nl_F176Y enzyme and active EasG.
 B.) Starting material chanoclavine-I-aldehyde **7** $[M+H]^+ = 255$ and the cyclized iminium ion enzymatic product **9** $[M]^+ = 239$ was observed in the presence of active EasA_Af_F176Y + boiled EasG.
 C.) Agroclavine **10** with $[M+H]^+ = 239$ and festuclavine **11** $[M+H]^+ = 241$ was observed with active EasA_Nl_F176Y and EasG.
 D.) Agroclavine standard **10** $[M+H]^+ = 239$
 E.) Festuclavine standard **11** $[M+H]^+ = 241$

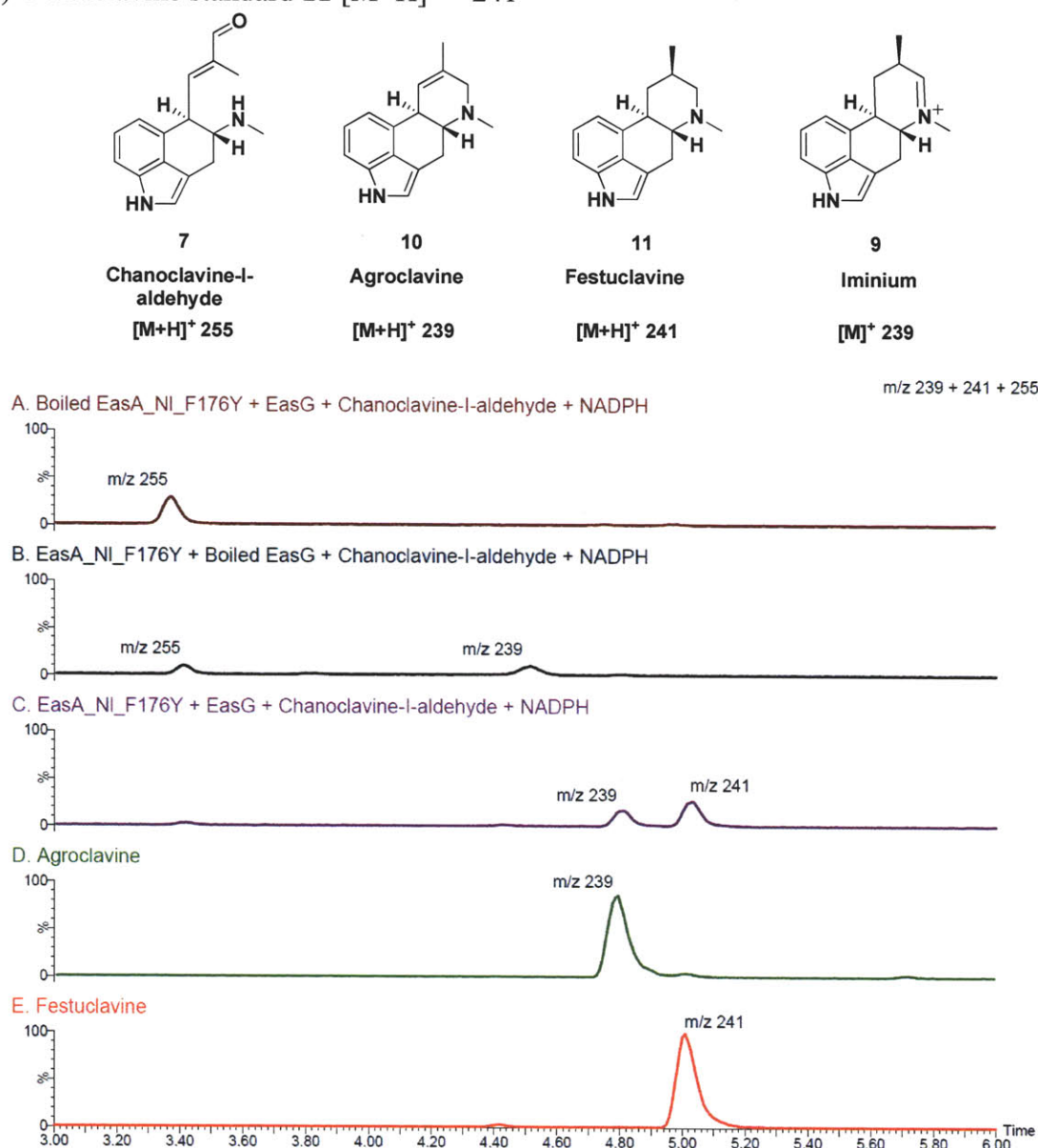
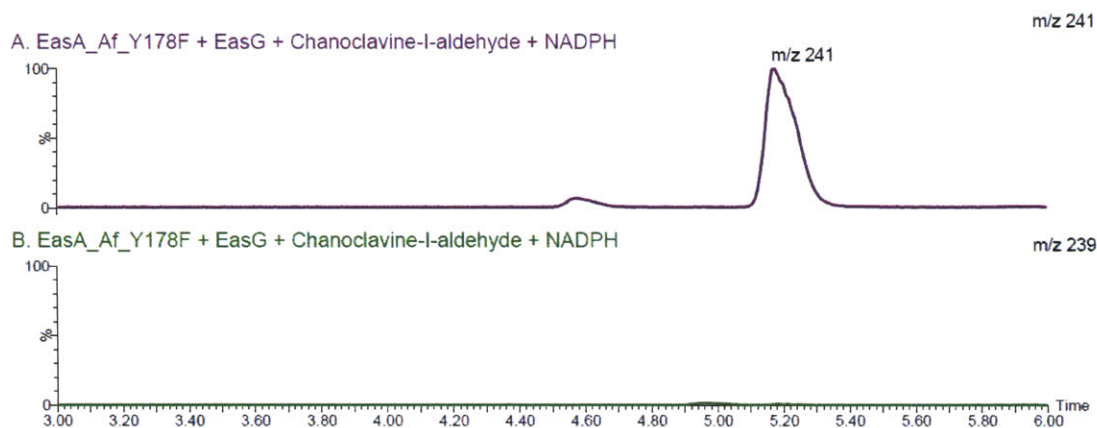
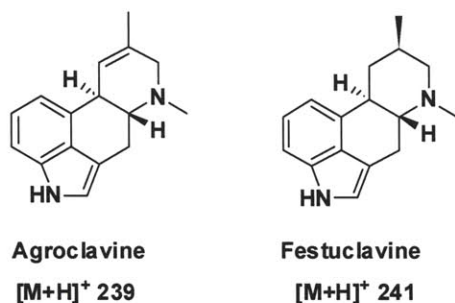


Figure 4.15. LC-MS chromatograms with selected ion monitoring comparing active EasA_Af_Y178F + EasG. Peak intensities for this set of chromatograms have been normalized to allow relative comparison of compound masses present.

- A. Selected ion monitoring at m/z 241. Festuclavine **11** $[M+H]^+ = 241$ was observed with the active EasA_Af_Y178F mutant.
- B. Selected ion monitoring at m/z 239. Agroclavine **10** $[M+H]^+ = 239$ was not observed.



Conclusion

This chapter describes the functional characterization of an EasA homologue from *N. lolii* that functions as an isomerase, in contrast to the EasA from *A. fumigatus* in Chapter 3, which acts as a reductase. The ability of EasA_Nl to produce agroclavine **10** in the presence of EasG allows us to propose an isomerase type mechanism for EasA_Nl involving isomerization of the C8-C9 bond. However, details regarding the cyclized iminium intermediate **8** resulting from the isomerization remain only speculative. Thus far we propose that the NADPH iminium reductase EasG was capable of trapping the intermediate from the EasA_Nl isomerization of the alkene of chanoclavine-I-aldehyde **7** to yield agroclavine **10** (Figure 4.1).

The production of agroclavine **10** by EasA_Nl in combination with EasG also demonstrated that EasA homologues function with unique active site differences that exert mechanistic control over the production of either festuclavine **11** or agroclavine **10** derived alkaloids at the branch point of ergot alkaloid biosynthesis. These findings also demonstrated that chanoclavine-I-aldehyde **7** was the common pathway intermediate prior to ergot alkaloid pathway divergence across different fungal species.

Our mutational analysis successfully showed that replacement of the phenylalanine with tyrosine in EasA_Nl_F176Y produced festuclavine **11** in addition to agroclavine **10**, thus engineering an additional reductase function into the wild type EasA_Nl isomerase. This finding also substantiated that the tyrosine or phenylalanine residue in the enzyme active site was a key mechanistic difference that defined a reductase or isomerase type EasA in the production of either festuclavine **11** or agroclavine **10** derived downstream ergot alkaloids. Other more subtle differences

between these homologues that contribute to isomerase or reductase function will need to be explored in future mutational analyses that extend beyond the active site residues. The work presented in this chapter demonstrated that EasA homologues in divergent fungal species were capable of having isomerase or reductase functions and gives precedence for future experiments to explore the mechanistic details that govern ergoline ring D formation.

References

1. Coyle, C.M. and D.G. Panaccione, *An Ergot Alkaloid Biosynthesis Gene and Clustered Hypothetical Genes from Aspergillus fumigatus*. Applied and Environmental Microbiology, 2005. **71**(6): p. 3112-3118.
2. Cheng, J.Z., C.M. Coyle, D.G. Panaccione, and S.E. O'Connor, *A Role for Old Yellow Enzyme in Ergot Alkaloid Biosynthesis*. Journal of the American Chemical Society, 2010. **132**(6): p. 1776-1777.
3. Coyle, C.M., J.Z. Cheng, S.E. O'Connor, and D.G. Panaccione, *An Old Yellow Enzyme Gene Controls the Branch Point between Aspergillus fumigatus and Claviceps purpurea Ergot Alkaloid Pathways*. Applied and Environmental Microbiology, 2010. **76**(12): p. 3898-3903.
4. Floss, H.G., *From Ergot to Ansamycins - 45 Years in Biosynthesis*. Journal of Natural Products, 2006. **69**: p. 158-169.
5. Floss, H.G. and J. Anderson, *The Biosynthesis of Mycotoxins*, P. Steyn, Editor. 1980, Academic Press. p. 17-67.
6. Schardl, C.L., D.G. Panaccione, and P. Tudzynski, *Ergot Alkaloids - Biology and Molecular Biology*, in *The Alkaloids* G. Cordell, Editor. 2006, Elsevier. p. 45-86.
7. Wallwey, C. and S.-M. Li, *Ergot alkaloids: structure diversity, biosynthetic gene clusters and functional proof of biosynthetic genes*. Natural Products Reports, 2011. **28**(3): p. 496-510.
8. Pachlatko, P., C. Tabacik, W. Acklin, and D. Arigoni, *Natural and unnatural precursors in the biosynthesis of ergot alkaloids*. Chimia, 1975. **29**: p. 526-527.
9. Fehr, T., W. Acklin, and D. Arigoni, *The role of the chanoclavines in the biosynthesis of ergot alkaloids*. Chemical Communications, 1966: p. 801-802.
10. Floss, H.G., U. Hornemann, N. Schilling, K. Kelley, D. Groger, and D. Erge, *Biosynthesis of ergot alkaloids. Evidence for two isomerizations in the isoprenoid moiety during the formation of tetracyclic ergolines*. Journal of the American Chemical Society, 1968. **90**: p. 6500-6507.
11. Groger, D. and H.G. Floss, *Biochemistry of Ergot Alkaloids-achievements and challenges*, in *The Alkaloids*, G. Cordell, Editor. 1998, Academic Press. p. 171-218.
12. Baxter, R.M., S.I. Kandel, and A. Okany, *Biosynthesis of Ergot Alkaloids: Incorporation of Mevalonic Acid into Ergosine*. Journal of the American Chemical Society, 1962. **84**(15): p. 2997-2999.
13. Bhattacharji, S., A.J. Birch, A. Brack, A. Hofmann, H. Kobel, D.C.C. Smith, H. Smith, and J. Winter, *Studies in Relation to Biosynthesis. Part XXVII. The Biosynthesis of Ergot Alkaloids*. Journal of the Chemical Society, 1962: p. 421-425.
14. Brown, B., Z. Deng, P.A. Karplus, and V. Massey, *On the Active Site of Old Yellow Enzyme Role of Histidine 191 and Asparagine 194*. The Journal of Biological Chemistry, 1998. **273**(49): p. 32753-32762.
15. Brown, B.J., J. Hyun, S. Duwuri, P.A. Karplus, and V. Massey, *The Role of Glutamine 114 in Old Yellow Enzyme*. The Journal of Biological Chemistry, 2002. **277**(3): p. 2138-2145.

16. Kohli, R. and V. Massey, *The Oxidative Half-reaction of Old Yellow Enzyme The Role of Tyrosine 196*. The Journal of Biological Chemistry, 1998. **273**(49): p. 32763-32770.
17. Meah, Y., B. Brown, S. Chakraborty, and V. Massey, *Old yellow enzyme: Reduction of nitrate esters, glycerin trinitrate, and propylene 1,2-dinitrate*. Proceedings of the National Academy of Sciences of the United States of America, 2001. **98**(15): p. 8560-8565.
18. Xu, D., R. Kohli, and V. Massey, *The Role of Threonine 37 in Flavin Reactivity of the Old Yellow Enzyme*. Proceedings of the National Academy of Sciences of the United States of America, 1999. **96**: p. 3556-3561.
19. Macheroux, P., *UV-visible spectroscopy as a tool to study flavoproteins*, in *Methods in Molecular Biology: Flavoprotein Protocols*, S. Chapman and G. Reid, Editors. 1999, Humana Press Inc.: Totowa, NJ.
20. Fox, K. and P.A. Karplus, *Old yellow enzyme at 2 Å resolution: overall structure, ligand binding, and comparison with related flavoproteins*. Structure, 1994. **15**(2): p. 1089-1105.
21. Floss, H.G., M. Tchong-Lin, C. Chang, B. Naidoo, G. Blair, C. Abou-Chaar, and J. Cassady, *Biosynthesis of ergot alkaloids. Mechanism of the conversion of chanoclavine-I into tetracyclic ergolines*. Journal of the American Chemical Society, 1974: p. 1898-1909.

Chapter 5 . Role of Redox Enzymes Involved with the Formation of Ergoline Ring C

Introduction

Ergoline ring C formation, which starts from pathway intermediate *N*-Me-DMAT **4** to form chanoclavine-I **6**, has been previously proposed to occur through two successive oxidation steps (Figure 5.1). The occurrence of these two oxidation steps were based on isotope feeding studies conducted by the Floss group.^{1,2} These studies yielded two important insights into ring C formation: (1) observation that a proposed diene intermediate **5** was incorporated into downstream ergot alkaloids of *C. purpurea*¹ and (2) molecular oxygen was incorporated into chanoclavine-I **6**.²

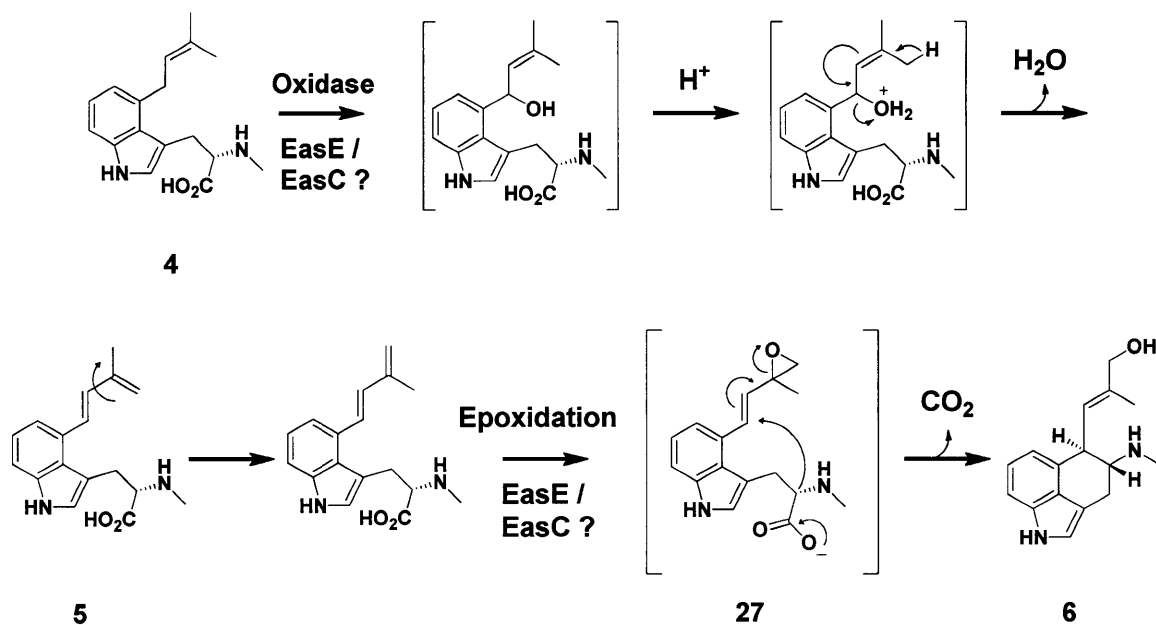
Bioinformatics analysis of ergot biosynthetic gene clusters demonstrated that *easC* and *easE* were two remaining functionally unassigned genes that encode for enzymes capable of carrying out oxidation reactions. Notably *easE* and *easC* have homologues in ergot gene clusters that were conserved across divergent fungal species, signifying their likely involvement in the early steps of ergot alkaloid biosynthesis as introduced in Chapter 1. The biosynthetic function of *easC* and *easE* had remained speculative, although their protein sequence similarity to catalases and FAD oxygenases suggested their likelihood to function in the cyclization of the ergoline ring C.

Gene disruption experiments described in Chapter 2, with the goal of assigning function to EasC and EasE, demonstrated that knockout strains of $\Delta easC$ and $\Delta easE$ in *A. fumigatus* failed to accumulate the downstream ergot alkaloids that were observed in the wildtype. Instead, the knockout strains accumulated upstream pathway intermediate *N*-Me-DMAT **4**. It was also demonstrated that feeding chanoclavine-I **6** to $\Delta easC$ strains restored production of downstream ergot alkaloids.³ In a separate study, Lorenz et al. disrupted an *easE* gene homologue (*ccsA*) in *Claviceps*, which resulted in the

accumulation of *N*-Me-DMAT **4** as a pathway intermediate with the loss of downstream ergot alkaloids.⁴ Collectively, these findings demonstrated that gene disruption of *easE* or *easC* accumulated the same pathway intermediate *N*-Me-DMAT **4**, and suggested that both gene products were required to observe the formation of ergoline ring C. However, information regarding the mechanistic details of EasC or EasE catalyzed ring C cyclization have yet to be established.

In this chapter, we describe our efforts to clone and characterize EasC and EasE enzymes which are involved in the early steps of ergot alkaloid biosynthesis. This chapter also describes the enzymatic preparation of the *N*-Me-DMAT **4** ergot pathway intermediate to assay the activity of EasC and EasE. While conditions for expression of *easC* and *easE* gene products were realized, we did not observe the production of chanoclavine-I **6** from *N*-Me-DMAT **4**. We followed this by an analysis of proposed mechanisms of ring C formation and hypothesize whether other enzymes and conditions may be required to study the functional role with EasC and EasE *in vitro*. Alternative future approaches to reconcile how EasE and EasC may catalyze ergoline ring C formation are described in Chapter 6.

Figure 5.1. Proposed EasE and EasC mechanism for the cyclization of ergoline ring C to form chanoclavine-I **6** from starting substrate *N*-Me-DMAT **4**. Hypothetical intermediates that have not been observed are shown in brackets.



Experimental Methods

General materials and methods

General recombinant DNA cloning procedures were performed using pGEM-T vector (Promega) propagated in *E. coli* Top10 (Invitrogen). Protein expression for *A. fumigatus* EasE was conducted in DsbC SHuffle® T7 Express Competent *E. coli* (New England Biolabs). Protein expression for DmaW and EasC were conducted in *E. coli* BL-21 (DE3) (Invitrogen). PCR amplification utilized Platinum Taq DNA Polymerase (Invitrogen). Recombinant DNA plasmids were prepared using Qiaprep Spin Miniprep and Qiaquick Gel Extraction kits (Qiagen). Restriction enzymes and T4 DNA ligase were purchased from New England Biolabs. Primers for cloning were synthesized by Integrated DNA Technologies and DNA sequencing was conducted by the MIT Biopolymers Laboratory (Cambridge, MA).

For HPLC analysis the samples were chromatographed using a Hibar 250-4 LiChrosorb RP-Select B 5 µm column (Merck) with a mobile phase of acetonitrile/0.1% trifluoroacetic acid in water. LC-MS analysis was conducted on an Acquity Ultra Performance BEH C18 column (2.1 x 100 mm; 1.7 µm particle size) and eluted with an acetonitrile/0.1% formic acid water. Mass detection was conducted on a Micromass LCT Premier TOF MS (Waters, Milford, MA) with an electrospray ionization source set in positive mode.

Cloning and expression of *C. purpurea dmaW*

The *C. purpurea dmaW* gene was PCR amplified using primers designed based on the nucleotide sequence of *dmaW* from the NCBI database (AY259840) encoding the

DmaW protein (AAP81209). The coding sequences were amplified from the *C. purpurea* *dmaW* construct pKAES154 previously studied by Wang et al.⁵ A pair of oligonucleotide primers were used to amplify the *dmaW* gene: forward primer 5'- TT **CATATG** GGTGTGTACGAAATTTTGAGTCTGA-3' (with NdeI restriction site in bold) and reverse primer 5'- **GACTCGAGTTAAAGCTTCTTCGTTGAGAGTTCACAGCGCCGG**-3' (XhoI restriction site in bold). (Additional restriction sites were incorporated into the primers to allow for cloning of *dmaW* as either an N-His₆ or C-His₆ construct.)

The PCR amplified *dmaW* gene was inserted into pGEM-T vector (Promega) for propagation and sequencing. Subsequently, the *dmaW* sequence was excised from pGEM-T by restriction digest and ligated into the NdeI/XhoI site of pET-28a(+) (Novagen) expression vector as an N-His₆ construct. Expression was carried out in LB media supplemented with kanamycin (50 µg/mL).

Optimal conditions for N-His₆ tagged DmaW over expression were achieved at 5 µM IPTG and at 15 °C for 68 hours. The enzyme was purified by Ni-NTA affinity chromatography where the purest fraction was obtained in elution buffer (100mM imidazole, 20 mM Tris-HCl, 300 mM NaCl, and 10% (v:v) glycerol, pH = 8.0) (Figure 5.2). The purest DmaW fraction was collected and exchanged with dialysis buffer (50 mM Tris-HCl, 100 mM NaCl, 1 mM Dithiothreitol (DTT), 10% (v:v) glycerol, pH = 8.0).

Endpoint Assay of DmaW for production of DMAT 3 and N-Me-DMAT 4

The expressed and purified DmaW enzyme was assayed under previously reported conditions (50 mM Tris-HCl, pH = 7.5, 5 mM CaCl₂)^{6, 7}. The purified DmaW

was assayed for prenylation of its natural substrate L-tryptophan **1** to produce 4-dimethylallyltryptophan (DMAT) **3** by incubation of 0.6 μ M DmaW with 1 mM dimethylallyl pyrophosphate (DMAPP) **2** and 1 mM L-tryptophan **1** at room temperature 25 °C. DmaW was also tested for the prenylation of *N* $_{\alpha}$ -Me-tryptophan (L-abrine) **26** by incubation of 0.6 μ M DmaW with 1 mM dimethylallyl pyrophosphate (DMAPP) and 1 mM L-abrine at room temperature 25°C to produce *N*-Me-DMAT **4**. Aliquots of the enzyme assay were quenched with 10% trichloroacetic acid over time and subsequently analyzed by HPLC and LC-MS.

For HPLC analysis, the samples were chromatographed with an acetonitrile/0.1% trifluoroacetic acid in water mobile phase (12:88 to 95:5 from 0-15 min, 95:5 to 12:88 from 15–23 min, at a constant flow rate of 1 mL/min) with the UV detection range set at 168-280 nm. For LC-MS analysis the samples were chromatographed with a linear gradient (0.5 mL/min) of 20:80 to 80:20 (acetonitrile:0.1% formic acid water) over 5 min.

Cloning and expression of *A. fumigatus easC*

The *A. fumigatus easC* gene was PCR amplified using *A. fumigatus* cDNA. To clone the desired gene, total RNA was extracted from *A. fumigatus* mycelia tissue using the Trizol RNA extraction procedure (Invitrogen).⁸ Using Creator SMART MMLV reverse transcriptase (Clontech), cDNA was constructed from the extracted total RNA. Primers were designed based on the nucleotide sequence of *easA* from the NCBI database (XM_751047). A pair of oligonucleotide primers were used to amplify the *easC* gene: forward primer 5'- TT CCATGG GC **CATATGCTAATTGAGCGTGGGTTATTGTC**

-3' (with NdeI restriction site in bold) and reverse primer 5'-TT**CTCGAG**TTAAGCTTT GAGCCTGGAAAGAGAGACTTGTGTTG-3' (XhoI restriction site in bold).

The PCR amplified *easC* gene was inserted into pGEM-T vector (Promega) for propagation and sequencing. Subsequently, the *easC* sequence was excised from pGEM-T by restriction digest and ligated into the NdeI/XhoI site of pET-28a(+) (Novagen) expression vector as an N-His₆ construct. Expression was carried out in LB media with kanamycin (50 µg/mL), aminolevulinic acid (0.4 mM) and ferric ammonium sulfate (0.2 mM). *E. coli* BL-21(DE3) cells were grown to an OD₆₀₀ of 0.8 prior to induction with IPTG (5 µM) and grown for an additional 68 hours at 15 °C prior to harvesting. EasC enzyme was purified by Ni-NTA agarose (Qiagen).

Fractions containing pure EasC, as demonstrated by SDS-PAGE (Figure 5.5), were collected and exchanged with dialysis buffer 50 mM Tris-HCl, 100 mM NaCl, 1 mM Dithiothreitol (DTT), 10% (v:v) glycerol, pH = 8.0. The final stock concentration of EasC was at 0.1 mg/mL. The catalase assay was conducted in a quartz cuvette with 0.1 µM EasC with 10 mM H₂O₂ in dialysis buffer.

Cloning and expression of *A. fumigatus easE*

Starting with the reference sequence for EasE (XM_751049), an alternative splicing of the *easE* gene was suggested by Dan Panaccione based on re-analysis sequence alignments of EasE homologues in fungi and other FAD dependent oxidoreductases. This newly assembled *E. coli* codon optimized EasE gene was synthesized and ligated as an N-terminal His construct in pET28a(+) with restriction sites in NdeI and EcoRI (Genscript). EasE was expressed using an *E. coli* strain that

produces a disulfide bond isomerase (DsbC SHuffle® T7 Express Competent *E. coli*, New England Biolabs). Fractions containing pure EasE, as demonstrated by SDS-PAGE (Figure 5.7), were collected and exchanged with dialysis buffer (50 mM K₂HPO₄, 100 mM NaCl, 10% (v/v) glycerol, pH = 7.0). Final holoenzyme stock concentration was at 6 μM. Analysis of the co-purified flavin of EasE was conducted with a UV-Vis spectrophotometer.

Endpoint assay of EasC and EasE with *N*-Me-DMAT 4 substrate

DmaW (0.6 μM) was incubated with DMAPP (1 mM) and L-tryptophan (*N*_α-methyl-L-tryptophan) **26** (1 mM) for 2 hours to prepare the *N*-Me-DMAT **4** substrate. The substrate **4** was then assayed with EasC (0.2 μM) and EasE (1.2 μM) under various combinations of added H₂O₂ (10 mM), NADPH (500 μM), and Dithiothreitol (DTT) (20 mM) in 100 mM K₂HPO₄ buffer (pH = 7.0) at 25°C for 60 min. Aliquots were quenched by dilution in 0.1% formic acid in water and analyzed by LC-MS.

For LC-MS analysis, the samples were chromatographed using a gradient of acetonitrile/0.1% formic acid in water mobile phase (10:90 to 20:80 from 0-5 min, 20:80 to 90:10 from 5-6 min, and 90:10 to 10:90 from 6-7 min at a constant flow rate of 0.5 mL/min). UV-Vis spectra were acquired on a Varian Cary 50 Bio Scanning Spectrometer.

Results and Discussion

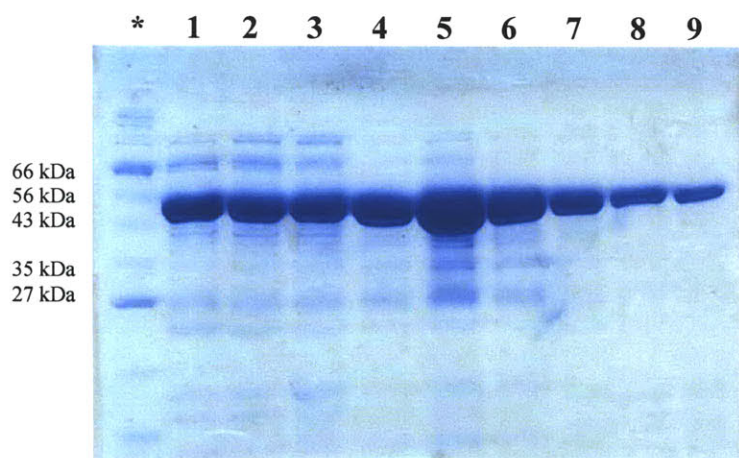
Enzymatic preparation of pathway intermediate *N*-Me-DMAT **4**

DmaW was successfully cloned, heterologously expressed, and purified by Ni-NTA agarose to yield enzyme at 3.0 mg/L culture (Figure 5.2). The purified DmaW was incubated with L-tryptophan **1** (1 mM) and DMAPP **2** (1 mM) and formation of DMAT **3** was observed using HPLC. Approximately 75% conversion of the starting substrate L-tryptophan was observed after 3 hours (Figure 5.3A). DmaW enzymatic activity for the prenylation of natural substrate L-tryptophan **1** was also observed by LC-MS analysis, which indicated decrease of the $[M+H]^+$ 205 peak and accumulation of the $[M+H]^+$ 273 product peak (Figure 5.4). This activity shown by DmaW was consistent with the function of this enzyme previously reported by Wang et al.⁵

Previous work by Steffan et al. also demonstrated that the DmaW homologue from *A. fumigatus* could prenylate L-abrine **26** in addition to its natural substrate L-tryptophan **1**.⁹ Therefore, DmaW can potentially be used to generate the *N*-Me-DMAT **4** substrate needed to test EasE and EasC directly. DmaW was incubated with L-abrine **26** (1 mM) and DMAPP **2** (1 mM) and formation of *N*-Me-DMAT **4** was observed by HPLC, giving approximately 59% conversion of the starting substrate L-abrine **26** in 3 hours (Figure 5.3B). DmaW enzyme activity was also observed by LC-MS by monitoring the L-abrine **26** peak at $[M+H]^+$ 219 and observing the accumulation of a $[M+H]^+$ 287 peak corresponding to the expected mass of *N*-Me-DMAT **4** (Figure 5.3). The identity of the *N*-Me-DMAT **4** product of DmaW prenylation of L-abrine **26** was further substantiated as it shared an identical mass and retention time as the intermediates that accumulated in the $\Delta easC$ and $\Delta easE$ *A. fumigatus* mutants as presented in Chapter 2

(Table 2.1, Figure 2.5).³ The successful expression of DmaW allowed preparation of the *N*-Me-DMAT 4 pathway intermediate required to assay EasE and EasC oxidases.

Figure 5.2. SDS-PAGE gel of DmaW (expected size 52 kDa)



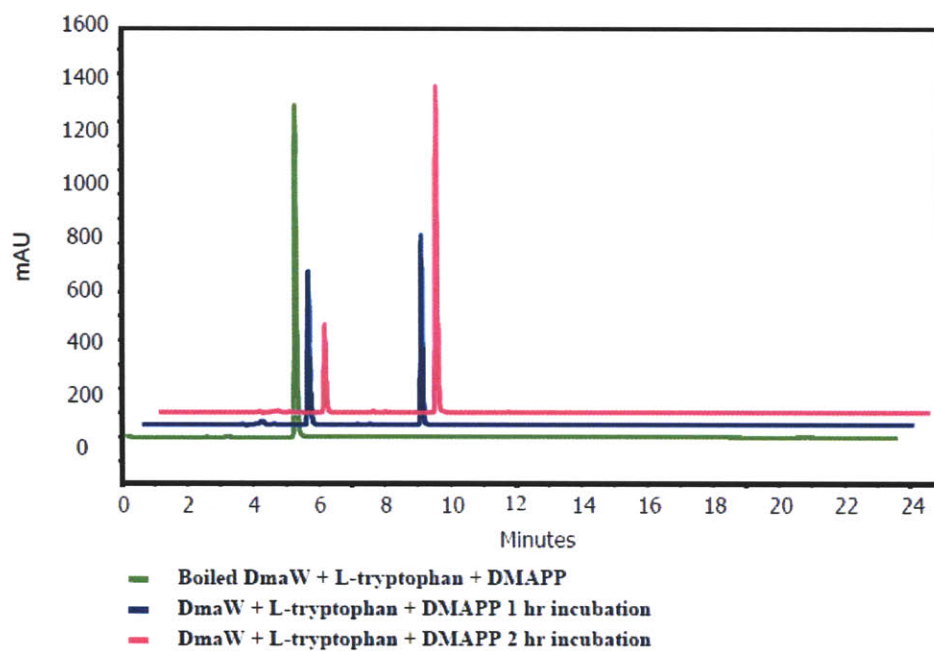
*. NEB Broad Range Protein Ladder (2-212 kDa)

1. 50 mM Imidazole

2-9. 100 mM Imidazole

Figure 5.3. HPLC chromatogram of DmaW enzyme assayed with A. L-tryptophan **1** and DMAPP **2** and B. L-abrine (N_α -L-tryptophan) **26** and DMAPP **2** (Detector 168-280nm)

A)



B)

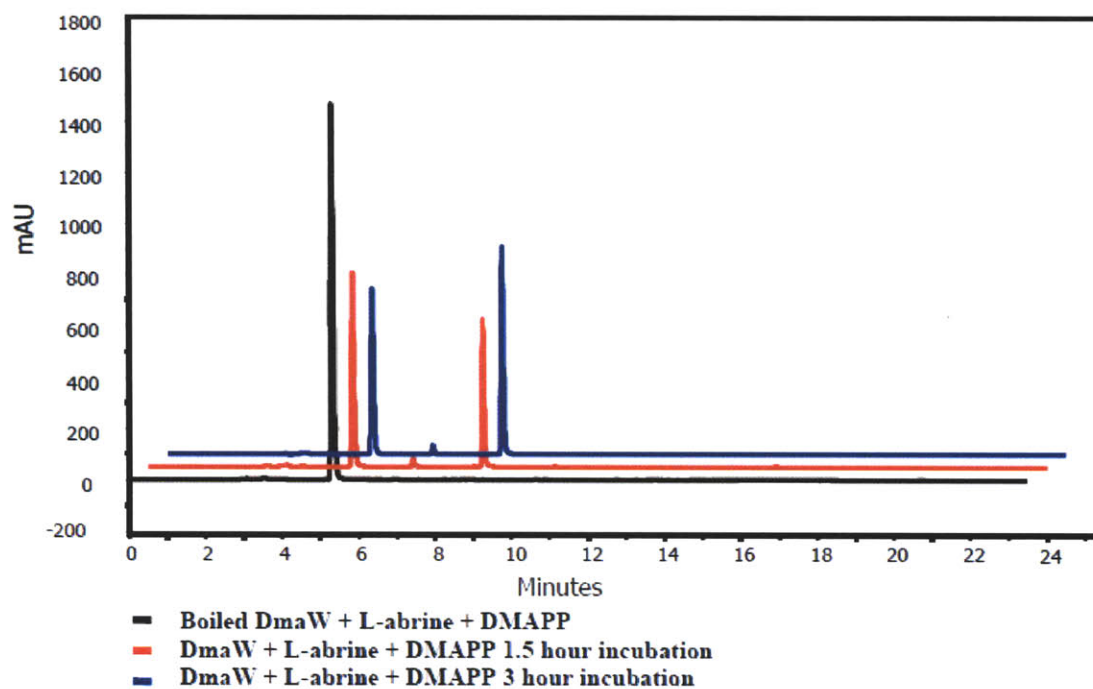
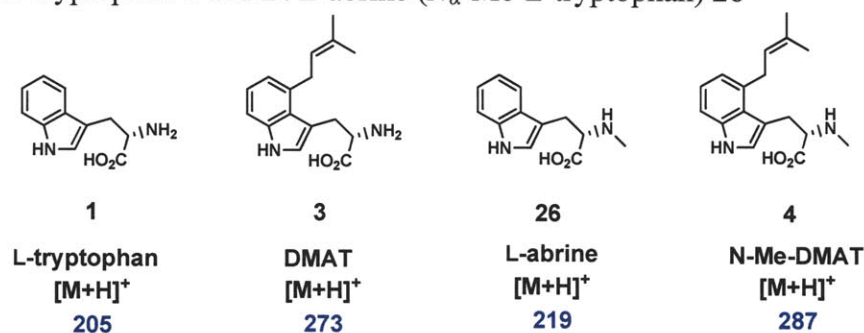
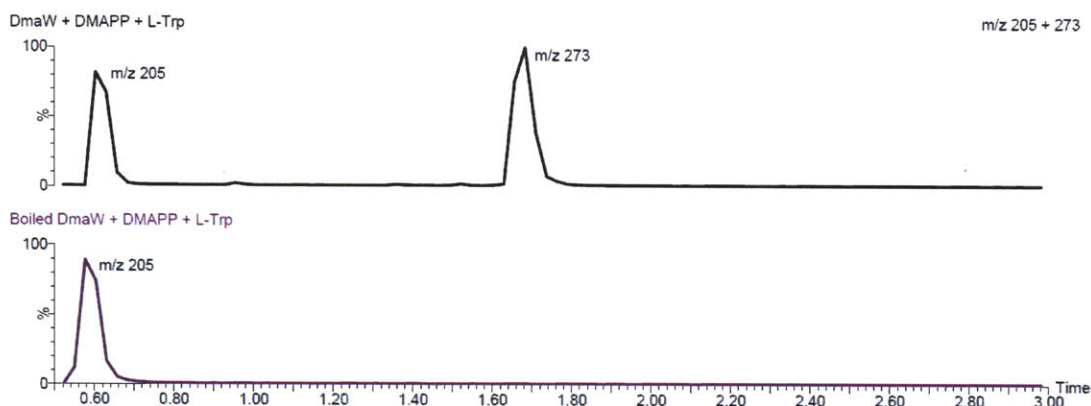


Figure 5.4. LC-MS chromatograms of endpoint activity assay (1 hour reaction) for purified DmaW dimethylallyl prenyltransferase. Peak intensities for this set of chromatograms have been normalized to allow relative comparison of compound masses present. A. L-tryptophan **1** and B. L-abrine (*N*_α-Me-L-tryptophan) **26**



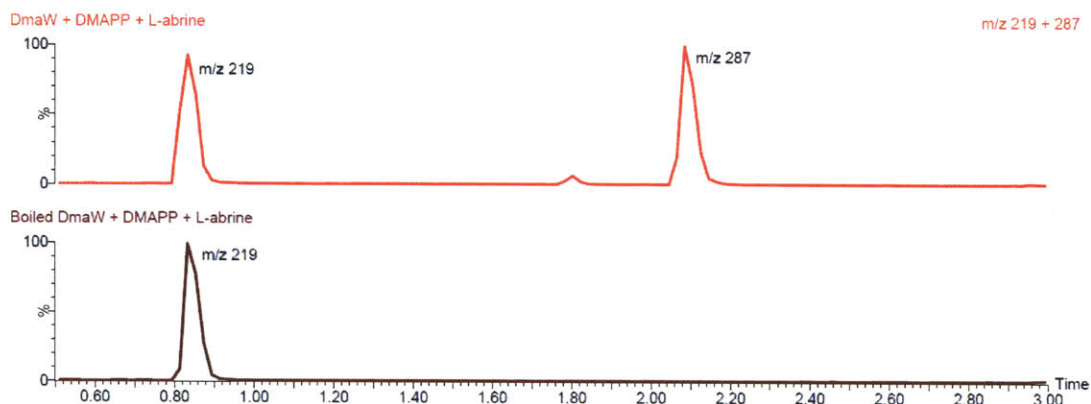
A. DmaW + DMAPP + L-Trp: Observed masses for L-tryptophan **1** [M+H]⁺ = 205 and product DMAT **3** [M+H]⁺ = 273.

Boiled DmaW + DMAPP + L-Trp (negative control): Observed mass for L-tryptophan **1** [M+H]⁺ = 205 only.



B. DmaW + DMAPP + L-abrine: observed masses for L-abrine **26** [M+H]⁺ = 219 and product *N*-Me-DMAT **4** [M+H]⁺ = 287.

Boiled DmaW + DMAPP + L-abrine (negative control): observed mass for L-abrine **26** [M+H]⁺ = 219 only.



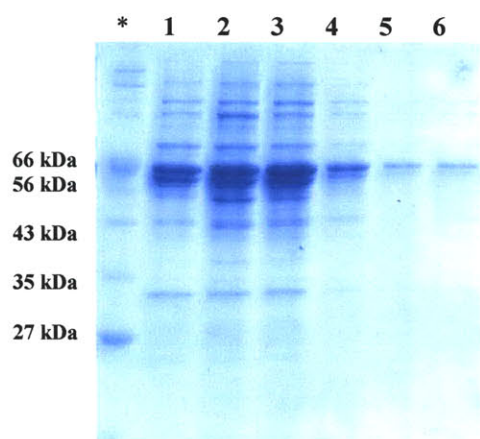
Expression and functional characterization of *easC* catalase

The *easC* gene was successfully cloned, yet initial expression attempts were low yielding and did not display catalase activity when tested with H_2O_2 . Due to the protein sequence homology of EasC to catalases, we added precursors ferric ammonium sulfate (0.2 mM) and aminolevulinic acid (0.4 mM) previously reported to support heme formation to our expression cultures.^{10, 11}

Under this new set of expression conditions, EasC was purified using Ni-NTA agarose at a yield of 0.3 mg/L (Figure 5.5) culture and displayed catalase activity when assayed with H_2O_2 . The activity of EasC was determined by an assay for catalase monitoring the decomposition of H_2O_2 with a spectrophotometer at 240 nM, as previously reported.¹²⁻¹⁴ The reaction mixture of EasC (0.1 μM) and H_2O_2 (10 mM) at pH = 8.0 displayed a gradual decrease in absorbance intensity over time when compared with the inactive boiled EasC control, which maintained a constant absorbance over the same time interval (Figure 5.6). These observations supported the catalase functionality expected for EasC.

To further characterize the functionality of EasC catalase relative to other known enzymes with oxidase activity, a UV-visible spectrum of EasC (1.6 μM) at pH = 8.0 was also taken from 250 nm to 550 nm, where the local maxima usually associated with heme containing enzymes were observed at 277 nm and 412 nm (Figure 5.7). The absorbance ratio of A_{406}/A_{280} was determined to be 0.13. From previous studies, typical catalases were observed with A_{406}/A_{280} ratios closer to 1 while catalases that also exhibited peroxidase activity had values less than 1.^{15, 16} Therefore, EasC, as produced under these expression conditions, was not completely reconstituted with heme.

Figure 5.5. SDS-PAGE gel of EasC (Expected Size 59 kDa)



Lane *. NEB Protein Marker Broad Range (2-212 kDa).
Lanes 1-6. 150 mM imidazole fractions

Figure 5.6. EasC catalase activity for decomposition of H_2O_2 . Absorbance monitored by spectrophotometer at 240 nm over a time course with 0.1 μM EasC + 10 mM H_2O_2 .

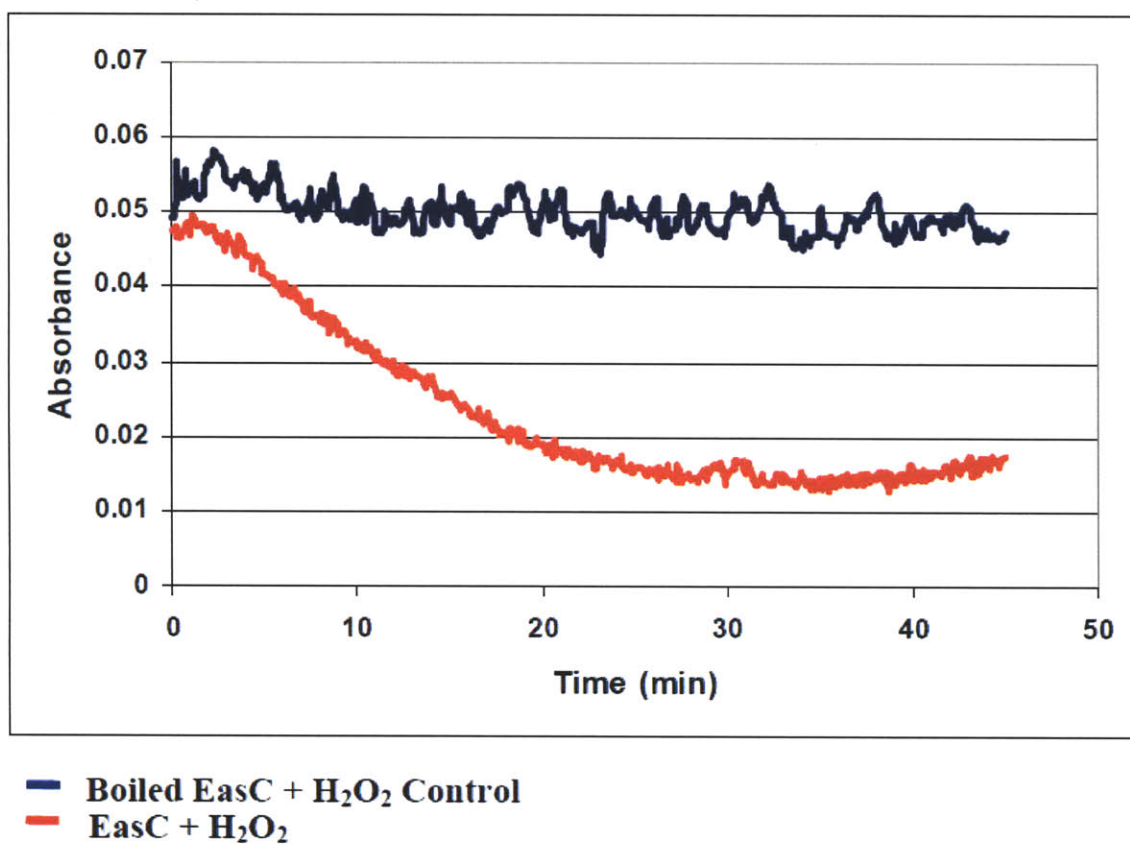
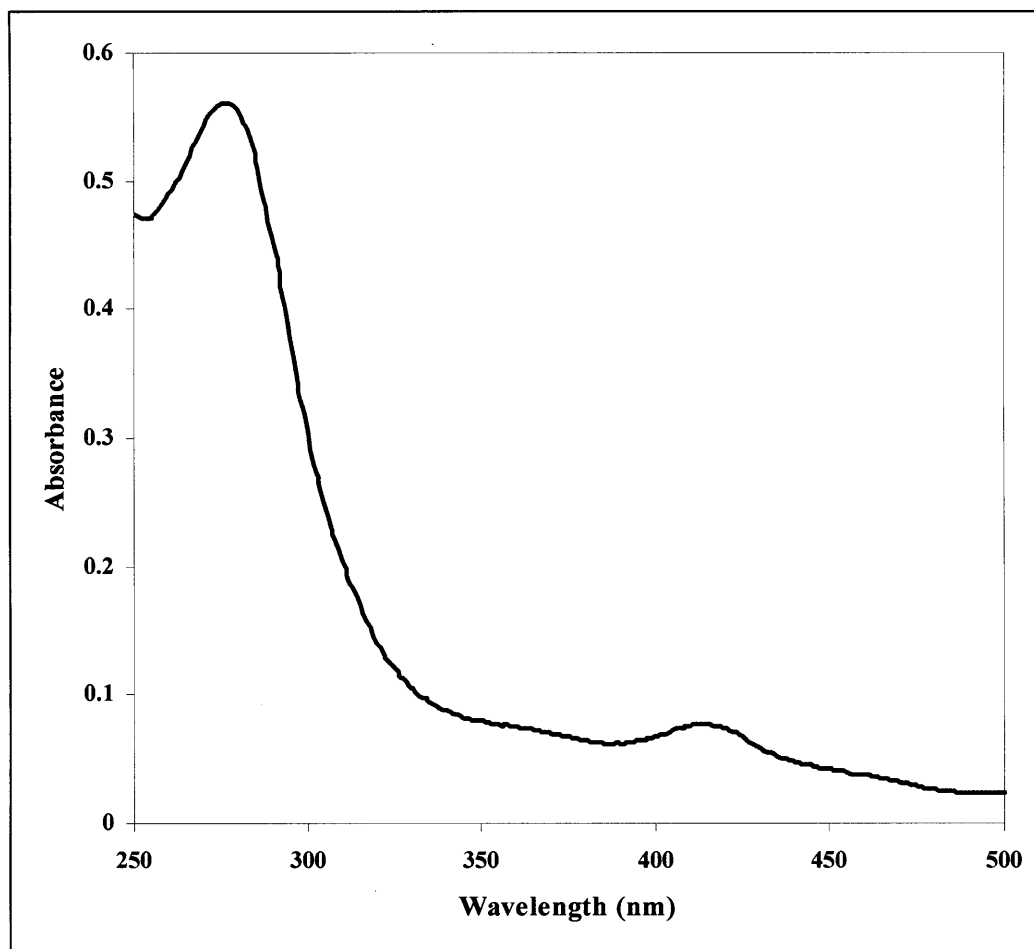


Figure 5.7. UV-Vis spectrum EasC (1.64 μM) local maxima at 277 nm and 412 nm.



To test the idea that EasC was involved in chanoclavine-I **6** formation, EasC (0.2 μ M) was incubated with *N*-Me-DMAT **4** produced from incubating DmaW (0.6 μ M) with DMAPP **2** (1 mM) and L-abrine **26** (1 mM) for 2 hours. The assay was also conducted with and without the addition of H₂O₂ (10 mM), but no downstream product intermediates were detected by HPLC or LC-MS analysis.

These data demonstrated that EasC displayed only standard catalase activity, which suggest that EasC may play a general protective role for the fungus from other oxidative enzymes that generate H₂O₂.^{15, 17} To test this hypothesis, our collaborators in the Panaccione lab conducted *in vivo* feeding studies of chanoclavine-I **6** to gene disrupted cultures of *easC*, as described in Chapter 2. They observed that downstream ergot alkaloid production was restored to similar levels as the *dmaW* gene disrupted control culture upon feeding. This finding suggested that *easC* does not act solely as a general protective enzyme to the fungus but provided a functional role in the cyclization of ergoline ring C.³ Yet the exact role of EasC as a catalase with possible peroxidase function in the cyclization of ring C remains speculative. Therefore, it was necessary to assay EasC in combination with other relevant pathway enzymes, such as EasE of the cluster, as described in the next section in order to investigate its potential as a peroxidase in ring C formation.

Expression and functional characterization of EasE

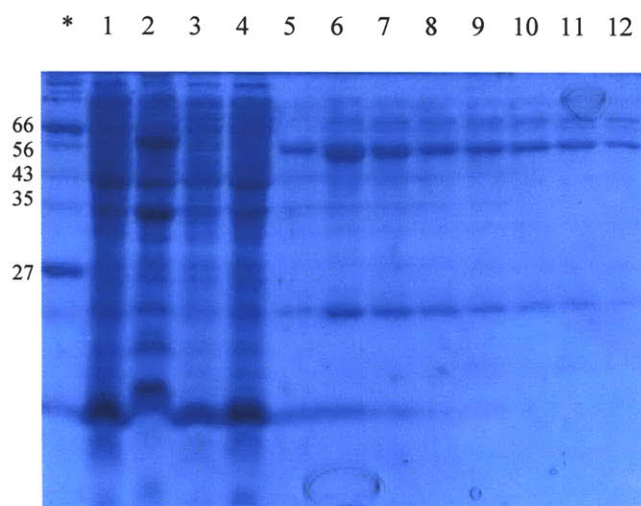
Initial attempts to express the *easE* gene product in *E. coli* BL-21 (DE3) were unsuccessful. More reasonable yields of EasE protein were obtained by using *S. cerevisiae* as an expression host; however, EasE did not co-purify with any flavin co-factor as evidenced by UV-Vis spectroscopy. Screening by assay of EasE in various

conditions with combinations of added FMN (60 μ M), FAD (30 μ M), H₂O₂ (10 mM), and EasC (0.2 μ M) protein did not display turnover of the *N*-Me-DMAT **4** substrate or accumulate any discernable product when analyzed by LC-MS.

These findings led us to re-analyze the splicing sequence of the EasE gene with other homologues in ergot producing gene clusters and retrieval expression with an *E. coli* codon optimized EasE sequence. Due to the cysteine rich protein sequence of EasE, we also tried to further optimize the proper folding and expression of this protein by using an *E. coli* strain that expressed a disulfide bond isomerase (DsbC SHuffle® T7 Express Competent *E.coli*, New England Biolabs).

Improved expression of EasE was realized after codon optimization and expression in *E. coli* DsbC SHuffle® and purification using Ni-NTA agarose yielded a yellow colored protein at 1.2 mg/L of culture (Figure 5.8). When analyzed by UV-Vis spectrometry, EasE exhibited the characteristic flavin profile (Figure 5.9). EasE was denatured and precipitated by the addition of 0.2% SDS, leaving a yellow supernatant that displayed the characteristic flavin spectra and was identified as flavin adenine dinucleotide (FAD) by comparison with an authentic standard (Figure 5.9). Concentration of the holoenzyme was calculated using the reported extinction co-efficient of FAD at 11,300 M⁻¹ cm⁻¹ at 450 nm.¹⁸

Figure 5.8. SDS-PAGE of EasE (*A. fumigatus*) (64 kDa)



*. NEB Broad Range Protein Ladder (2-212 kDa)

1. crude lysate

2. debris

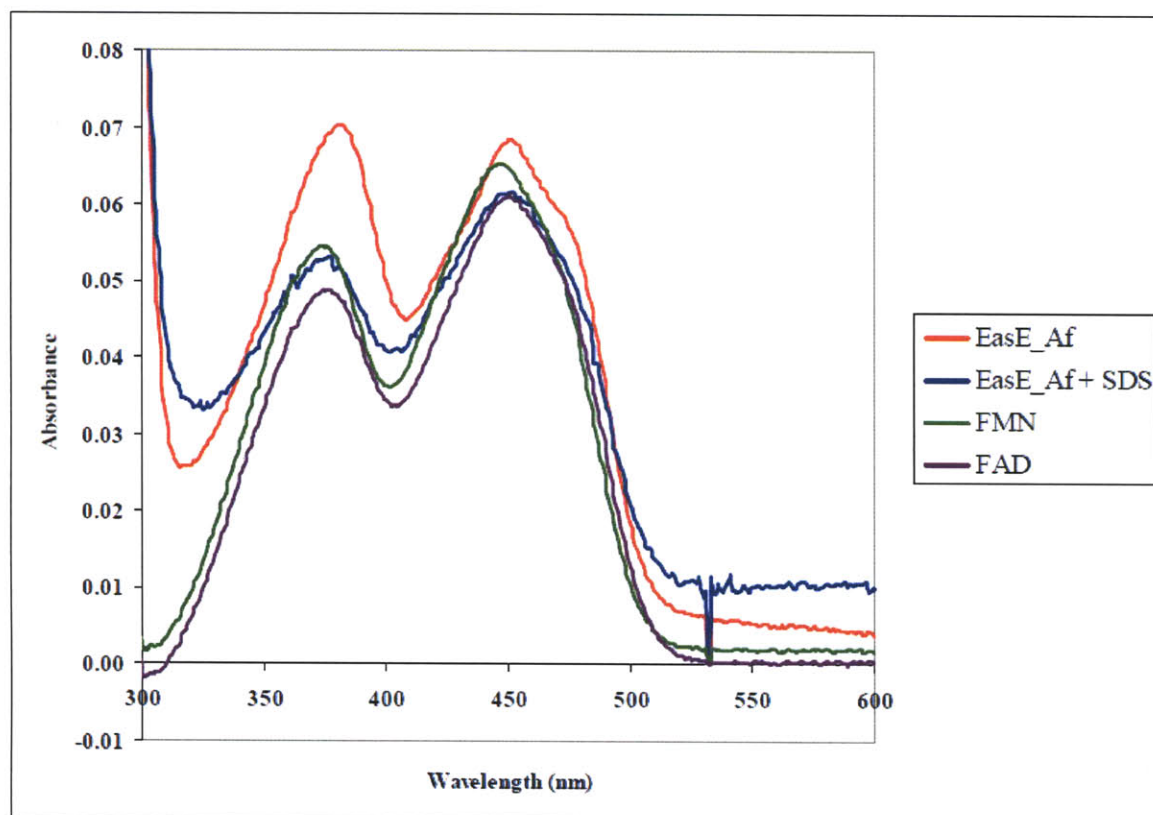
3. column flow through

4. buffer wash 10 mM imidazole

5. 25 mM imidazole

6-12. 50 mM imidazole

Figure 5.9. UV-Vis spectra of EasE_Af (300 nm to 600 nm)



Subsequent assay of the holoenzyme EasE (1.2 μ M) with substrate *N*-Me-DMAT **4** in different conditions and combinations with EasC (0.2 μ M), NADPH (500 μ M), and H₂O₂ (10 mM) did not lead to decrease of the substrate or accumulation of an intermediate. DTT (20 mM), which has been previously used as a synthetic reductant for flavins,¹⁹⁻²¹ was also added to the assay in order to see if EasE with a reduced FAD would exhibit activity; however, no substrate turnover was observed.

While EasC and EasE had good precedence for their involvement in the formation of ring C, we were challenged by difficulties in reconstituting their activity *in vitro* for the conversion of *N*-Me-DMAT **4** to chanoclavine-I **6**. These results led us to speculate on the functional role of EasC and EasE in terms of their mechanism and contribution to ring C cyclization. These speculations serve as guided hypotheses toward characterizing these enzymes *in vitro*.

Proposed mechanisms of ergoline ring C formation

The formation of chanoclavine-I **6**, the immediate product of ring C cyclization, from substrate *N*-Me-DMAT **4** required a net four electron oxidation, which is likely to occur in two successive two electron oxidation steps.^{1, 22, 23} The proposed mechanism of ring C cyclization was based on previous isotope feeding studies by the Floss group. They demonstrated that the diene **5** was a stable pathway intermediate that was well incorporated into downstream ergot alkaloids¹ and that the oxygen of chanoclavine-I **6** is derived from molecular oxygen.² Furthermore, data from our previous gene disruption studies of *easC* and *easE*, as described in Chapter 2, suggested that *N*-Me-DMAT **4** was the substrate for oxidation by EasC and EasE to form chanoclavine-I **6**.³

On the basis of these previous studies and our observations of the heterologously expressed EasC catalase activity and the co-purification of EasE with bound FAD, we explored mechanistic scenarios which could account for the challenges that need to be addressed before EasE and EasC activity can be successfully reconstituted *in vitro*. We proposed several schemes in which EasC and EasE may function to form ring C.

(1) *EasC as a catalase with peroxidatic activity and EasE as a FAD oxidase*

EasE may be involved with the direct oxidation of *N*-Me-DMAT **4** to form the proposed diene **5** intermediate as the first oxidation step. Like other known flavin oxidases, EasE may be able to carry out the direct oxidation of *N*-Me-DMAT **4**. The oxidation is proposed to occur via the transfer of a hydride from the substrate to the EasE flavin with a concerted deprotonation by an active site general base (Figure 5.10A). Precedence for this type of reaction had been observed in FAD oxidoreductases berberine bridge enzyme and isoamyl alcohol oxidase.²⁴⁻²⁶

EasE shares regions of protein sequence homology to the berberine bridge enzyme from *Eschscholzia californica* (California poppy) (Figure 5.10 B) which has been well characterized in its conversion of (S)-reticuline to (S)-scoulerine.^{24, 25} The proposed set of residues in berberine bridge enzyme which have been reported to be linked covalently to the FAD and involved in catalysis have identical or similar counterparts in the *A. fumigatus* EasE sequence alignments (Figure 5.11).^{24, 27}

The proposed mechanism for the initial oxidation in berberine bridge enzyme was reported to proceed via a concerted proton abstraction and hydride transfer to FAD (Figure 5.10B).^{24, 27} In our proposed mechanism for EasE, we believe that the diene **5**

could be formed directly from *N*-Me-DMAT **4** in an analogous fashion (Figure 5.10A). The berberine bridge enzyme also generated H₂O₂ as a byproduct during re-oxidation of FAD. Similarly, we can envision that EasE would also generate H₂O₂ by product.

Additionally, EasE also contained regions of protein sequence homology to fungal enzyme isoamyl alcohol oxidase from *Aspergillus oryzae* (Figure 5.12).²⁶ Isoamyl alcohol oxidase (Mre) from *A. oryzae* has been reported previously to catalyze the oxidation of isoamyl alcohol to isovaleraldehyde and shares homology to FAD dependent oxidoreductases.^{26, 28} Unlike the berberine bridge enzyme, mechanistic details for isoamyl alcohol oxidase have not been reported. Yet, based on the reaction catalyzed by isoamyl alcohol oxidase, it seemed likely that this oxidation may proceed via deprotonation of the alcohol along with the transfer of a hydride to the FAD of the enzyme (Figure 5.10C). The re-oxidation of the reduced FAD with molecular oxygen would generate H₂O₂ as a byproduct.

We propose that the EasC catalase / peroxidase may decompose the H₂O₂ byproduct of the EasE reaction to water and oxygen or use it to activate the heme for epoxidation of the diene **5** intermediate.²⁹ It has been observed previously that some catalases demonstrate peroxidatic activity, where the first molecule of H₂O₂ activates the heme iron in order to oxidize either a second molecule of H₂O₂ or organic compounds via a paired electron transfer or through sequential one electron transfer steps.^{15, 29-33}

Notably, EasC displayed protein sequence homology to *S. cerevisiae* catalase-A, which demonstrates both peroxidatic and catalatic activity (Figure 5.13).¹⁷ In order to facilitate ring C cyclization, we speculated that EasC may be involved with the epoxidation of proposed intermediate diene **5** (Figure 5.1 diene **5** to chanoclavine-I **6**).

The heme may be activated by H₂O₂ generated as a byproduct from the EasE reaction or other metabolic processes that reduce molecular oxygen O₂.^{32, 34, 35} This scenario would be consistent with results from previous isotope feeding studies where incorporation of molecular O₂ into formation of the chanoclavine-I **6** was observed.²

Alternatively, EasE flavin may act only on the later pathway of ring C cyclization serving as an epoxidase on the intermediate diene **5** prior to cyclization or the ring (Figure 5.14).³⁶ Enzymes capable of carrying out these reactions for the epoxidation of alkenes have been previously identified and are observed to require NADPH.³⁷⁻³⁹

In this scenario EasC would function to hydroxylate the benzylic C10 position, resulting in diene **5** formation. Subsequent epoxidation of the diene **5** by EasE would yield chanoclavine-I **6** (Figure 5.14). It is also possible that EasC may just act as a dedicated catalase to prevent undesired accumulation of H₂O₂ from the EasE reaction as described in the following section.

Figure 5.10. Comparison of proposed mechanisms for the FAD dependent oxidation of

A. *N*-Me-DMAT **4** to the diene **5** intermediate by *A. fumigatus* EasE

B. (S)-reticuline to (S)-scoulerine by *E. californica* Berberine Bridge Enzyme²⁴

C. Isoamyl alcohol to isovaleraldehyde by *A. oryzae* MreA Isoamyl Alcohol Oxidase
(Hypothetical mechanism based on our interpretation of reaction catalyzed by MreA^{26, 28}, no detailed mechanistic studies have been reported for this enzyme)

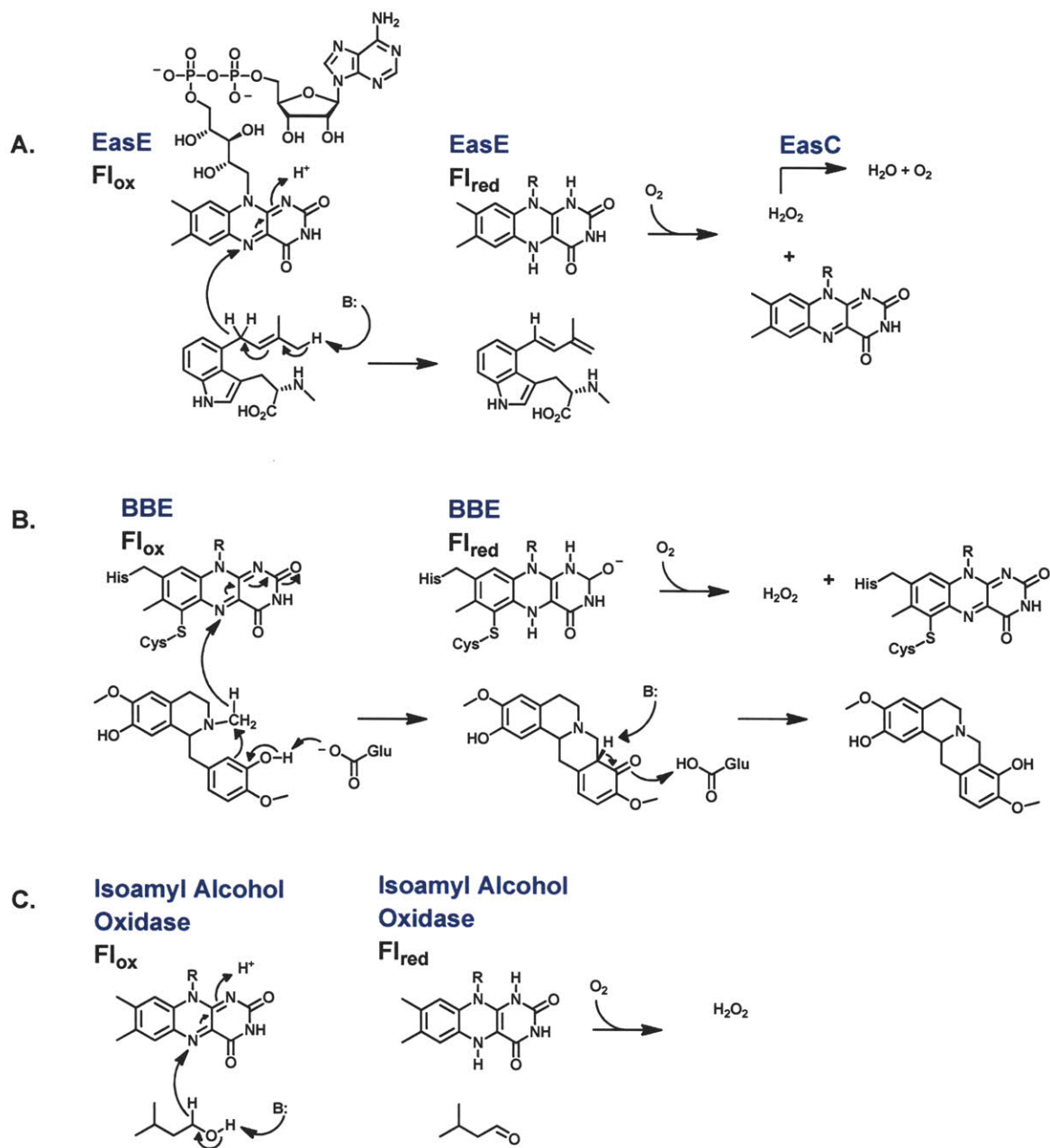


Figure 5.11. The *A_fumigatus* EasE and *E_californica*_BBE region proposed to interact with FAD (positions 131 to 292) shares 31% protein sequence identity and 48% similarity. Residues involved with covalent attachment of FAD to BBE were His 104 and Cys166 highlighted in green. These residues were identical in EasE.

```

A_fumigatus_EasE      --MPFVFSFLLGAFLSCIWLSLGGSTCRCPGESCWSPSEWAALNTTLRGDLVEVRPI 58
E_californica_BBE     MENKTPIFFSLSIFLSLLNCALGGNDLLSCLTFNGVRNHTVFSADSDSDFN-----RFL 54
                        : * *. *** : :*. *.. * . :. . * : :. * :

A_fumigatus_EasE      AHICHDPFYDHSACQNLRLDAKDSGWRASQAGTLQGWVVEVGRTEDETHAHSRPGAPCH 118
E_californica_BBE     HLSIQNPLFQNSLISKPSAIIIPG----- 78
                        ::*:::* .: : .

A_fumigatus_EasE      QGRIPLYSAAVESVDQIQVAVRFAQRHRLRLVVRNTGDTAGRSSGSDSFQIHCHRMKQI 178
E_californica_BBE     -----SKEELSNTRCIRKGSWTIRLRSGGSEGLSYTSDTPFILIDLNM-- 124
                        * : :. :.* : : : :. *. * * *: * . *:

A_fumigatus_EasE      EYHDNFRALGSDIDRGPVSVGAGVTLGEMYARGARDG--WVVVGGEPTVGAAGGFLQG 236
E_californica_BBE     -----LNRVSIDLES-ETAWVESGSLGELYAITESSKLGFTAGWPTVTGG-HISG 177
                        :. :. *: :. * : * *****: * :. . * *****: * . :.*

A_fumigatus_EasE      GGVSSFHSFIDGLAVDNVLEFEVVTAKGDVVVANDHQNPDIWFALRGGGGGTGIVTRAT 296
E_californica_BBE     GGFG-MMSRKYGLAADNVVDAILIDANG-AILDRQAMGEDVFWAIRGGGGVWGAIYAWK 235
                        **.. : * ***.***: : :*: * :. :. . *:***:*****: * : .

A_fumigatus_EasE      MRVHLNSPVCVSEVAVSGLRNSLLWTKGITGLFSILRSFNQQGIPGQFILRPLSKDQVN 356
E_californica_BBE     IKLLP-VPEKVTVFRVT--KNVAIDEATSLHKWQFVAEELEEDFT-LSVLGGADEKQVW 291
                        : : * * : . * : * : : : : : : : : : * . :.*

A_fumigatus_EasE      ASLTLYSLNTDDTRRSANMLSIRN-ILESTTLPTLAS--RCLPKISDALRKGPDMPLV 413
E_californica_BBE     LTMLGFHFGLKTVAKSTFDLLFPELGLVEEDYLEMSWGSEFAYLAGLETVSQNNRFLKF 351
                        : : : . . . *: : * . :*. * : :. . * . . . . * .

A_fumigatus_EasE      NYGIITGSVLVSEDLFNSSEEGPLHLAKQLEHFPMPDMLFTSNLGGNV SANTGKKHRDT 473
E_californica_BBE     DERAFTKVDLTKEPLPSK---AFYGLLERLSKEPNGFIALNGFGGQMSKIS---SDF 403
                        : :. . * : : : : * : : **:. * : :. :.***: * : *

A_fumigatus_EasE      SMHPGWRQAAHLINFVRSVSTPTAHEKARSLEELHSVQMRQLYDIEPDRVSYRNLGDPL 533
E_californica_BBE     TFPFHRSGTRLMEYIYAWNQSEQKKKTEFLDWLEKVYEFMKPFVSKNPRLYGVNH---I 460
                        : .* : : : : : . . :*: . *: *..* :. : *: * * :

A_fumigatus_EasE      ESDAAQVYWG--PNYKRLLLEIKRKWDPEDLFFS---QLGVGSEGWTEDQMCKRQRLQQM 588
E_californica_BBE     DLDLGGIDWGNKTVVNNAIEISRSWG-ESYFLSNYERLIRAKTLIDPNNVFNHPQSIPPM 519
                        : * . : ** . :. :*. *.. * . * : * .. : : : * : *

A_fumigatus_EasE      L--QYLMSSIAQRVYR-- 602
E_californica_BBE     ANFDYLEKTLGSDGGEVVI 538
                        : ** . :. . .

```


Figure 5.12. *A_oryzae_MreA* and *A_fumigatus_EasE* share approximately 39% protein sequence identity and 56% similarity.

A_oryzae_MreA	---MKSLIWALPFIPLAYANGNSSSCRCQPHQSCWPSEQWNSLSSSINGNLVAVQPIAA	57
A_fumigatus_Ease	MPFVFSFLLGAFLLSCLWLSLSGGSTCRCRPGESCWPSPSEWAALNTTLRGDLVEVRIAH	60
	: *: : . : : : ...*:***:* :***** .** :*: :*: :*: :*: :*	
A_oryzae_MreA	VCHEGDWDSSACKEVMASWTNSTWRAAQPGAVQWENWESWPEHNQTCYIESPRNTPCGQG	117
A_fumigatus_Ease	ICHDPFYDHSACQNLRLDLAKDSGWRASQAGTLQGVVWVEVGRTETEDTCHAHSPRGAPCHQG	120
	::*: :* ***::: :.* ***:*.*:* ** :*: :*.***:.* **	
A_oryzae_MreA	QISLYSTLAKSAFDIQETVKFAKHNLRLAIKNSGHDFLGRASAPESLQILTNGMKDIKM	177
A_fumigatus_Ease	RIPLYSAAVESVDQIQVAVRFAQRHRLRLVVRNTGHDTAGRSSGSDSFQIHCRRMKQIEY	180
	::*.**: :*. :*: :*: :*: :*.***:*.***:~::~*** **~::~*: :*: :*	
A_oryzae_MreA	VDKFTPAGAPQKGDEQAVTIAAGVSLQELYAAVAANNRTTVAGSAHTVGAAGGYIQGGG	237
A_fumigatus_Ease	HDNFRALGS--DIDRGPVSVGAGVTLGEMYARGARDGWVVVGGECPTVGAAGGFLQGGG	238
	: . * : . *.* **::~***:* *.* ** * :. .*.~.. *****:****	
A_oryzae_MreA	HSALGPWKG-MASDNALFTIVTANGDLVVANEYQNKDLFWALRGGGGGTFGVVVSVTVR	296
A_fumigatus_Ease	VSSFHSFIDGLAVDNVLEFEVVTAKGDVVVANDHQNPDIFWALRGGGGGTFGIVTRATMR	298
	:: :. : . : **.* ** :***.**:***::~** *:*****~::~*: . .*:*	
A_oryzae_MreA	TFDDAPLILVNFNITTSAGNPQYWDAVTTFHASLPKINDAKGGGYWIAPDTELTTENTSV	356
A_fumigatus_Ease	VHLNSPVCVSEVAVSGLRNNSLLWTKGITGLFSILRSFNQOG----IPGQFILRPLSKD	353
	.. :*: : : . : : .*. * * *: : : :* *. : * :.	
A_oryzae_MreA	SAITQTFTIFPNQTDTAQIDRLYAPLISKNGTTGVYTYQYASYPISVGFGLFSKIFLTGNS	416
A_fumigatus_Ease	QVNASLTLYSLNTDDTRSAENMLSIRNILESTTLPFTLASRCLP----KISDALRKGPD	409
	.. :. :. :. :*: :. : * : : : : ** :* :. : . *	
A_oryzae_MreA	DLAGTGTLG-SRLFSRDLLSSNNGSKKLSSALRSIRVDPGSAILGHLVAGGAVADN-AG	474
A_fumigatus_Ease	MLPVNYGIITGSVLVSEDLFNSEEGPLHLAKQLEHFPMPGMDLLFTSNLGGNVSAANTGKK	469
	*. . *: : * *.~***::~*.* :*: . * : : * . : : :*.~.* :	
A_oryzae_MreA	KVDSALNPAPWRKAITHIVIPRGWEPNATLAEQEAVKKNLTDVEIPILRSVEGTDKMGAYL	534
A_fumigatus_Ease	HRDTSMHPGWRQAAHLINFVR-SVSTPTAHEKARSLEELHSVQMRQLYDIEP-DFRVSYR	527
	: ~*: :*:~* * : * ...* *: :*: ~*: * .*: * :*	
A_oryzae_MreA	NEANAYESEFQSSFWGENYQRLLEVKKKWDPESLFFVVRGVGSEEWDEWGLCRAAK----	590
A_fumigatus_Ease	NLGDPLESDAAQVYWGPNYKRLLEIKRKWDPEDLFFSQLGVGSEGWTEDQMCKRQRLQ	587
	* :. . ** : . :* **.****:~*~*****~*~* : ***** * * :*: :	
A_oryzae_MreA	-----	
A_fumigatus_Ease	MLQYLMSSIAQRVYR	602

Figure 5.13. A_fumigatus_EasC and S_cerevisiae_CatalaseA protein sequence share approximately 43% identity and 60% similarity. The majority of residues proposed to interact with the heme in S_cerevisiae_catalaseA (green) were conserved for A_fumigatus_EasC (green). The V111A S_cerevisiae_CatalaseA mutant (pink) was reported to have increase peroxidatic activity over catalase activity.¹⁵ This residue was not conserved in A_fumigatus_EasC.

```

A_fumigatus_EasC      -MLIERGLLSIMASKCSGTWSTYKTYTTANGCPFMKPEGPPADGRTLALN 49
S_cerevisiae_CatalaseA DVREDR-----VVTNSTGN-PINEPFVTQR-----IGEHGP-----LLLQ 34
      :  :*      :.:.:.*. . :.:.*. . :  .**      *  *:

A_fumigatus_EasC      DHHLVESLAHFNREKIPERAVAKGAAAYGEFEVTADISDICNIDMLLGV 99
S_cerevisiae_CatalaseA DYNLIDSLAHFNRENIPQRNPAHGSGAFGYFEVTDITDICGSAMFSKI 84
      *:.:.:*****:.*:  *:.:.*:  *****  *:.*:  *:  :

A_fumigatus_EasC      GKKTPCVTRFSTTGLERGSAEGMRDLKGMATKFYTKEGNWDWVCINFFFF 149
S_cerevisiae_CatalaseA GKRTKCLTRFSTVGGDKGSADTVRDRPGFATKFYTEEGNLDWVYNTPVF 134
      **:.*  *:.*:  *.  :.:.:  :.*  :.:*****:***  **  *  *.

A_fumigatus_EasC      FIRDPLKFPPLMHAQRRDPRTNLLNPNMYWDWVTS--NHESLHMVLLQFS 197
S_cerevisiae_CatalaseA FIRDPSKFPFHFIHTQKRNPQTNLRDADMFWDFLTTPENQVAIHQVMILFS 184
      *****  ***  :.:.*:.*:.*:  :.:.*:.*:  *:  :.*  *:  **

A_fumigatus_EasC      DFGTMFNWRSLSGYMGHAYKWVMPNGSFKYVHIFLSSDRGPNFSQGEQAK 247
S_cerevisiae_CatalaseA DRGTPANYRSMHGYSGHTYKWSNKNGDWHYVQVHIKTDQGIKNLTIEEAT 234
      *  **  *:.*:  **  *:.*:  **  :.:.*:.*:  :  :.*:  *.

A_fumigatus_EasC      DNSDLDPDHATRDLYEAIERGDYPTWTANVQVVDPAEAPDLGFNILDVTK 297
S_cerevisiae_CatalaseA KIAGSNPDYCCQDLFEAIQNGNYPSTVYIQTMTERDAKKLPFSVFDLTK 284
      .  .  :.:.*:  :.:.*:.*:.*:.*:.*:  :.*:  :*  .  *  :.:.*:

A_fumigatus_EasC      HWNLGTYPKDLPKIPSRPFGKLTNLNRIPDNFFAEVEQLAFSPSNMVPGLV 347
S_cerevisiae_CatalaseA VWPQGQFP-----LRRVGKIVLNENPLNFFAQVEQAAPSTTVPYQE 327
      *  *  :*      *  .*:.*:  *  *****:***  *:.*:  **

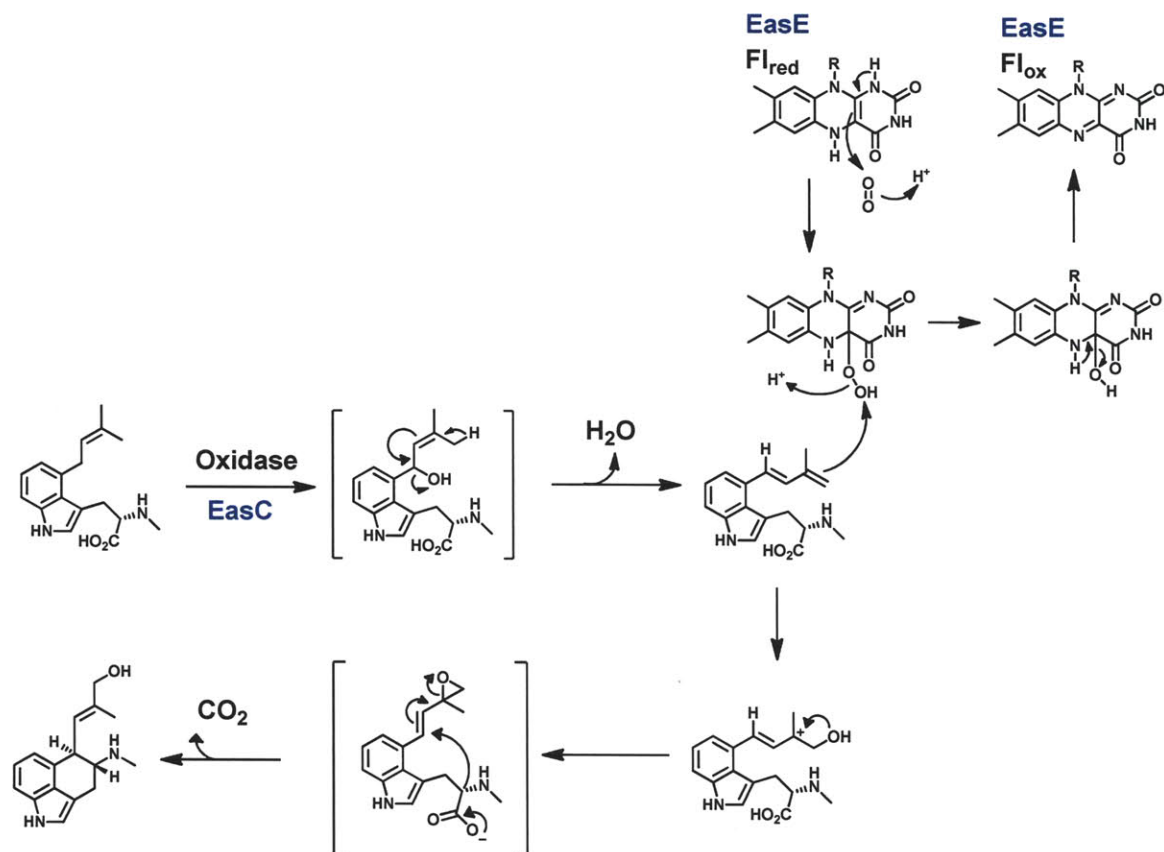
A_fumigatus_EasC      PSEDPIQAEMFAYPDAQRYRLGPNHHKIPVNQCMT--FNPTLRDGTG 394
S_cerevisiae_CatalaseA ASADPVLQAFLEFSYADAHRYRLGPNFHQIPVN-CPYASKFFNPAIRDGPM 376
      .  *  *:.*:.*:.*:  :.*:.*:.*:.*:.*:  **  :  ***:.*:

A_fumigatus_EasC      TFDANYGSLPGYVSESQGVNFARP-QEHDPKFNAWLSQLSSRPWMQTN-E 442
S_cerevisiae_CatalaseA NVNGNFGSEPTYLANDKSYTYIQQDRPIQQHQEVWNGPAIPYHWATSPGD 426
      :.:.*:.*:  *  :.:.:  .  :  :  :  :  :.*  .  .  *  :  :

A_fumigatus_EasC      NDYKFPRDFYNALPEFRSQEFQDKMVENIIASVAQTRREIREKVYHTFHL 492
S_cerevisiae_CatalaseA VDFVQARNLYRVLGKQPGQ--QKNLAYNIGIHVEGACPQIQQRVYDMFAR 474
      *:  .*:.*:.*:  :  .  *  *:.*:  **  *  :  :.:.*:.*:  *

A_fumigatus_EasC      VDPELSARVVRGVEKMDASFKQVLSRL 520
S_cerevisiae_CatalaseA VDKGLSEAIKKVAE----- 488
      **  **  :*:  .*
```

Figure 5.14. Proposed mechanism for EasC catalyzing the hydroxylation of C10 position of *N*-Me-DMAT **4** as the first oxidation step. EasE catalyzes the epoxidation of the diene **5** intermediate as the second oxidation step.



(2) *EasC as a catalase and EasE as a FAD oxidase catalyzing successive oxidations*

Alternatively, it is also possible that EasE may catalyze both oxidations in ring C cyclization (Figure 5.15). Numerous flavin dependent oxidases function to carry out oxidations with the transfer of a hydride equivalent from the substrate.^{25, 26, 40} If EasE were capable of carrying out the complete set of successive oxidations to cyclize ring C, then we propose that EasE could likely generate this diene **5** intermediate by the direct oxidation of *N*-Me-DMAT **4** (Figure 5.15).

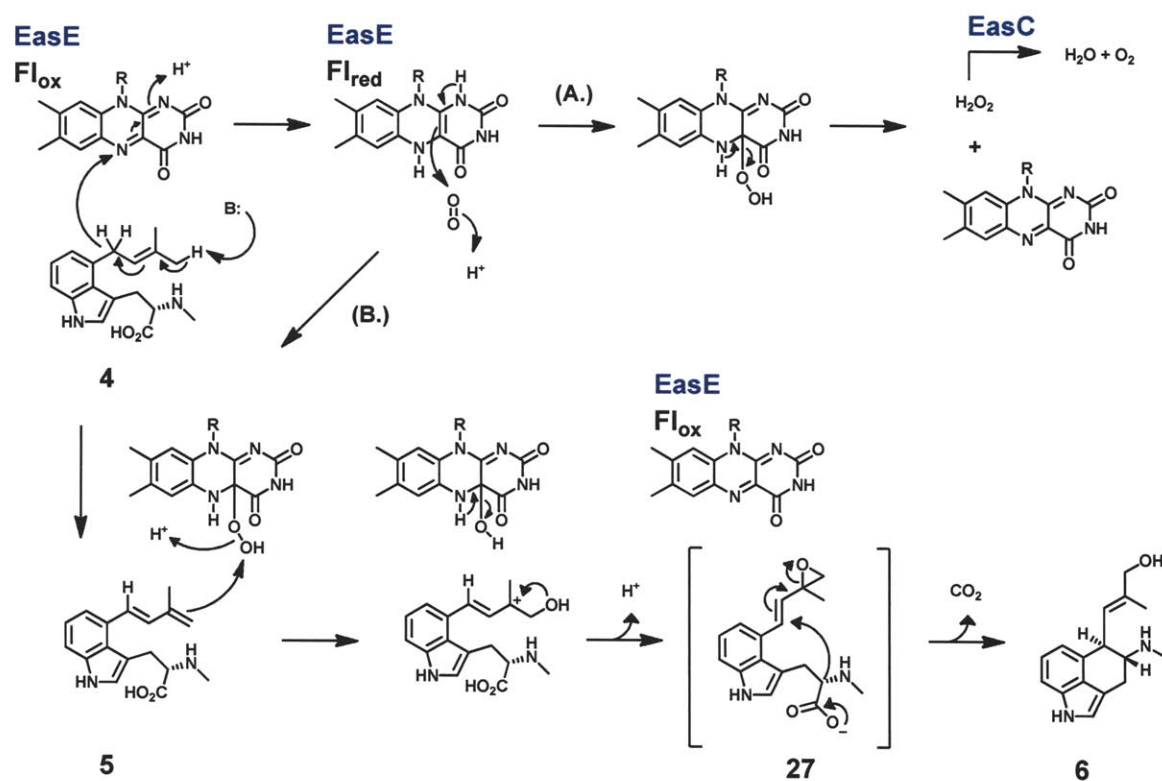
Subsequently, the EasE flavin C(4a)-hydroperoxide intermediate, generated from the reaction with reduced flavin and molecular oxygen⁴¹, could be used to form the epoxide **27** from the diene **5** in order to catalyze the formation of ring C to make chanoclavine-I-aldehyde **7** (Figure 5.15). Precedence for such a reaction has been previously reported for FAD catalyzed epoxidations.^{37, 42, 43} Whether EasE can carry out this further epoxidation reaction continues to be a focus of our future research. There has been precedence for a flavin enzyme to carry out such successive oxidations such as lactate monooxygenase, that oxidizes lactate to pyruvate then to acetate; however, these internal monooxygenases are rare.⁴⁴

If EasE carried out both oxidation steps, then EasC would only act as a protective enzyme to decompose the H₂O₂ byproduct in order to prevent undesired product formation or damage to the enzymes. Scenarios in which FAD oxidases like EasE have a partner catalase, like EasC, to act in such a protective role have been previously reported.^{45, 46}

From our assays described earlier we have observed that EasC and EasE together or in isolation did not turnover *N*-Me-DMAT **4** to form the proposed diene **5** or

chanoclavine-I **6** under our *in vitro* assay conditions. It remains a possibility that EasC and EasE act as part of a biosynthetic complex with other pathway enzymes to contribute to the initial formation of the diene **5**, aspects of which will be explored in the next section.

Figure 5.15. Proposed mechanism for EasE catalyzing successive oxidations on substrate *N*-Me-DMAT **4** and involvement of EasC in decomposing the H₂O₂ byproduct. A. Illustrates the re-oxidation of the flavin by molecular oxygen generating H₂O₂ as a byproduct for subsequent decomposition by EasC. B. Illustrates oxidation of the diene **5** intermediate by the flavin C(4a)-hydroperoxide intermediate resulting in the formation of the epoxide **27** followed by cyclization to yield chanoclavine-I **6**.



(3) *EasE and EasC function in a complex which may include other pathway enzymes*

Assays of EasE and EasC, in combination, have yet to demonstrate the conversion of *N*-Me-DMAT **4** to chanoclavine-I **6**. This suggests that other enzymes within or beyond the ergot alkaloid gene cluster may be involved in the cyclization of ring C. If EasC and EasE alone prove insufficient to catalyze the cyclization, this will guide efforts to search for other candidate oxidases that may support the formation of chanoclavine-I **6** from *N*-Me-DMAT **4**. Yet, it remains a possibility that EasE and EasC need to be present under strictly regulated ratios in order to observe cyclization of ring C. These ratios may govern the formation of a functioning enzyme complex in order to observe ring C cyclization from *N*-Me-DMAT **4** *in vitro*. It has been previously reported that successful reconstitution of active biosynthetic pathways *in vitro* often require the presence of other pathway enzymes in appropriate ratios in order to achieve product formation.⁴⁷

Due to the oxidations that were proposed in this step, greater control of the assay conditions may be necessary in order to reconstitute EasC and EasE function *in vitro*. In a study of the epoxidation reaction carried out by heme-peroxidases *Coprinus cinereus* peroxidase and myeloperoxidase, it had been reported that slow introduction of H₂O₂ into assays were required to observe epoxidation by heme-peroxidase *in vitro*, otherwise the accumulation of inactive intermediates were observed.³⁵ If EasC acts as a heme peroxidase to carry out the epoxidation of the diene **5**, then the H₂O₂ may need to be slowly introduced from a source, such as from the re-oxidation of the flavin EasE in order to observe activity. Therefore, EasC and EasE may need to be properly reconstituted in a biosynthetic complex in order to observe their proposed function for the cyclization of ergoline ring C *in vitro*.

These proposed mechanisms serve to guide our future efforts toward the successful reconstitution of EasC and EasE activity for the *in vitro* cyclization of the ergoline ring C. EasC and EasE will also be assayed in the presence of other pathway enzymes that may facilitate their proposed function in the production of chanoclavine-I **6**. Alternative approaches to assay these enzymes for their involvement of ergoline ring C formation will be discussed further in Chapter 6.

Conclusions

This chapter describes our current progress in efforts to characterize the enzymes of the ergot gene cluster that were necessary for the cyclization of ergoline ring C, which produces chanoclavine-I **6** from *N*-Me-DMAT **4**. We were able to express the active DmaW prenyltransferase from *C. purpurea*⁵ successfully and demonstrate its prenylation activity on the natural L-tryptophan **1** substrate in addition to L-abrine **26** substrate to yield *N*-Me-DMAT **4**. This allowed us to obtain the *N*-Me-DMAT **4** proposed substrate for EasE and EasC enzymes required for the cyclization of ergoline ring C to produce chanoclavine-I **6**. While expression of EasC catalase was successful and demonstrated activity for the decomposition of hydrogen peroxide, EasC did not display peroxidase activity alone or in the presence of EasE with *N*-Me-DMAT **4**. Likewise, our expressed EasE enzyme that co-purified with a bound FAD did not convert *N*-Me-DMAT **4** to product chanoclavine-I **6** when assayed alone or in various combinations with EasC.

Further analysis of possible mechanisms and sequences in which these two enzymes would function to form ring C, allowed us to speculate on possible reasons why enzymes when assayed *in vitro* do not display their proposed oxidase activities. It was possible that EasC and EasE may function as an enzyme complex given the instability of the proposed intermediates or reactivity of the diene **5** intermediate to the peroxides that may be generated in the reaction. Alternative approaches to further evaluate the role of EasE and EasC and conditions to achieve the cyclization of ergoline ring C *in vitro* will be discussed in Chapter 6.

References

1. Kozikowski, A., C. Chen, J. Wu, M. Shibuya, C. Kim, and H.G. Floss, *Probing ergot alkaloid biosynthesis: intermediates in the formation of ring C*. Journal of the American Chemical Society, 1993. **115** (6): p. 2482-2488.
2. Kobayashi, M. and H.G. Floss, *Biosynthesis of ergot alkaloids: origin of the oxygen atoms in chanoclavine-I and elymoclavine*. Journal of Organic Chemistry, 1987. **52**(19): p. 4350-4352.
3. Goetz, K.E., C.M. Coyle, J.Z. Cheng, S.E. O'Connor, and D.G. Panaccione, *Ergot cluster-encoded catalase is required for synthesis of chanoclavine-I in Aspergillus fumigatus*. Current Genetics, 2011(accepted).
4. Lorenz, N., J. Olsovska, M. Sulc, and P. Tudzynski, *Alkaloid Cluster Gene ccsA of the Ergot Fungus Claviceps purpurea Encodes Chanoclavine I Synthase, a Flavin Adenine Dinucleotide-Containing Oxidoreductase Mediating the Transformation of N-Methyl-Dimethylallyltryptophan to Chanoclavine I*. Applied and Environmental Microbiology, 2010. **76**(6): p. 1822-1830.
5. Wang, J., C. Machado, D.G. Panaccione, H.-F. Tsai, and C.L. Schardl, *The determinant step in ergot alkaloid biosynthesis by an endophyte of perennial ryegrass*. Fungal Genetics and Biology, 2004. **41**: p. 189-198.
6. Gebler, J., A. Woodside, and C. Poulter, *Dimethylallyltryptophan synthase. An enzyme-catalyzed electrophilic aromatic substitution*. Journal of the American Chemical Society, 1992. **114** (19): p. 7354-7360.
7. Unsold, I. and S.-M. Li, *Overproduction, purification and characterization of FgaPT2, a dimethylallyltryptophan synthase from Aspergillus fumigatus*. Microbiology, 2005. **151**: p. 1499-1505.
8. Chomczynski, P. and N. Sacchi, *The single-step method of RNA isolation by acid guanidinium thiocyanate-phenol-chloroform extraction: twenty-something years on*. Nature Protocols, 2006. **1**(2): p. 581-585.
9. Steffan, N., I. Unsold, and S.-M. Li, *Chemoenzymatic synthesis of prenylated indole derivatives by using a 4-dimethylallyltryptophan synthase from Aspergillus fumigatus*. ChemBiochem, 2007. **8**: p. 1298 - 1307.
10. Sengupta, R., R. Sahoo, S. Ray, T. Dutta, A. Dasgupta, and S. Ghosh, *Dissociation and unfolding of inducible nitric oxide synthase oxygenase domain identifies structural role of tetrahydrobiopterin in modulating the heme environment*. Molecular and Cellular Biochemistry, 2006. **284**: p. 117-126.
11. Weickert, M., D. Doherty, E. Best, and P. Olins, *Optimization of heterologous protein production in Escherichia coli*. Current Opinion in Biotechnology, 1996. **7**: p. 494-499.
12. Aebi, H., *Catalase in vitro*. Methods in Enzymology, 1984. **105**: p. 121-126.
13. Noble, R. and Q. Gibson, *The Reaction of Ferrous Horseradish Peroxidase with Hydrogen Peroxide*. The Journal of Biological Chemistry, 1970. **245**(9): p. 2409-2413.
14. Li, Y. and H.E. Schellhorn, *Rapid Kinetic Microassay for Catalase Activity*. Journal of Biomolecular Techniques, 2007. **18**(4): p. 185-187.

15. Zamocky, M., C. Herzog, L. Nykyri, and F. Koller, *Site-directed mutagenesis of the lower parts of the major substrate channel of yeast catalase A leads to highly increased peroxidatic activity*. FEBS Letters, 1995. **367**(241-245).
16. Kocabas, D., U. Bakir, S. Phillips, M. McPherson, and Z. Ogel, *Purification, characterization, and identification of a novel bifunctional catalase-phenol oxidase from Scytalidium thermophilum*. Applied Microbial Biotechnology, 2008. **79**: p. 407-415.
17. Mate, M., M. Zamocky, L. Nykyri, C. Herzog, P. Alzari, C. Betzel, F. Koller, and I. Fita, *Structure of catalase-A from Saccharomyces cerevisiae*. Journal of Molecular Biology, 1999. **286**(1): p. 135-149.
18. Macheroux, P., *UV-visible spectroscopy as a tool to study flavoproteins*, in *Methods in Molecular Biology: Flavoprotein Protocols*, S. Chapman and G. Reid, Editors. 1999, Humana Press Inc.: Totowa, NJ.
19. Bitto, E., Y. Huang, C.A. Bingman, S. Singh, J.S. Thorson, and G. Phillips, *The structure of flavin-dependent tryptophan 7-halogenase RebH*. Proteins: Structure, Function, and Bioinformatics, 2008. **70**(1): p. 289-293.
20. Penzkofer, A., A.K. Bansal, S.-H. Song, and B. Dick, *Fluorescence quenching of flavins by reductive agents*. Chemical Physics, 2007. **336**: p. 14-21.
21. Song, S.-H., B. Dick, and A. Penzkofer, *Photo-induced reduction of flavin mononucleotide in aqueous solutions*. Chemical Physics, 2007. **332**: p. 55-65.
22. Floss, H.G. and J. Anderson, *The Biosynthesis of Mycotoxins*, P. Steyn, Editor. 1980, Academic Press. p. 17-67.
23. Schardl, C.L., D.G. Panaccione, and P. Tudzynski, *Ergot Alkaloids - Biology and Molecular Biology*, in *The Alkaloids* G. Cordell, Editor. 2006, Elsevier. p. 45-86.
24. Winkler, A., A. Lyskowski, S. Riedl, M. Puhl, T. Kutchan, P. Macheroux, and K. Gruber, *A concerted mechanism for berberine bridge enzyme*. Nature Chemical Biology, 2008. **4**(12).
25. Diitrich, H. and T. Kutchan, *Characterization and Mechanism of the Berberine Bridge Enzyme, a Covalently Flavinylated Oxidase of Benzophenanthridine Alkaloid Biosynthesis in Plants*. The Journal of Biological Chemistry, 1995. **270**(41): p. 24475-24481.
26. Yamashita, N., T. Motoyoshi, and A. Nishimura, *Molecular Cloning of the Isoamyl Alcohol Oxidase-Encoding Gene (mreA) from Aspergillus oryzae*. Journal of Bioscience and Bioengineering, 2000. **89**(6): p. 522-527.
27. Fraaije, M. and A. Mattevi, *Cyclization in convert*. Nature Chemical Biology, 2008. **4**(12).
28. Kubodera, T., N. Yamashita, and A. Nishimura, *Molecular Breeding of the Mureka-Non-Forming Sake Koji Mold from Aspergillus oryzae by the Disruption of the mreA Gene*. Journal of Bioscience and Bioengineering, 2003. **95**(1).
29. Vlasits, V., C. Jakopitsch, M. Bernroitner, M. Zamocky, P. Furtmuller, and C. Obinger, *Mechanisms of catalase activity of heme peroxidases*. Archives of Biochemistry and Biophysics, 2010. **500**: p. 74-81.
30. Lah, L., N. Kras, P. Trontelj, and R. Komel, *High diversity and complex evolution of fungal cytochrome P450 reductase: cytochrome P450 systems*. Fungal Genetics and Biology, 2008. **45**: p. 446-458.

31. Perera R., J., S., Sono, M., and Dawson, J., *Cytochrome P450-Catalyzed Hydroxylations and Epoxidations*, in *Metal Ions in Life Science*, A. Sigel, Sigel, H., and Sigel, R., Editor. 2007, John Wiley & Sons Ltd.: England. p. 319-359.
32. Makris, T., I. Denisov, I. Schlichting, and S. Sligar, *Activation of molecular oxygen by cytochrome P450*, in *Cytochrome P450 Structure, Mechanism, and Biochemistry*, P. Ortiz de Montellano, Editor, Kluwer Academic/Plenum Publishers: New York. p. 149-182.
33. Loewen, P., M. Klotz, and D. Hassett, *Catalase - an "Old" Enzyme That Continues To Surprise Us*, in *American Society for Microbiology News*. 2000.
34. Gruschow, S. and D. Sherman, *The biosynthesis of epoxides*, in *Aziridines and Epoxides in Organic Synthesis*, A. Yudin, Editor. 2006, WILEY-VCH Verlag GmbH & Co. p. 349-376.
35. Tuynman, A., J.L. Spelberg, I.M. Kooter, H.E. Schoemaker, and R. Wever, *Enantioselective Epoxidation and Carbon-Carbon Bond Cleavage Catalyzed by Coprinus cinereus Peroxidase and Myeloperoxidase*. The Journal of Biological Chemistry, 2000. **275**(5): p. 3025-3030.
36. Palfrey, B. and C. McDonald, *Control of catalysis in flavin-dependent monooxygenases*. Archives of Biochemistry and Biophysics, 2010. **493**: p. 26-36.
37. Buch, K., H. Stransky, and A. Hager, *FAD is a further essential cofactor of the NAD(P)H and O₂-dependent zeaxanthin-epoxidase*. FEBS Letters, 1995. **376**: p. 45-48.
38. Reeves, C.D., Z. Hu, R. Reid, and J.T. Kealey, *Genes for the biosynthesis of the fungal polyketides hypothemycin from Hypomyces subiculosus and radicol from Pochonia chlamydosporia*. Applied and Environmental Microbiology, 2008. **74**: p. 5121-5129.
39. Tanaka, M. and S. Tahara, *FAD-dependent epoxidase as a key enzyme in fungal metabolism of prenylated flavonoids*. Phytochemistry, 1997. **46**: p. 433-439.
40. Gadda, G., *Hydride Transfer Made Easy in the Reaction of Alcohol Oxidation Catalyzed by Flavin-dependent Oxidases*. Biochemistry, 2008. **47**(52): p. 13745-13753.
41. Massey, V., *Activation of Molecular Oxygen by Flavins and Flavoproteins*. The Journal of Biological Chemistry, 1994. **269**(36): p. 22459-22462.
42. Kantz, A. and G.T. Gassner, *Nature of the Reaction Intermediates in the Flavin Adenine Dinucleotide-Dependent Epoxidation Mechanism of Styrene Monooxygenase*. Biochemistry, 2011. **50**: p. 523-532.
43. Laden, B.P., Y. Tang, and T.D. Porter, *Cloning, heterologous expression, and enzymological characterization of human squalene monooxygenase*. Archives of Biochemistry and Biophysics, 2000. **374**(2): p. 381-388.
44. Van Berkel, W.J.H., N.M. Kamerbeek, and M. Fraaije, *Flavoprotein monooxygenases, a diverse class of oxidative biocatalysts*. Journal of Biotechnology, 2006. **124**: p. 670-689.
45. Geissler, J., S. Ghisla, and P.M.H. Kroneck, *Flavin-dependent alcohol oxidase from yeast. Studies on the catalytic mechanism and inactivation during turnover*. European Journal of Biochemistry, 1986. **160**: p. 93-100.

46. Das, S., I.J.H. Glenn, and M. Subramanian, *Enantioselective oxidation of 2-hydroxy carboxylic acids by glycolate oxidase and catalase coexpressed in methylotropic Pichia pastoris*. . Biotechnology Progress, 2010. **26**: p. 607-615.
47. Kharel, M.K., P. Pahari, H. Lian, and J. Rohr, *Enzymatic Total Synthesis of Rabelomycin, and Angucycline Group Antibiotic*. Organic Letters, 2010. **12**: p. 2814-2817.

Chapter 6 . Conclusions and Future Directions

Conclusions

Chapter 2 described the *in vivo* approach toward the assignment of function to clustered genes associated with ergot alkaloid biosynthesis in *A. fumigatus*. In collaboration with the lab of Professor Daniel Panaccione we were able to confirm through targeted gene disruption that *dmaW* (prenyl transferase) and *easF* (SAM dependent *N*-methyltransferase) functioned as the first two enzymes of the ergot alkaloid pathway that precede ergoline ring C and D cyclization as had been previously suggested by feeding studies and *in vitro* characterization of DmaW and EasF enzymes.¹⁻⁴

Using this gene disruption strategy, we were able to identify *A. fumigatus* genes associated with the critical ergoline ring C and D cyclizations. Disruption of *easE* (FAD dependent oxidoreductase) and *easC* (catalase) genes led to the accumulation of the pathway intermediate *N*-Me-DMAT **4** which had been hypothesized to precede ring C cyclization.⁵ Disruption of *easA* (Old Yellow Enzyme homologue) demonstrated the accumulation of the pathway intermediate chanoclavine-I **6** and chanoclavine-I-aldehyde **7**, pathway intermediates that were believe to precede ring D cyclization.⁶

This finding signified that *easA* plays a functional role in the cyclization of ergoline ring D in festuclavine **11** derived alkaloids and suggested that it functions as a reductase similar to Old Yellow Enzyme.⁷ Subsequent augmentation of the *easA* gene with a homologue of *easA* from *C. purpurea* *in vivo*, resulted in a switch in the ergot alkaloid profile of *A. fumigatus* toward agroclavine **10** derived products in contrast to wild type *A. fumigatus*, which produces festuclavine **11** derived ergot alkaloids. This suggested that the gene product EasA from *C. purpurea* functions as an isomerase to catalyze ring D cyclization in agroclavine **10** derived ergot alkaloids.

Importantly, these results demonstrated that EasA was an enzyme acting at the critical branch point of ergot alkaloid biosynthesis across divergent fungal species, leading to the production of either festuclavine **11** or agroclavine **10** derived compounds. These *in vivo* gene disruption studies proved crucial to our efforts in understanding the sequence of catalytic events that led to ergoline ring formation and the enzymes associated with each step. These findings served as an essential guide toward our *in vitro* study of the gene products involved in ergoline ring cyclization.

Chapter 3 described our functional characterization of the *A. fumigatus* EasA Old Yellow Enzyme homologue *in vitro*. This study provided evidence that EasA_Af facilitates the reduction of the alkene in chanoclavine-I-aldehyde **7** catalyzes an intramolecular cyclization to form ring D of the ergoline structure via an intermediate cyclic iminium intermediate **9**.⁸ Trapping the iminium intermediate **9** either by synthetic reduction or by the addition of the NADPH dependent oxidoreductase EasG, also present in the ergot cluster, demonstrated that the cyclic iminium intermediate **9** precedes festuclavine **11** formation. These findings suggested that EasA_Af and EasG together catalyze the full set of transformations necessary to form ring D of festuclavine **11** starting from substrate chanoclavine-I-aldehyde **7**. The successful *in vitro* characterization of EasA_Af correlated with the findings of the *in vivo easA* gene disruption study, further substantiating that EasA functioned at the critical branch point of ergot alkaloid biosynthesis. These findings provided the platform upon which more detailed mechanistic studies can be performed to reconcile the mechanism and

stereoselectivity of this critical ring D cyclization across ergot alkaloid producing fungal species.

Chapter 4 described our functional characterization of the EasA Old Yellow Enzyme homologue from *N. lolii in vitro*.⁹ The work described in this chapter demonstrated that the function of the *N. lolii* EasA was uniquely different from *A. fumigatus* EasA. EasA_Nl, together with EasG, functioned to catalyze the set of transformations necessary to form ring D of agroclavine **10** starting from the substrate chanoclavine-I-aldehyde **7**. This observation suggested that EasA_Nl functioned with isomerase activity as opposed to the reductase activity observed for EasA_Af. Significantly, this finding showed that both EasA homologues utilized the same pathway intermediate chanoclavine-I-aldehyde **7**, yet produced a downstream product that was structurally different. EasA_Af and EasG produce festuclavine **11** with a reduced C8-C9 bond, while EasA_Nl and EasG retains a C8-C9 double bond yet in opposite geometrical configuration relative to the starting substrate chanoclavine-I-aldehyde **7**. These findings reinforced the idea that EasA homologues are at the critical branch point of ergot alkaloid biosynthesis across divergent fungal species.

Additionally, we obtained further insight into what mechanism governed this difference in activity among EasA homologues by identification of an active site tyrosine in EasA_Af homologues associated with festuclavine **11** producers versus an active site phenylalanine in EasA_Nl homologues associated with agroclavine **10** producers (Figure 4.3). The EasA_Nl_F176Y mutant demonstrated that the substitution of a tyrosine for phenylalanine in the isomerase type EasA resulted in newly acquired reductase activity

for the enzyme; therefore, the EasA_NI_F176Y along with EasG could yield both agroclavine **10** and festuclavine **11** from starting substrate chanoclavine-I-aldehyde **7**. These studies provided novel insight into the strategy *easA* homologues employ to modulate reductase activity into isomerase activity and thereby establishing structural diversity in ergot alkaloid biosynthesis. Findings from this study can be extended toward other biosynthetic systems to identify enzymes which may catalyze analogous reductase and isomerase reactions.

Chapter 5 described our efforts toward reconstitution of EasE and EasC enzymes *in vitro* to study their functional roles in the cyclization of ergoline ring C. Progress was made in establishing an enzymatic method for preparation of the *N*-Me-DMAT **4** substrate as well as for the expression of enzymes EasC with catalase activity and EasE that co-purifies with FAD. However, EasE and EasC, under various assay conditions and combinations, were not sufficient to catalyze the cyclization of *N*-Me-DMAT **4** to produce pathway intermediate chanoclavine-I **6** *in vitro*. Analysis of possible mechanisms of ring C cyclization by EasE and EasC, as well as the possible involvement of additional pathway enzymes, allowed us to speculate on alternative approaches to achieve reconstitution of these enzymes *in vitro*. These approaches of studying the cyclization of ring C *in vitro* are further described in future directions.

Future Directions

Exploring active site differences that define reductase versus isomerase EasA

EasA Mutants to Probe Mechanism

Further detailed study into the mechanism of EasA will be essential for understanding key active site differences that define a reductase or isomerase type enzyme. EasA_Af demonstrated the reduction of the C8-C9 carbon of substrate chanoclavine-I-aldehyde **7**, yet the contributions of other active site residues towards the stereoselective cyclization of ring D remain to be elucidated. In the case of EasA_Nl, isomerization of the C8-C9 double bond and stabilization of the proposed enolate intermediate remains a point of research focus. These future studies on EasA will be guided by the methods previously employed for the extensive enzyme characterization of Old Yellow Enzyme and homologs.¹⁰⁻¹⁶

As introduced in Chapters 3 and 4, OYE shares a conserved set of mechanistically important active site residues with EasA homologues. One approach will use site directed mutants to detail the mechanistic contributions of proposed active site residues towards the reductase or isomerase function of EasA. As a preliminary study, guided by protein sequence alignments of EasA_Af against *S. carlsbergensis* OYE (Figure 3.1), we made mutations to active site residues such as EasA_Af_H173N and N176H. Based on the previous studies of the OYE mechanism¹⁰, we proposed that the identical EasA_Af H173 and N176 residues also acted as hydrogen bond donors to the carbonyl oxygen of chanoclavine-I-aldehyde **7**, facilitating transfer of the hydride from FMN to reduce the C8-C9 double bond (Figure 3.4). However, the EasA_Af_H173N and EasA_Af_N176H mutations did not abolish reductase activity or significantly alter the enzyme's selectivity

toward production of the major cyclized iminium diastereoisomer **9**, yet rates of chanoclavine-I-aldehyde **7** substrate turnover were generally slower when compared to the wild type. A double mutant consisting of mutations to EasA H173N and N176H, however, did not show activity for the reduction of chanoclavine-I-aldehyde **7**. Collectively, these observations suggest that EasA_Af H173N and N176H residues are important contributors to the function of EasA_Af, similar to the H191 and N194 residues of OYE. To study these EasA mutants further, kinetic constants will be obtained to detail the contributions of each of these mutations toward NADPH and chanoclavine-I-aldehyde **7** binding. This preliminary study demonstrated that the *S. carlsbergensis* OYE serves as a good model toward the future design and characterization of additional EasA mutants. Recent work in the lab of Professor Audrey Lamb has resulted in a preliminary crystal structure that will guide more extensive mutations of EasA_Af to detail its mechanism.

While we were successful in engineering additional reductase function into isomerase Eas_Nl by a F176Y substitution, it is still a challenge to switch the function of EasA_Af from reductase to isomerase. As discussed in Chapter 4, EasA_Af_Y178F demonstrated the same reductase function as the wild type enzyme, leading us to believe that other active site residues may be contributing to EasA_Nl isomerization activity that are not present in EasA_Af. Such active site residues may, for example, preclude water from donating a proton to a reaction intermediate. To explore these possibilities fully with the ultimate goal of engineering isomerase function into the EasA_Af reductase, other mutations on EasA_Af that extend beyond its active site will be necessary. Similarly, we will also attempt to engineer the EasA_Nl_F176Y mutant from Chapter 4,

which exhibits both reductase and isomerase activity, to produce only the reductase product. This may in turn identify residues that are critical for facilitating isomerase function of EasA_Nl.

Exploring the Stereochemistry of EasA Catalysis by Deuterium Labeling

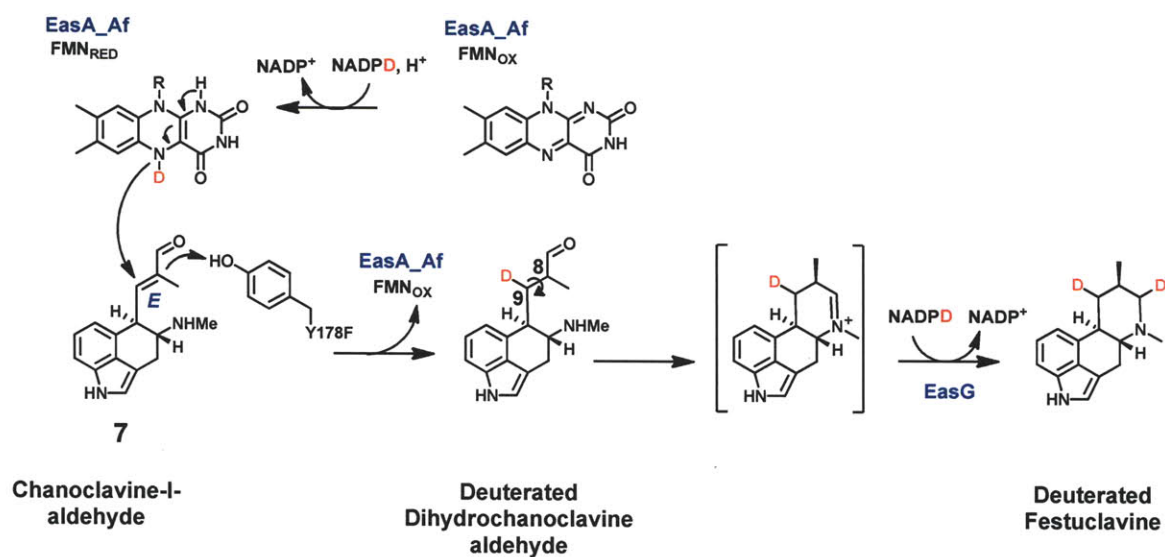
Although many of the Old Yellow Enzymes previously discovered have demonstrated their function to reduce the alkenes of α,β -unsaturated aldehydes and ketones on a variety of substrates, only a few studies have examined the stereoselectivity of the alkene reduction.^{17, 18} For *S. carlsbergensis* OYE, it has been proposed that the net anti-addition of H₂ across the alkene occurs via the transfer of hydride from flavin followed by protonation of the alpha carbon by the active site tyrosine.^{10, 12, 19} It will be of interest to study the stereoselectivity of EasA_Af and EasA_Nl given that they are unique OYE homologues which include an additional rotation step after hydride transfer in order to form ergoline ring D.

An approach to yield further insight into the stereoselectivity of EasA_Af reductase and EasA_Nl isomerase reactions will utilize deuterium labeled NADPH (NADPD) to monitor the incorporation of the deuterium label into the enzyme product. For EasA_Af reductase, the incorporation and location of deuterium label in the downstream product festuclavine **11** by NMR characterization, could yield information on the stereoselectivity of the hydride transfer from the flavin to the C9 position of chanoclavine-I-aldehyde **7** (Figure 6.1).

For EasA_Nl, vital details into the mechanism of the isomerization could be obtained by using NADPD and observing for the incorporation of the deuterium label

into downstream product agroclavine **10**. This would provide insight into the stereoselectivity of both the hydride transfer and the proposed re-oxidation of the C8-C9 double bond via hydride transfer from the substrate C9 position back to flavin (Figure 6.2). The distribution of the deuterium label by EasA_NI isomerase into the agroclavine **10** product will be useful toward studying the proposed intermolecular transfer of the hydrogen that has been previously proposed by the Floss group.²⁰

Figure 6.1. Proposed incorporation of deuterium label via NADPD during ergoline ring D formation as an approach to explore the stereoselectivity of the proposed EasA_Af reductase and EasG.



The diagram illustrates the biosynthetic pathway for the formation of deuterated agroclavine from chanoclavine-I-aldehyde (7). The process involves two parallel pathways, each initiated by the oxidation of FMN by EasA_{NI} to FMN_{ox}, which then reacts with NADP⁺ to form NADP^D and H⁺.

Left Pathway:

- Chanoclavine-I-aldehyde (7) reacts with NADP^D to form a deuterated intermediate (labeled 8 and 9).
- This intermediate is then converted to a deuterated intermediate (labeled 10 and 11) by EasA_{NI} (FMN_{ox}).
- The intermediate is further converted to a deuterated intermediate (labeled 12 and 13) by EasA_{NI} (FMN_{RED}).
- Dehydration (loss of H₂O) leads to a deuterated intermediate (labeled 14 and 15).
- Final conversion by EasG (NADP⁺ to NADP^D) yields **Deuterated Agroclavine**.

Right Pathway:

- Chanoclavine-I-aldehyde (7) reacts with NADP^D to form a deuterated intermediate (labeled 16 and 17).
- This intermediate is then converted to a deuterated intermediate (labeled 18 and 19) by EasA_{NI} (FMN_{ox}).
- The intermediate is further converted to a deuterated intermediate (labeled 20 and 21) by EasA_{NI} (FMN_{RED}).
- Dehydration (loss of H₂O) leads to a deuterated intermediate (labeled 22 and 23).
- Final conversion by EasG (NADP^D to NADP⁺) yields **Deuterated Agroclavine**.

The scheme shows the incorporation of deuterium (D) into the agroclavine molecule at various positions (C-8, C-9, C-10, C-11, C-12, C-13, C-14, C-15, C-16, C-17, C-18, C-19, C-20, C-21, C-22, C-23, C-24, C-25, C-26, C-27, C-28, C-29, C-30, C-31, C-32, C-33, C-34, C-35, C-36, C-37, C-38, C-39, C-40, C-41, C-42, C-43, C-44, C-45, C-46, C-47, C-48, C-49, C-50, C-51, C-52, C-53, C-54, C-55, C-56, C-57, C-58, C-59, C-60, C-61, C-62, C-63, C-64, C-65, C-66, C-67, C-68, C-69, C-70, C-71, C-72, C-73, C-74, C-75, C-76, C-77, C-78, C-79, C-80, C-81, C-82, C-83, C-84, C-85, C-86, C-87, C-88, C-89, C-90, C-91, C-92, C-93, C-94, C-95, C-96, C-97, C-98, C-99, C-100) during the biosynthesis of deuterated agroclavine.

In a complementary approach, an assay of EasA_Af or EasA_Nl in combination with EasG and NADPH in D₂O will also yield important mechanistic insight by examining the incorporation of deuterium label from solvent. After the transfer of the hydride from reduced flavin to the C9 position of chanoclavine-I-aldehyde **7**, EasA_Af reductase reaction is believed to proceed with the donation of a proton (active site tyrosine) to the C8 position, in contrast with the EasA_Nl isomerase reaction which is believed to proceed with no proton donation to the C8 position (active site phenylalanine). Currently we believe that the EasA_Af active site is more solvent accessible due to the finding that the EasA_Af_Y178F mutant was still able to carry out the production of festuclavine **11**, a reaction that is consistent with reductase EasA activity. This set of experiments carried out in D₂O could yield further information about differences in the solvent accessibility for active sites of EasA_Af and EasA_Nl, and mutants of these enzymes.

Kinetic Isotope Effects to Detail the Reductive and Oxidative Reactions of EasA Catalysis

Valuable details regarding the mechanism of the reductive and oxidative half reactions of EasA_Af and EasA_Nl enzymes will also be elucidated by the measurement of kinetic isotope effects in assays with NADPD and H₂O or D₂O.²¹ These kinetic isotope effects would yield mechanistic insights into the details of the hydride transfer to compare with those previously reported for other OYE homologues.^{11, 14, 22} Stopped flow spectroscopy approaches that had been previously used for measuring the kinetic isotope effects of the OYE homologue Morphinone Reductase, may be similarly applied to the study of EasA.²²

The characteristic flavin absorption spectrum of EasA FMN will serve as a spectroscopic handle to measure rates of the reductive half reaction with NADPH and the oxidative half reaction of reduced FMN and substrate chanoclavine-I-aldehyde **7**. This approach will provide the ability to deconvolute the details of the proposed mechanism of intermolecular hydrogen transfer with EasA_Nl and the isomerization of the C8-C9 chanoclavine-I-aldehyde **7** double bond (Figure 4.13A).²⁰ Additionally, it will be informative to contrast the flavin absorption spectra of EasA_Af reductase with EasA_Nl isomerase, as they may display different populations of oxidized and reduced states of flavin over time due to their proposed differences in mechanism.

As the kinetic isotope effect reveals greater mechanistic detail into the reductive and oxidative half reactions characteristic of EasA and OYE homologues, another interesting aspect of the reaction to study are the details of the hydrogen transfer between the EasA flavin, NADPH, and chanoclavine-I-aldehyde **7** substrate. Previous studies on OYE have proposed that the reactions proceed by hydride transfer, yet only a few studies have addressed the possibility of a radical based mechanism.²³⁻²⁵ Based on these previous studies, electron spin resonance (ESR) spectroscopy may be used to observe formation of radical intermediates generated in the redox half reactions catalyzed by EasA. The experimental setup will be guided by previous ESR studies that have been used to observe radical formation in similar reactions catalyzed by OYE homologues.^{23, 25, 26} This approach will allow for observation of significant differences in the mechanism of hydrogen transfer that may distinguish isomerase from reductase EasA.

It is necessary to yield greater mechanistic insight into EasA to understand the strategy these enzymes employ to catalyze reductase or isomerase reactions. These

strategies may well extend beyond the ergot alkaloid biosynthetic pathway given the abundance of OYE homologues across different species. Furthermore, this knowledge is also applicable toward the production or re-engineering of enzyme catalysts to carry out isomerization or reduction of alkenes that are not easily accessible by conventional synthetic approaches.

Exploring potential EasA and EasG interactions to form ergoline ring D

From Chapters 3 and 4, we observed that EasG NADPH reductase is important for reduction of the cyclic iminium intermediate **9** to form either festuclavine **11** (EasA_Af + EasG) or agroclavine **10** (EasA_Nl + EasG). The immediate product of EasA_Af and EasA_Nl are proposed to be cyclic iminium intermediates **9** and **8** respectively, which seem prone to decomposition or adduct formation with nucleophilic protein side chains. To prevent the formation of undesired byproducts or protein adducts, we speculate that there may be a physical protein-protein interaction between EasA and EasG that ensures efficient production of either festuclavine **11** or agroclavine **10** downstream products.

Preliminary experiments to demonstrate a physical interaction between EasA (42 kDa) and EasG (30 kDa) proteins would be to subject them to gel filtration chromatography under various buffer conditions and concentrations of protein, substrate, and co-factors. The elution profile of EasA and EasG together will be compared to the profiles of these enzymes when analyzed separately, in order to observe if they associate into a larger protein complex.^{27, 28} If results from gel filtration chromatography are supportive of interactions of EasA and EasG, analytical ultracentrifugation will be used

to look for additional evidence for protein-protein interactions.^{29, 30} In a complementary study, yeast two hybrid³¹⁻³³ or co-immunoprecipitation³⁴⁻³⁶ approaches may be used to examine interactions between EasA and EasG proteins. A crystal structure of this complex will also be pursued to provide novel insight into how these proteins may work together to facilitate either reductase or isomerase activity.

Reconstitution of EasE and EasC activity *in vitro* for ergoline ring C formation

While there is good evidence for the involvement of EasE and EasC in the cyclization of ergoline ring C as introduced in Chapter 2, there are still challenges to meet in order to reconstitute EasE and EasC activity *in vitro* as discussed in Chapter 5. While EasC displayed catalase activity for decomposing H₂O₂, we speculate that we have been unable to express EasE in its correct holoenzyme functional form. In Chapter 5, protein sequence analysis comparing EasE to similar FAD dependent oxidases berberine bridge enzyme and isoamyl alcohol oxidase suggested that FAD may be covalently linked to EasE, as they share identical residues for covalent attachment of flavin. In light of this observation, *E. coli* would not be an ideal host for expression of EasE, as the expression of active Berberine Bridge Enzyme was only achieved in *Pichia pastoris* while expression in *E. coli* yielded inactive protein.³⁷ Moving expression of EasE from *E. coli* into yeast such as *Saccharomyces cerevisiae* or *Pichia pastoris* seems to be a promising approach toward realizing active holoenzyme EasE.

To obtain proper EasE and EasC activity *in vitro*, it is also necessary to determine whether other enzymes in the ergot alkaloid cluster need to be present in order to observe proper function of EasE and EasC or whether these enzymes function in a larger

complex. One approach is to reconstitute the minimum set of genes necessary for chanoclavine-I 6 biosynthesis in the closely related model organism *Aspergillus nidulans*, which does not produce ergot alkaloids and has been previously used for the expression of other *A. fumigatus* genes.³⁸ *A. nidulans* is also an attractive host for expression of *A. fumigatus* associated genes as they share a similar sporulation developmental pathway, indicating that it is likely that native *A. fumigatus* promoters may be used successfully to regulate the expression of their respective ergot pathway genes.³⁹⁻⁴¹ Subsets of genes in the ergot alkaloid cluster starting with the first four genes of the pathway DmaW, EasF, EasC, and EasE would be transformed into *A. nidulans* to determine whether chanoclavine-I 6 production occurs. If this minimal set of genes do not provide sufficient evidence that chanoclavine-I 6 can be produced, additional ergot alkaloid genes of the cluster may also be added. Even though these additional pathway genes may not be directly associated with chanoclavine-I 6 biosynthesis, their presence may be required in order to observe product formation. The presence or absence of additional pathway associated genes and their relative ratios in polyketide biosynthesis have shown significant effects on product yield.⁴² The *A. nidulans* host would provide opportunities toward achieving proper reconstitution and expression of the ergot pathway enzymes.

Reconstitution of chanoclavine-I 6 production in *A. nidulans* would indicate that the minimal set of genes required for chanoclavine-I 6 biosynthesis are present. Identifying this correct subset of genes will guide efforts toward the *in vitro* reconstitution of EasC and EasE function, thus allowing for further characterization of their functional role and mechanism in ergoline ring C cyclization.

***In Vivo* Production of Novel Ergot Alkaloid Analogs**

In vivo feeding studies with substituted tryptophan derivatives to *A. fumigatus* culture will also be useful toward the production of novel ergot alkaloid analogs. Preliminary feeding studies conducted with our collaborators in the Panaccione lab have shown the incorporation of deuterated tryptophan from culture media into ergot alkaloids of *A. fumigatus*, yet fluorinated tryptophan analogs remain difficult to incorporate into downstream ergot alkaloids, most likely because of the high substrate specificity of DmaW.

From previous studies the first committed step to ergot alkaloid biosynthesis in *A. fumigatus* DmaW prenyltransferase is the pathway bottleneck for incorporation of substituted tryptophan analogs.² Expanding the substrate scope of this DmaW prenyltransferase by rational reengineering using the recently published crystal structure⁴³ as a model will be a useful approach toward studying the incorporation of other substrates into the downstream enzymes. Complementation of mutant DmaW with expanded substrate scope into the $\Delta dmaW$ strain of *A. fumigatus* may allow for the uptake of tryptophan derivatives that could be further incorporated into downstream enzymes to produce unique analogs of ergot alkaloids, and additionally serve as an entryway toward studying the substrate specificity of downstream ergot alkaloid pathway enzymes.

Furthermore, a similar strategy could also be used to complement alleles for genes such as *easA* from a different species origin to study their function in the presence of other ergot alkaloid pathway enzymes. In a parallel approach, the successful reconstitution of the minimal set of genes for ergot alkaloid biosynthesis in a more

tractable *A. nidulans* host will also allow us to gain a better perspective on the *in vivo* production of novel ergot alkaloid derivatives.

References

1. Tsai, H.F., H. Wang, J.C. Gebler, C.D. Poulter, and C.L. Schardl, *The Claviceps Purpurea gene encoding dimethylallyltryptophan synthase, the committed step for ergot alkaloid biosynthesis*. Biochemical and Biophysical Research Communications, 1995. **216**(1): p. 119-125.
2. Rigbers, O. and S.-M. Li, *Ergot Alkaloid Biosynthesis in Aspergillus fumigatus Overproduction and Biochemical Characterization of a 4-Dimethylallyltryptophan N-Methyltransferase*. The Journal of Biological Chemistry, 2008. **283**(40): p. 26859-26868.
3. Coyle, C.M. and D.G. Panaccione, *An Ergot Alkaloid Biosynthesis Gene and Clustered Hypothetical Genes from Aspergillus fumigatus*. Applied and Environmental Microbiology, 2005. **71**(6): p. 3112-3118.
4. Otsuka, H., F.R. Quigley, D. Groger, J.A. Anderson, and H.G. Floss, *In Vivo and In Vitro Evidence for N-Methylation as the Second Pathway-Specific Step in Ergoline Biosynthesis*. Planta Medica, 1980. **40**: p. 109-119.
5. Goetz, K.E., C.M. Coyle, J.Z. Cheng, S.E. O'Connor, and D.G. Panaccione, *Ergot cluster-encoded catalase is required for synthesis of chanoclavine-I in Aspergillus fumigatus*. Current Genetics, 2011(accepted).
6. Coyle, C.M., J.Z. Cheng, S.E. O'Connor, and D.G. Panaccione, *An Old Yellow Enzyme Gene Controls the Branch Point between Aspergillus fumigatus and Claviceps purpurea Ergot Alkaloid Pathways*. Applied and Environmental Microbiology, 2010. **76**(12): p. 3898-3903.
7. Saito, K., D. Thiele, M. Davio, O. Lockridge, and V. Massey, *The Cloning and Expression of a Gene Encoding Old Yellow Enzyme from Saccharomyces carlsbergensis*. The Journal of Biological Chemistry, 1991. **266**(31): p. 20720-20724.
8. Cheng, J.Z., C.M. Coyle, D.G. Panaccione, and S.E. O'Connor, *A Role for Old Yellow Enzyme in Ergot Alkaloid Biosynthesis*. Journal of the American Chemical Society, 2010. **132**(6): p. 1776-1777.
9. Cheng, J.Z., C.M. Coyle, D.G. Panaccione, and S.E. O'Connor, *Controlling a Structural Branch Point in Ergot Alkaloid Biosynthesis*. Journal of the American Chemical Society, 2010. **132**(37): p. 12835-12837.
10. Brown, B., Z. Deng, P.A. Karplus, and V. Massey, *On the Active Site of Old Yellow Enzyme Role of Histidine 191 and Asparagine 194*. The Journal of Biological Chemistry, 1998. **273**(49): p. 32753-32762.
11. Pudney, C.R., S. Hay, M. Sutcliffe, and N.S. Scrutton, *α -Secondary Isotope Effects as Probes of "Tunneling-Ready" Configurations in Enzymatic H-Tunneling: Insight from Environmentally Coupled Tunneling Models*. Journal of the American Chemical Society, 2006. **128**(43): p. 14053-14058.
12. Kohli, R. and V. Massey, *The Oxidative Half-reaction of Old Yellow Enzyme The Role of Tyrosine 196*. The Journal of Biological Chemistry, 1998. **273**(49): p. 32763-32770.
13. Vaz, A., S. Chakraborty, and V. Massey, *Old Yellow Enzyme: Aromatization of Cyclic Enones and the Mechanism of a Novel Dismutation Reaction*. Biochemistry, 1995. **34**: p. 4246-4256.

14. Massey, V. and L. Schopfer, *Reactivity of Old Yellow Enzyme with α -NADPH and Other Pyridine Nucleotide Derivatives*. The Journal of Biological Chemistry, 1986. **261**(3): p. 1215-1222.
15. Meah, Y. and V. Massey, *Old Yellow Enzyme: Stepwise reduction of nitro-olefins and catalysis of aci-nitro tautomerization*. Biochemistry, 2000. **97**(20): p. 10733–10738.
16. Fitzpatrick, T., N. Amrhein, and P. Macheroux, *Characterization of YqjM, an Old Yellow Enzyme Homolog from Bacillus subtilis Involved in the Oxidative Stress Response*. The Journal of Biological Chemistry, 2003. **278**(22): p. 19891-19897.
17. Muller, A., N. Hauer, and B. Rosche, *Asymmetric Alkene Reduction by Yeast Old Yellow Enzymes and by a Novel Zymomonas mobilis Reductase*. Biotechnology and Bioengineering, 2007. **98**(1): p. 22-29.
18. Swiderska, M.A. and J.D. Stewart, *Stereoselective enone reductions by Saccharomyces carlsbergensis old yellow enzyme*. Journal of Molecular Catalysis B: Enzymatic, 2006. **42**: p. 52-54.
19. Fox, K. and P.A. Karplus, *Old yellow enzyme at 2 Å resolution: overall structure, ligand binding, and comparison with related flavoproteins*. Structure, 1994. **15**(2): p. 1089-1105.
20. Floss, H.G., M. Tchong-Lin, C. Chang, B. Naidoo, G. Blair, C. Abou-Chaar, and J. Cassady, *Biosynthesis of ergot alkaloids. Mechanism of the conversion of chanoclavine-I into tetracyclic ergolines*. Journal of the American Chemical Society, 1974: p. 1898-1909.
21. Basran, J., R.J. Harris, M.J. Sutcliffe, and N.S. Scrutton, *H-tunneling in the Multiple H-transfers of the Catalytic Cycle of Morphinone Reductase and in the Reductive Half-reaction of the Homologous Pentaerythritol Tetranitrate Reductase*. The Journal of Biochemistry, 2003. **278**(45)(7): p. 43973-43982.
22. Hay, S., C.R. Pudney, and N.S. Scrutton, *Structural and mechanistic aspects of flavoproteins: probes of hydrogen tunnelling*. FEBS Journal, 2009. **276**: p. 3930-3941.
23. Honma, T. and Y. Ogura, *Kinetic Studies of the Old Yellow Enzyme*. Biochimica et Biophysica Acta, 1977. **484**: p. 9-23.
24. Nakamura, T. and J. Yoshimura, *Action Mechanism of the Old Yellow Enzyme*. The Journal of Biochemistry, 1965. **57**(4): p. 554-564.
25. Kubata, B.K., Z. Kabututu, T. Nozaki, C.J. Munday, S. Fukuzumi, K. Ohkubo, M. Lazarus, T. Maruyama, S.K. Martin, M. Duszenko, and Y. Urade, *A Key Role for Old Yellow Enzyme in the Metabolism of Drugs by Trypanosoma cruzi*. The Journal of Experimental Medicine, 2002. **196**(9): p. 1241-1251.
26. Murataliev, M.B., *Application of Electron Spin Resonance (ESR) for Detection and Characterization of Flavoprotein Semiquinones*, in *Methods in Molecular Biology: Flavoprotein Protocols*, S. Chapman and G. Reid, Editors. 1999, Humana Press Inc.: Totowa, NJ.
27. Tetlow, I.J., K.G. Beisel, S. Cameron, A. Makhmoudova, L. Fushan, N.S. Bresolin, R. Wait, M.K. Morell, and M.J. Emes, *Analysis of Protein Complexes in Wheat Amyloplasts Reveals Functional Interactions among Starch Biosynthetic Enzymes*. Plant Physiology, 2008. **146**: p. 1878-1891.

28. Wen, J., T. Arakawa, and J. Philo, *Size-Exclusion Chromatography with On-Line Light-Scattering, Absorbance, and Refractive Index Detectors for Studying Proteins and Their Interactions*. Analytical Biochemistry, 1996. **240**: p. 155-166.
29. Laue, T.M. and W.F. Stafford, *Modern Applications of Analytical Ultracentrifugation*. Annual Review of Biophysics and Biomolecular Structure, 1999. **28**: p. 75-100.
30. Lebowitz, J., M.S. Lewis, and P. Schuck, *Modern analytical ultracentrifugation in protein science: A tutorial review*. Protein Science, 2002. **11**: p. 2067-2079.
31. Suter, B., S. Kittanakom, and I. Stagljar, *Two-hybrid technologies in proteomics research*. Current Opinion in Biotechnology, 2008. **19**: p. 316-323.
32. Mukherjee, J., S. Bal, and P. Saha, *Protein interaction maps using yeast two-hybrid assay*. Current Science, 2001. **81**(5): p. 458-464.
33. Ishii, J., N. Fukuda, T. Tanaka, C. Ogino, and A. Kondo, *Protein-protein interactions and selection: yeast-based approaches that exploit guanine nucleotide-binding protein signaling*. FEBS Journal, 2010. **277**.
34. Miernyk, J.A. and J.J. Thelen, *Biochemical approaches for discovering protein-protein interactions*. The Plant Journal, 2008. **53**: p. 597-609.
35. Wittig, I. and H. Schagger, *Native electrophoretic techniques to identify protein-protein interactions*. Proteomics, 2009: p. 5214-5223.
36. Markham, K., Y. Bai, and G. Schmitt-Ulms, *Co-immunoprecipitations revisited: an update on experimental concepts and their implementation for sensitive interactome investigations of endogenous proteins*. Analytical and Bioanalytical Chemistry, 2007. **389**: p. 461-473.
37. Winkler, A., A. Lyskowski, S. Riedl, M. Puhl, T. Kutchan, P. Macheroux, and K. Gruber, *A concerted mechanism for berberine bridge enzyme*. Nature Chemical Biology, 2008. **4**(12).
38. Borgia, P.T., C.L. Dodge, L.E. Eagleton, and T.H. Adams, *Bidirectional gene transfer between Aspergillus fumigatus and Aspergillus nidulans*. FEMS Microbiology Letters, 1994. **122**(3): p. 227-231.
39. Mah, J.-H. and J.-H. Yu, *Upstream and Downstream Regulation of Asexual Development in Aspergillus fumigatus*. Eukaryotic Cell, 2006. **5**(10): p. 1585-1595.
40. Coyle, C.M., S. Kenaley, W. Rittenour, and D.G. Panaccione, *Association of ergot alkaloids with conidiation in Aspergillus fumigatus*. Mycologia, 2007. **99**(6): p. 804-811.
41. Twumasi-Boateng, K., Y. Yan, D. Chen, F.N. Gravelat, W.C. Nierman, and D.C. Sheppard, *Transcriptional Profiling Identifies a Role for BrlA in the Response to Nitrogen Depletion and for StuA in the Regulation of Secondary Metabolite Clusters in Aspergillus fumigatus*. Eukaryotic Cell, 2009. **8**: p. 104-115.
42. Kharel, M.K., P. Pahari, H. Lian, and J. Rohr, *Enzymatic Total Synthesis of Rabelomycin, and Angucycline Group Antibiotic*. Organic Letters, 2010. **12**: p. 2814-2817.
43. Metzger, U., C. Schall, G. Zocher, I. Unsold, E. Stec, S.-M. Li, L. Heide, and T. Stehle, *The structure of dimethylallyl tryptophan synthase reveals a common architecture of aromatic prenyltransferases in fungi and bacteria*. Proceedings of

the National Academy of Sciences of the United States of America., 2009.
106(34): p. 14309-14314.

Curriculum Vitae - Johnathan Zandrew Cheng

Education

2007-2011 Ph.D Chemistry, Massachusetts Institute of Technology
2003-2007 B.S. Chemistry, University of Hawaii

Research Experience

2011- Postdoctoral Researcher, John Innes Centre
2007-2011 Research Assistant, Massachusetts Institute of Technology
2004-2007 Undergraduate Research Assistant, University of Hawaii

Publications

Goetz, K.E., C.M. Coyle, J.Z. Cheng, S.E. O'Connor, and D.G. Panaccione, *Ergot cluster-encoded catalase is required for synthesis of chanoclavine-I in Aspergillus fumigatus*. Current Genetics, 2011(accepted).

Cheng, J.Z., C.M. Coyle, D.G. Panaccione, and S.E. O'Connor, *Controlling a Structural Branch Point in Ergot Alkaloid Biosynthesis*. Journal of the American Chemical Society, 2010. **132**(37): p. 12835-12837.

Cheng, J.Z., C.M. Coyle, D.G. Panaccione, and S.E. O'Connor, *A Role for Old Yellow Enzyme in Ergot Alkaloid Biosynthesis*. Journal of the American Chemical Society, 2010. **132**(6): p. 1776-1777.

Coyle, C.M., J.Z. Cheng, S.E. O'Connor, and D.G. Panaccione, *An Old Yellow Enzyme Gene Controls the Branch Point between Aspergillus fumigatus and Claviceps purpurea Ergot Alkaloid Pathways*. Applied and Environmental Microbiology, 2010. **76**(12): p. 3898-3903.

Selected Honors and Awards

2011 22nd Enzyme Mechanisms Conference Abstract
Honorable Mention Founders Travel Award
2007 MIT Presidential Fellow
2007 DuPont-MIT Alliance Fellow
2007 MIT Howard Hughes Medical Institute TA Fellow
2007 ACS Merck Outstanding Senior in Chemistry Award
2005 University of Hawaii Presidential Scholar
2005 ACS Award for Excellence in Analytical Chemistry
2004 ACS Award for Freshman Achievement in Chemistry